

**A TISSUE ENGINEERED APPROACH TO PROGENITOR CELL
DELIVERY AND MYOCARDIAL REPAIR**

A Dissertation
Presented to
The Academic Faculty

by

David Lemar Simpson

In Partial Fulfillment
Of the Requirements for the Degree
Doctor of Philosophy in Biomedical Engineering

Georgia Institute of Technology

December 2009

**A TISSUE ENGINEERED APPROACH TO PROGENITOR CELL
DELIVERY AND MYOCARDIAL REPAIR**

Approved by:

Dr. Samuel Dudley, Advisor
Department of Medicine
University of Illinois at Chicago

Dr. Robert M. Nerem, Advisor
School of Mechanical Engineering
Georgia Institute of Technology

Dr. Steve Stice
College of Agricultural and
Environmental Sciences
University of Georgia

Dr. Todd McDevitt
Department of Biomedical Engineering
*Georgia Institute of Technology and
Emory University*

Dr. Marie Csete
Chief Scientific Officer
*California Institute of Regenerative
Medicine*

Date Approved: August 18, 2009

Nothing in the world can take the place of persistence. Talent will not; nothing is more common than unsuccessful men [and women] with talent. Genius will not; unrewarded genius is almost a proverb. Education will not; the world is full of educated derelicts. The slogan, "Press on" has solved and always will solve the problems of the human race.

-Calvin Coolidge, January 17, 1914

To Mommy and Daddy

ACKNOWLEDGEMENTS

I would first like to thank my parents, Mable and David Evans (or as I like to call them, Mom and Dad). This journey of constant failure and success would not have been made possible without the values and drive they instilled in me at an early age. It is because of them that I continue to persevere. My persistence to becoming the best person I can be will never let down because I know they will always be with me...guiding me to the top. I love you both very much.

I am happy to have reached this stage in my professional endeavors. It has been a long and tedious journey filled with excitement, sleep deprivation, serendipity and colossal failure. As I have matured I have come to realize the advantages to all of these stages. I must admit that as a younger PhD student my "procrastination level" was quite high. I had come to rely on my ability to just "get by", which I was very good at doing. I maintained a good GPA at the University of Virginia with procrastination and was successful at a graduate student at Georgia Tech with procrastination. Research however, made me realize the importance of thorough planning and asking the right questions. These actions are not very friendly to the student who procrastinates...thus my mindset began to change. This change was not a divine realization that I had come to understand by myself. It took the guidance of my advisor, Dr. Samuel Dudley, to help me get back on track. Dr. Dudley has been a constant mentor and friend throughout my journey at Georgia Tech, Emory University and the University of Illinois at Chicago. He has guided me in becoming a better scientist and a better person. He has even extended a helping hand during my times of personal struggle and hardship. I am confident I will never forget his in depth knowledge about "everything" or his tales of science (the "CS" to "CS" converter comes to mind). He has always said that I need to

become famous so I can invite him to give a talk someday...he can rest assured he will be at the top of my list.

I would also like to acknowledge the contributions of the members on my PhD thesis committee: Dr. Robert Nerem, Dr. Marie Csete, Dr. Steve Stice and Dr. Todd McDevitt. Specifically, I would like to thank Dr. Nerem for his assistance, guidance and belief in me during my time at Georgia Tech. I have always considered him to be a second advisor and have enjoyed working with him and his laboratory. I would also like to thank Dr. Csete for her assistance with understanding oxygen tension and how it relates stem cell function and also her enthusiasm for my project. While at Emory University I was able to collaborate and work with members of Dr. Csete's research lab which was of great help in furthering my project. I would like to thank Dr. Steve Stice for his assistance with understanding embryonic stem cell culture and properties. In addition, I would like to thank the Stice Lab (specifically, Dr. Nolan Boyd) for providing SM1, SM4 and B4 progenitor cells which I have used over the past two years in my studies. Lastly, I would like to thank Dr. Todd McDevitt for his great advice and feedback which has helped me tailor my thesis into something I am quite proud of.

The laboratory of Dr. Samuel Dudley has been of immense help in aiding me through this stage of my life. They have assisted me with various techniques and made me feel welcome when I joined the lab. I would like to thank Jon Allen, Priyanka Karen, Georgia Gaconnet and Alana Reed for their friendship and assistance throughout the various facets of my work. I would like to thank Dr. Zhe Jiao, Dr. Hong Liu, Dr. Lisa Shang, Dr. Vijay Kasi, Dr. Grace Gao, Dr. Havey Lardin, Dr. Josh Lovelock, Dr. Man Liu, Dr. Michael Fan, Dr. Alice Huang and Dr. Susen Varghese for their willingness to assist me in learning new techniques or helping me in understanding some random piece of knowledge. In particular I'd like to thank Dr. Alice Huang and Dr. Hong Liu for having the

patience to work with me and teach me a variety of surgical techniques which I have come to rely on throughout my PhD research.

During my stay at Georgia Tech and Emory University I had the opportunity to work with many individuals. I would like to thank the members of the Nerem Lab for accepting me into the lab and teaching me various techniques that I continue to use to this day. Thank you Kara McCloskey, Ima Ibong, Tiffany Johnson, Ann Ensley, Jonathan Butcher, Josette Broiles, Stacy Schutte, Taby Ashan, Adele Doyle, Barbara Nsiah, Casey Holiday and Steve Woodard for all of your help. I would also like to acknowledge the staff of the IBB who aided me in understanding and performing additional techniques such as histology (Tracy Couse and Aqua Asberry), flow cytometry and confocal microscopy (Jonafel Crowe). I also want to thank all the secretaries, assistants and staff of the IBB front office and building. You are the ones who keep this institute running.

While at Georgia Tech and Emory University I worked with various faculty who gave me the opportunity to improve my teaching pedagogy. In particular I'd like to thank Dr. Barbara Boyan for allowing me to help reshape and improve the BMED 3160 lab and Dr. David Lynn for accepting me into the ORDER program at Emory University. I would also like to thank the program directors of the FACES program, NIH Cellular and Tissue Engineering Training Grant, George Fellowships and Gandy-Diaz Fellowships for all the financial assistance these programs have provided me over the years.

I would also like to acknowledge the faculty and staff at the University of Illinois at Chicago, Section of Cardiology. In particular I'd like to thank Dr. Dave Geenen for his assistance with fine tuning my myocardial infarct model and echocardiography technique. Also, I'd like to thank Dr. Mei Lin Chen for her assistance with confocal microscopy and Dr. Karen Hagen for her assistance with flow cytometry. Additionally, I'd like to thank the staff of the Section of Cardiology: Lisa Cox, Birgitta Kuehn, Jeffery

Kulik, Faith Thrumond and Richard Whitley. They are always willing to help me with any problem and I greatly appreciate their efforts.

Lastly, I'd like to thank my friends Anthony, Matt, Johnny, Adam, Tony and Augustus. Thank you Anthony, Matt, Johnny, Adam and Tony for always being there for me. You are great friends who I have come to rely on for peace of mind and great conversation. Augustus, I know we've had our ups and downs but thank you for being by my side during some of the toughest times of my life: my financial curses, the death of my grandmother, my sudden move to Chicago, the theft from my car and my personal struggles with life in general. You helped me to continue to strive for my goals and live life to its fullest. I can confidently say that because of you I have evolved into a better person. I can see my faults and am willing to venture outside my comfort zone to change them. Sometimes I do wish I would've realized this earlier, but I am confident that we are both much happier. Thank you for everything, I love you and I wish you the best.

TABLE OF CONTENTS

ACKNOWLEDGEMENTS	v
TABLE OF CONTENTS	ix
LIST OF TABLES	xvi
LIST OF FIGURES	xvii
LIST OF ABBREVIATIONS	xx
SUMMARY	xxiii

CHAPTER

1	Introduction	1
2	Background	5
2.1	A Brief Discussion on the Anatomy and Physiology of the Heart	5
2.2	Epidemiology and Etiology of Heart Failure	10
2.3	Myocardial Infarction (MI)	12
2.4	Diagnosis of Myocardial Infarction	16
2.4.1	The Electrocardiogram (ECG)	16
2.4.2	Echocardiography	18
2.5	Current Treatment Options and Limitations	21
2.5.1	Drug Therapies	21
2.5.2	Surgical Options	22
2.5.3	Cellular Cardiomyoplasty as a Potential Treatment	23
2.6	A Critical Review on the State of Progenitor Cell Cardiomyoplasty	23
2.6.1	Cell Sources for Cardiomyoplasty	23
2.6.1.1	Skeletal Myoblast	25

2.6.1.2	Cardiac Progenitors	26
2.6.1.3	Bone Marrow Stem Cells	28
2.6.1.4	Adipose-Derived Mesenchymal Stem Cells	29
2.6.1.5	Amniotic Fluid Stem Cells	30
2.6.1.6	Embryonic Stem Cells	31
2.6.1.7	Induced Pluripotent Stem Cells	32
2.6.2	Clinical Translation of Cellular Cardiomyoplasty	34
2.6.2.1	Phase I Clinical Trial Results	36
2.6.2.2	Phase II and III Clinical Trials	37
2.6.3	Translational Issues Concerning Cellular Cardiomyoplasty	41
2.6.3.1	Translational Roadblock #1: No Optimum Cell has been Identified	41
2.6.3.2	Translational Roadblock #2: Low Engraftment Rates	41
2.6.3.3	Translational Roadblock #3: Understanding the Mechanism of Repair	42
2.6.3.3.1	Do Cardiomyocytes Matter?	42
2.6.3.3.2	Trophic Factors – The Paracrine Hypothesis	45
2.6.4	Tissue Engineering for Addressing the Translational Issues	46
2.6.5	Summary	51
2.7	Conclusions	52
2.8	References	53
3	A TISSUE ENGINEERING APPROACH TO CELL DELIVERY RESULTS IN SIGNIFICANT CELL ENGRAFTMENT AND IMPROVED MYOCARDIAL REMODELING: A PROOF OF CONCEPT	
3.1	Introduction	64

3.2	Materials and Methods	65
3.2.1	Animal Handling	65
3.2.2	Production of Cardiac Patches	65
3.2.3	Characterization of hMSC in Cardiac Patch	69
3.2.4.1	Viability	69
3.2.4.2	Differentiation	69
3.2.4.3	Cellularity	70
3.2.4	Infarct Model and Patch Application	70
3.2.5	Echocardiography	71
3.2.6	Cardiac Hemodynamics	72
3.2.7	Myocardial Histology	72
3.2.8	Neonatal Cardiomyocyte and Cardiac Fibroblast Isolation	74
3.2.9	Real Time RT-PCR	74
3.2.10	Assessment of hMSC Paracrine Function	75
3.2.11	Statistical Analysis and Interpretation	77
3.3	Results	77
3.3.1	In Vitro Characterization of the Cardiac Patch	77
3.3.2	Progenitor Cell Engraftment and Distribution with Cardiac Patch Application	80
3.3.3	Efficacy of the Cardiac Patch in Post-infarct Remodeling	84
3.3.4	Increased Myofibroblast and c-Kit Expression with Patch Application	87
3.3.4	An <i>In Vitro</i> Model to Assess Possible Benefits of hMSC Conditioned Media	91
3.4	Discussion	95
3.5	Limitations and Recommendations	99

3.6	References	101
4	MODULATION OF HUMAN MESENCHYMAL STEM CELL FUNCTION IN COLLAGEN PATCHES	105
4.1	Introduction	105
4.2	Materials and Methods	106
4.2.1	Cell Culture	106
4.2.2	Formation of Cell Seeded Collagen Patches	106
4.2.3	Measurement of Patch Compaction	106
4.2.4	Viability Assays	107
4.2.5	Cellularity	107
4.2.6	Proliferation	108
4.2.7	Assessment of Cell Differentiation	109
4.2.7.1	Flow Cytometry	109
4.2.7.2	Histology	109
4.2.8	Antibody Arrays and Protein ELISAs	110
4.2.9	Real Time RT-PCR	111
4.2.10	Hypoxia Model and Endothelial Cell Function	112
4.2.11	Animal Handling	114
4.2.12	Infarct Model and Patch Application	114
4.2.13	Echocardiography	115
4.2.14	Cardiac Hemodynamics	116
4.2.15	Myocardial Histology	117
4.2.16	Statistical Analysis and Interpretation	118
4.3	Results	118
4.3.1	Culture within Collagen Patches Modulates	

	Proliferation, Differentiation and Viability of hMSC	118
4.3.2	Changes in Secretory Profiles of hMSC after Culture in Collagen Patches	123
4.3.3	hMSC Conditioned Media may Modulate Endothelial Cell function	129
4.3.4	hMSC Patch Application Results in Improved Myocardial Function Compared to Injected hMSC	131
4.4	Discussion	135
4.5	Limitations and Recommendations	140
4.6	References	141
5	HUMAN EMBRYONIC STEM CELL DERIVED-MESENCHYMAL CELLS: EXPLORING THE EFFICACY OF A POSSIBLE SUBSTITUTE FOR MESENCHYMAL STEM CELLS IN CELLULAR CARDIOMYOPLASTY	145
5.1	Introduction	145
5.2	Materials and Methods	147
5.2.1	Animal Handling	147
5.2.2	Cell Culture	147
5.2.3	Formation of Cell Seeded Collagen Patches	148
5.2.4	Viability Assays	148
5.2.5	Proliferation	149
5.2.6	Assessment of Cell Differentiation	150
5.2.7	Real Time RT-PCR	150
5.2.8	Infarct Model and Patch Application	151
5.2.9	Echocardiography	152
5.2.10	Cardiac Hemodynamics	153
5.2.11	Myocardial Histology	153
5.2.12	Statistical Analysis and Interpretation	154
5.3	Results	154

5.3.1	Culture within Collagen Patches Modulates Proliferation, Differentiation and Viability of hMSC and B4 Progenitor Cells	154
5.3.2	Culture within 3D Collagen Patches Modulates Growth mRNA Abundance of hMSC and B4 Progenitor Cells	157
5.3.3	Cardiac Patch Application to Injured Myocardium does not Alter the Developed Infarct Size	160
5.3.4	hMSC and B4 Progenitor Cell Cardiac Patch Application Improves Parameters of Cardiac Remodeling and Function after Myocardial Infarction	162
5.3.3	B4 Progenitor Cell Patch does not Alter Neovessel Formation after Myocardial Infarction	164
5.4	Discussion	166
5.5	Limitations and Recommendations	169
5.5	References	170
6	CONCLUSIONS AND FUTURE DIRECTIONS	174
6.1	Addressing Cellular Cardiomyoplasty in Five Stages	174
6.2	Conclusions	189
6.3	References	190

APPENDIX

A	PERFORMING A SUCCESSFUL LEFT ANTERIOR DESCENDING CORONARY ARTERY LIGATION	194
A.1	Introduction	194
A.2	Materials	194
A.3	Pre-op	195
A.4	Surgical Procedure	198
A.5	Post-op	201
B	MODULATION OF HUMAN EMBRYONIC STEM CELL FUNCTION IN COLLAGEN PATCHES	202

B.1	Introduction	202
B.2	Materials and Methods	202
B.2.1	Cell Culture	202
B.2.2	Formation of Cell Seeded Collagen Patches	202
B.2.3	Viability Assays	203
B.2.4	Proliferation	203
B.2.5	Assessment of Cell Differentiation	204
B.3	Results	205
B.3.1	Culture of hESCs within Collagen Patches Modulates Proliferation, Differentiations and Viability	205
B.4	Discussion	208
B.5	References	209
C	SECRETION PROFILE FOR B4 PROGENITOR CELLS	210
<u>VITA</u>		212

LIST OF TABLES

Table 2.1: Major human clinical studies involving stem cell therapy for heart failure	35
Table 2.2: Major preclinical studies involving tissue engineering for myocardial repair	48
Table 3.1: Echocardiographic measures of myocardial remodeling and function	85
Table 3.2: Hemodynamic measures of myocardial infarction	86
Table 4.1: Animal accounting for <i>in vivo</i> model of myocardial infarction	117
Table 4.2: Corrected echocardiographic measures after myocardial infarction	133
Table 4.3: Hemodynamic measures after myocardial infarction	134
Table 5.1: Animal accounting for <i>in vivo</i> model of myocardial infarction	160
Table 5.2: Corrected echocardiographic measures after myocardial infarction	163
Table 5.3: Hemodynamic measures after myocardial infarction	164
Table 6.1: Correlation of cell number to improved myocardial function	180

LIST OF FIGURES

Figure 2.1: The flow of blood in the heart	6
Figure 2.2: The cardiac action potential	8
Figure 2.3: Pressure-volume loop from the ventricle of a normal rat	10
Figure 2.4: The pathological progression of myocardial infarction	14
Figure 2.5: Mechanical changes in the infarcted heart	16
Figure 2.6: The standard ECG	17
Figure 2.7: The twelve lead ECG	18
Figure 2.8: Diagnosis of MI using echocardiography	20
Figure 2.9: Translational roadblocks of cellular cardiomyoplasty	40
Figure 2.10: Tissue engineering approaches to address roadblocks	51
Figure 3.1: Apparent cell migration with culture on tissue culture treated plates	67
Figure 3.2: A single freeze/thaw cycle leads to complete loss of viability in cardiac patches	68
Figure 3.3: Overview of induced infarct and patch placement methodology	71
Figure 3.4: Schematic of <i>in vitro</i> hypoxia model	77
Figure 3.5: <i>In vitro</i> characteristics of the cardiac patch	78
Figure 3.6: Remodeling of cardiac patches in culture	79
Figure 3.7: Loss of patch cellularity while in culture	80
Figure 3.8: Trends in hMSC engraftment	81
Figure 3.9: Engraftment of hMSC in infarcted rat heart at 1 week	83
Figure 3.10: Blood vessel density at 4 weeks post-infarction	88
Figure 3.11: Expression of α -SMA in infarcted hearts at 4 weeks	89
Figure 3.12: No change in the extent of fibrosis with cardiac patch application	90
Figure 3.13: Endogenous stem cell recruitment with cardiac patch treatment	91

Figure 3.14: NCM apoptosis with exposure to hMSC conditioned media	92
Figure 3.15: Downregulation of SCN5A transcript levels with exposure to hMSC conditioned media	93
Figure 3.16: Increased CFb presence after exposure to hMSC conditioned media	94
Figure 3.17: Attenuated collagen secretion from CFb exposed to hMSC conditioned media	95
Figure 4.1: Schematic of experiments to test the paracrine effects of hMSC	114
Figure 4.2: Initial seeding density influences cardiac patch cellularity and compaction	119
Figure 4.3: Culture of hMSC in collagen patches attenuates proliferation	120
Figure 4.4: Minimal loss of cell potency after culture in collagen patches	122
Figure 4.5: Viability of hMSC cells in collagen patches	123
Figure 4.6: hMSC secretion profile	126
Figure 4.7: Angiogenic factor gene expression in hMSC	128
Figure 4.8: hMSC conditioned media may support endothelial cell growth/proliferation	130
Figure 4.9: hMSC conditioned media may alter endothelial cell tube formation properties	131
Figure 4.10: No change in infarct size with cardiac patch transplantation	132
Figure 4.11: Application of hMSC patch does not change blood vessel presence	135
Figure 5.1: Proliferation of hMSC and B4 progenitor cells in collagen patches	155
Figure 5.2: No loss of hMSC or B4 progenitor cell potency after culture in collagen patches	156
Figure 5.3: Viability of hMSC and B4 progenitor cells in collagen patches	157
Figure 5.4: Angiogenic growth factor mRNA abundance fold change in hMSC and B4 progenitor cells	159
Figure 5.5: No change in infarct size with cardiac patch transplantation	161
Figure 5.2: Myocardial infarct development after treatment with a cardiac patch	162

Figure 5.6: Application of hMSC patch showed no improvement in neovessel formation	165
Figure 6.1: The five stages	175
Figure B.1: Culture of hESC in collagen patches attenuates proliferation	205
Figure B.2: Culture of hESC in collagen patches modulates potency	206
Figure B.3: Viability of hESC cells in collagen patches	207
Figure C.1: B4 progenitor cell secretion profile	210

LIST OF ABBREVIATIONS

ANG	Angiogenin
α -SMA	alpha-Smooth Muscle Actin
ATP	Adenosine Triphosphate
BSA	Bovine Serum Albumin
cDNA	Complementary Deoxyribonucleic Acid
CFb	Cardiac Fibroblast
CHF	Congestive Heart Failure
Cx43	Connexin 43
DAPI	4', 6-diamidino-2-phenylindole
DMEM	Dulbecco's Modified Eagle's Medium
DNA	Deoxyribonucleic Acid
ECG	Electrocardiography
ECHO	Echocardiography
ECM	Extracellular Matrix
EDP	End Diastolic Pressure
EdU	5-ethynyl-2'-deoxyuridine
ELISA	Enzyme-Linked Immunosorbent Assay
FBS	Fetal Bovine Serum
FGF-a	Fibroblast Growth Factor-acidic
FGF-b	Fibroblast Growth Factor-basic
FITC	Fluorescein Isothiocyanate
HCl	Hydrochloric Acid
hESC	Human Embryonic Stem Cell

hESC-MC/B4	Human Embryonic Stem Cell derived Mesenchymal Cell
HF	Heart Failure
HIF-1 α	Hypoxia Inducible Factor-1 alpha
HLA	Human Leukocyte Antigen
hMSC	Human Mesenchymal Stem Cell
IC	Intracoronary
IgG	Immunoglobulin
IHC	Immunohistochemistry
IL-6	Interleukin 6
IL-8	Interleukin 8
IM	Intramuscular
IRC	Intravenous Retrograde Intracoronary
LAD	Left Anterior Descending (Coronary Artery)
LV	Left Ventricle
MI	Myocardial Infarction
MM	Maintenance Media
MMP	Matrix Metalloproteinase
MSC	Mesenchymal Stem Cell
MTT	3-(4,5-Dimethylthiazol-2-yl)-2,5-diphenyltetrazolium bromide
NCM	Neonatal Cardiomyocyte
NV	Non-viable
OCT	Optimal Cutting Temperature
Oct 3/4	Octomer –binding transcription factor 3/4
PBS	Phosphate Buffered Saline
PCR	Polymerase Chain Reaction

R18s	Ribosomal Protein 18s
RLP13A	Ribosomal Protein 13A
RAS	Renin Angiotensin System
RNA	Ribonucleic Acid
RT-PCR	Reverse Transcription Polymerase Chain Reaction
SDF-1	Stromal Derived Factor-1
SERCA	Sarcoendoplasmic reticulum calcium ATPase
SSEA4	Stage Specific Embryonic Antigen 4
TE	Tissue Engineering
TIMP	Tissue Inhibitor of Metalloproteinase
TNF- α	Tissue Necrosis Factor-alpha
TnT	Troponin T
TUNEL	Terminal Deoxynucleotidyl Transferase mediated dUTP Nick End Labeling
VEGF	Vascular Endothelial Growth Factor

SUMMARY

Heart failure accounts for more deaths in the United States than any other pathology. Unfortunately, repairing the heart after pathological injury has become an overwhelming task for physicians and researchers to overcome. Fortunately, cellular cardiomyoplasty has emerged as a promising solution for sufferers of heart failure. Such a therapy is limited in efficacy due to poor engraftment efficiencies, however. To address this issue, we have developed a tissue engineered vehicle for cell delivery. Use of a “cardiac patch” resulted in localized and efficient delivery of human mesenchymal stem cells (hMSC) to infarcted myocardium. Application of a cardiac patch also attenuated adverse remodeling. Additionally, the culture of stem/progenitor cells within three dimensional collagen constructs led to modulations in cell function, which did not promote enhanced angiogenesis *in vitro* or *in vivo*. Despite enhanced neovessel formation, hMSC patches were more beneficial at augmenting myocardial repair compared to directly injected hMSC. Lastly, although hMSC represent an effective cell source option for enhancing cardiac repair they require additional purification and expansion steps which inherently delay the turnover before treatment. Therefore, suitable cell alternative are being sought. Human embryonic stem cell derived mesenchymal (B4) cells display several phenotypic similarities to hMSC. B4 progenitor cell responded similarly to hMSC in 3D culture. In addition B4 progenitor cell patch application to infarcted myocardium resulted in similar indices of repair compared to hMSC. Thus, a tissue engineering approach represents an effective cell delivery strategy and induces modulations in cell function which may demonstrate pathological significance.

Chapter 1

Introduction

Myocardial infarction (MI) is the death of heart muscle that results from impaired perfusion. Approximately 16.8 million American adults suffer from coronary heart disease, a common cause of MI. In addition, it is expected that over 151,000 individuals will die from severe MI, even with modern advances in devices and pharmaceuticals. Current research efforts involve replacing lost myocardial cells (due to MI) with other functional cells that act to restore contractile function or provide paracrine factors to enhance healing. In particular, fibroblasts, smooth muscle cells, skeletal myoblasts, bone marrow stem cells, and embryonic stem cells have been transplanted into infarcted myocardium. Typical approaches used to deliver cells to an infarcted heart include direct epicardial or endocardial injection, intravenous (IV), intracoronary (IC), and retrograde IC injection. Direct injection methods result in inhomogeneous cell delivery or washout of cells into vascular shunts, however. Additionally, IV and IC methods suffer from the failure of cells to reach the target area. The following thesis will provide evidence that a tissue engineered approach to cell delivery will help attenuate such limitations. We hypothesize that tissue engineered constructs will help to localize more cells in the damaged region, thus improving overall cardiac function after infarction.

Specific Aim I

The application of tissue engineering practices for cell delivery is not a novel concept. Translating this approach for cardiac repair however, does offer a unique approach to cellular cardiomyoplasty. Initially we set out to provide a “Proof of Concept” that tissue engineering could be used to deliver human mesenchymal stem cells to

infarcted myocardium. We also set out to demonstrate that engraftment would be relatively high with this approach.

Specific Aim: Determine the suitability of cell delivery using a collagen hydrogel disk embedded with human mesenchymal stem cells to infarcted heart.

Hypothesis: Tissue engineered cellularized vehicles can be used to efficiently deliver human mesenchymal stem cells to infarcted heart.

Specific Aim II

With conventional methods of delivery such as direct or IV injection, cells are grown as a monolayer before injection into the host. With a TE approach, cell delivery is achieved by applying a cellularized collagen patch onto the epicardial surface of the heart. These changes in culture configuration have the possibility of affecting cell function in numerous ways. Such changes in cell function can lead to downstream consequences which may promote or attenuate potential reparative mechanisms involved in cellular cardiomyoplasty. Thus we set out to investigate modulations in cell function due to culture in collagen patches. Two cell types were used in these studies: human mesenchymal stem cells (Chapter 4) and B4 progenitor cells (Chapter 5). Both cell types are thought to have cardiomyoplastic potential.

Specific Aim: Investigate how progenitor/stem cell function can be modulated through culture in collagen hydrogels.

Hypothesis: Culture of progenitor/stem cells within collagen gels will modulate cellular viability, proliferation, differentiation and secretory profiles compared to cells cultured as monolayer.

Specific Aim III

Our initial “Proof of Concept” experiments provided much insight as to how to optimize future experiments investigating tissue engineered approaches to cell delivery. Firstly, we changed from an immunocompetent animal model to an immunocompromised animal model. Ideally, this would provide for longer engraftment of human progenitor/stem cells. Additionally, the cardiac patch was slightly modified by lowering the initial seeding density. This effectively reduced cell crowding and was thought to also enhance long term viability. With these changes in place, we conducted a comparison of direct myocardial injection and cardiac patch cell delivery using human mesenchymal stem cells in an *in vivo* model for myocardial infarction (Chapter 4).

Specific Aim: Compare the efficacy of a tissue engineered approach to cell delivery to a direct injection approach on cardiac function.

Hypothesis: Localized delivery of a modest number of hMSC using cellularized collagen constructs will enhance global cardiac function and myocardial remodeling compared to delivery via direct injection.

Specific Aim IV

Human mesenchymal stem cells are a viable cell source for cellular cardiomyoplasty because they are easily maintained and have been implicated in several potential reparative mechanisms to heart failure (including cardiac/vascular cell differentiation and secretion of trophic factors). Although these properties are attractive, the time needed to purify and scale up mesenchymal stem cell production may lead to delayed treatment for severely ill patients in the clinic. Fortunately, a human embryonic stem cell derived mesenchymal stem cell has recently become available. The use of these cells could potentially eliminate the need for scale up and offer “off the shelf” availability of a cardiac cell therapy. These cells, termed human embryonic stem cell derived mesenchymal cells (referred to as B4 progenitor cells throughout the study),

were tested *in vitro* and *in vivo* model of myocardial infarction to determine their suitability and effectiveness for cellular cardiomyoplasty (Chapter 5).

Specific Aim: Explore the extent of cardiac repair and remodeling with the use of B4 progenitor cells delivered within tissue engineered constructs.

Hypothesis: Similar indices of myocardial improvement will be presented upon delivery of B4 progenitor cells to infarcted heart when compared to human mesenchymal stem cells.

Chapter 2

Background

2.1 A BREIF DISSCUSSION ON THE ANATOMY AND PHYSIOLOGY OF THE HEART

The human heart is a mechanical pump that facilitates the delivery of oxygen, biochemical molecules and blood cells to all vascularized tissues of the body. It achieves such delivery with the help of a vast vessel network. The human heart is composed of four chambers: two atrium and two ventricles. Associated with each chamber is a valve that aids in controlling the flow of blood in the systemic and pulmonary circulation. Under normal conditions, blood enters the heart from the vena cava into the right atria. Next, blood travels through the tricuspid valve into the right ventricle where it is sent through the pulmonic valve into the lung. While in the lung circulation, blood is re-oxygenated (heme groups in hemoglobin of erythrocytes bind oxygen) and returns to the left atrium. Blood then enters the left ventricle through the mitral valve. Once the pressure within the left ventricle exceeds that across the aortic valve, blood is ejected from the left ventricle into the systemic circulation (Figure 2.1).

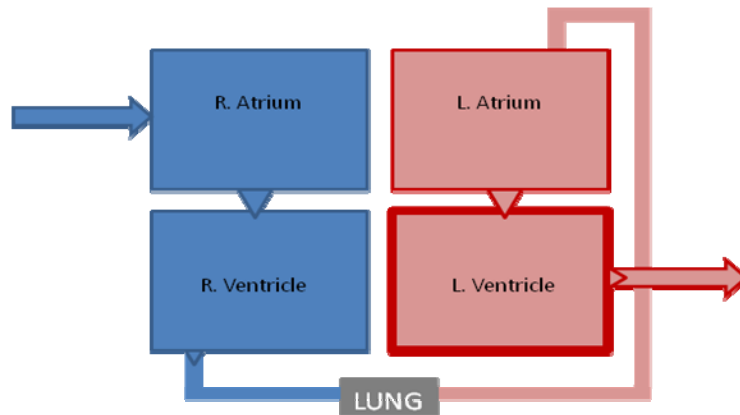


Figure 2.1) The flow of blood in the heart. Blood returns to the right (blue) side of the heart. This blood, which has diminished oxygen content, flows to the lung to bind more oxygen and returns to the left side of the heart (red). After entering the thick-walled left ventricle blood is ejected into the systemic circulation.

Several cell types found in the heart contribute to its overall function. These include working myocytes, Purkinje fibers, nodal cells, fibroblasts, endothelial cells, vascular smooth muscle cells and squamous cells (which line the endocardium and epicardium). The bulk of work produced by the heart is the result of active working myocytes. These cells are found in both the atria and ventricles and contain a contractile apparatus made of an array of sarcomeres. Located within the sarcomeres are thick (myosin and titin) and thin (actin, tropomyosin and troponin proteins) filaments. It is the interaction of these filaments which dictates the extent of force produced by a working myocyte. In general, as the overlap of myosin and actin increases, the generated tension also increases. This positive correlation does diminish, however, as the overlap continues to increase and the sarcomere length falls below $1.65 \mu\text{m}$ in humans. The collection of sarcomeres forms myofibrils which account for over 47% of the volume of myocytes. Mitochondria (36%), sarcoplasmic reticulum (3.5%) and nuclei (2%) occupy most of the remaining volume. Surrounding each myocyte is a sarcolemma which acts to separate the intracellular and extracellular environments. A system of transverse tubules emanates from the sarcolemma and helps to relay electrochemical

signals throughout the interior of the cell. Myocytes interact with each other via specialized junctions called intercalated discs. These structures allow for mechanical and electrical communication between cells.

The heart is innervated with both sympathetic and parasympathetic nerves which act to control the automaticity, rhythmicity and contractile properties of the heart. Excitation-contraction coupling mediates the translation of electrical impulses into mechanical work. This is mediated by Ca^{2+} -induced Ca^{2+} release from the sarcoplasmic reticulum. The propagation of an action potential initiates these cycles. This action potential is determined by the timed opening and closing of specific ion channels and is divided into 5 major phases (Figure 2.2). During phase 0, sodium channels (hH1 encoded by SCN5A) open, and there is a rapid depolarization event. This causes the membrane potential to depolarize from -90mV to +20mV. Ion flux is driven by an electrochemical gradient (I_{Na}). During phase 1, there is early repolarization caused by a transient outward current of potassium ions (I_{KR}). Repolarization does not complete, however, because of competing inward calcium currents through voltage gated L-type calcium ion channels (I_{Ca}). This balance of inward and outward currents leads to a plateau phase (phase 2). It is this influx of calcium ions which triggers sarcoplasmic reticulum Ca^{2+} release. When the efflux of potassium ions is greater than the influx of calcium ions, repolarization accelerates (phase 3). This process is typically mediated by delayed outward rectifying and inward rectifying potassium currents (I_{KS}). Eventually, rapid repolarization will occur as the inward rectifier current becomes active (I_{KI}). During phase 4 the sodium and calcium ions which entered the cell at earlier phases are ejected through ion-specific exchangers and pumps and the baseline membrane potential is restored.

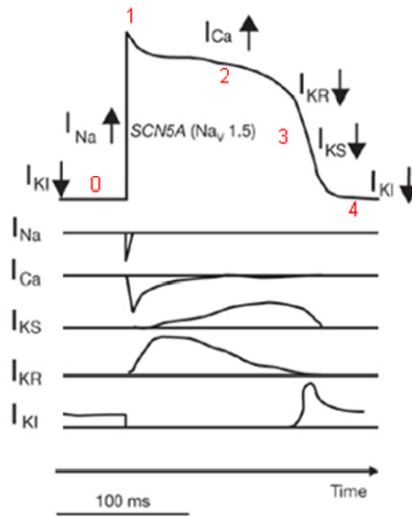


Figure 2.2) The cardiac action potential. The cardiac action potential can be divided into 5 phases (0-4). Each phase represents the well timed process of ion channel opening and closing that creates small currents. These currents allow for changes in membrane potential and action potential propagation. Adapted from *Nature Cell Biology* 2004. 6:1039 - 1047.

As discussed above, the cardiac action potential stimulates the opening of voltage gated L-type calcium ion channels. These “long-lasting” channels allow a relatively small influx of calcium ions to enter the cell. These calcium ions bind to calcium release channels (ryanodine receptors) in the sarcoplasmic reticulum. Interestingly, L-type calcium channels in the sarcolemma and calcium release channels in the sarcoplasmic reticulum are in close proximity as dyad structures, minimizing the diffusion distance. Once extracellular calcium ions bind to the calcium release channel, a surge of calcium is released into the cytosolic space. This level of internal calcium concentration allows for calcium binding to troponin C, a regulatory protein found in thin filaments of myofibrils. Upon binding to troponin C, a conformation change of the troponin complex displaces tropomyosin from the actin binding site for myosin. At this point, myosin can bind actin and initiate shortening of sarcomeres (contraction) in an ATP-dependent process. Afterwards, calcium is returned to the sarcoplasmic reticulum by the sarcoendoplasmic reticulum calcium pump ATPase (SERCA) and residual

calcium is ejected from the cytosol into the extracellular space by a sodium-calcium exchanger and the P-type plasma membrane calcium pump. This process occurs in each individual ventricular myocyte. When cells act together in a pseudo-anatomical syncytium, work can be performed to supply the entire body with a sufficient blood supply.

Within the left ventricle, the heart undergoes what is known as the cardiac cycle. The cycle involves isovolumic phases, ejection (systole), and filling (diastole). During the cardiac cycle, blood enters the left ventricle through the mitral valve from the left atrium. This rapid filling phase steadily increases the volume of blood in the ventricle as the pressure in both the atria and ventricle slightly decreases. Next, the filling rate declines (diastasis) as the ventricular, venous and atrial pressures increase slightly. Such pressures result from preload tensions produced within the ventricular wall as it is stressed. After a brief contraction of the atrium, the mitral valve closes and isovolumic contraction occurs in which the pressure within the ventricle rises to near that of the aorta. When the pressure within the ventricle is above the pressure across the aortic valve, the valve opens and blood flows into the systemic circulation. Normally about 50-75% of blood in the ventricular chamber is ejected across the aortic valve with each cycle. After ejection, onset of isovolumic relaxation occurs in which the pressure within the ventricle returns to basal levels before filling repeats. Often the cardiac cycle is represented by pressure-volume (P-V) loops (Figure 2.3).

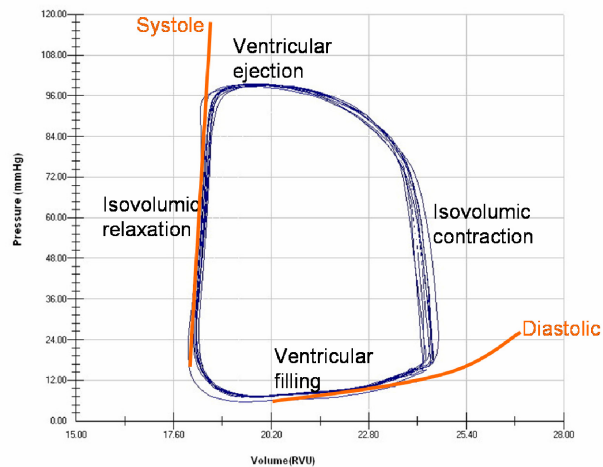


Figure 2.3) Pressure-Volume loop from ventricle of normal rat. The cardiac cycle can be represented via a pressure-volume loop. Stages of isovolumic contraction and relaxation, filling and ejection make up this cycle and contribute to the systolic and diastolic properties of the heart.

Abnormal heart function can be the result of problems with ejection (systole), relaxation (diastole), or arrhythmias. As these abnormalities progress, patients experience symptoms of congestive heart failure (CHF).

2.2 EPIDEMIOLOGY AND ETIOLOGY OF HEART FAILURE

CHF is the leading cause of death in the Western world. It is estimated that as many as 4.9 million people suffer from this disease in the U.S. with 550,000 new cases emerging each year. Additionally, approximately \$27.9 billion per year is spent on more than 900,000 hospitalizations related to CHF annually. Several studies have been undertaken to determine the incidence and prevalence of the disease. The Framingham Heart Study indicated that the prevalence of heart failure increased with age from 1% in individuals aged 50-59 to 10% in individuals aged 80-89 [1]. In addition, the annual incidence also increased with age from 0.4% in individuals aged 45-54 to 4% in individuals aged 85-94.

The Framingham Heart Study first suggested that the majority of CHF events were a result of hypertension. More recent data from the “Studies of Left Ventricular Dysfunction” (SOLVD) study indicates that over 70% of people with CHF have coronary artery disease as the underlying etiology [2]. The SOLVD study was specifically designed such that the majority of patients have ventricular dysfunction or congestive heart disease (CHD). For instance, in the Framingham Heart Study, 76% of men had a predisposition to hypertension while only 46% had coronary heart disease. The SOLVD study, however, included a patient population where 70% were predisposed to some form of ischemic heart disease and 7% were hypertensive [2]. Regardless of the underlying etiology, CHF occurs because of 1) mechanical abnormalities, 2) myocardial failure, 3) arrhythmias or a combination of these processes.

One underlying etiology of CHF is myocardial infarction (MI). MI is the death of heart muscle that results when the heart's blood supply is impaired. The myocardium does not regenerate itself like other organs in our body because it lacks the sizable pool of endogenous progenitor cells, and because adult cardiac muscle cells are not capable of extensive proliferation. Therefore, the dead tissue is replaced with fibrous scar tissue and the left ventricle dilates. MI is generally a result of atherosclerosis; a disease characterized by the formation of fibrofatty plaques in the coronary arteries accelerated by hypertension, diabetes mellitus, and/or hypercholesterolemia. MI results when there is impairment of perfusion of the myocardial tissue typically mediated by thrombus formation. Just like CHF, the prevalence and incidence of MI related deaths increases with age, peaking between 35-64 in men and 80-89 in women. Men are generally more prone to MI than are women.[3] Increased risk of MI is associated with smoking, use of oral contraceptives, lack of exercise, and stress.

2.3 MYOCARDIAL INFARCTION (MI)

MI typically leads to mechanical abnormalities, myocardial failure and arrhythmias. When the demand for blood exceeds the perfusion of blood a sequence of events begins which can ultimately lead to heart failure. The first event is known as “angina pectoris” or chest pain that is caused by ischemia. With time, acute ischemia within the myocardium leads to no contractile function. Depending on the extent of impaired perfusion, a subendocardial or transmural infarct can develop. Subendocardial infarcts occur on the endocardial side of the myocardial wall leaving healthy or hibernating myocardium towards the epicardium. A subendocardial infarct will develop first because the endocardium has a higher metabolic demand but decreased perfusion. A transmural infarct, however, occurs throughout the myocardial wall stretching from endocardium to epicardium and results from thrombosis or vasospasm of the major coronary arteries (left anterior descending, right coronary, and left circumflex coronary artery).

Most infarctions involve the left ventricle because it is more highly perfused than the right ventricle. The most apparent gross morphological change of an infarcted area is the color (grayish brown). Typically pallor occurs within twenty-four hours after an infarct in humans. This change in color is also apparent in small animals (purple-pink), occurring within minutes after induced infarction. By the fourth day after MI in humans, the border of the infarct becomes more apparent and the infarct itself begins to change to a yellow-brown color. By day ten, the peri-infarct region is bright red (due to the high vascularity) and the infarct is yellow and soft because of a progressive fatty change. By six weeks the infarct will contain fibrous and vascularized scar tissue.

In addition to gross morphological changes, several microscopic changes occur. The first noticeable change is termed coagulative necrosis. During this process, cross

striations of the cells as well as their nuclei begin to disappear (pyknosis). Also, the cytoplasm becomes granular as eosinophilia develops and cells begin to condense. By forty-eight hours hemorrhagic exudate leads to the accumulation of neutrophils and eventual myofibrosis. Eventually the neutrophils become replaced by macrophages and the cytoplasm of necrotic cells accumulates fat. Over time, necrotic cells will be phagocytosed by scavenging macrophages and a fibrovascular response will occur. During this time there is marked in-growth of neo-vessels and fibroblasts. These changes in morphology have many functional consequences that ultimately lead to heart failure (Figure 2.4).

The onset of cardiac ischemia typically reflects a lack of (or diminished) blood perfusion in the myocardium. This gives rise to reduced oxygen tensions which ultimately affect the energetic output of cardiomyocytes. The lack of oxygen halts the process of oxidative phosphorylation and thus aerobic respiration shuts down. This results in decreased adenosine triphosphate (ATP) production and reduced ATP hydrolysis. Reduced ATP levels lead to abnormalities in several ATP-dependent processes including actin-myosin interactions (physiologic response: negatively lusitropic), calcium channels (physiologic response: negatively inotropic), P-Type plasma membrane calcium pump (physiologic response: negatively lusitropic), SERCA (physiologic response: negatively lusitropic), sodium-calcium exchangers (physiologic response: negatively lusitropic) and Ryanodine receptors (physiologic response: negatively inotropic). The halting of aerobic respiration puts increased strain on the anaerobic process of glycolysis to deliver the myocyte's energy content. Eventually, falling glucose and glycogen content ceases any energetic output. Ischemia also gives rise to acidosis (due to lactic acid and inorganic phosphate build up) and cellular depolarization (which can inactivate sodium channels and is due to potassium efflux).

All of these events constrain normal cardiac function. This results in slow conduction, irritable ectopic foci and mechanical failure which are the features for heart failure.

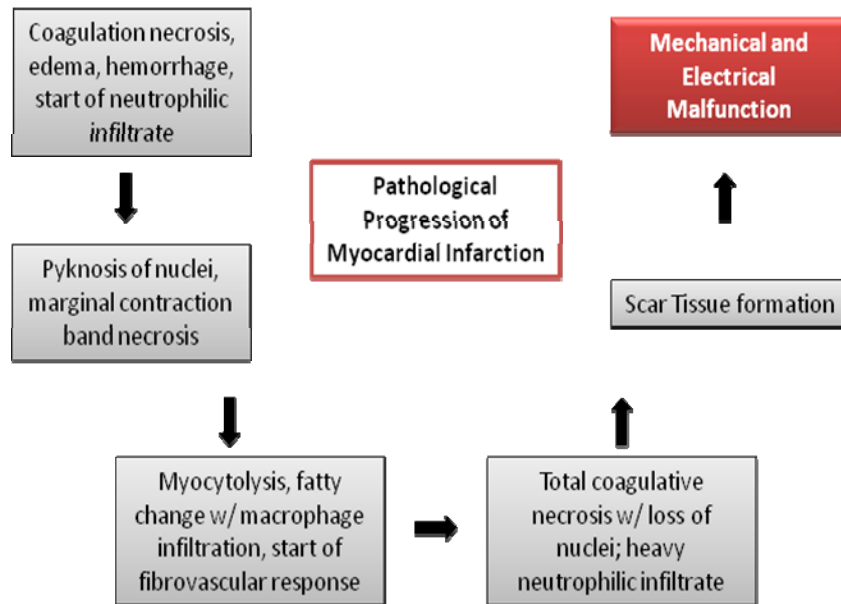


Figure 2.4) The pathological progression of myocardial infarction. MI proceeds as a series of events which include gross morphological, cellular and metabolic changes. Cellular necrosis due to ischemia gives rise to macrophage and neutrophil infiltration. Ultimately, scar tissue is formed which leads to mechanical and electrical malfunction.

The process of MI can be broken into four phases: acute ischemia, necrosis, fibrosis and remodeling. Each phase has a distinct effect on the mechanical properties and function of the infarcted myocardium. Acute ischemia occurs within hours after the impaired perfusion of a coronary artery. During this time oxygen tension steadily decreases and what was once active, contracting myocardium becomes flaccid. At this point the affected myocardium has mechanical properties which are similar to passive constitutive (elastic) myocardium although matrix associated proteins and collagen content decrease. Thus, the myocardium retains its diastolic properties, however the systolic properties are severely impaired (Figure 2.5; Holmes et al). Within 24 hours of chronic coronary artery stenosis, necrosis of the native myocardium begins to occur within the infarcted segment of the heart. During this time matrix metalloproteinase

activity increases, disrupting the extracellular matrix (ECM) composition and cardiomyocytes lose viability. Despite the reduction in cell density and ECM proteins the infarct area does stiffen over time during this phase. It is thought that interstitial edema contributes to this increase in elastic modulus and may help prevent infarct rupture during this critical stage. During the fibrotic stage the infarct area is infiltrated with fibroblasts and new collagen is deposited. The increase in anisotropic collagen stiffens the infarcted area over a period of several weeks. Unfortunately, this increase in chamber stiffness impairs both chamber filling and systolic function of neighboring (non-infarcted) tissue. Lastly, remodeling occurs when the mechanical properties of the infarcted heart are no longer determined by the collagen content (i.e. fibrotic phase). Although the collagen content may continue to increase during remodeling, stiffness drops. This has to do with the degree of collagen cross-linking which occurs during the remodeling phase. Typically LV dilation occurs during this phase as wall stress increases over each cardiac cycle. This occurs because the limited systolic function the heart has to offer reduces the cardiac output and stroke volume. Thus more volume is left in the LV chamber at end diastole which imparts increased wall stress on the LV wall (wall stress = $PR / 2T$; where P is pressure, R is radius of chamber, T is wall thickness). This leads to thinning of the infarcted wall segment.

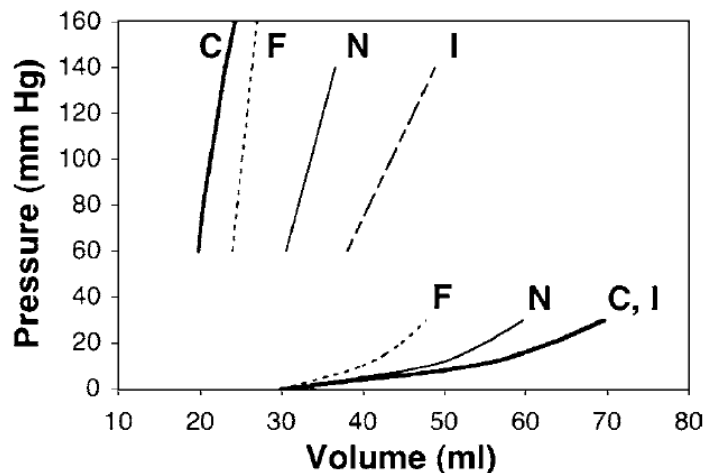


Figure 2.5) Mechanical changes in the infarcted heart. Myocardial infarction leads to pressure-volume changes as MI develops. Control (C), Acute Ischemia (I), Nectrotic (N), and Fibrotic (F) hearts display differences in diastolic and systolic function. Adapted from, *Annu. Rev. Biomed. Eng.* 2005. 7:223–53.

2.4 DIAGNOSIS OF MYOCARDIAL INFARCTION

2.4.1 The Electrocardiogram (ECG)

The typical twelve lead ECG consist of three limb leads, three augmented limb leads and six chest leads. The twelve lead ECG give a concise and non-invasive assessment of cardiac rhythm function. In general, ECG leads measure the flow of positive ions during the cardiac cycle. Positive ions that flow toward the lead gives an upward deflection while those that flow away from the lead create a downward deflection. The typical ECG waveform is composed of several parts including the P-wave, QRS complex and T-wave (Figure 2.6).

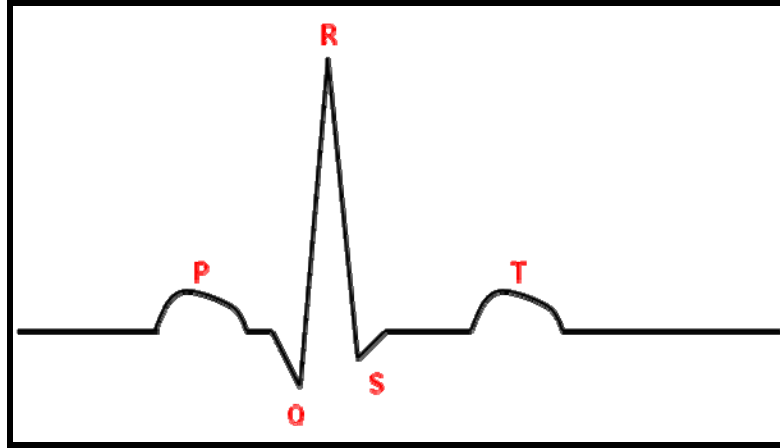


Figure 2.6) The standard ECG waveform. The ECG is composed of several parts including a P-wave, QRS complex and T-wave. The figure represents a generic ECG although depending on the axis of depolarization, other patterns may exist. This includes inverted QRS complexes or very large (non-pathological) Q-waves.

The P-wave reflects atrial contraction. The QRS complex reflects ventricular contraction. The T-wave reflects ventricular repolarization. Normal tracings for the twelve lead ECG are shown in Figure 2.7. After the onset of myocardial infarction, acute ischemia gives rise to reduced free energy and subsequent myocardial death. This creates an electrical void which can be detected with the ECG. Acute changes include ST segment elevation and depressed QRS amplitude. The ECG of well developed myocardial infarcts evolves to generate significant Q waves and T-wave inversion (although this can also be an acute characterization). ST-segment elevation may also persist if a transmural infarct develops.

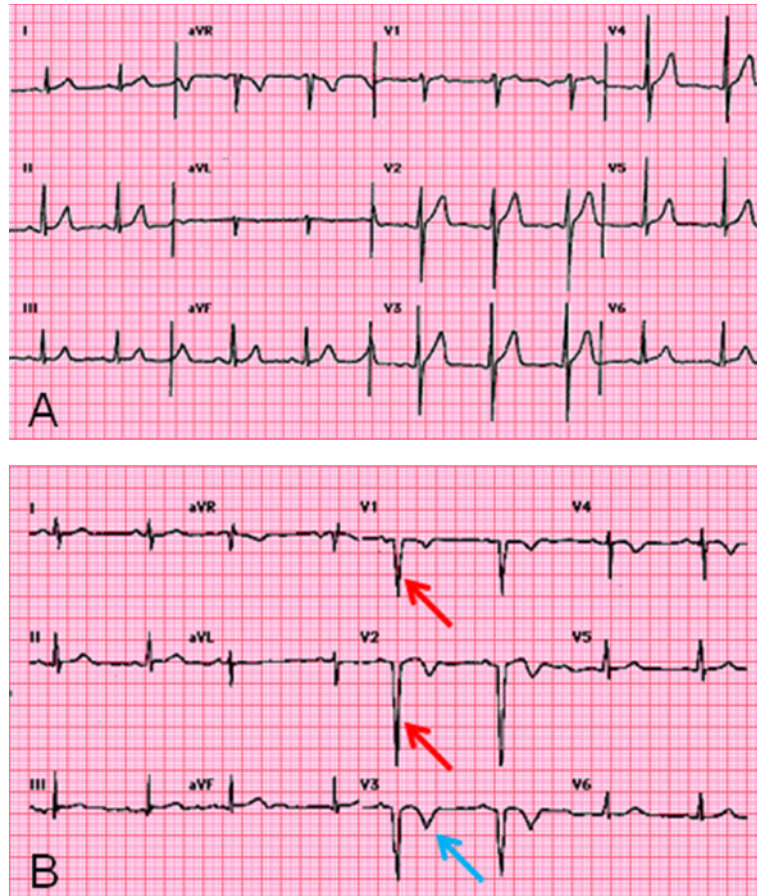


Figure 2.7) The twelve lead ECG. A) A normal twelve lead ECG taken from a healthy patient. B) A twelve lead ECG taken from a patient with an old anterior infarct. The appearance of significant Q-waves (red arrows) and T-wave inversion (blue arrow) signifies necrotic or infarcted myocardium. Adapted from www.uptodate.com.

2.4.2 Echocardiography

Ultrasound is a versatile non-invasive technique which relies on the propagation, scatter and detection of sound waves in anatomical structures. Ultrasonic study intended to visualize the heart is referred to as echocardiography. In general, piezoelectric materials capable of producing electric currents through conformational changes are used to generate ultrasounds. These materials can also detect scattered or reflected ultrasounds (echos). Echo detection causes a conformation change in the piezoelectric material and gives rise to an electric current which can be processed as an

analog signal. Echocardiography can be used for B-mode two-dimensional images, M-Mode one-dimensional motion analysis and Doppler analysis, all of which play a vital role in the analysis of cardiac function. B-mode in conjunction with M-mode can be used to measure ventricular dimensions, volume and fractional shortening. Doppler can be used to measure hemodynamic-related parameters such as mitral valve function, stroke volume and cardiac output. Doppler relies on the frequency components of generated (F_0) and detected (F_d) ultrasounds to measure an apparent velocity or V ($F_d = (2F_0/C) * V\cos\theta$). After the onset of myocardial infarction, echocardiography will reveal ventricular dilation, ventricular wall thinning, reduced fractional shortening and attenuated hemodynamic measures compared to normal heart (Figure 2.8).

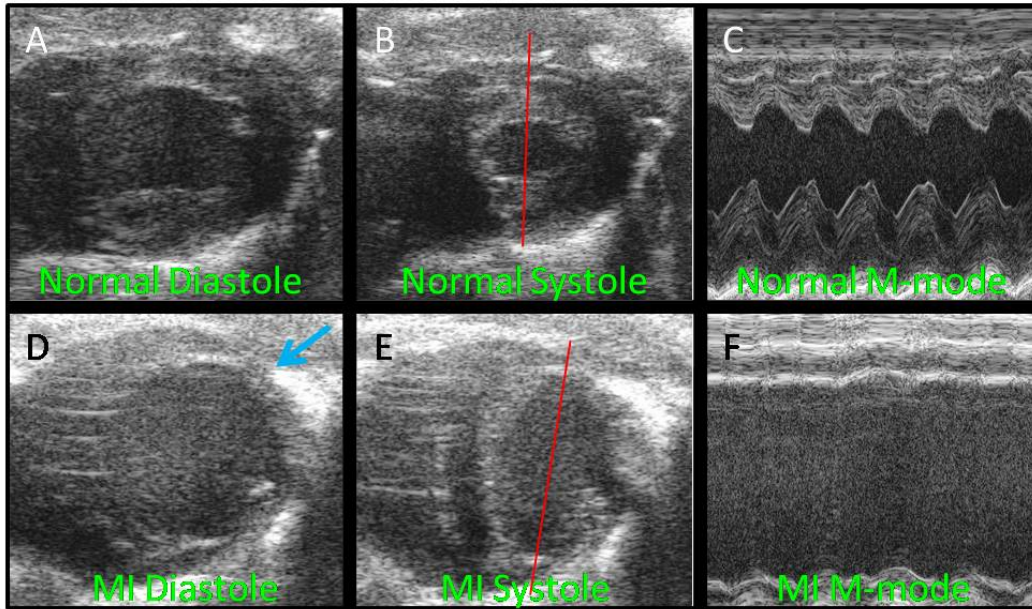


Figure 2.8) Diagnosis of MI using echocardiography. Normal cardiac function is represented by myocardial thickening during a complete cycle which includes diastole (A) and systole (B). B-mode images are acquired as a short axis view at the mid-papillary level. Cardiac measurements can be made by looking along a single line through the ventricle (Red line shown in B and E). This produces an M-mode view where chamber dimensions and function can be assessed and calculated. Infarcted myocardium displays little systolic function during the cardiac cycle (D and E). This loss of function is also apparent in M-mode (F). Images acquired by author using Vevo 770 Ultrasound Unit from Visual Sonics (Toronto, Canada).

2.5 CURRENT TREATMENT OPTIONS AND LIMITATIONS

2.5.1 Drug Therapies

The current clinical approaches to treating heart failure are pharmaceuticals and/or surgery. One common class of drugs is diuretics. When the heart begins to fail (decreased cardiac output and subsequent decrease in circulating blood volume), a compensatory neurohormonal response is elicited in which the circulating renin-angiotensin system (RAS) is activated. In addition to heightened sympathetic nervous activity, the RAS acts by increasing the amount of circulating angiotensin II, a potent vasoconstrictor, as well as atrial natriuretic peptide, aldosterone and vasopressin. The increase in activity of these circulating compounds leads to arterial and venous vasoconstriction, increased tubular sodium reabsorption due to decreased renal perfusion and eventual increases in blood volume. Although these actions appear to compensate for the failing heart, they also aggravate failure by increasing atrial and ventricular preload and afterload and increasing intracardiac and intravascular congestion and edema. Diuretics act by eliminating intravascular congestion and thus aid in the removal of water and salt from blood vessels. Extensive use of diuretics, however, can lead to hypokalemia (potassium deficiency) and ventricular arrhythmias. In addition, steroid glycoside compounds such as digitalis have been used as drug therapy for arrhythmias in the setting of congestive heart failure. Digitalis acts as a positive inotropic (contraction) agent by inhibiting the actions of the sodium-potassium ATPase pump. In doing so, intracellular sodium increases and is later exchanged for extracellular calcium via the sodium-calcium exchanger (see above). The increase in calcium leads to heightened contractility. Digitalis also results in vasodilation, diuresis, reduction of circulating neurohormones, slowing of rapid ventricular rate, and increased baroreceptor sensitivity. If digitalis is not effectively removed from circulation, however,

it can become toxic and lead to deficiencies of many electrolytes, hypothyroidism, and renal failure.

Another drug class used in heart failure is the angiotensin-converting enzyme (ACE) inhibitors. These drugs act by inhibiting the enzyme responsible for converting the decapeptide angiotensin I to the octapeptide, vasoconstrictor angiotensin II. Thus the effect of ACE inhibitors is vasodilation of constricted vessels mediated by the RAS. ACE inhibitors also reduce plasma norepinephrine levels which decreases sympathetic nervous activity. ACE inhibitors, however, can also lead to hypotension and angioedema. Finally, β -adrenergic blockers act at β -receptors and are a class of drugs that act by reducing the synthesis of cyclic AMP and reducing pacemaker activity. They have proven benefit in decreasing the heart's energy demand and risk for tachycardia and other arrhythmias. Unfortunately, the decrease in adrenergic activity also leads to decreased cardiac output.

Thus, current pharmaceutical therapies have focused on restoring and enhancing inotropic function, reducing congestion, and decreasing α -adrenergic stimulation, but such approaches are not able to prevent remodeling and are associated with several negative side effects.

2.5.2 Surgical Options

In addition to pharmaceuticals, several surgical options have emerged to treat the failing heart. These include left ventricular assist devices, which augment cardiac output, implanted defibrillators, which attempt to combat the occurrence of arrhythmias, percutaneous coronary intervention, which removes stenosis in diseased coronary arteries, coronary bypass surgery and heart transplants. Except for heart transplants, no treatments are able to fully restore cardiac function. Heart transplants require a matched donor (heart size and blood group), and the number of hearts available is significantly

lower than the number of patients who require this procedure. Recently, cell based methods of heart repair have been established which attempt to regenerate lost myocardium after ischemic events.

2.5.3 Cellular Cardiomyoplasty as a Potential Treatment

Regenerative medicine has emerged as a strategy to repair myocardial damage after injury. This strategy, called cellular cardiomyoplasty, involves transplanting cells into injured myocardium to assist in the repair and restoration of myocardial function. In particular, stem cells have gained much attention over the past decade because of their ability to differentiate into cardiomyocytes as well as provide trophic factors to assist in the repair of an injured heart. Translating this approach into the clinical realm has proven to be difficult, however. Questions have arisen regarding cell source, stem cell fate once transplanted, and cell delivery and site of delivery strategies.

2.6 A CRITICAL REVIEW ON THE STATE OF PROGENITOR CELL CARDIOMYOPLASTY

2.6.1 Cell Sources for Cardiomyoplasty

In order to achieve successful clinical translation of cellular cardiomyoplasty, a cell capable of improving cardiac function without induction of adverse consequences must be identified. One elegantly simple solution would be exogenous cardiomyocytes. Several preclinical studies have been undertaken to show the potential of these cells in restoring cardiac function after infarction. In particular, Koh et al. demonstrated that mouse AT-1 cardiomyocytes (derived by expressing an atrial natriuretic factor-simian virus 40 T antigen fusion gene) were able to survive up to four months and proliferate when injected into normal mouse myocardium [4]. The ability of these cells to survive suggests that cardiomyocytes may provide a useful platform for cardiac therapy.

Additional studies showed that injection of rat fetal ventricular cells into infarcted rat myocardium resulted in reduced scar formation and improved systolic pressure over eight weeks [5]. A study comparing rat fetal cardiomyocytes, rat smooth muscle cells, and rat fibroblast concluded that the contractile potential of a cell (cardiomyocytes > smooth muscle cell > fibroblast) determined the extent of improved muscle function in infarcted rat hearts [6]. Although these studies are promising, successful translation has been difficult given the inability of obtaining large numbers of primary cardiomyocytes (adult or neonatal) and immunological limitations.

The choice of progenitor cell is more challenging than comparing cardiomyocytes and carries additional potential complications. After the onset of myocardial infarction and other cardiomyopathies, fibroblast infiltration gives rise to collagen deposition [7]. This increase in fibrosis leads to changes in the mechanical properties of the muscle and usually is associated with reduced myocardial performance [8]. An ideal cell for cardiomyoplasty might reduce cardiac fibrosis and migrate to areas of myocardial damage to induce a favorable effect. Other desirable characteristics might include the ability to promote endogenous cardiomyocyte proliferation or to differentiate into working cardiomyocytes. Thus, a suitable cell might provide a therapeutic scaffold for myocardial repair and preservation by stimulating endogenous cardiac progenitors to proliferate and migrate to areas of myocardial injury, or by production of trophic factors. Whatever the mechanism of benefit, a suitable cell would have to be free from significant adverse effects such as arrhythmias, tumor formation or aberrant differentiation.

Unfortunately, no known cell exists which demonstrates all of these properties, and the notion of engineering suitable cells seems decades away. Several progenitor cells do provide many desirable traits, however. The selection is vast and continues to grow as new progenitor cells are characterized. These cells may hold the key to successful cellular cardiomyoplasty. Many progenitor cells have already been tested in

preclinical and clinical studies and in most cases a beneficial effect was observed, at least transiently [9].

2.6.1.1 Skeletal Muscle Satellite Cells

Skeletal muscle satellite cells are precursor cells for skeletal muscle and are found in the basal lamina of muscle fibers. They are typically characterized by their expression of Pax 7 (quiescent) and MyoD (activated) [10]. Activated satellite cells are typically referred to as skeletal myoblasts. Because of their contractile potential and resistance to ischemia, early efforts in cellular cardiomyoplasty involved the direct injection of skeletal myoblasts into injured hearts. Murry et al. demonstrated that rat skeletal myoblasts could engraft in infarcted rat myocardium, form myotubes, and mature into β -myosin heavy chain expressing muscle [11]. Additionally, this muscle could be induced to contract *ex vivo* and was able to convert into fatigue resistant, slow twitch fibers. There is still some debate whether these cells assume a cardiac-like phenotype *in vivo*. Reinecke et al. were not able to show transdifferentiation of rat skeletal muscle satellite cells into cardiomyocytes once grafted [12]. Other reports suggest partial transdifferentiation potential of skeletal muscle satellite cells [13, 14]. One possible explanation for the disparity between reports is that skeletal muscle satellite cells may fuse with surrounding myocardium, developing a hybrid phenotype [15, 16].

Regardless of the fate of the myoblasts or satellite cells after *in vivo* intracardiac transplantation, improvements in myocardial performance have been demonstrated over four to five weeks after transplantation in several studies. Discrepancies between reports, however, make it difficult to assess the mechanism of action by which myoblasts or satellite cells assist in myocardial repair. Additionally, myoblasts and satellite cells require *ex vivo* expansion to increase cell number for autologous transplantation.

Inherently, this delays the time until treatment can be administered and may contribute to variability in cell behavior.

2.6.1.2 Cardiac Progenitors

Several variations of cardiac progenitors are currently being studied. Stem cell antigen-1 (Sca-1) has previously been shown to exist on several tissue-specific progenitor cells [17, 18]. Sca-1⁺ cardiac progenitors have also been reported. These cells maintain the ability to proliferate *ex vivo* allowing for cell expansion. Also, these cells can be induced to differentiate into beating cardiomyocytes with the application of the demethylating agent, 5' azacytadine and oxytocin [19, 20]. Notably, beating frequency increases with isoproterenol treatment demonstrating the physiological responsiveness of mouse cardiac Sca-1⁺ derived cardiac cells. When injected, these cells are able to home to the border zone of infarcted myocardium [19]. Nevertheless, the regenerative ability of mouse cardiac Sca-1⁺ cells has yet to be determined.

Cardiac side population (CSP) cells have been isolated via the selection of cells which efflux Hoechst dye. Such cells have a varied phenotypic profile in regards to the expression of Sca-1, c-kit, Abcg2, CD34 and CD31 depending on the donor from which they are isolated. High expression of Sca-1 and low expression of c-kit are observed typically [21, 22] in CSP cells from mouse heart. Mouse CSP cells have been shown to differentiate into a cardiac phenotype (Nkx2.5 and GATA4 positive) via co-culture with cardiomyocytes and demonstrate a high proclivity for *ex vivo* proliferation [21-23]. The efficacy of these cells in an *in vivo* myocardial injury model has yet to be determined, although it has been demonstrated that the proliferation of CSP cells increases after MI and that these cells can be replenished by bone marrow derived progenitors during MI [24].

Another cardiac progenitor that has been isolated from the myocardium is characterized by its high expression of c-kit and negative expression for CD34 and

CD45. These cells can be isolated from an enzymatically dissociated heart lysate using c-kit specific antibodies and antibody-based cell sorting techniques. 7-10% of isolated rat c-kit⁺ cells express the cardiac specific transcription factors Nkx2.5, GATA-4, and MEF-2 [25]. Further signs of differentiation are exhibited when c-kit⁺ cells are cultured in differentiation media. Although no morphological signs are observed in regards to cardiac cell differentiation, many molecular resemblances emerged. Beltrami et al. injected BrdU-labeled rat c-kit⁺ cells into the border zone of infarcted rat myocardium. These cells engrafted, reduced infarct size and differentiated into cardiac muscle, smooth muscle and endothelial cells. Additionally, injection of c-kit⁺ cells enhances cardiac remodeling and improves myocardial performance [26].

Cardiospheres (CSph) are a heterogeneous progenitor cell population derived from an adult cardiac biopsy. Upon isolation and enzymatic dissociation, the cells are cultured in suspension where they spontaneously form small clusters and differentially express markers such as c-kit, Sca-1, CD31, CD34 and CD105 [27, 28]. CSph can spontaneously differentiate into beating cardiac muscle, alone or as a co-culture with cardiomyocytes. When mouse CSph are injected into infarcted mouse hearts, a marked increase in fractional shortening and myogenesis is observed. Similar effects are also observed when enzymatically dissociated CSph (used to form single cells) are injected into infarcted myocardium [28]. The use of CSph-derived single cells offers the option of expanding the progenitor cell population, given the small number of cells initially isolated, and avoids using large cell clusters *in vivo*.

The presence of the LIM-homeodomain transcription factor islet-1 (*isl1*) has been used as a marker to identify a progenitor cell population in the mouse, rat and human postnatal heart. These “cardioblasts” are observed to primarily reside in areas of the second heart field (i.e. right ventricle, both atria, and the outflow tract). Although the number of *isl1*⁺ cells substantially decreases after birth, they are able to propagate ex

vivo when cultured on a cardiac mesenchymal feeder layer. Mouse *isl1*⁺ cardioblasts are positive for *Nkx2.5* and *GATA4* but fail to express both *Sca-1* and *c-kit* indicating they are phenotypically distinct from other reported cardiac progenitors [29].

Interestingly, mouse *isl1*⁺ cardioblasts are able to differentiate spontaneously into functional cardiomyocytes when co-cultured with neonatal mouse cardiomyocytes.

These cardioblast-derived cardiomyocytes express cardiac structural proteins, exhibit calcium transients, and have the ability to undergo excitation contraction coupling. The role of *isl1*⁺ cardioblast in myocardial repair after injury has yet to be determined.

Although cardiac progenitors show a high proclivity for cardiac differentiation, it is difficult to isolate large numbers of these cells. Therefore, *ex vivo* expansion is typically performed to allow for a suitable size graft. Cardiac progenitor cell therapies would benefit from methods to decrease the time from cell isolation to cell transplantation.

2.6.1.3 Bone Marrow Stem Cells

Bone marrow stem cells (BMSC) include both mesenchymal and hematopoietic cell types. Both have been used extensively as a cell therapy for myocardial infarction. Mesenchymal stem cell (MSCs) are adult progenitor cells that have the potential to differentiate into tissues from the mesoderm [30]. These include fibroblast, muscle, bone, cartilage, and adipose tissue. Such cells are characterized by their expression of SH2 (type III TGF receptor), SH3, SH4 (ecto-5'-nucleotidase), and STRO-1 [31] and by their lack of expression of CD45 and CD34. These cells have also been shown to successfully differentiate into cardiomyocytes *in vitro* [32]. In landmark papers by Orlic and his co-workers, they showed that mouse *Lin*⁻, *c-kit*⁺ BMSC differentiated into premature cardiomyocytes, endothelial cells, and smooth muscle cells after injection into infarcted mouse myocardium. Functional assessments of infarcted hearts with BMSC grafts also revealed improvement in several hemodynamic measures [33, 34]. Other reports showed lesser functional improvements, and hematopoietic stem cell

differentiation into cardiomyocytes was not observed [35, 36]. Functional cardiac improvement without cardiomyocyte differentiation raises questions about the mechanisms by which these cells can impact cardiac function. When human MSCs are injected into normal mouse myocardium they attain a “cardiac-like” phenotype [37] as tested by the expression of several cardiac related markers. Unfortunately, few studies have shown well-defined cardiomyogenic differentiation of MSCs delivered to infarcted hearts [9, 38-40]. In addition, these studies indicate a need for *ex vivo* expansion of MSCs before implantation. Other fractions of the bone marrow do not require extensive *ex vivo* manipulation and can be readily used as autologous grafts. Nevertheless, most studies do report improvements in remodeling, hemodynamic measures, and mechanical parameters upon delivery of MSCs to injured myocardium. One theory to explain such improvements without substantial cardiomyocyte repopulation is that MSCs secrete paracrine factors that act on host cells in a beneficial manner [41, 42].

Some benefit of BMSC transplantation in myocardial repair seems clear. Nevertheless, the extent and mechanism of repair are still uncertain. In addition, unfractionated BMSCs represent a heterogenous cell population. The use of BMSCs for cellular cardiomyoplasty may benefit from advancements in bioprocessing to identify different marrow populations with enhanced cardiomyogenic or angiogenic potential.

2.6.1.4 Adipose-Derived Mesenchymal Stem Cells

MSCs are not only found in the bone marrow but can be found in several tissues throughout the body. In particular, cells isolated from liposuction aspirates have demonstrated mesenchymal-like properties and offer an alternative to bone marrow-derived MSCs [43]. Adipose-derived stem cells (ADSC) express similar markers expressed by MSCs such as CD105, CD29, CD44 and CD90. One difference appears in the expression of the VLA-VCAM-1 receptor-ligand pair. ADSCs express Very Late Antigen (VLA) but fail to express Vascular Cell Adhesion Molecule-1 (VCAM-1), while

MSCs express VCAM-1 but not VLA. Such differences in adhesion molecule/integrin expression may account for the distinct differences in tissue localization [44]. There appears to be 500 times more ADSCs per gram of fat than MSCs per gram of marrow thus possibly eliminating the need for *ex vivo* scale up for cellular cardiomyoplasty. In addition, ADSCs differentiate into a α actinin and β -myosin heavy chain expressing cardiac phenotype with the use of 5-azacytidine, co-culture with neonatal cardiomyocytes, or spontaneously under defined culture conditions [45-47]. Observations indicate that cardiomyocytes derived from ADSCs can generate action potentials and respond appropriately to pharmacological stimuli such as isoproterenol [47]. Mouse ADSCs injected into the LV of a mouse cryoinjured myocardial infarct model determined that these cells engraft and differentiate into Nkx2.5, troponin I, and myosin heavy chain expressing cells. These cells were not shown to integrate with healthy myocardium, however [48]. Others studies have shown the angiogenic potential of ADSCs upon enrichment of the CD34+/CD31- population [49] and the beneficial effect these cells have on global myocardial function after LV chamber injection [50]. Also, ADSCs secrete angiogenic paracrine factors (VEGF) that may contribute to tissue repair after injury [51].

The ability of ADSCs to differentiate into cardiomyocytes, secrete paracrine factors, provide functional augmentation after myocardial infarction, and not require *ex vivo* expansion suggests these cells represent an important advancement in the search for useful cell sources. An understanding of the mechanism by which these cells contribute to cardiac repair is lacking, however.

2.6.1.5 Amniotic Fluid Stem Cells

Amniotic fluid stem cells (AFSC) are a multipotent cell population isolated from amniocentesis specimens. Although cultures of amniocentesis contain a heterogeneous population of cells with diverse potencies, AFSC can be isolated and enriched for by

using antibody selection for the c-kit receptor. Upon isolation, human AFSC express markers characteristic of mesenchymal, neural, and embryonic stem cells. These include the expression of CD90, CD44, CD105, CD29, CD73, Oct4, and SSEA4. AFSCs fail to express the hematopoietic markers CD45, CD34 and CD133 [52]. AFSCs differentiate into a cardiomyogenic phenotype in the presence of neonatal cardiomyocytes as evidenced by the expression of Nkx2.5, cardiac troponin I, GATA-4, and MLC-2v, but cell fusion with host myocytes has not been excluded. When swine AFSCs are injected into infarcted pig hearts, they differentiate into endothelial, fibroblast, and smooth muscle phenotypes, but no cardiogenic phenotypes are observed [53]. Human AFSCs are acutely rejected when used in normal or immunosuppressed rat myocardial infarct models [54].

AFSC represent another abundant cell source. The efficacy of AFSCs in cardiac repair is still ill defined, however. In order for further progress, more studies will have to be performed to investigate issues of cell integration, rejection, and efficacy for myocardial repair.

2.6.1.6 Embryonic Stem Cells

Embryonic stem cells (ESCs) are another cell type which has garnered attention lately because of their relative availability, expansion capabilities, and proven cardiomyocyte differentiation. Most ESC lines are isolated from the inner cell mass of a developing blastocyst, are defined by their ability to differentiate into tissues from all three germ layers, and express pluripotency markers such as OCT 3/4 and Tra 1-81 [55-58]. Mouse and human embryonic stem cells have been shown to successfully differentiate into cardiomyocytes through the formation of embryoid bodies [59] or co-culture with the visceral endoderm-like cell line END-2 [60, 61]. ESCs have also been extensively tested *in vivo* for potential to differentiate into cardiomyocytes [62].

Limitations of undifferentiated ESCs include the formation of teratomas and susceptibility

to ischemia after delivery [63]. Both Swijnenburg et al. [64] and Nussbaum et al. [65] report significant teratoma formation after undifferentiated mouse ESC transplantation into infarcted mouse myocardium. To avoid teratoma formation, investigators are starting to differentiate cells into cardiomyocytes before transplantation. Differentiated mouse ESC-derived cardiomyocytes have shown arrhythmic potential *in vitro* [42], however. In addition, ESC-derived cardiomyocytes continued to display susceptibility to ischemia [63].

The use of undifferentiated ESCs risks teratoma formation and low graft viability. Addressing these issues has resulted in many investigators differentiating ESCs into cardiomyocytes before implantation. This approach focuses on remuscularization of damaged heart, although other mechanisms may play a significant role. Additionally, integration of these grafts with host myocardium is poor and may result in unwanted arrhythmias. The issue of rejection is also a concern.

2.6.1.7 Induced Pluripotent Stem Cells

Induced pluripotent stem (iPS) cells represent a major breakthrough in regenerative medicine and involve the transdifferentiation of an unipotent or multipotent cell into a pluripotent state. Typical approaches to inducing pluripotency include retroviral transduction of somatic cells with four transcription factors: octamer-binding transcription factor 3/4 (oct 3/4), SRY-related high-mobility-group-box protein-2 (Sox2), Myc, and Kruppel-like factor-4 (Klf4) [66-68], although variations on which factors can be used or excluded are being explored [69-71]. Additional methods intended to avoid genomic integration of the expression vectors have been undertaken and include use of adenoviral vectors and plasmid transfection and membrane soluble proteins [70, 72, 73]. iPS cell formation suffers from low induction efficiencies, however. Also, retroviral-based transduction has resulted in tumor formation in chimeric animals [74]. Recently, it was demonstrated that functional cardiomyocytes could be derived from iPS cells [75]. After

induced pluripotency, cardiomyocytes were derived through embryoid body formation. iPS cell-derived cardiomyocytes expressed many cardiac markers and displayed cardiomyocyte-specific action potentials.

Despite several obstacles, iPS cells hold potential in providing an autologous cell therapy without the ethical or immunological concerns surrounding the use of ESCs. There are still many questions surrounding iPS cells (mechanism of induced pluripotency, safety, and similarity to ESCs), and thus their potential for myocardial repair has yet to be explored.

In summary, several progenitor cell populations have been used or are being studied for use in myocardial repair. In most cases, the delivery and engraftment of cells to infarcted myocardium leads to improvements in function after injury. Such improvements seem transient, indicating the goal of myocardial “regeneration” has transitioned into myocardial “preservation” marked by reduced fibrosis, attenuated remodeling, and improved myocardial perfusion. Although several studies have shown viable muscular grafts, the mechanism by which these grafts induce myocardial improvement is still lacking. Given the similarity in outcome with the progenitor cells used for cellular cardiomyoplasty, how do we choose which is the best? Recently, van der Bogt et al. reported a direct comparison of how mouse mononuclear cells (fresh unfractionated bone marrow), mouse MSCs, mouse skeletal myoblasts, and mouse fibroblasts acted as mediators for infarct repair [76]. The authors conclude that mononuclear cells provide a superior regimen for cardiac repair and preservation compared to the other cell types given their capacity for long term survival. Such comparisons between cell types were lacking previously in the field and are likely necessary in the future to determine if an optimal cell type exists. The transient nature of cellular cardiomyoplasty also raises the question as to whether only one cell type is needed or if multiple cell doses would be required to have an extended effect [77, 78].

As discussed below, some of these cell sources have been used in humans, and the results have not always paralleled the preclinical outcomes, raising another level of complexity in choosing the right cell.

2.6.2 Clinical Translation of Cellular Cardiomyoplasty

Many phase I human clinical trials indicate that cellular cardiomyoplasty is safe and feasible. Efficacy reports from larger controlled trials revealed transient and somewhat limited effects for primary endpoints (Table 2.1). Thus far, autologous bone marrow derived stem cells, skeletal myoblasts, MSCs, and circulating blood-derived progenitor cells have been used in human clinical trials.

Table 2.1) Major Human Clinical Studies involving Stem Cell Therapy for Heart Failure

Study	Primary End Point	Cells Used	Randomized Controlled	# Cells	# Patients	Time after PCI	Delivery	Results
Hamono et al. [79]	Myocardial Perfusion	BMMC	N	50x10 ⁶ – 100x10 ⁶	5		Direct injection	60% Efficacy
Strauer et al. [80]	LVEF %	BMMC	N	9x10 ⁶ – 28x10 ⁶	20	5-9d	Intracoronary (IC)	Increased LVEF (not significant), decreased ESV
Assmus et al. [82]	LVEF %	CPC / BMMC	N	10x10 ⁶	20	4.3±1.5d	IC	Increased LVEF%, ESV and myocardial viability. No difference between CPC and BMMC
Stamm et al. [84]	LVEF% and Perfusion	AC133+ BMMC	N	--	6		Direct injection	Increased LVEF% and blood perfusion through heart
Menasche et al. [89]	LVEF %	Skeletal Myoblast	N	5-17x10 ⁶	10		Direct injection	Increased LVEF% and systolic thickening. Increased risk of arrhythmia
Tse et al. [85]	LVEF %	BMMC	N	--			Trans-Endocardial injection	No significant increase in LVEF%, increased wall thickening and motion
Patel et al. [87]	LVEF %	CD34+ BMMC	N	--	20		Direct injection	Increased LVEF% and LVEDV
Wollert et al. [88]	LVEF %	BMMC	Y	--	60		IC	Increased LVEF% and decreased infarct size
Perin et al. [86]	LVEF %	BMMC	N	25.5x10 ⁶	14		Trans-Endocardial injection	Increased LVEF% and decreased ESV. Results decline by 4 months
Assmus et al. [91]	LVEF%	BMMC	Y	200x10 ⁶	92		IC	Increased LVEF%
Lunde et al. [95]	LVEF%	BMMC	Y	68x10 ⁶	100	4-8d	IC	No Change in LVEF % or infarct size
Schachinger et al. [93]	LVEF%	BMMC	Y	236x10 ⁶	204	3-7d	IC	Increased LVEF%, ESV. The more time after PCI the better the result

ESV - End systolic volume, LVEDV – Left ventricular end diastolic volume, PCI – Percutaneous coronary intervention, LVEF – Left ventricular ejection fraction, CPC – Circulating blood-derived progenitor cell, BMMS – Bone marrow mononuclear cell

2.6.2.1 Phase I Clinical Trial Results

Many of the first human clinical trials for cellular cardiomyoplasty were small and non-randomized. In 1999, Hamano and colleagues [79] directly injected bone marrow mononuclear cells (BMMC) into the ischemic area of patients undergoing coronary artery bypass graft (CABG) surgery. Results indicated that three out of five patients obtained increased blood perfusion in the area where the cells were grafted. This increase in blood flow was persistent after a one-year follow-up. Strauer et al. [80]. demonstrated that intracoronary infusion was a feasible approach for the delivery of autologous BMMC. In this study, cells were injected 5-9 days after percutaneous transluminal coronary angioplasty and resulted in a significant reduction of 18% in end systolic volume and a 12% increase in stroke volume index at a three-month follow-up. This was the first human study to not only consider alternate delivery strategies for cellular cardiomyoplasty but also the time of delivery after acute myocardial infarction (AMI), showing less invasive procedures could be used to deliver cells. The contribution of time of delivery to improved cardiac function was not tested, but it was thought that waiting until after the inflammatory response has subdued would allow for enhanced cell engraftment. Such an idea has been validated in animal studies [81].

Additional studies followed, including the TOPCARE-AMI (Transplantation of Progenitor Cells and Regeneration Enhancement in Acute Myocardial Infarction) [82, 83] clinical trial that delivered either circulating blood-derived progenitor cells (CPC) or BMMC to patients diagnosed with acute myocardial infarction (AMI). Cells were delivered an average of 4.3 days after AMI and resulted in reduced end systolic volume and in increased LV ejection fraction, coronary flow reserve, and myocardial viability. Although both cell types gave rise to improved functional outcomes, there were no differences observed between the two cell types. Given the angiogenic potential of both cell types, the similarity in results seems likely to arise from each cell type's ability to

promote neovascularization, endothelial cell migration, and proliferation. This conclusion is similar to many preclinical studies discussed above. Supporting this idea, neovascularization was observed when Stamm and colleagues [84] directly injected BMMC enriched for AC133+ cells into the border zone of infarcted myocardium. After a three-month follow-up, patients receiving AC133+ enriched cell treatment had increased ejection fraction and perfusion in infarcted segments of the heart. Similar results were seen by Tse et al. [85], Perin et al. [86], and Patel et al. [87].

In 2004, the BOOST (Bone Marrow Transfer to Enhance ST-Elevation Infarct Regeneration) clinical trial represented the first randomized, controlled and blinded human clinical trial for cellular cardiomyoplasty [88]. Sixty patients were randomly assigned to a control or BMMC transplant groups. BMMC-treated patients were injected via intracoronary infusion, five days after percutaneous coronary intervention. After six months, cardiac magnetic resonance imaging revealed BMMC-treated patients had a significant increase in LV ejection fraction from baseline value after infarct and as compared to controls. Additionally, systolic wall motion in the border zone increased over this period. There were no major adverse events after infusion of BMMC.

Autologous skeletal myoblasts have also been used in human clinical trials for cellular cardiomyoplasty. In an initial feasibility study, $\sim 871 \times 10^6$ skeletal myoblasts were injected directly into 37 sites within and around the injured myocardium in 10 patients undergoing CABG [89]. At an average follow-up of 11 months, most patients had increased ejection fraction and improved systolic thickening, but an increase in arrhythmias was observed in four patients. A similar result was observed when Pagani and colleagues [90] directly injected autologous skeletal myoblasts into five patients undergoing implantation of a left ventricular assist device. Of the five patients treated, four developed cardiac arrhythmias.

2.6.2.2 Phase II and III Clinical Trials

After the demonstration of feasibility in several smaller human clinical trials, larger, randomized, controlled clinical trials were initiated. In 2005, Assmus and colleagues [91] expanded upon their previous investigation using both autologous BMMC and circulating blood derived progenitor cells (CPCs). Patients were randomized into control (no cell treatment), BMMC and CPC groups. After a three month follow-up, patients were entered into a crossover phase whereby patients initially designated into the BMMC group were given CPCs and vice versa. Patients in the control group were randomized into either BMMC or CPC groups at crossover. In general, BMMC performed better than CPCs as demonstrated by significant improvements in LV ejection fraction (4% by MRI) over control at three months. This observation was further confirmed at crossover as patients given BMMC at the three-month follow-up examination also showed increased improvements in LV ejection fraction. Additionally, Schachinger and colleagues [92-94] demonstrated similar trends of LV ejection fraction (4% over placebo) improvement at four months with intracoronary delivery of autologous BMMC. Interestingly, they found that the degree of improvement was correlated to the time of cell delivery after reperfusion therapy and the extent of impaired cardiac function at enrollment.

Not all larger clinical trials, however, have shown comparable improvements in cardiac function after cell treatment. Lunde and colleagues [95] delivered autologous BMMC via intracoronary injection and showed no change in LV ejection fraction or infarct size versus control at a six month follow-up. This might be ascribed to differences in cell preparation [96] and number of delivered cells in the Autologous Stem Cell Transplantation in Acute Myocardial Infarction (ASTAMI) trial.

The US registry of federally and privately supported clinical trials, Clinicaltrials.gov, reports several ongoing studies aimed at cellular cardiomyoplasty. The majority of these trials use autologous BMMC as the cell source. Several trials,

however, are taking new approaches to cardiac cell therapy. For instance, the Combination Stem Cell Therapy for Utilization and Rescue of Infarcted Myocardium (MESENDO) trial is attempting to use an autologous mixture of two cell sources (BMMCs and MSCs in equal proportions); one which would promote neovascularization and the other would promote cardiac remuscularization. In addition, the Study of Allogeneic Mesenchymal Precursor Cells (MPCs) in Subjects with Recent Acute Myocardial Infarction is attempting to determine the suitability of an allogeneic progenitor cell source. This work and others could prove beneficial to optimizing cellular cardiomyoplasty in the future.

In summary, of the two major cell types used in clinical trials, only one has emerged as a viable option. BMMC appear to have a beneficial effect on myocardial function while the threat of adverse arrhythmias precludes the use of skeletal myoblasts. Unfortunately, the extent of repair with BMMC appears less robust than that reported in preclinical studies using the same or a similar cell source. The lack of expansion beyond the use of BMMC in clinical trials has provided a significant roadblock to the progression of cellular cardiomyoplasty. Are there other cells which could supply even greater benefit? The answer is likely to be yes, but there are roadblocks to be addressed (Figure 2.9).

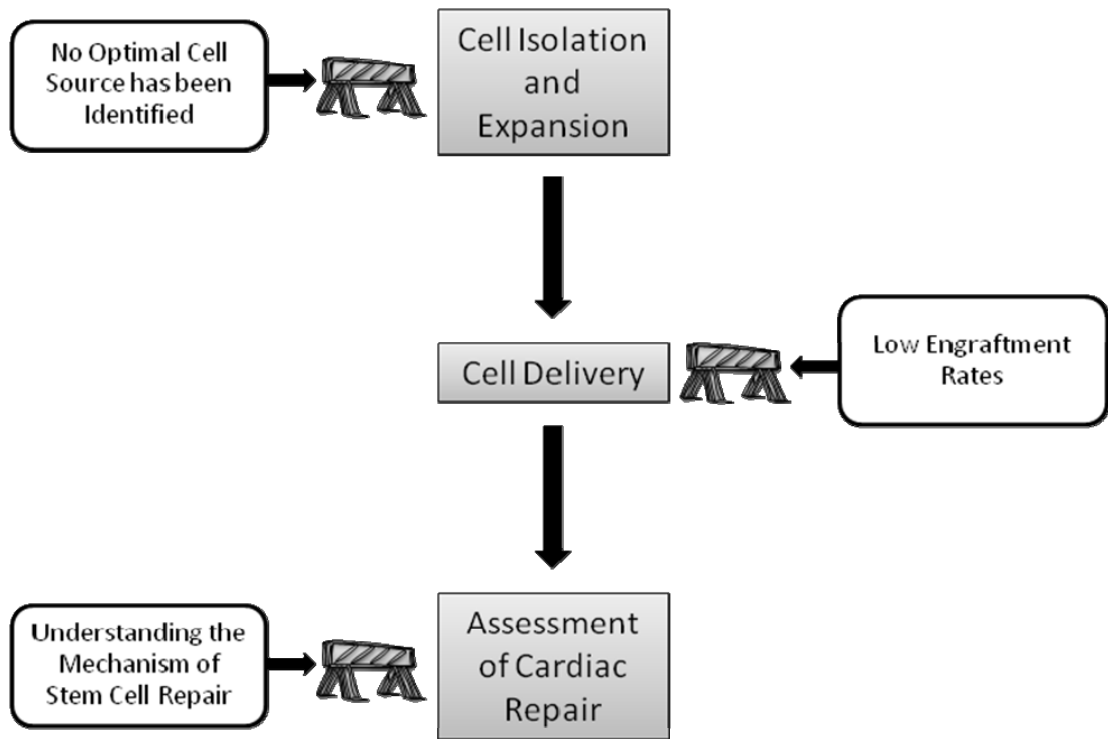


Figure 2.9) Translational roadblocks which are preventing the successful application of cellular cardiomyoplasty in the clinic include determining an optimal cell source, increasing engraftment rates, and understanding the mechanism of stem cell repair.

2.6.3 Translational Issues Concerning Cellular Cardiomyoplasty

2.6.3.1 Translational Roadblock #1: No Optimum Cell has been Identified.

The progression of clinical cellular cardiomyoplasty appears to be moving forward, but as noted above, the extent of repair in humans is limited when compared to preclinical models. One reason for this is that the cell source pool is limited. Cell sources are constrained by immunological rejection and the need for large numbers. Autologous sources address the issue of rejection but prevent “off-the-shelf” availability of cell therapies for efficient treatment. In addition, patients likely to be treated with autologous cell cardiomyoplasty maybe the same ones that have deficiencies in source number or efficacy. Ongoing clinical trials continue to utilize previously suggested cell sources in their experimental design, [97] although the number of cell sources used in preclinical studies is vast. This disconnect will likely have to be addressed.

2.6.3.2 Translational Roadblock #2: Low Engraftments Rates

The rate of cell engraftment is a factor in determining the initial outcomes and may explain the lack of durable results seen in some studies. Assmus and colleagues and Schachinger and colleagues delivered 200×10^6 and 236×10^6 autologous human BMSCs, respectively and observed modest improvements in LV ejection fraction compared to placebo [91, 93]. Lunde and colleagues however, reported no change in LV ejection fraction with the delivery of 68×10^6 autologous human BMSCs cells [95]. This suggests cell number may play an important role in the repair of myocardial damage.

Engraftment rates can be influenced in a number of ways, one of which is the cell delivery method. Typical approaches to deliver cells include intravenous (IV) injection, intracoronary (IC) injection, retrograde venous intracoronary (RIC) infusion, and intramyocardial (IM) injection. Although IV injection offers the advantage of being minimally invasive, there is low cell engraftment (< 1%) into the injured area [98, 99]. IC

injection and RIC infusion provide more localized delivery of cells, resulting in improved but still limited cell engraftment (3-6%) [98, 100]. IM injection offers direct localization of cells to the injured area, but engraftment (6-12%) is limited by leakage out of the injection sites and cellular washout into the native venous shunts [99]. Moreover, this technique results in inhomogeneous cell delivery with emerging cell clusters within the myocardial scar [82]. This could act as a substrate for adverse electrical remodeling [101]. In a study comparing the relative efficiency of cell delivery by intramyocardial (IM), intracoronary (IC), and interstitial retrograde coronary venous (IRV) delivery, each method resulted in only modest engraftment [100]. Specifically, IM injection resulted in 11% engraftment, while IC and IRV injections resulted in 2.6% and 3.2% engraftment, respectively. Similar studies performed by Freyman et al. [98] showed that 14 days after IC infusion, engraftment was 6%, and this delivery procedure was also accompanied by reduced coronary blood flow and subsequent myocardial injury. The low engraftment rates reported with conventional delivery strategies may not allow for optimal reparative ability from individual cells. Therefore, methods aimed at improving engraftment may help bring cellular cardiomyoplasty to its full potential.

2.6.3.3 Translational Roadblock #3: Understanding the Mechanism of Repair

Just how cells might fix hearts is not understood, and this lack of understanding slows the design of future trials. Competing hypotheses include stem cell differentiation into cardiac or vascular cells and the secretion of beneficial trophic factors to modulate endogenous functions or to lower cell death thresholds.

2.6.3.3.1 Do Cardiomyocytes Matter?

ESCs, MSCs, and skeletal myoblasts have been extensively tested *in vivo* for their potential for differentiation into myocytes. For these myocytes to be functional, they would have to be electrically integrated and be able to produce sufficient force to explain

the observed preclinical and clinical results. As of yet, it is unclear if any of these cell types meets these criteria.

Early studies involving the injection of undifferentiated ESCs into infarcted hearts reported enhanced cardiac function after cell transplantation with evidence that these cells engraft and differentiate into cardiomyocytes [62]. In addition, there was also evidence of ESC differentiation into vascular smooth muscle and endothelial cells. These cells were able to attenuate apoptosis and adverse cardiac remodeling [102]. The uncertainty about teratoma formation, however, has led many investigators to initially differentiate ESCs into cardiomyocytes before transplantation. Early investigations by Min et al. [103] showed that delivery of a modest number of mouse ESC-derived cardiomyocytes could improve cardiac function after infarction in rat. Engraftment was calculated to be 7.3% after direct injection of cells and was complemented with improvements in ventricular function and myocardial remodeling after six weeks. These results appeared to be maintained out to thirty-two weeks, suggesting a potential long term benefit [104]. Human ESC-derived cardiomyocytes were also shown to engraft into healthy rat myocardium with no teratoma formation by four weeks [105]. Additionally, the cardiomyogenic grafts exhibited a substantial proliferative capacity and an ability to interact with host myocardium through the formation of vascular beds. Other studies which delivered human ESC-derived cardiomyocyte grafts into infarcted myocardium accompanied by pro-survival factors reported improved cardiac function and remodeling [63]. Improvements in cardiac function, ventricular wall remodeling, and remuscularization were observed at four weeks after cell delivery. Despite evidence of remuscularization and neovascularization, it is yet to be established that these grafts are functional and contribute to the improvements in cardiac function observed.

A similar circumstance is the case for MSCs. MSCs have also demonstrated cardiomyogenic differentiation potential *in vivo*. Human MSCs injected into healthy

mouse heart upregulated their expression of cardiac proteins out to 40 days after delivery [37]. Unfortunately, the percent engraftment was extremely low with only 0.44% MSCs detected after only four days. Min et al. [42] showed that human MSCs had a beneficial effect on myocardial perfusion in a pig model and that MSCs could differentiate into a cardiac α -myosin heavy chain and troponin I expressing cell phenotype. Myocardial perfusion was further enhanced when human MSCs were co-transplanted with fetal cardiomyocytes. Dai et al. [9] studied the short and long term effects of rat MSC therapy on infarcted rat myocardium. These studies revealed that allogeneic rat MSCs could differentiate to express cardiac-specific proteins, that MSC therapy resulted in improved cardiac function, but that the effect of MSCs on global cardiac function was transient (lasting only one month after delivery). Moreover, the number of MSCs expressing cardiac proteins decreased over time. Contrary to these results, Amado et al. [106] reported improved cardiac function with reduced scar formation in Yorkshire pigs undergoing myocardial infarction but without swine MSC differentiation into a cardiac-expressing phenotype. Unfortunately, none of these studies have investigated the function of MSC-derived cardiac gene expressing cells. Thus, even if MSCs can differentiate toward the cardiac lineage, it is unclear that they can make myocytes with sufficient contractile properties to explain the observed effects of cell transplantation.

More evidence that factors other than myocyte differentiation may be important come from the experiments with skeletal muscle progenitors. The transdifferentiation potential of skeletal myoblasts and satellite cells into cardiomyocytes is unclear. In one study, Reinecke et al. reported that skeletal muscle satellite cells are unable to transdifferentiate into cardiomyocytes after delivery to the myocardium [12]. Skeletal muscle satellite cells differentiated into mature skeletal muscle but failed to co-express a cardiomyogenic phenotype. On the other hand, Horackova et al. reported that over time

engrafted skeletal myoblasts downregulated their expression of skeletal muscle markers and partially transdifferentiated into a cardiac phenotype through the expression of cardiac troponin T in addition to other markers [13]. Additionally, Invernici and colleagues [14] reported that upon treatment with retinoic acid, human skeletal myoblasts would differentiate into spontaneously beating cells which expressed cardiomyogenic markers. These differentiated skeletal myoblasts also mediated improved cardiac function after they were injected into infarcted myocardium. Since skeletal myoblasts are capable of mediating myocardial improvement but may have a limited ability to differentiate into cardiac myocytes and since they do not electrically couple with native cardiac cells, it seems unlikely that their ability to improve outcomes is the sole result of generation of new, functional cardiac myocytes.

In summary, although many studies have focused on cardiomyocyte differentiation, function of these donor-derived myocytes is unclear, and engraftment and differentiation rates seem too low to explain the full effect of exogenous cell transplant. Therefore, it seems likely that, despite the original idea of regenerating myocardium, other mechanisms are at work with current therapeutic strategies.

2.6.3.3.2 Trophic Factors – The Paracrine Hypothesis

It now seems possible that the main effect of improved cardiac function after cell delivery results from secreted factors that preserve native cells, induce neovascularization, or attract resident stem cells [107]. *In vitro* studies with MSCs show that they secrete paracrine factors under hypoxic and normoxic conditions. MSC-conditioned media can attenuate fibroblast proliferation [108], induce electrical remodeling of cardiomyocytes [109], stimulate endothelial cell proliferation and activation [110, 111], and inhibit apoptosis [112, 113]. These results provide a basis for possible paracrine mechanisms by which stem cells may repair and/or preserve myocardial function after AMI.

Potential paracrine factors mediating these effects include VEGF, basic FGF, SDF-1 α , IGF-1 and secreted frizzled related protein [114]. Studies using only conditioned media from Akt over-expressing MSCs confirmed that paracrine factors can mediate myocardial repair [115]. Pro-survival cocktails have also been used with the intention of prolonging engraftment of progenitor cells in ischemic conditions [63]. Results show improved engraftment and survivability after graft delivery. Additionally, Korf-Klingebiel et al. [116] recently described human bone marrow cells as rich sources for pro-angiogenic and cytoprotective factors. This suggests that current clinical trials which have focused on the use of autologous bone marrow progenitor cells may promote myocardial repair via a paracrine pathway. ESC-derived cardiomyocytes have also been shown to secrete beneficial paracrine factors [117].

These studies and others suggest that exogenous cells secrete factors that affect the host tissue. This observation may explain why so many different cell types can mediate repair and why differentiation seems poorly correlated to functional improvement. Also, it would suggest that the field would seem to be at an implementation bifurcation point, having to choose between understanding and refining the paracrine effect with or without cells or moving on to identify cells with more potential to generate cardiac myocytes.

2.6.4 Tissue Engineering for Addressing the Translational Issues

Tissue engineering may help address the obstacles noted above. Tissue engineering involves the restoration, maintenance, or enhancement of tissue and organ function.

Initial tissue engineering treatment options for heart failure involved acellular synthetic materials which surrounded the ventricle to prevent ventricular dilation [118].

Cellularized scaffolds have been constructed as alternative delivery and graft solutions to cardiomyoplasty. Tissue engineered approaches include neonatal rat ventricular cells

embedded in gelatin mesh (Gelfoam®) [119] and skeletal myoblasts suspended in fibrin glue [120]. Zimmerman et al. [121] have demonstrated electrical integration with host myocardium in addition to improved myocardial performance and remodeling after application of engineered heart tissue (EHT). EHTs created by combining neonatal cardiomyocytes and collagen achieved spontaneous contraction while in culture. Currently fibroblasts [122, 123], skeletal myoblasts [120], embryonic stem cells [124, 125], cardiomyocytes [121, 126-131] and BMSCs [132-135] have been used in conjunction with a variety of biomaterials to form “cardiac patches” (Table 2.2). Some groups have also used acellular biodegradable materials as cardiac grafts and have seen improvements in remodeling and cardiac function [136] in preclinical studies. Another benefit of tissue engineered constructs that may prove useful is that materials have been shown to induce differentiation or modulate cell function [137, 138]. Therefore, tissue engineering is likely to direct progenitor cell fate more efficiently through the combination of biomaterials, bioactive factors, and physical forces. This would provide more controllable methods for optimization of cell source in cellular cardiomyoplasty. Unfortunately, cellularized constructs are restricted in size due to diffusion limitations. In order to sustain cell viability with tissue engineered constructs, methods to induce angiogenesis and cell survival within cardiac patches will need to be explored. Other considerations will involve optimizing construct size and delivery.

Table 2.2) Major Preclinical Studies Involving Tissue Engineering for Myocardial Repair

Study	Cell Type (Seeding Density)	Construct Type	Animal Model	Immune Status	Time of Measurements	Results of Outcome Measures	TE Controls
Christman et al. [120]	Skeletal Myoblast (5×10^6 / construct)	Fibrin Glue	Female SD Rats	IC	ECHO 1 weeks and 5 weeks Histology 5 weeks	Improved FS% and LV AWTh	Fibrin Glue only
Li et al. [119]	Rat Fetal Ventricular Cells (4×10^7 / mL)	Gelatin	Male Lewis Rats	IC	5 weeks	Little effect on cardiac function, formed junctions with host myocardium	Acellular Gelatin
Zimmerman et al. [121]	Rat Neonatal Heart Cells (2.5×10^6 / construct)	Collagen Type I	Male Wistar Rats	IS	4 weeks in vivo histology 2 weeks all other measures	Electrical integration with host myocardium, improved LVDD, LVEDD, FS%, max LV volume, tau (relaxation index) LVEDP and LVEDV	formaldehyde fixed, Non-cardiomyocyte construct
Leor et al. [130]	Rat Fetal Heart Cells (3×10^5 / construct)	Alginate	Female SD Rats	IC	5-7 days after MI and 65 days after implantation	Improvement in FS%, LVIDs and LVIDd	none
Kellar et al. [122, 123]	Human Dermal Fibroblast (N/A)	Vicryl Mesh	Female Mice	SCID	2 weeks	Increased overall survival, increased microvessel formation, improved EF, preload recruitable stroke work, and volume at end-systole	Non-viable construct
Miyagawa et al. [131]	Rat Neonatal Cardiomyocytes (1×10^6 / sheet)	N/A	Male Lewis Rats	IC	ECHO 2, 4, 8 weeks; Histology 2, 8 weeks, Electrophysiology	Improved LV AWTh, vessel density, FS%, EF electrical communication with host myocardium	Fibroblast Sheet, collagen membrane
Kofidis et al. [124]	Mouse Embryonic Stem Cells (2.5×10^9 / mL)	Collagen Type I	Rat	Athymic Nude	2 weeks	Improved LV AWTh and FS%	Acellular Collagen
Kofidis et al. [125]	Mouse Embryonic Stem Cells (1×10^6 / 50 μ L)	Matrigel	BALB/c Mice	IC	2 weeks after in situ injection	Increased graft/scar ratio, improved FS%	Matrigel only
Miyahara et al. [133]	Rat Mesenchymal Stem Cells (5×10^5 / sheet)	N/A	Male SD Rats	IC	ECHO, Hemodynamics 4 and 8 weeks; Histology 1-4 weeks	MSC differentiation within host, improved LVDD, FS%, LV AWTh, +/- dP/dt, and LVEDP	Fibroblast sheet
Gaballa et al. [136]	N/A	Collagen Foam	Male Fischer Rats	IC	6 weeks	No change in Hemodynamics, increase vascular density, improved cardiac remodeling	none
Simpson et al. [137]	Human Mesenchymal Stem Cells (1×10^6)	Collagen Type I	Male CDF Rats	IC	4 weeks	Decreased adverse myocardial remodeling, increased myofibroblast presence	Non-viable construct
Wei et al. [135]	Rat Mesenchymal Stem Cells (1.5×10^9 / sheets)	Acellular bovine pericardia	Lewis Rats	IC	12 weeks	Improved FS%, LVEDP and LVESP, increased neovessel formation	none

FS% - Percent fractional shortening, AWTh - Anterior wall thickness, LVDD - Left ventricular diastolic diameter, LVESP - Left ventricular end systolic pressure, LVEDP - Left ventricular end diastolic pressure, LVEDV - Left ventricular end diastolic volume, IC - Immuno-competent, IS - Immuno-suppressed, ECHO – Echocardiography, LVIDd – Left ventricular internal diameter at diastole, LVIDs – Left ventricular internal diameter at systole, SCID - Severe combined immunodeficiency, dP/dt – Change in pressure over time

Tissue engineering, in conjunction with bioreactors and biomimetics, can be used to expand and prepare cells and tissues and offers the ability to develop and test tissue function *in vitro* in a controlled manner [139]. Bioreactors are culture devices and schemes used for scalable cell and tissue production. Bioreactors can be used to reduce time between cell isolation and cell transplantation and to promote progenitor cell differentiation. Biomimetics is a functional system which serves to mimic a biological process. This allows for an *in vitro* test situation for various strategies. Currently, investigators are taking steps to optimize cardiac tissue formation through the combination of cells, biomaterials, and electrical or mechanical stimulation [140-143]. For instance, cardiac organoids have been formed with the intent to develop a working biological model of the left ventricle. This tissue engineered model was shown to contract, develop a small pressure and even eject fluid. This model was responsive to cryoinjury [142], a technique commonly used in animal models to induce myocardial infarction. Bioreactors and biomimetics may allow researchers to develop systems to rapidly optimize cell bioprocessing and cardiomyoplasty.

The versatility of tissue engineering also extends to making chemical modifications to biomaterials for the attachment of proteins, immunosuppressive, or biochemical agents. Such techniques can provide localized bulk delivery of paracrine factors [144, 145] or other molecules which may directly benefit the myocardium or act to enhance engraftment and reduce rejection after cell transplantation. Local delivery of defined factors may also help elucidate the role of these factors in cardiac repair and help overcome roadblocks in understanding the mechanism by which cellular cardiomyoplasty is effective. The rate of release of these factors can also be modulated to prolong their effects or provide a temporal augmentation to the repair process. Furthermore, by using their inherent mechanical properties, the material may also be tailored to provide mechanical support for the ailing heart either transiently, using

biodegradable materials, or permanently in the case of non-degradable substrates. Therefore, tissue engineering may promote higher engraftment rates, improved differentiation, maintenance of progenitor cells, an ability to tailor and sustain the release of various paracrine factors, and assistance in the understanding of cardiac repair via cellular cardiomyoplasty, helping to address the two major issues identified above (Figure 2.10). The issue of engraftment, however relies on the use of tissue engineering as a delivery vehicle. It can be hypothesized that the application of a biocompatible material seeded with progenitor cells will allow for localized and enhanced engraftment beyond that observed with conventional delivery techniques.

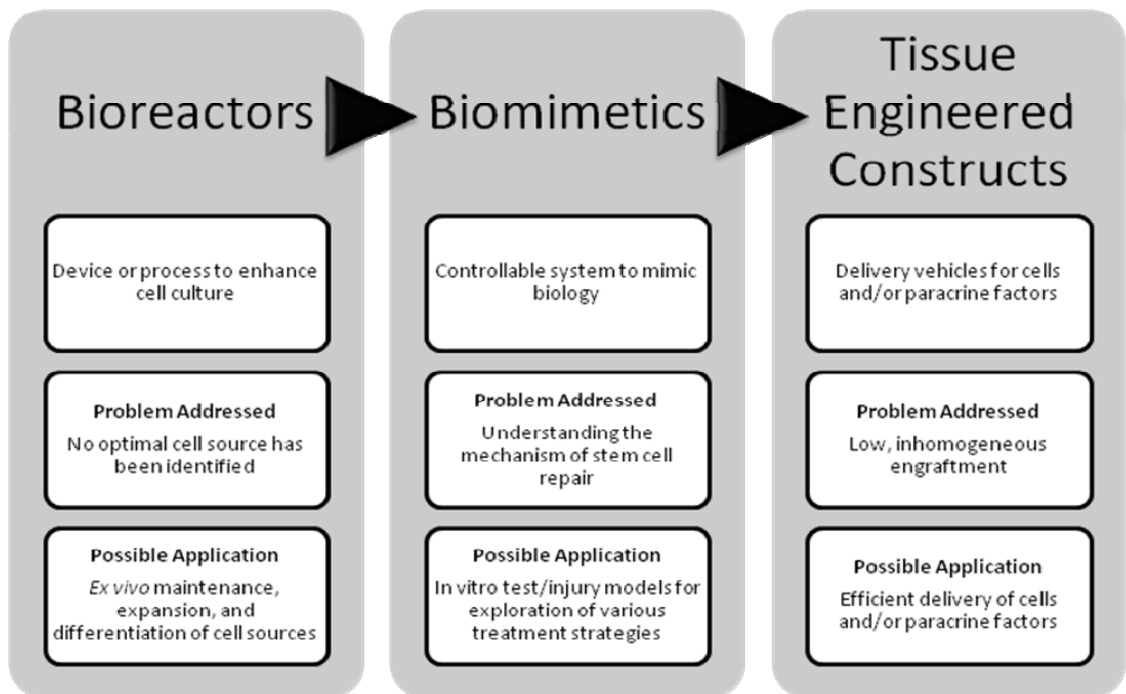


Figure 2.10) Tissue engineering principles are likely to help overcome roadblocks that are slowing the progress of cellular cardiomyoplasty. Bioreactors and biomimetics can be used to create and test functional tissue engineered constructs. These constructs can act to modulate cell function and enhance delivery of cells or paracrine factors.

2.6.5 Summary

The issues preventing clinical success for cellular cardiomyoplasty have proved more formidable than first expected. Although this therapy is a viable option for the treatment of ischemic cardiomyopathy, there are many questions which still need to be addressed. In particular, issues related to optimizing cell source, understanding the mechanism of repair, and enhancing engraftment need to be optimized before maximally successful transition from the laboratory to the clinic will be possible. The use of autologous cells appears to be the safest route, yet obtaining large numbers of cells needed for transplantation limits the cell source pool. Also, there is a lack of understanding the mechanism by which progenitor cells can repair injured myocardium. Enhancing cell engraftment may also play a critical role in enhancing clinical outcomes. Tissue engineering may offer solutions to current problems by allowing for *ex vivo* cell

expansion and differentiation, suitable test models, cell and paracrine factor delivery systems, and replacement tissue, which may bring us a step closer to making cardiomyoplasty a therapeutic option for heart disease patients.

2.7 CONCLUSIONS

The heart is an essential organ. When abnormalities of the heart occur, the progression of several events can lead to a deterioration of cardiac function and secondary damage to other organ systems. Although there are several proposed therapeutic options for patients with degenerative cardiomyopathies, the limited regenerative capacity of the heart, potential side effects of treatment and limited reparative potential of these therapies prevents successful recovery. In addition, a heart transplant, which appears to be the one true cure, is limited by the number of hearts available, matching criteria and significant side effects. Fortunately, research has begun to investigate other potentially useful therapies for cardiac repair. Cellular cardiomyoplasty, which involves the transplantation of a cell source with regenerative properties, has emerged as an exciting option. Unfortunately, issue regarding cell source, mechanisms of repair and enhancement of cell engraftment have made it difficult to translate basic research efforts into the clinic. Biomedical researchers are beginning to decipher the challenges in understanding the heart and treating the heart after injury. In particular, tissue engineering may hold the key to unlocking a vast vault of solutions regarding these roadblocks to cell therapy. There is no end to cardiac regenerative medicine in sight and it is expected that tissue engineering will provide many contributions to the field of cellular cardiomyoplasty.

2.8 REFERENCES

1. W. B. Kannel and A. J. Belanger. Epidemiology of heart failure. *Am Heart J.* 1991 Mar;121:951-7.
2. D. McCall. Epidemiology, Etiology and Natural History. *Heart Failure: Current Topics in Cardiology.* 1995:1-13.
3. S. L. Robbins, R. S. Cotran and V. Kumar. *The Heart. Pathologic Basis of Disease.* 1984:547-609.
4. G. Y. Koh, M. H. Soonpaa, M. G. Klug and L. J. Field. Long-term survival of AT-1 cardiomyocyte grafts in syngeneic myocardium. *Am J Physiol.* 1993 May;264:H1727-33.
5. R. K. Li, Z. Q. Jia, R. D. Weisel, et al. Cardiomyocyte transplantation improves heart function. *Ann Thorac Surg.* 1996 Sep;62:654-60; discussion 60-1.
6. T. Sakai, R. K. Li, R. D. Weisel, et al. Fetal cell transplantation: a comparison of three cell types. *J Thorac Cardiovasc Surg.* 1999 Oct;118:715-24.
7. K. B. Gupta, M. B. Ratcliffe, M. A. Fallert, L. H. Edmunds, Jr. and D. K. Bogen. Changes in passive mechanical stiffness of myocardial tissue with aneurysm formation. *Circulation.* 1994 May;89:2315-26.
8. J. W. Holmes, T. K. Borg and J. W. Covell. Structure and mechanics of healing myocardial infarcts. *Annu Rev Biomed Eng.* 2005;7:223-53.
9. W. Dai, S. L. Hale, B. J. Martin, et al. Allogeneic mesenchymal stem cell transplantation in postinfarcted rat myocardium: short- and long-term effects. *Circulation.* 2005 Jul 12;112:214-23.
10. P. S. Zammit, T. A. Partridge and Z. Yablonka-Reuveni. The skeletal muscle satellite cell: the stem cell that came in from the cold. *J Histochem Cytochem.* 2006 Nov;54:1177-91.
11. C. E. Murry, R. W. Wiseman, S. M. Schwartz and S. D. Hauschka. Skeletal myoblast transplantation for repair of myocardial necrosis. *J Clin Invest.* 1996 Dec 1;98:2512-23.
12. H. Reinecke, V. Poppa and C. E. Murry. Skeletal muscle stem cells do not transdifferentiate into cardiomyocytes after cardiac grafting. *J Mol Cell Cardiol.* 2002 Feb;34:241-9.
13. M. Horackova, R. Arora, R. Chen, et al. Cell transplantation for treatment of acute myocardial infarction: unique capacity for repair by skeletal muscle satellite cells. *Am J Physiol Heart Circ Physiol.* 2004 Oct;287:H1599-608.
14. G. Invernici, S. Cristini, P. Madeddu, et al. Human adult skeletal muscle stem cells differentiate into cardiomyocyte phenotype in vitro. *Exp Cell Res.* 2007 Aug 16.

15. K. V. Pajcini, J. H. Pomerantz, O. Alkan, R. Doyonnas and H. M. Blau. Myoblasts and macrophages share molecular components that contribute to cell-cell fusion. *J Cell Biol.* 2008 Mar 10;180:1005-19.
16. V. Horsley and G. K. Pavlath. Forming a multinucleated cell: molecules that regulate myoblast fusion. *Cells Tissues Organs.* 2004;176:67-78.
17. S. Cherqui, S. M. Kurian, O. Schussler, J. A. Hewel, J. R. Yates, 3rd and D. R. Salomon. Isolation and angiogenesis by endothelial progenitors in the fetal liver. *Stem Cells.* 2006 Jan;24:44-54.
18. G. Parise, I. W. McKinnell and M. A. Rudnicki. Muscle satellite cell and atypical myogenic progenitor response following exercise. *Muscle Nerve.* 2008 May;37:611-9.
19. H. Oh, S. B. Bradfute, T. D. Gallardo, et al. Cardiac progenitor cells from adult myocardium: homing, differentiation, and fusion after infarction. *Proc Natl Acad Sci U S A.* 2003 Oct 14;100:12313-8.
20. K. Matsuura, T. Nagai, N. Nishigaki, et al. Adult cardiac Sca-1-positive cells differentiate into beating cardiomyocytes. *J Biol Chem.* 2004 Mar 19;279:11384-91.
21. C. M. Martin, A. P. Meeson, S. M. Robertson, et al. Persistent expression of the ATP-binding cassette transporter, *Abcg2*, identifies cardiac SP cells in the developing and adult heart. *Dev Biol.* 2004 Jan 1;265:262-75.
22. A. M. Hierlihy, P. Seale, C. G. Lobe, M. A. Rudnicki and L. A. Megeney. The post-natal heart contains a myocardial stem cell population. *FEBS Lett.* 2002 Oct 23;530:239-43.
23. O. Pfister, F. Mouquet, M. Jain, et al. CD31- but Not CD31+ cardiac side population cells exhibit functional cardiomyogenic differentiation. *Circ Res.* 2005 Jul 8;97:52-61.
24. F. Mouquet, O. Pfister, M. Jain, et al. Restoration of cardiac progenitor cells after myocardial infarction by self-proliferation and selective homing of bone marrow-derived stem cells. *Circ Res.* 2005 Nov 25;97:1090-2.
25. A. P. Beltrami, L. Barlucchi, D. Torella, et al. Adult cardiac stem cells are multipotent and support myocardial regeneration. *Cell.* 2003 Sep 19;114:763-76.
26. B. Dawn, A. B. Stein, K. Urbanek, et al. Cardiac stem cells delivered intravascularly traverse the vessel barrier, regenerate infarcted myocardium, and improve cardiac function. *Proc Natl Acad Sci U S A.* 2005 Mar 8;102:3766-71.
27. E. Messina, L. De Angelis, G. Frati, et al. Isolation and expansion of adult cardiac stem cells from human and murine heart. *Circ Res.* 2004 Oct 29;95:911-21.
28. L. Barile, E. Messina, A. Giacomello and E. Marban. Endogenous cardiac stem cells. *Prog Cardiovasc Dis.* 2007 Jul-Aug;50:31-48.

29. K. L. Laugwitz, A. Moretti, J. Lam, et al. Postnatal isl1+ cardioblasts enter fully differentiated cardiomyocyte lineages. *Nature*. 2005 Feb 10;433:647-53.
30. M. F. Pittenger, A. M. Mackay, S. C. Beck, et al. Multilineage potential of adult human mesenchymal stem cells. *Science*. 1999 Apr 2;284:143-7.
31. C. A. Dennis JE. Bone Marrow Mesechymal Stem Cells. *Stem Cells Handbook*.107-17.
32. W. S. Shim, S. Jiang, P. Wong, et al. Ex vivo differentiation of human adult bone marrow stem cells into cardiomyocyte-like cells. *Biochem Biophys Res Commun*. 2004 Nov 12;324:481-8.
33. D. Orlic, J. Kajstura, S. Chimenti, D. M. Bodine, A. Leri and P. Anversa. Transplanted adult bone marrow cells repair myocardial infarcts in mice. *Ann N Y Acad Sci*. 2001 Jun;938:221-9; discussion 9-30.
34. D. Orlic, J. Kajstura, S. Chimenti, et al. Bone marrow cells regenerate infarcted myocardium. *Nature*. 2001 Apr 5;410:701-5.
35. C. E. Murry, M. H. Soonpaa, H. Reinecke, et al. Haematopoietic stem cells do not transdifferentiate into cardiac myocytes in myocardial infarcts. *Nature*. 2004 Apr 8;428:664-8.
36. L. B. Balsam, A. J. Wagers, J. L. Christensen, T. Kofidis, I. L. Weissman and R. C. Robbins. Haematopoietic stem cells adopt mature haematopoietic fates in ischaemic myocardium. *Nature*. 2004 Apr 8;428:668-73.
37. C. Toma, M. F. Pittenger, K. S. Cahill, B. J. Byrne and P. D. Kessler. Human mesenchymal stem cells differentiate to a cardiomyocyte phenotype in the adult murine heart. *Circulation*. 2002 Jan 1;105:93-8.
38. A. A. Mangi, N. Noiseux, D. Kong, et al. Mesenchymal stem cells modified with Akt prevent remodeling and restore performance of infarcted hearts. *Nat Med*. 2003 Sep;9:1195-201.
39. W. Jiang, A. Ma, T. Wang, et al. Homing and differentiation of mesenchymal stem cells delivered intravenously to ischemic myocardium in vivo: a time-series study. *Pflugers Arch*. 2006 Aug 17.
40. M. Kudo, Y. Wang, M. A. Wani, M. Xu, A. Ayub and M. Ashraf. Implantation of bone marrow stem cells reduces the infarction and fibrosis in ischemic mouse heart. *J Mol Cell Cardiol*. 2003 Sep;35:1113-9.
41. Y. L. Tang, Q. Zhao, Y. C. Zhang, et al. Autologous mesenchymal stem cell transplantation induce VEGF and neovascularization in ischemic myocardium. *Regul Pept*. 2004 Jan 15;117:3-10.
42. J. Y. Min, M. F. Sullivan, Y. Yang, et al. Significant improvement of heart function by cotransplantation of human mesenchymal stem cells and fetal cardiomyocytes in postinfarcted pigs. *Ann Thorac Surg*. 2002 Nov;74:1568-75.

43. P. A. Zuk, M. Zhu, H. Mizuno, et al. Multilineage cells from human adipose tissue: implications for cell-based therapies. *Tissue Eng.* 2001 Apr;7:211-28.
44. P. A. Zuk, M. Zhu, P. Ashjian, et al. Human adipose tissue is a source of multipotent stem cells. *Mol Biol Cell.* 2002 Dec;13:4279-95.
45. S. Rangappa, C. Fen, E. H. Lee, A. Bongso and E. K. Sim. Transformation of adult mesenchymal stem cells isolated from the fatty tissue into cardiomyocytes. *Ann Thorac Surg.* 2003 Mar;75:775-9.
46. K. G. Gaustad, A. C. Boquest, B. E. Anderson, A. M. Gerdes and P. Collas. Differentiation of human adipose tissue stem cells using extracts of rat cardiomyocytes. *Biochem Biophys Res Commun.* 2004 Feb 6;314:420-7.
47. V. Planat-Benard, C. Menard, M. Andre, et al. Spontaneous cardiomyocyte differentiation from adipose tissue stroma cells. *Circ Res.* 2004 Feb 6;94:223-9.
48. B. M. Strem, M. Zhu, Z. Alfonso, et al. Expression of cardiomyocytic markers on adipose tissue-derived cells in a murine model of acute myocardial injury. *Cytotherapy.* 2005;7:282-91.
49. A. Miranville, C. Heeschen, C. Sengenès, C. A. Curat, R. Busse and A. Bouloumie. Improvement of postnatal neovascularization by human adipose tissue-derived stem cells. *Circulation.* 2004 Jul 20;110:349-55.
50. K. Schenke-Layland, B. M. Strem, M. C. Jordan, et al. Adipose Tissue-Derived Cells Improve Cardiac Function Following Myocardial Infarction. *J Surg Res.* 2008 Apr 10.
51. J. Rehman, D. Traktuev, J. Li, et al. Secretion of angiogenic and antiapoptotic factors by human adipose stromal cells. *Circulation.* 2004 Mar 16;109:1292-8.
52. P. De Coppi, G. Bartsch, Jr., M. M. Siddiqui, et al. Isolation of amniotic stem cell lines with potential for therapy. *Nat Biotechnol.* 2007 Jan;25:100-6.
53. S. Sartore, M. Lenzi, A. Angelini, et al. Amniotic mesenchymal cells autotransplanted in a porcine model of cardiac ischemia do not differentiate to cardiogenic phenotypes. *Eur J Cardiothorac Surg.* 2005 Nov;28:677-84.
54. A. Chiavegato, S. Bollini, M. Pozzobon, et al. Human amniotic fluid-derived stem cells are rejected after transplantation in the myocardium of normal, ischemic, immunosuppressed or immuno-deficient rat. *J Mol Cell Cardiol.* 2007 Apr;42:746-59.
55. X. Zeng, T. Miura, Y. Luo, et al. Properties of pluripotent human embryonic stem cells BG01 and BG02. *Stem Cells.* 2004;22:292-312.
56. J. Itskovitz-Eldor, M. Schuldiner, D. Karsenti, et al. Differentiation of human embryonic stem cells into embryoid bodies compromising the three embryonic germ layers. *Mol Med.* 2000 Feb;6:88-95.

57. J. A. Thomson, J. Itskovitz-Eldor, S. S. Shapiro, et al. Embryonic stem cell lines derived from human blastocysts. *Science*. 1998 Nov 6;282:1145-7.
58. M. Mitalipova, J. Calhoun, S. Shin, et al. Human embryonic stem cell lines derived from discarded embryos. *Stem Cells*. 2003;21:521-6.
59. I. Kehat and L. Gepstein. Human embryonic stem cells for myocardial regeneration. *Heart Fail Rev*. 2003 Jul;8:229-36.
60. C. Mummery, D. Ward-van Oostwaard, P. Doevendans, et al. Differentiation of human embryonic stem cells to cardiomyocytes: role of coculture with visceral endoderm-like cells. *Circulation*. 2003 Jun 3;107:2733-40.
61. C. Mummery, D. Ward, C. E. van den Brink, et al. Cardiomyocyte differentiation of mouse and human embryonic stem cells. *J Anat*. 2002 Mar;200:233-42.
62. D. K. Singla, T. A. Hacker, L. Ma, et al. Transplantation of embryonic stem cells into the infarcted mouse heart: formation of multiple cell types. *J Mol Cell Cardiol*. 2006 Jan;40:195-200.
63. M. A. Laflamme, K. Y. Chen, A. V. Naumova, et al. Cardiomyocytes derived from human embryonic stem cells in pro-survival factors enhance function of infarcted rat hearts. *Nat Biotechnol*. 2007 Sep;25:1015-24.
64. R. J. Swijnenburg, M. Tanaka, H. Vogel, et al. Embryonic stem cell immunogenicity increases upon differentiation after transplantation into ischemic myocardium. *Circulation*. 2005 Aug 30;112:1166-72.
65. J. Nussbaum, E. Minami, M. A. Laflamme, et al. Transplantation of undifferentiated murine embryonic stem cells in the heart: teratoma formation and immune response. *FASEB J*. 2007 May;21:1345-57.
66. K. Takahashi, K. Tanabe, M. Ohnuki, et al. Induction of pluripotent stem cells from adult human fibroblasts by defined factors. *Cell*. 2007 Nov 30;131:861-72.
67. K. Takahashi and S. Yamanaka. Induction of pluripotent stem cells from mouse embryonic and adult fibroblast cultures by defined factors. *Cell*. 2006 Aug 25;126:663-76.
68. W. E. Lowry, L. Richter, R. Yachechko, et al. Generation of human induced pluripotent stem cells from dermal fibroblasts. *Proc Natl Acad Sci U S A*. 2008 Feb 26;105:2883-8.
69. Y. Shi, C. Desponts, J. T. Do, H. S. Hahm, H. R. Scholer and S. Ding. Induction of pluripotent stem cells from mouse embryonic fibroblasts by Oct4 and Klf4 with small-molecule compounds. *Cell Stem Cell*. 2008 Nov 6;3:568-74.
70. D. Huangfu, K. Osafune, R. Maehr, et al. Induction of pluripotent stem cells from primary human fibroblasts with only Oct4 and Sox2. *Nat Biotechnol*. 2008 Nov;26:1269-75.

71. M. Nakagawa, M. Koyanagi, K. Tanabe, et al. Generation of induced pluripotent stem cells without Myc from mouse and human fibroblasts. *Nat Biotechnol.* 2008 Jan;26:101-6.
72. M. Stadtfeld, M. Nagaya, J. Utikal, G. Weir and K. Hochedlinger. Induced pluripotent stem cells generated without viral integration. *Science.* 2008 Nov 7;322:945-9.
73. K. Okita, M. Nakagawa, H. Hyenjong, T. Ichisaka and S. Yamanaka. Generation of mouse induced pluripotent stem cells without viral vectors. *Science.* 2008 Nov 7;322:949-53.
74. K. Okita, T. Ichisaka and S. Yamanaka. Generation of germline-competent induced pluripotent stem cells. *Nature.* 2007 Jul 19;448:313-7.
75. J. Zhang, G. F. Wilson, A. G. Soerens, et al. Functional cardiomyocytes derived from human induced pluripotent stem cells. *Circ Res.* 2009 Feb 27;104:e30-41.
76. K. E. van der Bogt, A. Y. Sheikh, S. Schrepfer, et al. Comparison of different adult stem cell types for treatment of myocardial ischemia. *Circulation.* 2008 Sep 30;118:S121-9.
77. K. K. Poh, E. Sperry, R. G. Young, T. Freyman, K. G. Barringhaus and C. A. Thompson. Repeated direct endomyocardial transplantation of allogeneic mesenchymal stem cells: safety of a high dose, "off-the-shelf", cellular cardiomyoplasty strategy. *Int J Cardiol.* 2007 May 2;117:360-4.
78. A. C. Diederichsen, J. E. Moller, P. Thayssen, et al. Effect of repeated intracoronary injection of bone marrow cells in patients with ischaemic heart failure the Danish stem cell study--congestive heart failure trial (DanCell-CHF). *Eur J Heart Fail.* 2008 Jul;10:661-7.
79. K. Hamano, M. Nishida, K. Hirata, et al. Local implantation of autologous bone marrow cells for therapeutic angiogenesis in patients with ischemic heart disease: clinical trial and preliminary results. *Jpn Circ J.* 2001 Sep;65:845-7.
80. B. E. Strauer, M. Brehm, T. Zeus, et al. Repair of infarcted myocardium by autologous intracoronary mononuclear bone marrow cell transplantation in humans. *Circulation.* 2002 Oct 8;106:1913-8.
81. X. Hu, J. Wang, J. Chen, et al. Optimal temporal delivery of bone marrow mesenchymal stem cells in rats with myocardial infarction. *Eur J Cardiothorac Surg.* 2007 Mar;31:438-43.
82. B. Assmus, V. Schachinger, C. Teupe, et al. Transplantation of Progenitor Cells and Regeneration Enhancement in Acute Myocardial Infarction (TOPCARE-AMI). *Circulation.* 2002 Dec 10;106:3009-17.
83. V. Schachinger, B. Assmus, M. B. Britten, et al. Transplantation of progenitor cells and regeneration enhancement in acute myocardial infarction: final one-year results of the TOPCARE-AMI Trial. *J Am Coll Cardiol.* 2004 Oct 19;44:1690-9.

84. C. Stamm, B. Westphal, H. D. Kleine, et al. Autologous bone-marrow stem-cell transplantation for myocardial regeneration. *Lancet*. 2003 Jan 4;361:45-6.
85. H. F. Tse, Y. L. Kwong, J. K. Chan, G. Lo, C. L. Ho and C. P. Lau. Angiogenesis in ischaemic myocardium by intramyocardial autologous bone marrow mononuclear cell implantation. *Lancet*. 2003 Jan 4;361:47-9.
86. E. C. Perin, H. F. Dohmann, R. Borojevic, et al. Transendocardial, autologous bone marrow cell transplantation for severe, chronic ischemic heart failure. *Circulation*. 2003 May 13;107:2294-302.
87. A. N. Patel, L. Geffner, R. F. Vina, et al. Surgical treatment for congestive heart failure with autologous adult stem cell transplantation: a prospective randomized study. *J Thorac Cardiovasc Surg*. 2005 Dec;130:1631-8.
88. K. C. Wollert, G. P. Meyer, J. Lotz, et al. Intracoronary autologous bone-marrow cell transfer after myocardial infarction: the BOOST randomised controlled clinical trial. *Lancet*. 2004 Jul 10-16;364:141-8.
89. P. Menasche, A. A. Hagege, J. T. Vilquin, et al. Autologous skeletal myoblast transplantation for severe postinfarction left ventricular dysfunction. *J Am Coll Cardiol*. 2003 Apr 2;41:1078-83.
90. F. D. Pagani, H. DerSimonian, A. Zawadzka, et al. Autologous skeletal myoblasts transplanted to ischemia-damaged myocardium in humans. Histological analysis of cell survival and differentiation. *J Am Coll Cardiol*. 2003 Mar 5;41:879-88.
91. B. Assmus, J. Honold, V. Schachinger, et al. Transcoronary transplantation of progenitor cells after myocardial infarction. *N Engl J Med*. 2006 Sep 21;355:1222-32.
92. G. Marenzi and A. L. Bartorelli. Improved clinical outcome after intracoronary administration of bone marrow-derived progenitor cells in acute myocardial infarction: final 1-year results of the REPAIR-AMI trial. *Eur Heart J*. 2007 Sep;28:2172-3; author reply 3-4.
93. V. Schachinger, S. Erbs, A. Elsasser, et al. Intracoronary bone marrow-derived progenitor cells in acute myocardial infarction. *N Engl J Med*. 2006 Sep 21;355:1210-21.
94. V. Schachinger, S. Erbs, A. Elsasser, et al. Improved clinical outcome after intracoronary administration of bone-marrow-derived progenitor cells in acute myocardial infarction: final 1-year results of the REPAIR-AMI trial. *Eur Heart J*. 2006 Dec;27:2775-83.
95. K. Lunde, S. Solheim, S. Aakhus, et al. Intracoronary injection of mononuclear bone marrow cells in acute myocardial infarction. *N Engl J Med*. 2006 Sep 21;355:1199-209.
96. T. Egeland and J. E. Brinchmann. The REPAIR-AMI and ASTAMI trials: cell isolation procedures. *Eur Heart J*. 2007 Sep;28:2174-5; author reply 5.

97. clinicaltrials.gov. 2008.
98. T. Freyman, G. Polin, H. Osman, et al. A quantitative, randomized study evaluating three methods of mesenchymal stem cell delivery following myocardial infarction. *Eur Heart J*. 2006 May;27:1114-22.
99. I. M. Barbash, P. Chouraqui, J. Baron, et al. Systemic delivery of bone marrow-derived mesenchymal stem cells to the infarcted myocardium: feasibility, cell migration, and body distribution. *Circulation*. 2003 Aug 19;108:863-8.
100. T. H. Park, S. F. Nagueh, D. S. Khoury, et al. Impact of myocardial structure and function postinfarction on diastolic strain measurements: implications for assessment of myocardial viability. *Am J Physiol Heart Circ Physiol*. 2006 Feb;290:H724-31.
101. S. Fukushima, S. R. Coppen, J. Lee, et al. Choice of cell-delivery route for skeletal myoblast transplantation for treating post-infarction chronic heart failure in rat. *PLoS ONE*. 2008;3:e3071.
102. D. K. Singla, G. E. Lyons and T. J. Kamp. Transplanted embryonic stem cells following mouse myocardial infarction inhibit apoptosis and cardiac remodeling. *Am J Physiol Heart Circ Physiol*. 2007 Aug;293:H1308-14.
103. J. Y. Min, Y. Yang, K. L. Converso, et al. Transplantation of embryonic stem cells improves cardiac function in postinfarcted rats. *J Appl Physiol*. 2002 Jan;92:288-96.
104. J. Y. Min, Y. Yang, M. F. Sullivan, et al. Long-term improvement of cardiac function in rats after infarction by transplantation of embryonic stem cells. *J Thorac Cardiovasc Surg*. 2003 Feb;125:361-9.
105. M. A. Laflamme, J. Gold, C. Xu, et al. Formation of human myocardium in the rat heart from human embryonic stem cells. *Am J Pathol*. 2005 Sep;167:663-71.
106. L. C. Amado, A. P. Saliaris, K. H. Schuleri, et al. Cardiac repair with intramyocardial injection of allogeneic mesenchymal stem cells after myocardial infarction. *Proc Natl Acad Sci U S A*. 2005 Aug 9;102:11474-9.
107. Y. L. Tang, Q. Zhao, X. Qin, et al. Paracrine action enhances the effects of autologous mesenchymal stem cell transplantation on vascular regeneration in rat model of myocardial infarction. *Ann Thorac Surg*. 2005 Jul;80:229-36; discussion 36-7.
108. S. Ohnishi, H. Sumiyoshi, S. Kitamura and N. Nagaya. Mesenchymal stem cells attenuate cardiac fibroblast proliferation and collagen synthesis through paracrine actions. *FEBS Lett*. 2007 Aug 21;581:3961-6.
109. M. G. Chang, L. Tung, R. B. Sekar, et al. Proarrhythmic potential of mesenchymal stem cell transplantation revealed in an in vitro coculture model. *Circulation*. 2006 Apr 18;113:1832-41.
110. M. Takahashi, T. S. Li, R. Suzuki, et al. Cytokines produced by bone marrow cells can contribute to functional improvement of the infarcted heart by protecting

cardiomyocytes from ischemic injury. *Am J Physiol Heart Circ Physiol*. 2006 Aug;291:H886-93.

111. D. Ladage, K. Brixius, C. Steingen, et al. Mesenchymal stem cells induce endothelial activation via paracrine mechanisms. *Endothelium*. 2007 Mar-Apr;14:53-63.

112. W. Li, N. Ma, L. L. Ong, et al. Bcl-2 engineered MSCs inhibited apoptosis and improved heart function. *Stem Cells*. 2007 Aug;25:2118-27.

113. M. Xu, R. Uemura, Y. Dai, Y. Wang, Z. Pasha and M. Ashraf. In vitro and in vivo effects of bone marrow stem cells on cardiac structure and function. *J Mol Cell Cardiol*. 2007 Feb;42:441-8.

114. M. Mirotsov, Z. Zhang, A. Deb, et al. Secreted frizzled related protein 2 (Sfrp2) is the key Akt-mesenchymal stem cell-released paracrine factor mediating myocardial survival and repair. *Proc Natl Acad Sci U S A*. 2007 Jan 30;104:1643-8.

115. M. Gnecci, H. He, N. Noiseux, et al. Evidence supporting paracrine hypothesis for Akt-modified mesenchymal stem cell-mediated cardiac protection and functional improvement. *FASEB J*. 2006 Apr;20:661-9.

116. M. Korf-Klingebiel, T. Kempf, T. Sauer, et al. Bone marrow cells are a rich source of growth factors and cytokines: implications for cell therapy trials after myocardial infarction. *Eur Heart J*. 2008 Oct 25.

117. H. Ebel, M. Jungblut, Y. Zhang, et al. Cellular cardiomyoplasty: improvement of left ventricular function correlates with the release of cardioactive cytokines. *Stem Cells*. 2007 Jan;25:236-44.

118. A. S. Blom, R. Mukherjee, J. J. Pilla, et al. Cardiac support device modifies left ventricular geometry and myocardial structure after myocardial infarction. *Circulation*. 2005 Aug 30;112:1274-83.

119. R. K. Li, Z. Q. Jia, R. D. Weisel, D. A. Mickle, A. Choi and T. M. Yau. Survival and function of bioengineered cardiac grafts. *Circulation*. 1999 Nov 9;100:II63-9.

120. K. L. Christman, H. H. Fok, R. E. Sievers, Q. Fang and R. J. Lee. Fibrin glue alone and skeletal myoblasts in a fibrin scaffold preserve cardiac function after myocardial infarction. *Tissue Eng*. 2004 Mar-Apr;10:403-9.

121. W. H. Zimmermann, I. Melnychenko, G. Wasmeier, et al. Engineered heart tissue grafts improve systolic and diastolic function in infarcted rat hearts. *Nat Med*. 2006 Apr;12:452-8.

122. R. S. Kellar, L. K. Landeen, B. R. Shepherd, G. K. Naughton, A. Ratcliffe and S. K. Williams. Scaffold-based three-dimensional human fibroblast culture provides a structural matrix that supports angiogenesis in infarcted heart tissue. *Circulation*. 2001 Oct 23;104:2063-8.

123. R. S. Kellar, B. R. Shepherd, D. F. Larson, G. K. Naughton and S. K. Williams. Cardiac patch constructed from human fibroblasts attenuates reduction in cardiac function after acute infarct. *Tissue Eng.* 2005 Nov-Dec;11:1678-87.
124. T. Kofidis, J. L. de Bruin, G. Hoyt, et al. Myocardial restoration with embryonic stem cell bioartificial tissue transplantation. *J Heart Lung Transplant.* 2005 Jun;24:737-44.
125. T. Kofidis, J. L. de Bruin, G. Hoyt, et al. Injectable bioartificial myocardial tissue for large-scale intramural cell transfer and functional recovery of injured heart muscle. *J Thorac Cardiovasc Surg.* 2004 Oct;128:571-8.
126. W. H. Zimmermann and T. Eschenhagen. Cardiac tissue engineering for replacement therapy. *Heart Fail Rev.* 2003 Jul;8:259-69.
127. R. L. Carrier, M. Papadaki, M. Rupnick, et al. Cardiac tissue engineering: cell seeding, cultivation parameters, and tissue construct characterization. *Biotechnol Bioeng.* 1999 Sep 5;64:580-9.
128. T. Shimizu, M. Yamato, A. Kikuchi and T. Okano. Two-dimensional manipulation of cardiac myocyte sheets utilizing temperature-responsive culture dishes augments the pulsatile amplitude. *Tissue Eng.* 2001 Apr;7:141-51.
129. I. A. Memon, Y. Sawa, N. Fukushima, et al. Repair of impaired myocardium by means of implantation of engineered autologous myoblast sheets. *J Thorac Cardiovasc Surg.* 2005 Nov;130:1333-41.
130. J. Leor, S. Aboulafia-Etzion, A. Dar, et al. Bioengineered cardiac grafts: A new approach to repair the infarcted myocardium? *Circulation.* 2000 Nov 7;102:III56-61.
131. S. Miyagawa, Y. Sawa, S. Sakakida, et al. Tissue cardiomyoplasty using bioengineered contractile cardiomyocyte sheets to repair damaged myocardium: their integration with recipient myocardium. *Transplantation.* 2005 Dec 15;80:1586-95.
132. J. Liu, Q. Hu, Z. Wang, et al. Autologous stem cell transplantation for myocardial repair. *Am J Physiol Heart Circ Physiol.* 2004 Aug;287:H501-11.
133. Y. Miyahara, N. Nagaya, M. Kataoka, et al. Monolayered mesenchymal stem cells repair scarred myocardium after myocardial infarction. *Nat Med.* 2006 Apr;12:459-65.
134. G. Zhang, X. Wang, Z. Wang, J. Zhang and L. Suggs. A PEGylated fibrin patch for mesenchymal stem cell delivery. *Tissue Eng.* 2006 Jan;12:9-19.
135. H. J. Wei, C. H. Chen, W. Y. Lee, et al. Bioengineered cardiac patch constructed from multilayered mesenchymal stem cells for myocardial repair. *Biomaterials.* 2008 Sep;29:3547-56.
136. M. A. Gaballa, J. N. Sunkomat, H. Thai, E. Morkin, G. Ewy and S. Goldman. Grafting an acellular 3-dimensional collagen scaffold onto a non-transmural infarcted

myocardium induces neo-angiogenesis and reduces cardiac remodeling. *J Heart Lung Transplant*. 2006 Aug;25:946-54.

137. E. Engel, E. Martinez, C. A. Mills, M. Funes, J. A. Planell and J. Samitier. Mesenchymal stem cell differentiation on microstructured poly (methyl methacrylate) substrates. *Ann Anat*. 2008 Sep 27.

138. J. Xie, S. M. Willerth, X. Li, et al. The differentiation of embryonic stem cells seeded on electrospun nanofibers into neural lineages. *Biomaterials*. 2009 Jan;30:354-62.

139. W. L. Grayson, T. P. Martens, G. M. Eng, M. Radisic and G. Vunjak-Novakovic. Biomimetic approach to tissue engineering. *Semin Cell Dev Biol*. 2008 Dec 25.

140. M. Radisic, H. Park, S. Gerecht, C. Cannizzaro, R. Langer and G. Vunjak-Novakovic. Biomimetic approach to cardiac tissue engineering. *Philos Trans R Soc Lond B Biol Sci*. 2007 Aug 29;362:1357-68.

141. M. Radisic, H. Park, H. Shing, et al. Functional assembly of engineered myocardium by electrical stimulation of cardiac myocytes cultured on scaffolds. *Proc Natl Acad Sci U S A*. 2004 Dec 28;101:18129-34.

142. E. J. Lee, E. Kim do, E. U. Azeloglu and K. D. Costa. Engineered cardiac organoid chambers: toward a functional biological model ventricle. *Tissue Eng Part A*. 2008 Feb;14:215-25.

143. W. H. Zimmermann, K. Schneiderbanger, P. Schubert, et al. Tissue engineering of a differentiated cardiac muscle construct. *Circ Res*. 2002 Feb 8;90:223-30.

144. M. E. Davis, P. C. Hsieh, T. Takahashi, et al. Local myocardial insulin-like growth factor 1 (IGF-1) delivery with biotinylated peptide nanofibers improves cell therapy for myocardial infarction. *Proc Natl Acad Sci U S A*. 2006 May 23;103:8155-60.

145. I. Kutschka, I. Y. Chen, T. Kofidis, et al. Collagen matrices enhance survival of transplanted cardiomyoblasts and contribute to functional improvement of ischemic rat hearts. *Circulation*. 2006 Jul 4;114:1167-73.

Chapter 3

A Tissue Engineering Approach to Cell Delivery Results in Significant Cell Engraftment and Improved Myocardial Remodeling: A Proof of Concept*

3.1 INTRODUCTION

Myocardial infarction is the term for heart muscle death, either apoptotic or necrotic, resulting from an impaired myocardial blood supply. Repair of infarcted myocardium is mediated largely by fibroblast proliferation, collagen deposition, and scar formation[1, 2]. The myocardium does not regenerate appreciably because of the limited pool of cardiac specific progenitor cells present and the inability of adult cardiomyocytes to proliferate[3]. Recently, cellular cardiomyoplasty has been proposed as a strategy to repair myocardial damage after injury. This strategy involves encouraging replacement of lost myocardium with new cells having desirable properties. To date, addition of skeletal myoblasts[4-6], smooth muscle cells[7], fibroblast[8], hematopoietic stem cells[9], cardiomyocytes[10, 11], umbilical cord blood derived cells[12], embryonic stem cells[13, 14] and mesenchymal stem cells[15, 16] have shown improvement in cardiac function after myocardial infarction in animal models. Despite some disappointing results, several clinical trials suggest efficacy of cellular cardiomyoplasty in the treatment of human heart disease[17-20].

One factor likely to influence the success of cellular cardiomyoplasty is the number of cells delivered to the area of damage. Typical approaches to deliver cells to infarcted myocardium include intravenous (IV) injection, intracoronary (IC) injection, retrograde venous intracoronary (RIC) infusion, and intramyocardial (IM) injection. Although IV injection offers the advantage of being minimally invasive, it suffers from low cell engraftment (< 1%) into the injury area [21, 22]. IC injection and RIC infusion provide somewhat more localized delivery of cells, resulting in improved but still limited

cell engraftment (3-6%)[21, 23]. IM injection offers direct localization of cells to the injured area, but engraftment (6-12%) is limited by leakage out of the injection sites and cellular washout into the native venous shunts[22]. Moreover, this technique results in inhomogeneous cell delivery with cell “islands” within the myocardial scar [18].

Therefore, we tested the possibility that a biodegradable, cellularized construct applied directly on the epicardial surface of the infarction could result in uniform delivery of cells with better engraftment efficacy than the more traditional cell delivery techniques. We refer to this construct as a “cardiac patch”.

3.2 MATERIALS and METHODS

3.2.1 Animal Handling

Male CDF rats obtained from Charles River (Wilmington, MA) were allowed to acclimate to housing conditions for one week before use. All animals received care in compliance with federal and institutional guidelines with approval from the Institutional Animal Care and Use Committee.

3.2.2 Production of Cardiac Patches

We used patches containing bone marrow-derived human mesenchymal stem cells (hMSCs) because several studies have shown benefits with the use of these cells and because they are currently being used in several human clinical trials[17-19, 24]. CD34 negative hMSC obtained from Cambrex Inc. (Walkersville, MD) were expanded to P3 – P6 before being embedded into a rat tail type I collagen matrix (BD Biosciences; San Jose, California). hMSC were cultured in complete media consisting of Dulbecco’s Modified Eagle’s Medium (DMEM) containing 10% MSC qualified serum, L-glutamine and penicillin/streptomycin at 37°C in 5% CO₂ (Cambrex Inc.). To produce cardiac patches for progenitor cell delivery, one million hMSCs were resuspended in a solution

of rat tail collagen type I (BD Biosciences, Bedford, MA), 10% fetal bovine serum (FBS) 0.1 M NaOH and adjusted with 5x DMEM (Gibco, Carlsbad, CA) such that the final collagen concentration was 2 mg/mL and the initial volume was 200 μ L. Then, the solution was placed in individual wells of a non-tissue culture-treated 48-well plate in order to create a patch that was between 0.3 – 0.7 cm in diameter. Non-tissue culture-treated plates were chosen to minimize cell lost due to migration. As shown in figure 3.1, there appeared to be decreased cellularity within patches (See section 3.2.4.3) cultured in treated plates compared to non-treated plates after four days.

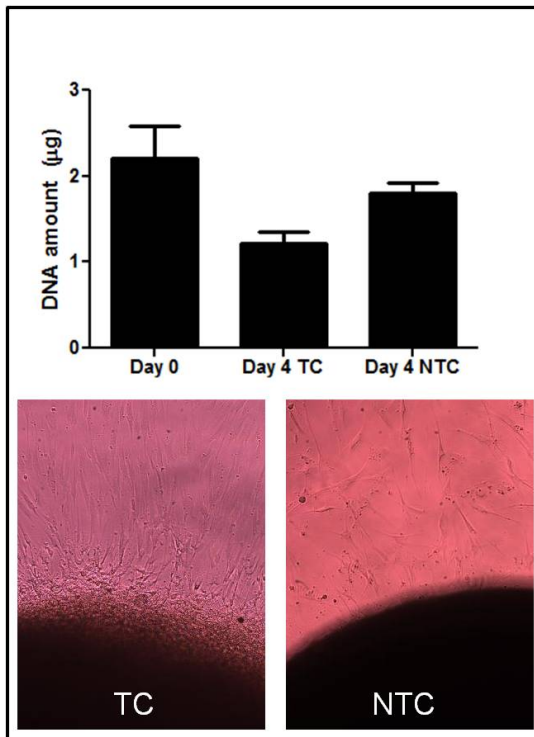


Figure 3.1) Apparent cell migration with culture on tissue culture (TC) treated plates. There is a nonsignificant reduction in cellularity (DNA content) of cardiac patches over four days under normal culture conditions. Additionally, more cells appear to be attaching and migrating from the patch over two days in culture. This data set provided rationale to culture cardiac patches in non-tissue culture (NTC) treated plates.

Patches were cultured at 37°C in 5% CO₂ for 4-7 d before usage. For the control experiments, non-viable cardiac patches were prepared by freezing four day old patches overnight in phosphate buffered saline at -80°C. The patches were thawed at room temperature and used for subsequent experiments. The resulting non-viable (NV) patches demonstrated significantly reduced viability (figure 3.2).

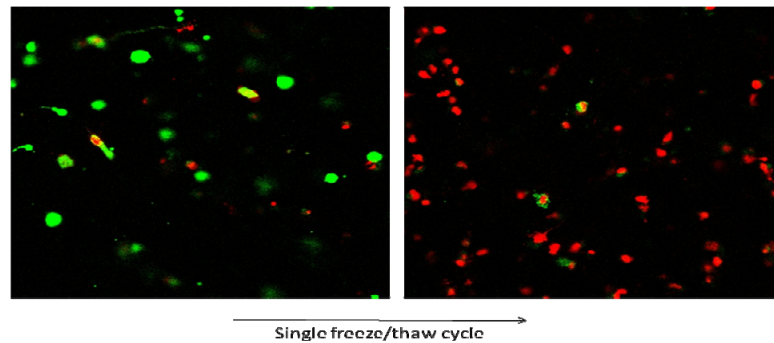


Figure 3.2) A single freeze/thaw cycle leads to complete loss of viability in cardiac patches. To create NV patches, we quickly froze viable cardiac patches at -80°C in sterile PBS. Afterwards patches were thawed and used as controls in animal experiments. A live/dead assay was performed to assess the efficacy of the single freeze/thaw cycle to promote cellular death. This assay revealed complete loss of viability within cardiac patches.

Compaction of the patch, a property thought to describe cell interaction with the collagen, was determined by measuring the change in area of the patch over 5 d. The change in cross-sectional area was measured by taking images of the construct every 24 h and measuring the diameter along at least three different dimensions using Matrox Inspector 3.0 software (Dorval, Québec, Canada). Diameters were converted into areas, and change was represented as the percent reduction in area over five days. In addition, compaction of hMSC patches was determined by measuring the change in volume of the patch over 7 d. Patches were removed from culture dishes and washed several times to remove media/serum using PBS. Afterwards patches were placed in a 10 mL volumetric flask (containing 10mL of serum-free DMEM). The location of the initial

volume was indicated using the “10 mL” marking on the side of the flask. The change in volume was measured after submersing patches in DMEM. The change in volume after submersion was obtained using a micro-volume syringe. DMEM was removed from the flask until the volume reached the initial location as indicated by the “10 mL” marking. The volume removed after submersion was recorded as the volume of the patches at one to five days.

3.2.3 Characterization of hMSC in the Cardiac Patch

3.2.3.1 Viability

To assess cell viability within the construct, patches were digested in type I collagenase (650 U/mL, Worthington Biochemical Corporation; Lakewood, NJ) for 45 min at 37°C. Collagenase activity was inhibited by the addition of FBS and complete hMSC media. Viability was measured using trypan blue with a hemocytometer. In addition, viability was assessed via fluorescence microscopy. Briefly, constructs were washed 3x in phosphate buffered saline (PBS) to remove serum. Fluorescent EthD-1 (4 µM, red) and Calcein AM (4 µM, green) (Molecular Probes; Eugene, Oregon) were then added for 45 min. Afterwards, constructs were washed 3x in PBS and viewed with a confocal microscope.

3.2.3.2 Differentiation

Differentiation of hMSCs within the patch was measured by monitoring the expression of CD73 (SH3) and CD105 (SH2) over seven days. Cells were isolated from the patch by treatment in collagenase (650 U/mL) for 30 min at 37°C. Collagenase activity was inhibited by the addition of FBS and complete media, and cells were washed in complete media. Cells were stained with anti-CD73 and anti-CD105 diluted in 0.3%

bovine serum albumin at 2-4°C for 30 min. Cells were then washed with PBS and analyzed by flow cytometry (BD; San Jose, CA).

3.2.3.3 Cellularity

Cellularity was measured by quantifying the amount of DNA within cardiac patches. Constructs were digested in a mild detergent with proteinase K for 1-2 hours at 55°C and DNA was isolated and purified using a DNeasy kit (Qiagen; Valencia, CA). The amount of DNA was quantified by incubating DNA with PicoGreen reagent for five minutes at room temperature and analyzed with a fluorescent plate reader at an excitation of 480nm and emission of 520nm. RFU values were compared with a standard curve and DNA concentrations were calculated at zero to five days after patch formation.

3.2.4 Infarct Model and Patch Application

Myocardial infarction (MI) was induced by permanent ligation of the left anterior descending (LAD) coronary artery in immuno-competent male CDF rats. Briefly, rats were anesthetized with 1.5% isoflurane. After endotracheal intubation and initiation of ventilation, the heart was exposed via a left thoracotomy and the proximal LAD was ligated. Ten minutes after ligation, patches were applied onto the anterior wall of infarct site and secured with fibrin glue (Baxter; Deerfield, IL; Figure 3.3). Rats with induced infarction and without construct application or with an acellular construct served as controls. Buprenorphine (0.03mg/kg) was injected subcutaneously after surgery (and as necessary), and rats were allowed to recover under close supervision.

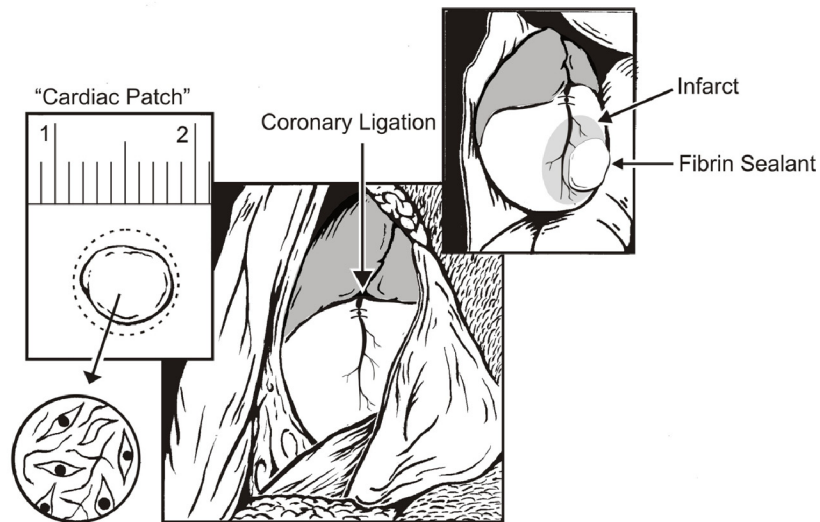


Figure 3.3) Overview of induced infarct and patch placement methodology. Collagen based patches seeded with human mesenchymal stem cells are allowed to culture for 4 days before placement. A permanent ligation of the left anterior descending artery is used to induce myocardial infarction. Afterwards the cardiac patch is placed onto the anterior wall of the heart below the ligation point and held in place with fibrin sealant.

3.2.5 Echocardiography

Transthoracic echocardiograms were performed on rats using a SONOS 5500 ultrasound unit (Philips Medical Systems, Bothell, WA) equipped with a 15-MHz linear-array transducer and a 12-MHz phase-array transducer. The animals were maintained lightly anesthetized during the procedure with 1% isoflurane delivered through a face mask at a rate of 5 L/min. The animals were kept warm on a heating pad. The body temperature was continuously monitored using a rectal thermometer probe and maintained between 36 and 37 °C by adjusting the distance of a ceramic heating lamp. Under these conditions, the animal's heart rate could be maintained above 300 beats per minute. Two-dimensional and M-mode echocardiography were used to assess wall motion, chamber dimensions, wall thickness, and fractional shortening. Color flow Doppler was used to assess valve function. Images were obtained from the parasternal

long axis, parasternal short axis at the mid-papillary level, apical 4-chamber, apical 2-chamber, and apical 3-chamber views.

Baseline echocardiograms were acquired at 2-3 days post-MI with additional echocardiograms acquired at 4 weeks post-MI. The baseline post-MI echocardiograms served two purposes: 1) they allowed us to determine whether there were initial differences in infarct size between the MI control group and the patch-treated groups, and 2) they allowed us to select only animals with sufficiently large MI. We have prospectively established that an animal must have sustained a sizable anterior MI in order to be included in subsequent studies. We defined sizable anterior MI as wall motion abnormalities involving at least two of the three anterior myocardial segments. Using this pre-established criterion, we excluded a total of two animals from our study: one from the MI control group and one from the MI + Patch group.

3.2.6 Cardiac hemodynamics

Cardiac hemodynamics were measured after the final echocardiographic examination. Rats were anesthetized with 1% isoflurane, and a 1.4F Millar Mikro-Tip catheter (SPR-671, Millar Instruments, Houston, TX) was inserted into the right carotid artery and advanced into left ventricle. Aortic and left ventricular (LV) pressures were recorded on a PowerLab system and analyzed using Chart v4.2.4 software (ADInstruments, Colorado Springs, CO).

3.2.7 Myocardial Histology

After the hemodynamics study, hearts were removed, perfused with 4% paraformaldehyde and then cryo-protected by immersion in 30% sucrose for 48-96 h. Isopentane cooled in liquid nitrogen was used to freeze hearts immersed in optimal cutting temperature (OCT) medium. Sections were cut to 7 μm using a commercial

cyrostat and used for either immunohistochemistry or staining with hematoxylin and eosin or Masson's Trichrome. To calculate fibrosis, at least three Masson's Trichrome stained sections at various levels along the long axis were analyzed for collagen deposition using the histogram-based color selection function of Image-Pro[®] Plus software v6.3 (Media Cybernetics, Inc; Bethesda, MD). To assess engraftment efficiency, serial sections were taken at 1 mm intervals along the axis of the heart from the apex to the base. Total cell number was interpolated using a physical dissector methodology for stereology[25]. Using fluorescence microscopy, the numbers for human and 4',6-diamidino-2-phenylindole (DAPI)-positive cells were counted within the mid-infarct and peri-infarct region, and serial sections were compared to exclude points of cell intersection. Human cells were detected using a fluorescein isothiocyanate (FITC) conjugated anti-human IgG (Sigma, St. Louis, MO 1:20). Equivalent results were obtained using anti-human HLA (Sigma 1:20) and a lack of fluorescence in the hearts without applied cells confirmed the antibody specificity. Engraftment was calculated as the number of FITC-positive cells within the native tissue divided by the number of intact cells initially delivered within the patch. Immunohistochemical staining with antibodies against α -smooth muscle actin (α -SMA, Sigma, St. Louis, MO; 1:200), von Willebrand Factor (vWF, Sigma; 1:500) and c-kit (Santa Cruz Biotechnology; 1:100) with appropriate secondary antibodies (anti-mouse IgG, Jackson ImmunoResearch Inc, West Grove, PA; anti-goat IgG, anti-rabbit IgG) were used to show blood vessel (calculated as vessels per field) and myofibroblast and endogenous stem cell locations within and around the infarct zone. Frozen sections were air dried, and OCT was removed by rinsing slides in PBS. Non-specific binding was blocked by incubating slides with 5% donkey or goat serum (Sigma) for 1 h. The primary antibody was then added for 2 h at room temperature or overnight at 4°C. After rinsing in 0.45% fish skin gelatin oil

(Sigma), the secondary antibody is added for 1 h then counterstained with DAPI and mounted with DAKO anti-fade aqueous mounting media (DAKO, Carpinteria, CA).

3.2.8 Neonatal Cardiomyocyte and Cardiac Fibroblast Isolation

Ventricular cardiomyocytes were isolated from 2 to 3 day-old Sprague-Dawley rats (Charles River Laboratories, Wilmington, MA) using an isolation kit purchased from Worthington Biochemical Corporation (Lakewood, NJ). Briefly, the beating hearts of anesthetized Sprague-Dawley neonates were surgically removed and then immediately placed in a centrifuge tube containing 35 mL sterile calcium- and magnesium-free Hanks Balanced Salt Solution (pH 7.4). The suspension was incubated overnight at 4°C with trypsin (50µg/ml). On the following day, the tissue was treated with a trypsin inhibitor for 30 min, followed by collagenase for 45 min both at 37°C. The tissue was titrated and the supernatant was filtered through a cell strainer. Then, the cells were centrifuged at 1000 rpm for 3 min, and the cell pellet was re-suspended in media consisting of DMEM, 10% FBS, and 200µg/mL penicillin/streptomycin. After measuring cell yield and viability with the trypan blue exclusion test, cells were plated on tissue culture dishes for 1.5 h to allow for the attachment of non-myocyte fibroblasts. The non-adherent neonatal cardiomyocytes (NCM) were collected and re-plated in a new culture dish. The remaining cardiac fibroblasts (CFb) were cultured at 37°C and 5% CO₂.

3.2.9 Real Time RT-PCR

RNA was isolated from cell monolayers using a commercial RNeasy kit (Qiagen; Valencia, CA). RNA concentration was measured using a spectrophotometer (abs: 260nm). Afterwards, 1µg of RNA was converted into cDNA using a BioRad iScript cDNA synthesis kit (BioRad; Hercules, CA). The reaction mixture was run for 30 minutes at 55°C. Real Time PCR was run using a total of 50ng template cDNA for each sample.

For each run a negative control (water only, no template) was also run. Each sample was run in triplicate using a BioRad SYBR green master mix for multiple genes including: rat SCN5A, rat bax and rat bcl2. Primer assays for bax and bcl2 was obtained from Qiagen. Unfortunately, primer sequence information is proprietary and is not available. Primer sequence information for SCN5A is listed below. The PCR protocol consists of an initial denaturing step at 95°C for 15 minutes. Next, samples are run at 94°C (denaturation) for 15 seconds, 60°C (annealing) for 30 seconds and 72°C (extension) for 30 seconds for 35 cycles. Relative RNA abundance was calculated using the following equation: $2^{-\Delta\Delta CT}$.

SCN5A Primer Sequence:

Fwd: TTACGCACCTTCCGAGTCCTCC

Rev: GATGAGGGCAAAGACGCTGAGG

3.2.10 Assessment of hMSC Paracrine Function

To assess the likelihood of paracrine functionality, hMSC were cultured under hypoxic conditions (1% O₂) for 3 d (Figure 3.3) in DMEM supplemented with L-Glutamine and penicillin/streptomycin only (Maintenance Media; MM). Afterwards the conditioned media was removed from the hMSC, spun at 2000 rpm to remove debris and placed on beating and confluent NCM cultures or 24 hour serum starved CFb for 1 d. Conditioned media that was not immediately used was frozen at -80°C. Frozen media was also used for experiments, but would only be used after at most a single freeze/thaw cycle. After a one day culture period under hypoxic or normoxic (20% O₂) conditions with conditioned media, NCM were collected and the RNA was isolated as described in 3.2.10. RT-PCR was run for the expression of SCN5a, bax and bcl2. Additionally, after 1 d in culture under hypoxic or normoxic conditions, conditioned media was removed from CFb (initial

seeding density was 20,000 cells/well) and MTT (3-(4,5-Dimethylthiazol-2-yl)-2,5-diphenyltetrazolium bromide; Sigma) reagent was added for 4 hours (Figure 3.4). Afterwards, the MTT reagent was removed and an ice cold solution of 0.1 N hydrochloric acid (HCL) in anhydrous isopropyl alcohol was added to dissolve formazan crystals. The resulting colored solution was collected and the absorbance was spectrophotometrically measured at 570nm with background subtraction at 690nm. Also, a picosirius red assay was performed on media collected from CFb (initial seeding density was 500,000 cells/T-25 flask) after 1 d of culture in hMSC conditioned media. Briefly, the media was collected and dried onto a non-tissue culture treated multi-well dish in a 37°C humidified chamber for 16 hours than a 37°C dry oven for at least 24 hours. The wells were washed with deionized H₂O and than stained with a 0.1% picosirius red solution (Direct Red dissolved in picric acid; Sigma) for 2 hours. The wells were washed five times with 10mM HCL and bound collagen was eluted using 0.1 M sodium hydroxide. The resulting colored solution was collected and the absorbance was spectrophotometrically measured at 540nm. Absolute concentrations were determined through the use of a standard curve utilizing rat tail type I collagen. Background collagen secreted from hMSC was subtracted by measuring picosirius red absorbance from media taken directly off of hMSC.

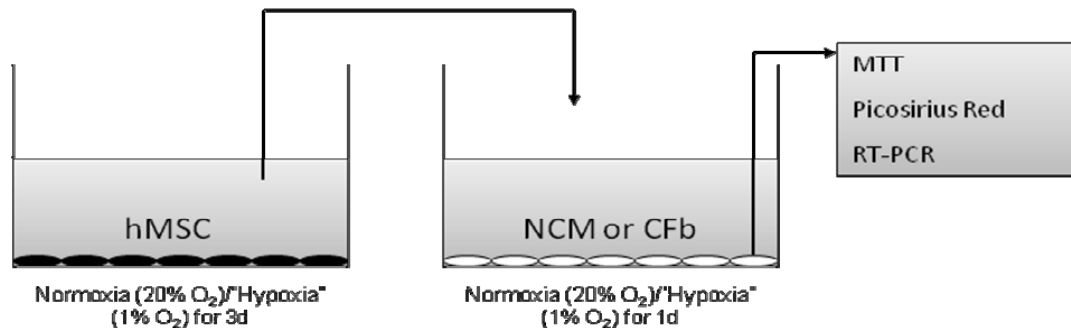


Figure 3.4) Schematic of *in vitro* hypoxia model. In order to investigate the paracrine effects of hMSC on NCM and CFb, a model was set up in which conditioned media from hMSC under hypoxia was removed and placed on viable NCM or CFb. After defined periods, the function of either cell was analyzed.

3.2.11 Statistical Analysis and Interpretation

A Student's t-test was used for comparison of data sets with two groups. Data sets involving three or more groups were analyzed using a one-way analysis of variance (ANOVA). Appropriate post-hoc testing (Bonerroni or Dunnett) was performed for the interpretation of several data sets. A p-value less than 0.05 indicated statistical significance.

3.3 RESULTS

3.3.1 In Vitro Characterization of the Cardiac Patch

To determine the suitability of the cardiac patch for transplantation of progenitor cells, we performed a series of experiments to assess hMSC differentiation, collagen compaction, patch cellularity and hMSC viability *in vitro* after casting cells in the collagen hydrogel. Progenitor cell potency is thought to be an important factor determining the degree of cardiac repair with cell replacement therapy. On days 4 and 7 of culture, the extent of hMSC differentiation was measured by monitoring the expression of two markers of hMSC potency, CD105 and CD73[26]. As shown in figure 3.5a, there was no

significant decrease in either marker after 4 d, the day patches were applied in our experiments. Longer incubation resulted in a modest decrease in CD73 but not CD105 expression at 7 d. Therefore, hMSCs retained their original potency on the day the patch constructs were used.

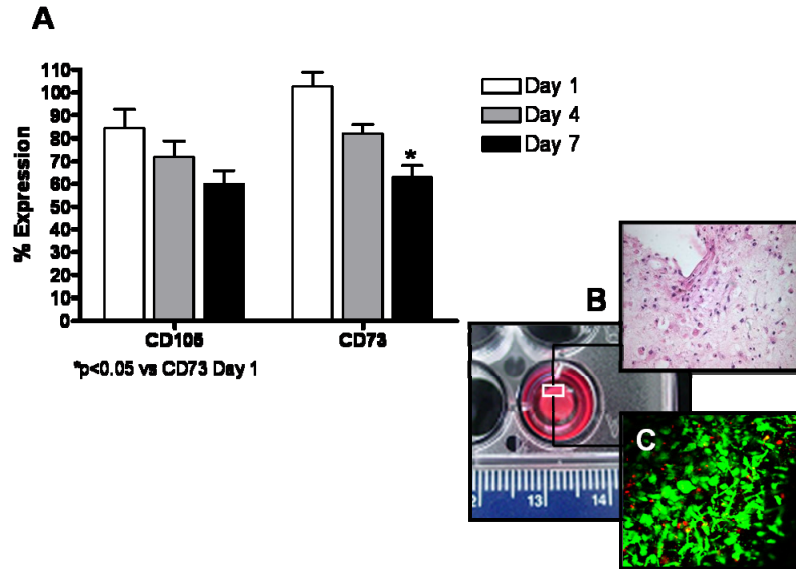


Figure 3.5) *In vitro* characteristic of the cardiac patch. In order to determine the feasibility of this cell-matrix combination a series of *in vitro* experiments were performed to assess hMSC differentiation, collagen compaction and hMSC viability. A) hMSC potency was measured by monitoring the expression of CD105 and CD73 via flow cytometry over 7 d. B) The change in diameter of the cardiac patch was measured over several days to determine the extent of collagen compaction. In addition, H&E staining was performed (20X magnification) on compacted cardiac patches to view the distribution of cells. C) A representative picture of a live/dead assay on a cardiac patch (20X magnification). High hMSC viability was retained before placement of cardiac patch onto infarcted heart.

During the *in vitro* culture period, there was evidence of cell-matrix interactions. Compaction is a measure of the interaction of cells and matrix. Compaction of the collagen construct imparted increased mechanical strength to the patch, providing for easier manipulation during transplantation. Compaction was quantified by the measurement of the maximum construct diameter on days 0 and 4. After 24 h, constructs compacted maximally to $38 \pm 2\%$ (n=5) of their original area to a diameter of

3.7 ± 0.4 mm (figure 3.5b, 3.6). The degree of volumetric compaction was similar (23 ± 7 μl; n=3). This degree of compaction is similar to that seen using other cell types embedded in a collagen matrix[27].

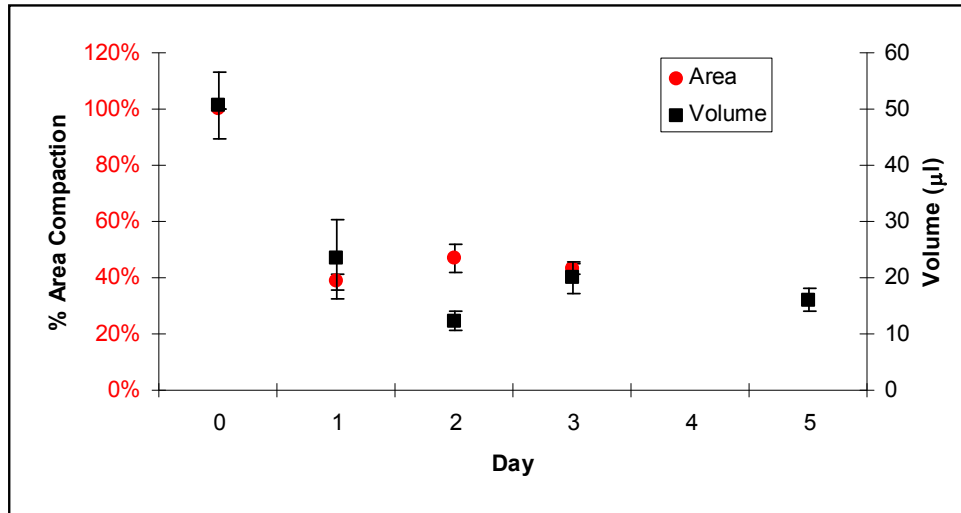


Figure 3.6) Remodeling of cardiac patches in culture. To assess the extent of remodeling of cardiac patches, compaction was measured to gauge percent change in cross-sectional area and volumetric change over five days.

Also, in order for successful delivery to the infarct, cells must remain viable in the patch. hMSC viability was found to be 94 ± 2% over 4 d in culture (figure 3.5c). Therefore, patches developed suitable mechanical properties and embedded cells retained appropriate characteristics for *in vivo* application. Although viability remained relatively high, we observed a progressive non-significant reduction in patch cellularity over five days. Overall there was an apparent 55% drop in patch cellularity from day zero to day five. As shown in figure 3.1 this may be partly due to cell migration from the patch onto the culture surface. Additionally, cell apoptosis could contribute to these effects. It should be noted that the viability assay used to determine hMSC survival was not designed to differentiate apoptotic cells.

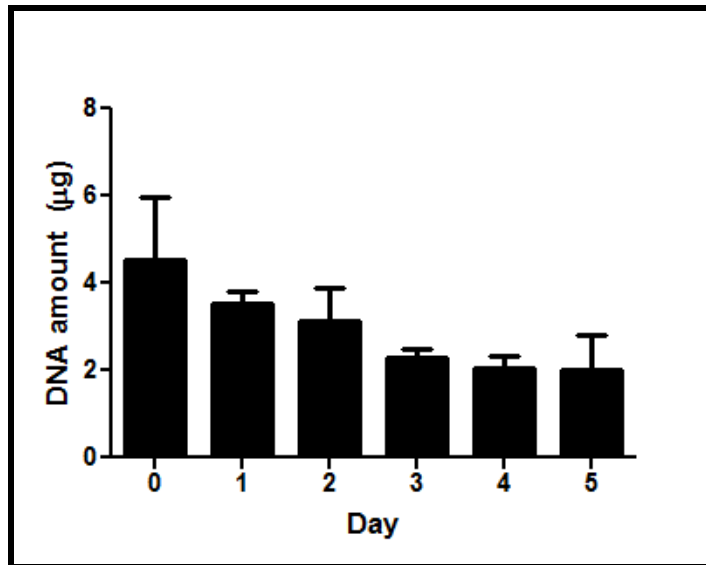


Figure 3.7) Loss of cardiac patch cellularity while in culture. The absolute DNA content of cardiac patches was measured using a Picogreen DNA binding dye. There was an apparent 55% drop in cellularity measured over five days. (n=3, Day 0-3; n=4 Day 4-5)

3.3.2 Progenitor Cell Engraftment and Distribution with Cardiac Patch Application

Cardiac patches were fixed in place on the epicardial surface of the heart, and cell engraftment was determined at one week. After the removal of rat hearts, they were fixed, cryopreserved, and embedded in OCT medium. Serial sections at 1 mm intervals were cut and stained for human antigen. Engraftment was analyzed across the infarcted region with fluorescence microscopy. Only cells which were positive for human antigen and DAPI and located within the myocardium were counted as being engrafted (figure 3.8 and figure 3.9a). We found that $23 \pm 4\%$ of the applied cells engrafted at this time (i.e., one week after patch application, n=6). Cell distribution within animals which received a cardiac patch tended to show low engraftment at the apex and base of the heart (figure 3.8). We also noticed the fusion of collagen patches with the native tissue. This event made it difficult to differentiate between the patch and host myocardium in histological evaluations.

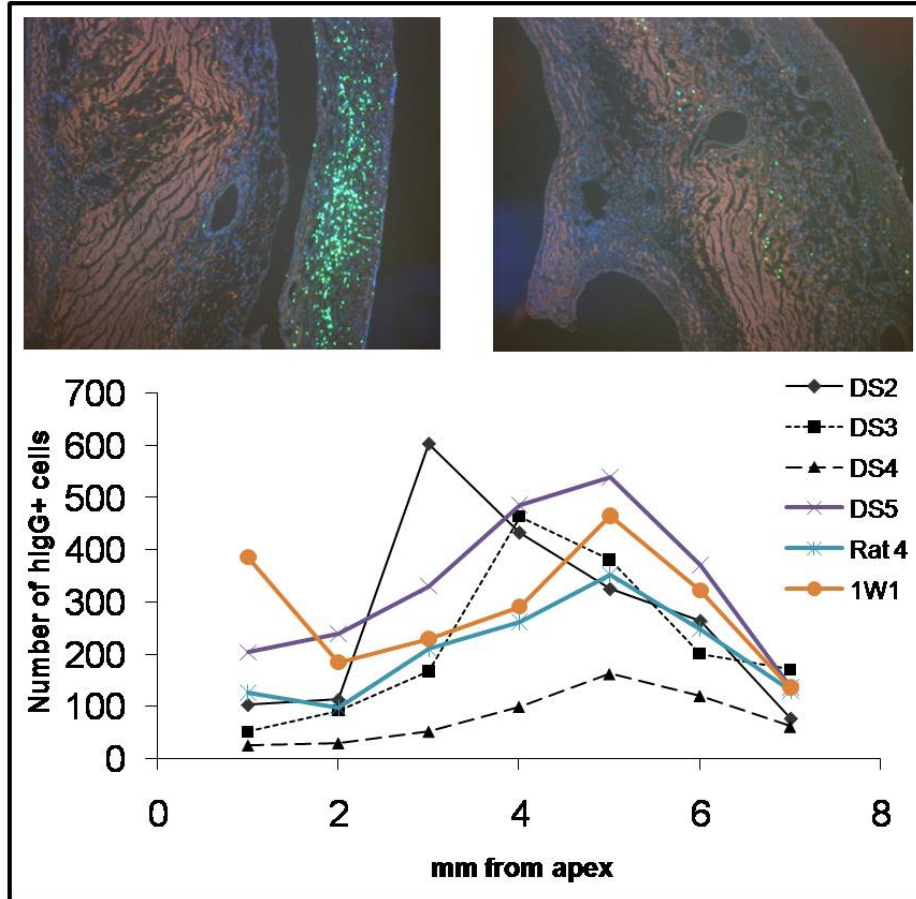


Figure 3.8) Trends in hMSC engraftment. One week post-infarcted rat hearts were stained with anti-human IgG or anti-human HLA to determine the extent of engraftment after patch application. In general, most stem cells were observed to engraft in the area between the apical and basal portions of the heart.

Most engraftment occurred directly underneath the applied patch with $80 \pm 3\%$ of the hMSCs found in this area of the myocardial anterior wall (figure 3.9a and c). Of these engrafted cells, $1.0 \pm 0.2\%$, $14 \pm 3\%$, and $85 \pm 3\%$ were found in the endocardial, mid-myocardial, and epicardial regions, respectively. Nevertheless, some cell migration away from the patch occurred. Of the engrafted hMSCs, $20 \pm 3\%$ were found in the infarcted region not covered by the patch. These cells showed a similar proclivity to engraft in the epicardial region. Of the cells engrafted away from the patch, $3 \pm 1\%$, $39 \pm 4\%$, and $58 \pm 4\%$ were found in the endocardium, mid-myocardium, and epicardium, respectively. Cells within the mid-myocardium were typically found amongst necrotic myocardium. Occasionally, we observed hMSC engraftment in regions as far as 1 mm from the apex of the heart (figure 3.9b).

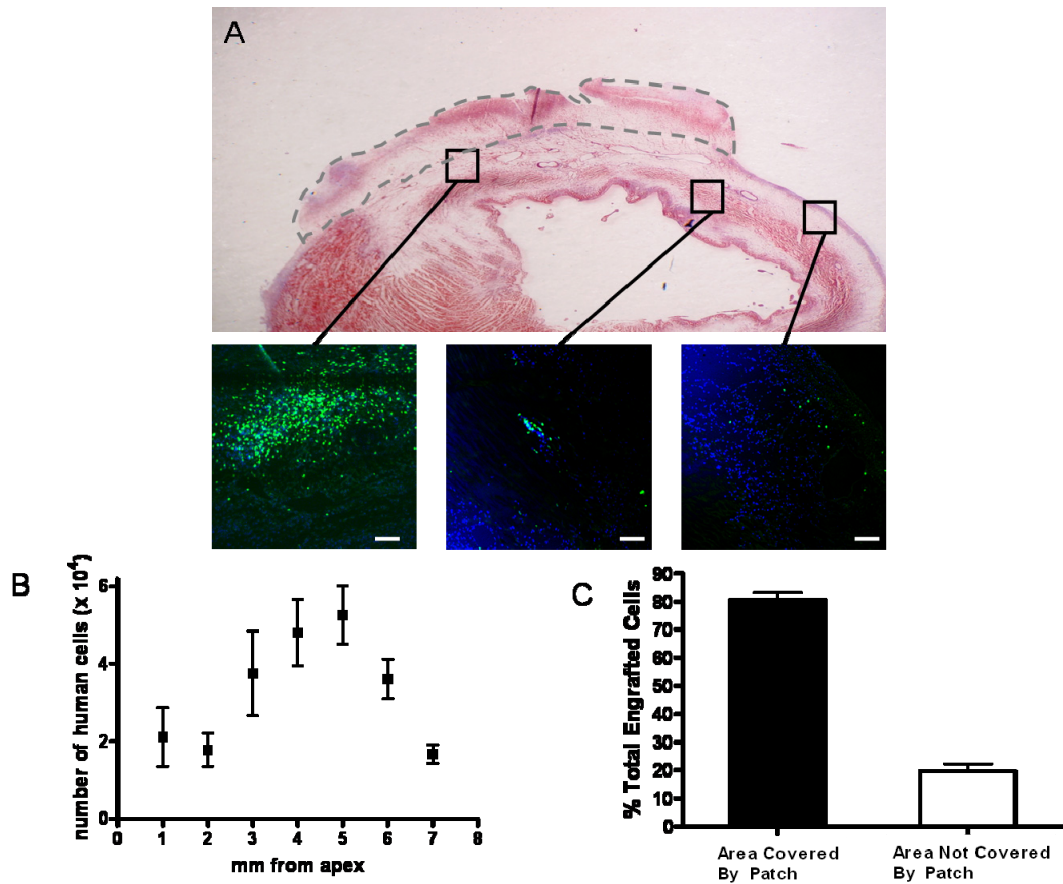


Figure 3.9) Engraftment of hMSC in infarcted rat heart at 1 week. Histology was performed on 1 week old infarcted hearts to determine the location and number of hMSC. As shown on the left, hMSC stained with an anti-human IgG (verified with human anti HLA class I) are able to migrate from the patch to the infarcted region of the heart (A and B). Cells typically migrated to the epicardial side of the heart though they were found in more distal in areas not covered by the patch (C and D). Engraftment was calculated to be $22 \pm 5\%$ (n=4). E) In addition, engraftment was distributed across the entire infarct, spreading from apex to base. (20X magnification; bar equals $100\mu\text{m}$)

3.3.3 Efficacy of the Cardiac Patch in Post-Infarct Remodeling

In order to assess the efficacy of this cell delivery method, post-infarct remodeling was studied using echocardiography and invasive hemodynamics. Baseline echocardiograms at day 2-3, presumably before any substantial effects of the applied progenitor cells, showed no difference in the initial infarct size between the MI control group and patch-treated animals, $39 \pm 1\%$ and $38 \pm 2\%$ of the left ventricle (LV), respectively. At four weeks, MI resulted in statistically significant adverse remodeling in all five parameters measured, as shown in Table 3.1. Application of patches containing hMSCs statistically significantly improved all five parameters as compared to MI only animals. At four weeks after infarction, the hearts of patch-treated animals showed less dilatation in LV internal dimensions and better preserved anterior wall thickness. These findings were consistent with a -11.5% reduction in internal LV diameter and a 29.8% increase in wall thickness in the MI + patch group when compared to the MI only group as assessed by histological morphometry. Fractional shortening was also better preserved in patch-treated hearts as compared to MI control hearts ($25 \pm 2\%$ vs. $19 \pm 1\%$, $p < 0.05$), and the L/S ratios suggested a less spherical LV in the patch-treated animals as compared to the MI control group.

To determine if the improvements were mediated by hMSC or by cardiac patch placement itself, we used patches without viable cells (i.e. non-viable patches). A freeze/thaw cycle was used to eliminate hMSCs within 4-day old patches, and these non-viable patches of equivalent size and mechanical properties to the cellular patches were transplanted onto infarcted myocardium in an identical manner. As shown in Table 3.1, all remodeling parameters were statistically unchanged between MI control animals and non-viable patch-treated animals. Also, animals treated with the cardiac patch showed improvements in all five parameters when compared to animals treated with

non-viable patches, suggesting that hMSCs and not the collagen alone were responsible for favorable remodeling.

Table 3.1: Echocardiographic measures of myocardial remodeling and function

	Sham (n=4)	MI (n=8)	MI + NV Patch (n=7)	MI + Patch (n=7)
LVIDd (mm)	7.5±0.2	9.5±0.1 ^a	9.7±0.4 ^a	8.8±0.1 ^{a,b}
LVIDs (mm)	3.9±0.2	7.7±0.1 ^a	8.0±0.5 ^a	6.4±0.3 ^{a,b,c}
FS (%)	48±2	19±1 ^a	18±2 ^a	27±3 ^{a,c}
AWTh (mm)	1.01±0.01	0.35±0.03 ^a	0.37±0.04 ^a	0.60±0.03 ^{a,b,c}
L/S	1.55±0.04	1.27±0.02 ^a	1.26±0.03 ^a	1.40±0.02 ^{a,b,c}

^a p<0.05, vs. Sham; ^b p<0.05 vs. MI; ^c p<0.05 vs. MI + NV Patch

MI: Myocardial Infarction

NV: Non-viable

LVIDd: Left ventricular internal diameter at diastole

LVIDs: Left ventricular internal diameter at systole

FS%: Percent fractional shortening

AWTh: Anterior wall thickness

L/S: Ratio of long to short axis; sphericity index

In general, hemodynamic measures were less sensitive to infarction and subsequent patch application. Despite creating relatively uniform, large infarcts, only +dp/dt, the rate of rise of pressure LV pressure, and -dp/dt, a measure of diastolic relaxation, were statistically different between the control and MI groups, and despite the improvements in post-infarct structural remodeling as assessed by echocardiography, there was no statistical differences in hemodynamic parameters between the MI and MI + patch groups (Table 3.2).

Table 3.2 Hemodynamic measures of myocardial function

	Sham (n=5)	MI (n=10)	MI+Patch (n=13)	MI+NV (n=7)	Patch
SBP (mmHg)	132 ± 3	126 ± 3	131 ± 2	123 ± 2	
DBP (mmHg)	98 ± 1	96 ± 3	99 ± 2	93 ± 2	
LVESP (mmHg)	136 ± 4	126 ± 4	128 ± 3	124 ± 1	
LVEDP (mmHg)	5.1 ± 0.3	8.9 ± 1.2	9.1 ± 1.2	7.6 ± 1.6	
+ dp/dt (mmHg/s)	10080 ± 567	8320 ± 213 ^a	8774 ± 228 ^a	8518 ± 229 ^a	
- dp/dt (mmHg/s)	-9476 ± 463	-6960 ± 245 ^a	-7065 ± 168 ^a	-6396 ± 202 ^a	

^a p<0.05 vs. Sham

SBP: Systolic blood pressure

DBP: Diastolic blood pressure

LVESP: Left ventricular end-systolic pressure

LVEDP: Left ventricular end-diastolic pressure

+ dp/dt: Maximum rate of rise in left ventricular pressure during systole

- dp/dt: Maximum rate of decrease in left ventricular pressure during diastole

3.3.4 Increased Myofibroblast and c-Kit Expression with Patch Application

The mechanism whereby bone marrow-derived progenitor cell replacement therapy improves myocardial function is unknown. Possibilities include proliferation and differentiation of exogenously applied MSCs or paracrine effects on native cells[28, 29]. To investigate these two possibilities further in our system, we replicated the histological analysis for MSCs at four weeks. This analysis showed that despite high initial engraftment rates at one week, no hMSCs or residual patch were detectable at four weeks. This suggested that the advantageous effect of patches containing MSCs was not the result of long-term MSC proliferation and differentiation.

Since MSC application has been reported to increase angiogenesis[30], we performed additional histological analysis for this possibility. Immunohistochemical staining for vWF at four weeks after MI showed only a trend toward an increased number of blood vessels throughout the peri-infarct and infarcted regions of patch-treated animals (7.2 ± 2.1 vs. 10.3 ± 1.3 vessels per field for control and patch-treated animals respectively; figures 3.10a, b and c). Additionally, there were generally more vessels toward the endocardium compared to the epicardium in both MI control and cardiac patch treated animals (figure 3.10d). Interestingly, there is a non-significant trend for increased vessel density on the epicardial side of the infarct zone compared to MI controls. Cardiac patches were placed on the epicardial surface of hearts and showed heightened engraftment in the area, which may contribute to these observations.

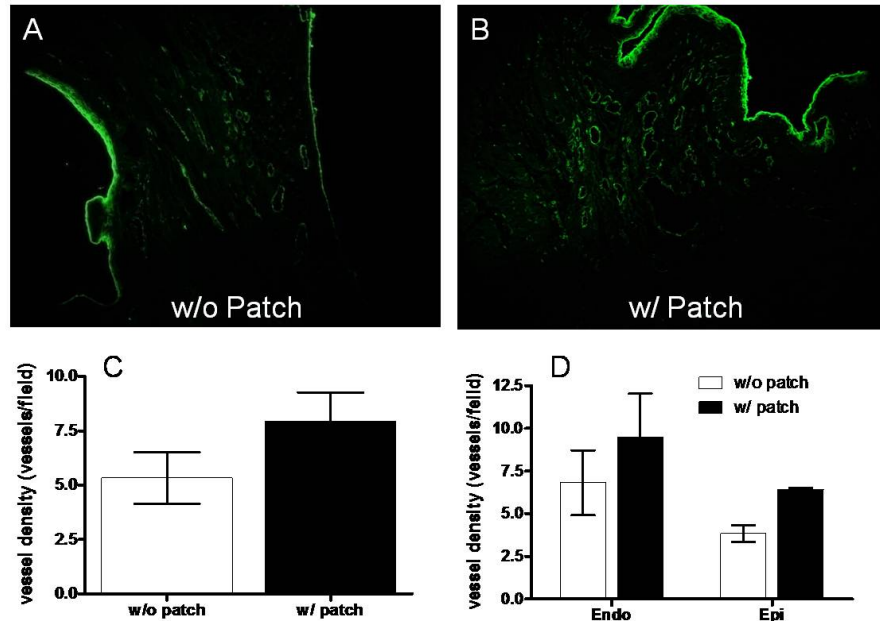


Figure 3.10) Blood vessel density at 4 weeks post-infarction. A) and B) vwf expression was used to determine the vessel density in infarcted hearts with and without cardiac patch treatment (20X magnification). C) Although there was a trend for increased vessel density across the border zone and infarct zone there was no statistically significant difference. D) In general there were more blood vessels on the endocardial side of the heart versus the epicardium.

On the other hand, we found a marked increase in the number of cells in the infarct area expressing α -SMA. α -SMA positive cells were increased in patch-treated animals ($1.5 \pm 0.5\%$ vs. $4.6 \pm 1.1\%$; $p < 0.01$; figure 3.11a). Most of these α -SMA expressing cells were located in the mid myocardium, away from blood vessels and along the border zone of the mid-infarcted region. (figure 3.11b, c and d). Since α -SMA expression is a marker for vascular smooth muscle cells and myofibroblasts and most cells expressing the marker were not associated with blood vessels, these cells likely represent an increase in myofibroblasts within the infarct region in response to patch application. Finally, these α -SMA positive cells did not stain for human antigen, suggesting that patch application encouraged recruitment, differentiation, or both of native cells.

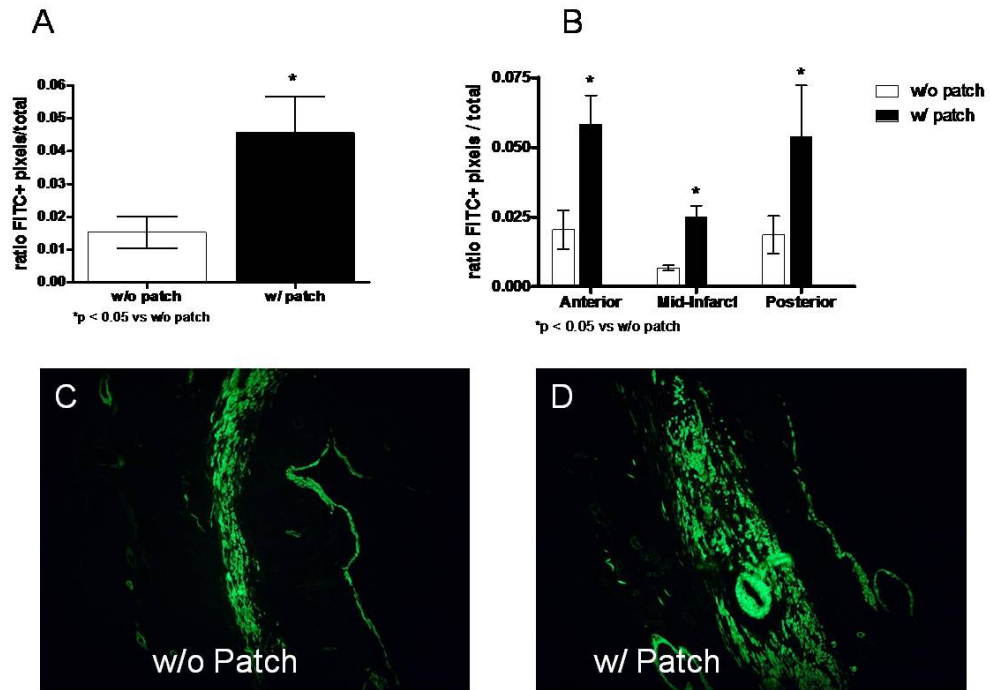


Figure 3.11) Expression of α -SMA in infarcted hearts at 4 weeks. A) α -SMA expression was significantly increased with the application of constructs when compared to an infarcted control ($4.6 \pm 1.1\%$ vs. $1.5 \pm 0.5\%$, $p < 0.01$; $n=4$). B) Increased α -SMA expression was consistently augmented across the LV wall. C) and D) Fluorescence microscopy images show higher α -SMA expression in patch treated hearts versus controls (20X magnification).

Although we observed a significant increase in myofibroblast presence, this did not result in increased collagen deposition. Several sections along the long axis of the heart were stained with a Masson's Trichrome tinctorial stain and analyzed for fibrosis using Image Pro Plus software. Analysis revealed there was no difference in the amount of fibrosis at the anterior, mid and posterior regions of the infarct in MI control hearts versus hearts treated with a cardiac patch (figure 3.12a-d) Therefore, although cell presence is increased in samples treated with a cardiac patch, the extent of collagen production appears attenuated.

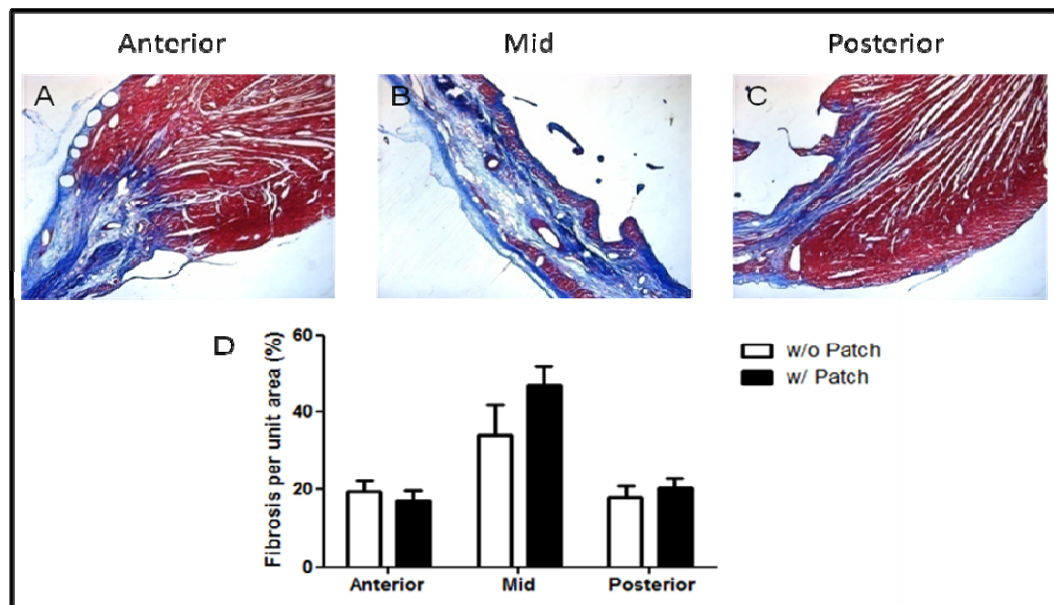


Figure 3.12) No change in the extent of fibrosis with cardiac patch application. Fibrosis was measure using Masson's Trichrome stained sections from MI control and cardiac patch treated hearts. D) There was no difference in the extent of fibrosis at the anterior (A) and posterior (C) border zones or the mid-infarct region (B); 10X magnification.

In addition, to determine the extent of endogenous stem cell recruitment to the infarct site we performed immunohistochemistry for the presence of the c-kit antigen. As shown in figures 3.13a and b, there is an apparent increase in the number of c-kit-positive cells present in infarcted hearts treated with a cardiac patch versus MI controls.

We also noticed that many hMSC appeared c-kit-positive (figure 3.13c). Such expression may represent cell fusion of hMSC with endogenous progenitors or possible dedifferentiation of hMSC after transplantation.

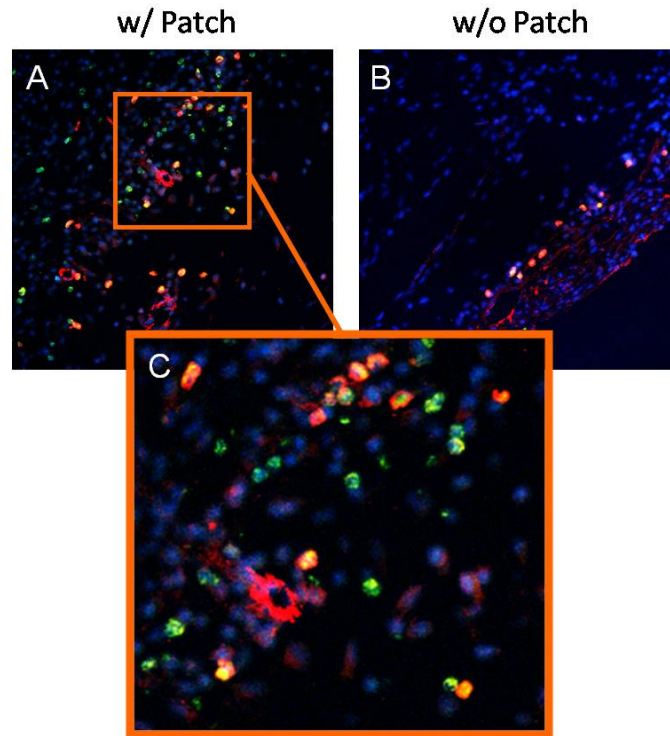


Figure 3.13) Endogenous stem cell recruitment with cardiac patch treatment. A) and B) Infarcted rat hearts treated with cardiac patches demonstrated an apparent increase in c-kit-positive cells (Red) in the infarct zone compared to those without cardiac patches one week after infarction and patch placement. (20X magnification) (C) hMSC are stained with anti-human HLA (Green) and show apparent colocalization (Yellow) with c-kit antigen.

3.3.5 An In Vitro Model to Assess Possible Benefits of hMSC Conditioned Media

The results obtained from *in vivo* experimentation predict that repair of infarcted myocardium may be mediated via a paracrine mechanism. To further assess this possibility, we developed an *in vitro* hypoxia model (figure 3.4). Conditioned media from hMSC cultured under hypoxia for 3 d was removed and placed on NCM or CFb to determine downstream functions. NCM cultured with hMSC conditioned media or maintenance media (MM) were cultured for 1 d under normoxia or hypoxia. RT-PCR of

RNA collected from NCM revealed there was no change in the extent of apoptosis (bcl2:bax) with or without hMSC conditioned media (Figure 3.14). Additionally, NCM cultured with hMSC conditioned media showed a relative downregulation of SCN5A (sodium channel) transcripts compared to cells in MM at 1% oxygen or cells in MM at 20% oxygen (Control: 1.04 ± 0.06 ; Hypoxia: 0.68 ± 0.1 ; hMSC Hypoxia: 0.37 ± 0.07 ; Figure 3.15).

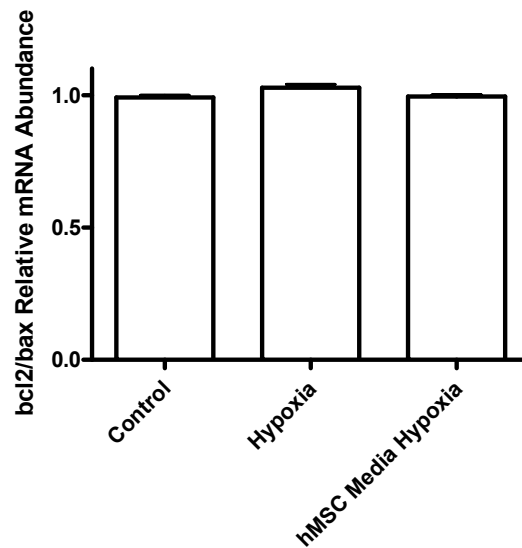


Figure 3.14) NCM apoptosis with exposure to hMSC conditioned media. RT-PCR for bcl2 and bax transcripts revealed no change in the extent of apoptosis with exposure of NCM to hypoxia. Control represents NCM at 20% oxygen in MM. Hypoxia represents NCM at 1% oxygen in MM. hMSC media hypoxia represents NCM at 1% oxygen in hMSC conditioned media.

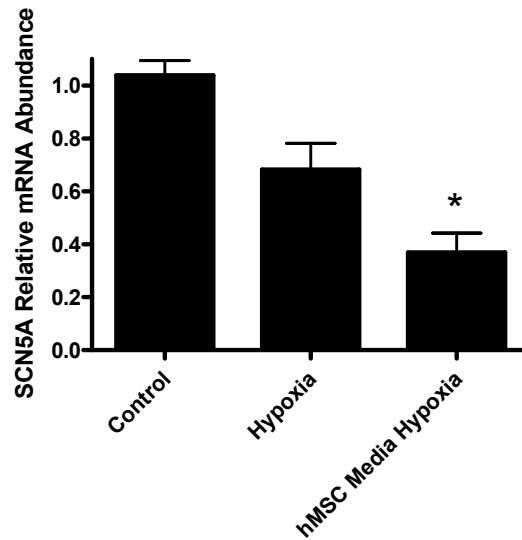


Figure 3.15) Downregulation of SCN5A transcript levels with exposure to hMSC conditioned media. SCN5A transcript were downregulated upon exposure to hypoxia alone and further upon exposure to hMSC conditioned media (Control: 1.04 ± 0.06 ; Hypoxia: 0.68 ± 0.1 ; hMSC Hypoxia: 0.37 ± 0.07 ; * $p < 0.05$ vs. Control).

CFb cultured in hMSC conditioned media or maintenance media at differing oxygen tensions was performed to determine the effect of hMSC paracrine factors on CFb presence and collagen secretion. hMSC were cultured with MM for 3 d at 1% or 20% oxygen. hMSC conditioned media was collected and added to primary CFb at passage two or three under normoxic or hypoxic conditions. MM was also added to a subset CFb as control media. MTT and cell counts were used to quantify cell growth and proliferation while a picosirius red assay was used to quantify collagen secretion from CFb. As shown in figures 3.16a and b, after exposure to hMSC conditioned media in hypoxic culture for 24 hours, CFb demonstrated increased formazan formation (0.07 ± 0.02 vs. 0.13 ± 0.01 AU; $p < 0.05$) and increased cell number ($2.7 \pm 0.3 \times 10^5$ vs. $4.5 \pm 0.8 \times 10^5$ cells; $p = 0.06$).

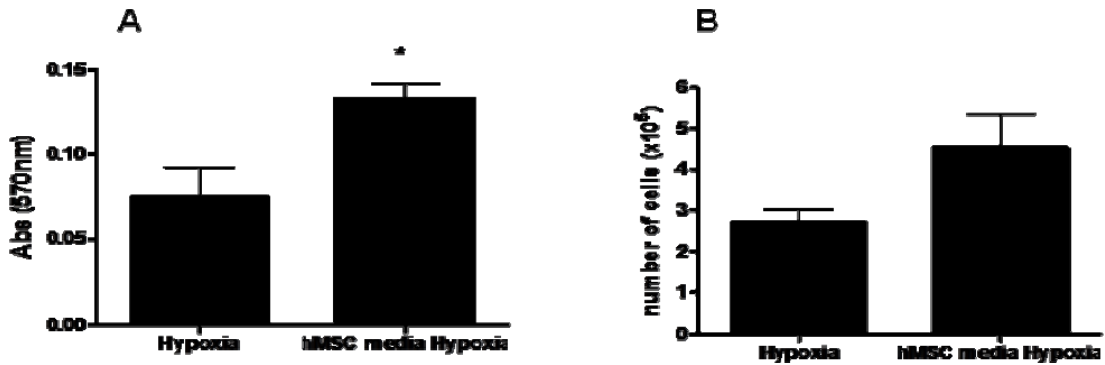


Figure 3.16) Increased CFb presence after exposure to hMSC conditioned media. After 24 hour exposure to hypoxia, CFb demonstrated heightened presence as indicated by A) formazan absorbance (MTT assay; 0.07 ± 0.02 vs. 0.13 ± 0.01 AU; $*p < 0.05$; $n=3$) and B) cell number ($2.7 \pm 0.3 \times 10^5$ vs. $4.5 \pm 0.8 \times 10^5$ cells; $p=0.06$, $n=3$).

Additionally, we performed a picosirius red assay to assess collagen secretion from CFbs. Conditioned media from CFbs with hMSC conditioned media or MM at differing oxygen tensions was collected and dried onto a multiwell plate to allow for collagen absorption. Plates were stained with picosirius red dye, washed and absorbance values measured with a spectrophotometer. hMSC conditioned media was also used in this process to subtract any background collagen secreted into hMSC conditioned media by hMSC. Originally we found that there was no change in the amount of collagen in the conditioned media taken from CFbs under hypoxia. Considering, however, that more CFbs exist in the wells after exposure to hMSC conditioned media we normalized absorbance values obtained from the picosirius red assay to those obtained from the MTT assay. This normalization gives a relative value for collagen secretion based on cell presence. As shown in figure 3.17 this correction reveals attenuated collagen secretion from CFb exposed to hMSC conditioned media under hypoxia (0.45 ± 0.12 ($n=6$) vs. 0.14 ± 0.06 ($n=4$) AU; $p=0.08$).

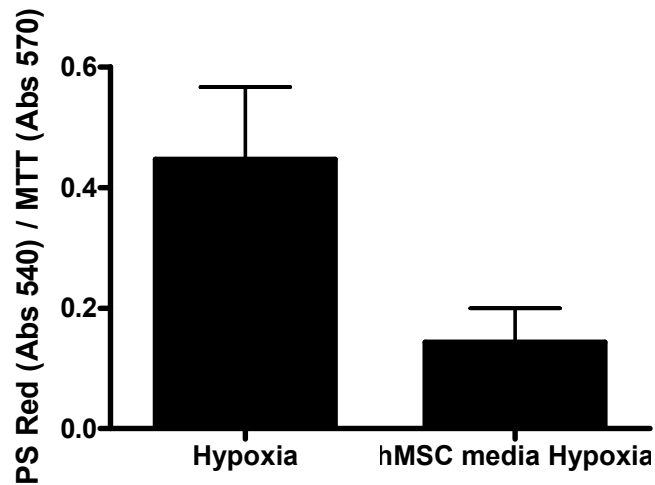


Figure 3.17) Attenuated collagen secretion from CFb exposed to hMSC conditioned media. Upon exposure to hMSC conditioned media a statistically non-significant reduction in collagen secretion was observed (0.45 ± 0.12 (n=6) vs. 0.14 ± 0.06 (n=4) AU; $p=0.08$). Picosirius red absorbance was normalized to MTT absorbance to account for differences in CFb presence as shown in figure 3.16.

3.4 DISCUSSION

Reconstituting infarcted tissue with cells capable of performing the functions of the heart or providing beneficial trophic factors for native cells are attractive solutions for myocardial repair[31]. In order to reconstitute myocardium, a large number of cells will need to be delivered efficiently. In this study, we tested the feasibility of a tissue engineered approach to stem cell delivery by delivering hMSC embedded in a biodegradable collagen matrix to the site of an infarct. Using this approach, we were able to achieve high levels of cell engraftment and show improvements in post-infarct remodeling, despite the relatively modest number of cells initially delivered.

Several tissue engineering approaches have been undertaken for cardiac cell replacement therapy[6, 14, 32-37]. These include the use of biomaterial-based cellular patches to restore myocardial function. Additional studies have attempted to optimize different cardiac constructs for myocardial repair *in vitro*[38-40]. Our approach, however, differs in several regards. First, previous studies utilizing a type I collagen hydrogel were

conducted in immunosuppressed models, making comparison with our results difficult. Second, to date, no study has investigated the use of hMSC embedded in a collagen matrix as a repair tool *in vivo*. Finally, we have attempted to quantify the extent of early cell engraftment using the cardiac patch as a delivery vehicle.

This method of cell delivery leads to engraftment which exceeds reported rates for other delivery techniques. In a study comparing the relative efficiency of cell delivery by intramyocardial (IM), intracoronary (IC), and interstitial retrograde coronary venous (IRV) delivery, it was found that these injection procedures resulted in only modest engraftment[23]. Specifically, IM injection resulted in 11% engraftment while IC and IRV injections resulted in 2.6% and 3.2% engraftment, respectively. Similar studies performed by Freyman et al. [21] showed that 14 days after IC infusion, engraftment was 6%, and this delivery procedure was also accompanied by reduced coronary blood flow and subsequent myocardial injury. In our study, patch delivery achieved an initial cell engraftment of 23%. While this is an improvement over the other techniques, calculating the exact percentage of cells delivered is complicated by an unknown rate of hMSC proliferation and loss. Nevertheless, these rates are likely to be similar between delivery techniques. Possible explanations for this increased delivery include that exogenously applied cells remained fixed in proximity to the infarct area increasing the opportunities for engraftment. The technique had the further advantage of delivering cells in a relatively homogenous manner as compared to the next most efficacious delivery technique, direct injection.

While our purpose in these experiments was to demonstrate the feasibility of the patch delivery system, applied MSCs showed favorable effects on post-infarct myocardial remodeling. This outcome is similar to that described by others using MSCs. For example, Uemura et al. found that, with a similar number of applied bone marrow stem cells delivered via intraventricular injection, there was significant improvements in LV ejection

fraction and LV internal diameter at systole[29] Other measures of remodeling and function in their study, however, were unchanged including wall thickness and infarct size.

Despite the improvements in echocardiographic measures of remodeling, we were not able to show significant changes in hemodynamic parameters at four weeks after patch placement. This result is consistent with reports using a similar number of MSC [30, 41]. At higher doses of five million or more cells, there is evidence of improvements in hemodynamic measures as well as structural remodeling, however [28, 42]. This observation reinforces the need for high engraftment rates to maximally affect myocardial remodeling. Nevertheless, the fact that echocardiographic parameters showed improvements with only trends toward improvement in hemodynamic parameters in our experiments suggests that pressure measurements in rats are a relatively insensitive measure of myocardial function. Alternatively, it is possible that hemodynamic improvements might have been noted if remodeling had been allowed to continue longer.

Based on the experiments with non-viable patches, it seems likely that the improvement in remodeling seen was mediated by the applied cells rather than some effect of the biodegradable matrix. Despite this conclusion, it is possible that future permutations with different matrices or different configurations of the same matrix will allow improvements in the results with the patch approach. For example, Gaballa et al. found that acellular 3-D collagen foam scaffolds can reduce cardiac remodeling and induce angiogenesis,[43] reporting that these scaffolds can lead to reduced LV dilation and scar area.

While the mechanism of any benefit of MSC application in humans is likely multifactorial, our experiments imply that favorable remodeling can be seen in the absence of long-term cell engraftment. Probably related to the xenograft nature of our experiments and the application of cells into immuno-competent animals, we observed no retained hMSC four weeks after patch application. Our results are similar to those of Leor et

al.[44] where the injection of activated human macrophages into immuno-competent male Sprague-Dawley rats resulted in improved myocardial healing and function. In these experiments, human macrophages survived only 4-7 days, but their presence during early healing led to significant improvements in LV dimensions and fractional shortening at five weeks. Alternatively, we observed an increased number of cells in the infarct region that expressed α -SMA, presumably mostly myofibroblasts, since most of the additional cells were not associated with blood vessels. Myofibroblasts have previously been shown to assist in favorable post-infarct remodeling [45], and therefore, may represent a novel mechanism for the observed remodeling effects of the patch. In any event, our experiments evaluating myofibroblast, neovessel formation and endogenous stem cell recruitment confirm that some improvement in myocardial repair with MSCs is mediated through a paracrine effect.

The paracrine effects of hMSC were further investigated using an in vitro hypoxia model with NCM and CFb. When NCM cultured with hMSC conditioned media are subjected to hypoxia for 24 hours there was no change in the bcl2:bax ratio compared to NCM cultured with MM. This suggests hypoxia alone may not mediate significant apoptosis of NCM. For instance Malhotra et al. have demonstrated a need for glucose inhibitors or glucose depleted media in addition to hypoxia to induce substantial apoptosis in NCM[46]. Although no apoptosis of NCM was observed under hypoxia, we did observe a significant reduction in SCN5A transcripts with hypoxia. This effect was further attenuated with the addition of hMSC conditioned media. A reduction in sodium channels has been correlated with arrhythmias[47, 48] and thus this data suggests the proarrhythmic potential of hMSC paracrine factors. MSC transplantation into infarcted myocardium has not revealed increased arrhythmogenicity[49], however. Regardless, the substantial change observed with addition of conditioned media suggests hMSC can effect NCM via paracrine mechanisms.

CFbs were also used in an *in vitro* hypoxia model to investigate the effect of hMSC conditioned media on CFbs presence and collagen secretion. CFbs exposed to hMSC conditioned media exhibited increased presence after exposure to hypoxia and decreased collagen secretion. Similar results have also shown increased CFbs presence after culture with MSC conditioned media[50]. Collagen synthesis remained constant in studies by Li et al.[50] and Ohnishi et al.[51], however. Notably, the MSC source was different in these two studies versus our study and collagen expression was measured using RT-PCR. Thus, transcript levels may not correlate well with secreted protein levels. This *in vitro* data set also follows trends seen in our *in vivo* results. For instance, there are correlations for increased myofibroblast presence. Although there is an increase in myofibroblasts there is no change in fibrosis, suggesting fibroblasts are secreting less collagen. A similar trend was observed *in vitro*. This data as well as the *in vivo* data highlight possible paracrine mechanisms that may act to repair injured heart after cell therapy.

In conclusion, these experiments suggest that it is possible to deliver progenitor cells to injured myocardium using a collagen hydrogel. Moreover, this approach appears to result in higher initial engraftment rates than conventional approaches. Refinements of this approach, such as using matrices with desirable effects on cell differentiation or maintenance, may serve to enhance any benefits gained by cellular cardiomyoplasty.

3.5 LIMITATIONS and RECOMMENDATIONS

This proof of concept study details the use of TE constructs for the delivery of hMSC to infarcted myocardium. Application of cardiac patches resulted in high engraftment and prevention of adverse remodeling. There are several limitations to this study, however. For instance, it was noted that the culture of hMSC in collagen patches led to reduced potency and cellularity. This response may indicate that cells are

exposed to high stresses that modulate their function. This could be due a number of possibilities including cell crowding, mechanical strain or increased oxidative stress within the patch. Unfortunately, our does not directly support any one of these possibilities. Future studies should include investigations into stem cell function within collagen patches and the mechanisms for any observed modulations. Additionally, although our *in vivo* studies clearly demonstrate improved myocardial remodeling, it is unclear whether this effect is mediated by cell presence or via a possible immune response. The immunocompetent model used in this study has the capacity to elicit an immune response (to the xenograft). The presence of a strong immune response may also aid in the repair of infarcted myocardium. This model also limits the extent of engraftment over long periods. Therefore, use of an immunocompromised model may help to circumvent these limitations allowing for long term culture, uninhibited by a detrimental host response.

3.6 REFERENCES

1. Y. Sun, J. Q. Zhang, J. Zhang and S. Lamparter. Cardiac remodeling by fibrous tissue after infarction in rats. *J Lab Clin Med.* 2000 Apr;135:316-23.
2. M. C. Fishbein, D. Maclean and P. R. Maroko. The histopathologic evolution of myocardial infarction. *Chest.* 1978 Jun;73:843-9.
3. M. G. Klug, M. H. Soonpaa, G. Y. Koh and L. J. Field. Genetically selected cardiomyocytes from differentiating embryonic stem cells form stable intracardiac grafts. *J Clin Invest.* 1996 Jul 1;98:216-24.
4. C. E. Murry, R. W. Wiseman, S. M. Schwartz and S. D. Hauschka. Skeletal myoblast transplantation for repair of myocardial necrosis. *J Clin Invest.* 1996 Dec 1;98:2512-23.
5. P. Menasche. Skeletal myoblast transplantation for cardiac repair. *Expert Rev Cardiovasc Ther.* 2004 Jan;2:21-8.
6. K. L. Christman, H. H. Fok, R. E. Sievers, Q. Fang and R. J. Lee. Fibrin glue alone and skeletal myoblasts in a fibrin scaffold preserve cardiac function after myocardial infarction. *Tissue Eng.* 2004 Mar-Apr;10:403-9.
7. R. K. Li, Z. Q. Jia, R. D. Weisel, F. Merante and D. A. Mickle. Smooth muscle cell transplantation into myocardial scar tissue improves heart function. *J Mol Cell Cardiol.* 1999 Mar;31:513-22.
8. K. A. Hutcheson, B. Z. Atkins, M. T. Hueman, M. B. Hopkins, D. D. Glower and D. A. Taylor. Comparison of benefits on myocardial performance of cellular cardiomyoplasty with skeletal myoblasts and fibroblasts. *Cell Transplant.* 2000 May-Jun;9:359-68.
9. C. E. Murry, M. H. Soonpaa, H. Reinecke, et al. Haematopoietic stem cells do not transdifferentiate into cardiac myocytes in myocardial infarcts. *Nature.* 2004 Apr 8;428:664-8.
10. W. H. Zimmermann, M. Didie, S. Doker, et al. Heart muscle engineering: An update on cardiac muscle replacement therapy. *Cardiovasc Res.* 2006 Aug 1;71:419-29.
11. H. Oh, S. B. Bradfute, T. D. Gallardo, et al. Cardiac progenitor cells from adult myocardium: homing, differentiation, and fusion after infarction. *Proc Natl Acad Sci U S A.* 2003 Oct 14;100:12313-8.
12. J. Leor, E. Guetta, M. S. Feinberg, et al. Human umbilical cord blood-derived CD133+ cells enhance function and repair of the infarcted myocardium. *Stem Cells.* 2006 Mar;24:772-80.
13. M. A. Laflamme, J. Gold, C. Xu, et al. Formation of human myocardium in the rat heart from human embryonic stem cells. *Am J Pathol.* 2005 Sep;167:663-71.

14. T. Kofidis, J. L. de Bruin, G. Hoyt, et al. Myocardial restoration with embryonic stem cell bioartificial tissue transplantation. *J Heart Lung Transplant*. 2005 Jun;24:737-44.
15. Y. L. Tang, Q. Zhao, Y. C. Zhang, et al. Autologous mesenchymal stem cell transplantation induce VEGF and neovascularization in ischemic myocardium. *Regul Pept*. 2004 Jan 15;117:3-10.
16. D. Orlic, J. Kajstura, S. Chimenti, et al. Bone marrow cells regenerate infarcted myocardium. *Nature*. 2001 Apr 5;410:701-5.
17. V. Schachinger, S. Erbs, A. Elsasser, et al. Intracoronary bone marrow-derived progenitor cells in acute myocardial infarction. *N Engl J Med*. 2006 Sep 21;355:1210-21.
18. B. Assmus, V. Schachinger, C. Teupe, et al. Transplantation of Progenitor Cells and Regeneration Enhancement in Acute Myocardial Infarction (TOPCARE-AMI). *Circulation*. 2002 Dec 10;106:3009-17.
19. B. Assmus, J. Honold, V. Schachinger, et al. Transcoronary transplantation of progenitor cells after myocardial infarction. *N Engl J Med*. 2006 Sep 21;355:1222-32.
20. K. Lunde, S. Solheim, S. Aakhus, et al. Intracoronary injection of mononuclear bone marrow cells in acute myocardial infarction. *N Engl J Med*. 2006 Sep 21;355:1199-209.
21. T. Freyman, G. Polin, H. Osman, et al. A quantitative, randomized study evaluating three methods of mesenchymal stem cell delivery following myocardial infarction. *Eur Heart J*. 2006 May;27:1114-22.
22. I. M. Barbash, P. Chouraqui, J. Baron, et al. Systemic delivery of bone marrow-derived mesenchymal stem cells to the infarcted myocardium: feasibility, cell migration, and body distribution. *Circulation*. 2003 Aug 19;108:863-8.
23. C. Alperin, P. W. Zandstra and K. A. Woodhouse. Polyurethane films seeded with embryonic stem cell-derived cardiomyocytes for use in cardiac tissue engineering applications. *Biomaterials*. 2005 Dec;26:7377-86.
24. K. C. Wollert, G. P. Meyer, J. Lotz, et al. Intracoronary autologous bone-marrow cell transfer after myocardial infarction: the BOOST randomised controlled clinical trial. *Lancet*. 2004 Jul 10-16;364:141-8.
25. R. E. Coggeshall and H. A. Lekan. Methods for determining numbers of cells and synapses: a case for more uniform standards of review. *J Comp Neurol*. 1996 Jan 1;364:6-15.
26. M. F. Pittenger and B. J. Martin. Mesenchymal stem cells and their potential as cardiac therapeutics. *Circ Res*. 2004 Jul 9;95:9-20.
27. C. J. Hunter, S. M. Imler, P. Malaviya, R. M. Nerem and M. E. Levenston. Mechanical compression alters gene expression and extracellular matrix synthesis by chondrocytes cultured in collagen I gels. *Biomaterials*. 2002 Feb;23:1249-59.

28. Y. L. Tang, Q. Zhao, X. Qin, et al. Paracrine action enhances the effects of autologous mesenchymal stem cell transplantation on vascular regeneration in rat model of myocardial infarction. *Ann Thorac Surg.* 2005 Jul;80:229-36; discussion 36-7.
29. R. Uemura, M. Xu, N. Ahmad and M. Ashraf. Bone marrow stem cells prevent left ventricular remodeling of ischemic heart through paracrine signaling. *Circ Res.* 2006 Jun 9;98:1414-21.
30. A. A. Kocher, M. D. Schuster, M. J. Szabolcs, et al. Neovascularization of ischemic myocardium by human bone-marrow-derived angioblasts prevents cardiomyocyte apoptosis, reduces remodeling and improves cardiac function. *Nat Med.* 2001 Apr;7:430-6.
31. C. E. Murry, H. Reinecke and L. M. Pabon. Regeneration gaps: observations on stem cells and cardiac repair. *J Am Coll Cardiol.* 2006 May 2;47:1777-85.
32. R. S. Kellar, B. R. Shepherd, D. F. Larson, G. K. Naughton and S. K. Williams. Cardiac patch constructed from human fibroblasts attenuates reduction in cardiac function after acute infarct. *Tissue Eng.* 2005 Nov-Dec;11:1678-87.
33. T. Kofidis, J. L. de Bruin, G. Hoyt, et al. Injectable bioartificial myocardial tissue for large-scale intramural cell transfer and functional recovery of injured heart muscle. *J Thorac Cardiovasc Surg.* 2004 Oct;128:571-8.
34. S. Miyagawa, Y. Sawa, S. Sakakida, et al. Tissue cardiomyoplasty using bioengineered contractile cardiomyocyte sheets to repair damaged myocardium: their integration with recipient myocardium. *Transplantation.* 2005 Dec 15;80:1586-95.
35. W. H. Zimmermann, I. Melnychenko, G. Wasmeier, et al. Engineered heart tissue grafts improve systolic and diastolic function in infarcted rat hearts. *Nat Med.* 2006 Apr;12:452-8.
36. Y. Miyahara, N. Nagaya, M. Kataoka, et al. Monolayered mesenchymal stem cells repair scarred myocardium after myocardial infarction. *Nat Med.* 2006 Apr;12:459-65.
37. J. Leor, S. Aboulafia-Etzion, A. Dar, et al. Bioengineered cardiac grafts: A new approach to repair the infarcted myocardium? *Circulation.* 2000 Nov 7;102:III56-61.
38. G. Zhang, X. Wang, Z. Wang, J. Zhang and L. Suggs. A PEGylated fibrin patch for mesenchymal stem cell delivery. *Tissue Eng.* 2006 Jan;12:9-19.
39. T. Shimizu, H. Sekine, Y. Isoi, M. Yamato, A. Kikuchi and T. Okano. Long-term survival and growth of pulsatile myocardial tissue grafts engineered by the layering of cardiomyocyte sheets. *Tissue Eng.* 2006 Mar;12:499-507.
40. R. L. Carrier, M. Papadaki, M. Rupnick, et al. Cardiac tissue engineering: cell seeding, cultivation parameters, and tissue construct characterization. *Biotechnol Bioeng.* 1999 Sep 5;64:580-9.

41. W. Dai, S. L. Hale, B. J. Martin, et al. Allogeneic mesenchymal stem cell transplantation in postinfarcted rat myocardium: short- and long-term effects. *Circulation*. 2005 Jul 12;112:214-23.
42. N. Nagaya, K. Kangawa, T. Itoh, et al. Transplantation of mesenchymal stem cells improves cardiac function in a rat model of dilated cardiomyopathy. *Circulation*. 2005 Aug 23;112:1128-35.
43. M. A. Gaballa, J. N. Sunkomat, H. Thai, E. Morkin, G. Ewy and S. Goldman. Grafting an acellular 3-dimensional collagen scaffold onto a non-transmural infarcted myocardium induces neo-angiogenesis and reduces cardiac remodeling. *J Heart Lung Transplant*. 2006 Aug;25:946-54.
44. J. Leor, L. Rozen, A. Zulloff-Shani, et al. Ex vivo activated human macrophages improve healing, remodeling, and function of the infarcted heart. *Circulation*. 2006 Jul 4;114:194-100.
45. K. B. Gupta, M. B. Ratcliffe, M. A. Fallert, L. H. Edmunds, Jr. and D. K. Bogen. Changes in passive mechanical stiffness of myocardial tissue with aneurysm formation. *Circulation*. 1994 May;89:2315-26.
46. R. Malhotra and F. C. Brosius, 3rd. Glucose uptake and glycolysis reduce hypoxia-induced apoptosis in cultured neonatal rat cardiac myocytes. *J Biol Chem*. 1999 Apr 30;274:12567-75.
47. J. Akai, N. Makita, H. Sakurada, et al. A novel SCN5A mutation associated with idiopathic ventricular fibrillation without typical ECG findings of Brugada syndrome. *FEBS Lett*. 2000 Aug 11;479:29-34.
48. T. Makiyama, M. Akao, K. Tsuji, et al. High risk for bradyarrhythmic complications in patients with Brugada syndrome caused by SCN5A gene mutations. *J Am Coll Cardiol*. 2005 Dec 6;46:2100-6.
49. D. G. Katritsis, P. Sotiropoulou, E. Giazitzoglou, E. Karvouni and M. Papamichail. Electrophysiological effects of intracoronary transplantation of autologous mesenchymal and endothelial progenitor cells. *Europace*. 2007 Mar;9:167-71.
50. L. Li, S. Zhang, Y. Zhang, B. Yu, Y. Xu and Z. Guan. Paracrine action mediate the antifibrotic effect of transplanted mesenchymal stem cells in a rat model of global heart failure. *Mol Biol Rep*. 2009 Apr;36:725-31.
51. S. Ohnishi, H. Sumiyoshi, S. Kitamura and N. Nagaya. Mesenchymal stem cells attenuate cardiac fibroblast proliferation and collagen synthesis through paracrine actions. *FEBS Lett*. 2007 Aug 21;581:3961-6.

Chapter 4

Modulation of Human Mesenchymal Stem Cell Function in Collagen Patches

4.1 INTRODUCTION

Tissue engineering (TE) encompasses the combination of living cells with biological or synthetic scaffolds. Several attempts at engineering blood vessels, heart valves, heart tissue, bone, skin, ligament and nerve tissue have been undertaken recently and show promise as therapeutic substitutes [1-6]. In the field of cellular cardiomyoplasty, several cell types have been delivered to the myocardium, yet few cells actually engraft using conventional delivery methods such as direct or IV injection [7, 8]. To address this problem, we have developed a TE approach (combination of cells and matrix) to locally and homogeneously deliver cells to an infarct. We have selected collagen as the bioscaffold because it is easily available and relatively non-immunogenic. Its composition can be modified to vary how rapidly it is reabsorbed *in vivo* and to vary its elastic modulus. Collagen is relatively strong but flexible, and it contains signaling sequences for cells that are seeded into it; thus adhesion-dependent cell types are capable of attaching to and remodeling this fibrous protein. Adult stem cells such as hMSCs are attractive for cellular cardiomyoplasty because they are relatively easy to obtain and maintain in culture. In general, MSCs which engraft into infarcted heart improve global cardiac measures [9-11].

With conventional methods of delivery, cells grown as a monolayer are removed from culture, resuspended in an aqueous vehicle and injected into the host. With a TE approach, cell delivery is achieved by applying a cellularized collagen patch to the epicardial surface of the heart. Because these cells are cultured in a different configuration (i.e. a monolayer vs. in three dimensions in collagen), it is expected that the phenotype and function of cells in collagen constructs will be affected. We

hypothesize that culture of hMSC within collagen gels will modulate cellular viability, proliferation, differentiation and secretory profiles compared to cells cultured as monolayers. Such changes in cell function can lead to downstream consequences that may promote or attenuate potential reparative mechanisms involved in cellular cardiomyoplasty.

4.2 MATERIALS and METHODS

4.2.1 Cell Culture

CD34 negative female hMSC obtained from Lonza (Wakersville, Maryland) were cultured in complete medium consisting of Dulbecco's Modified Eagle's Medium (DMEM) containing 10% MSC qualified serum, L-glutamine and penicillin/streptomycin at 37°C in 5% CO₂. Human cardiac microvascular endothelial cells (hMVEC-C) were cultured in EGM-2V medium (Lonza; Wakersville, Maryland) containing 5% FBS at 37°C in 5% CO₂.

4.2.2 Formation of Cell Seeded Collagen Patches

hMSC (female) expanded to P3 – P6 were embedded into a rat tail type I collagen matrix to form cardiac patches. To produce cardiac patches for progenitor cell delivery, 0.2 million hMSCs were mixed in a solution of rat tail type I collagen, 5x DMEM and 10% fetal bovine serum such that the final collagen concentration was 2 mg/mL. The solution was placed in individual wells of a non-tissue culture-treated 48-well plate in order to create a patch that was between 0.3 – 0.7 cm in diameter. Patches were cultured at 37°C in 5% CO₂ for 1-7 d before usage.

4.2.3 Measurement of Patch Compaction

Compaction of hMSC patches was determined by measuring the change in volume of the patch over 7 d, using a water displacement strategy. Patches were

removed from culture dishes and washed several times to remove medium/serum using PBS. Afterwards, patches were placed in a 10 mL volumetric flask containing 10 mL of serum-free DMEM. The location of the initial volume was indicated using the “10 mL” marking on the side of the flask. The change in volume was measured after submersing patches in DMEM and was obtained using a micro-volume syringe. DMEM was removed from the flask until the volume reached the initial location as indicated by the “10 mL” marking. The volume removed after submersion was recorded as the volume of the patches at 0, 1 and 3 d.

4.2.4 Viability Assays

To assess cell viability within the construct, patches containing hMSC were digested in type I collagenase (500 U/mL) diluted in DMEM for 30 minutes at 37°C with intermittent mixing. Each patch was submerged in 2 mL of the collagenase solution and placed into at 37°C water bath. The solution was triturated every 5 minutes to assist in the digestion of the construct. At the end of the incubation period, collagenase activity was inhibited by the addition of 500 μ L of 100% FBS and 8 mL of complete hMSC medium (see section 4.2.1). Viability was measured using a 1:10 dilution of cell suspension to trypan blue. Counts were made using a hemocytometer on day three. Total cell number was counted in addition to the total number of live cells. Viability was recorded as (the number of live cells) / (the number of total cells). Viability of stem cells cultured on treated plastic was also determined using the same counting procedure as above. Cells were removed from culture dishes using 0.25% Trypsin/EDTA.

4.2.5 Cellularity

DNA within hMSC cardiac patches was used as an index of cellularity. Constructs were digested in a mild detergent with proteinase K for 1-2 hours at 55°C and

DNA was isolated and purified using a DNeasy kit (Qiagen; Valencia, CA). The amount of DNA was quantified by incubating DNA with PicoGreen reagent (Molecular Probes; Eugene, Oregon) for five minutes at room temperature and analyzed with a fluorescent plate reader at an excitation of 480 nm and emission of 520 nm. RFU values were compared with a standard curve and DNA concentrations were calculated at 1 and 3 d after patch formation.

4.2.6 Proliferation

Proliferation was determined by measuring the incorporation of 5-ethynyl-2'-deoxyuridine (EdU); a nucleoside analog to thymidine, which is incorporated into DNA during synthesis. Cellularized constructs or cells cultured as a monolayer were pulsed with 10 mM EdU (Invitrogen; Carlsbad, CA) for 72 hours after their initial formation. Afterwards constructs were washed in PBS and digested using collagenase to isolate cells as described above (4.2.4). Next, cells were washed using a 1% bovine serum albumin (BSA)/PBS solution and then fixed using the Click-iT fixative (Invitrogen; Carlsbad, CA) for 15 minutes at room temperature. Cells were permeabilized with Triton X-100 and then stained using the Click-iT cocktail mixture for 30 minutes at room temperature. Afterwards, cells were washed with 1% BSA/PBS and used for flow cytometry. To simplify analysis hMSC were gated using an unstained sample (no antibody) on a forward scatter vs. side scatter dot plot. This procedure helped to remove excess debris. Next, a positive control using hMSC cultured on treated plastic was run to determine the proper levels for positive signal. Samples were analyzed for positive fluorescein isothiocyanate (FITC) signal using the histogram option of the BD FACS Diva software package (BD Biosciences; San Jose, CA). Positive signal was compared with the appropriate isotype controls, which allowed for accurate background subtraction.

Analysis of data was performed using FCS Express 3.0 software (De Novo Software; Los Angeles, CA) and the histogram subtraction function.

4.2.7 Assessment of Cell Differentiation

4.2.7.1 Flow Cytometry

Differentiation of hMSC within collagen patches was measured by monitoring the expression of markers for stem cell potency over several days. hMSC were isolated from the patch via collagenase treatment, stained and analyzed for the expression of CD105 and CD73 by flow cytometry. After cells were isolated from the patch, they were fixed using 4% paraformaldehyde (PFA) for 15 minutes on ice. Next, cells were stained with the appropriate primary antibodies for 30 minutes on ice. If necessary, fluorescent conjugated secondary antibodies were added for 25 minutes on ice (Santa Cruz Biotechnology; Santa Cruz, CA). Cells were washed in a 0.3% BSA/PBS solution and analyzed via flow cytometry as described above (4.2.5).

4.2.7.2 Histology

Differentiation of hMSC toward cardiac lineages was further assessed using immunohistochemistry (IHC) and fluorescence or confocal microscopy. hMSC were cultured on glass slides coated with 0.1% gelatin until 80-90% confluency. Culture medium was removed, and the cells were fixed and permeabilized using 4% PFA and 0.1% Triton X-100, respectively. Cells were blocked with 3% BSA. Next, cells were stained for connexin 43 or troponin T (diluted in 0.3% BSA in PBS) followed by staining with appropriate fluorescent conjugated secondary antibodies (diluted in 5% goat serum), a phalloidin F-actin stain (Molecular Probes; Eugene, Oregon) and a nuclear DAPI (4',6-diamidino-2-phenylindole) stain (Sigma; St. Louis, MO). Cells were mounted using an antifade mounting medium and viewed under a confocal microscope (Carl Zeiss; Thornwood, NY). Additionally, patches at 3 d and 7 d were removed from culture

and washed in PBS to remove excess culture medium. Sections were fixed in 4% PFA for 24 hours then transferred into 70% ethanol until paraffin processing. The patches were embedded in paraffin wax and cut to 5 μ m sections using a microtome and dried onto a glass slide at 37°C for 24 hours. To stain patches, sections were rehydrated by washing in two changes each of the following: xylene (to remove paraffin wax), 100% ethanol, 95% ethanol, 70% ethanol and deionized water. Afterwards sections were pretreated with citrate buffer (10 mM citric acid in water; pH 6.0, microwaved on high) for 5 minutes for antigen retrieval. Next sections were blocked with 5% goat serum for one hour and incubated with primary antibodies (connexin 43 and Troponin T; diluted in 0.3% BSA in PBS) for two hours. Sections were washed using a 0.45% fish skin gelatin solution in PBS and the appropriate fluorescent conjugated secondary antibodies were added for one hour. DAPI was used to stain cell nuclei. Afterwards, sections were mounted using an antifade mounting medium and viewed under a fluorescence and confocal microscope (Nikon; Melville, NY).

4.2.8 Antibody Arrays and Protein ELISAs

To determine possible angiogenic growth factors secreted by hMSC, an antibody array was performed on four sets of conditioned media:

Room Air (20% Oxygen; also defined as normoxia for our experiments):

- 1) hMSC monolayer (hN), 2) hMSC patch (hNP)

Hypoxia (1% Oxygen):

- 3) hMSC monolayer (hH), 4) hMSC patch (hHP)

Conditioned medium was collected from each group after 24 hours with either room air or 1% O₂ and allowed to incubate with an angiogenesis specific antibody array

(Panomics; Fremont, CA) for two hours. Conditioned medium not immediately used was frozen at -80°C . Unused medium was used and discarded after a single freeze/thaw cycle. The antibody array was washed, labeled and visualized using the ECL plus chemiluminescence kit (Amersham Biosciences, Piscataway, NJ). Exposure times ranged from 15 seconds to two minutes. Several individual angiogenic factors were further assessed using an enzyme-linked immunosorbent assay (ELISA). In particular, vascular endothelial growth factor (VEGF), fibroblast growth factor-acidic (FGF-1), angiogenin (ANG) and interleukin-8 (IL-8) ELISAs were performed according to manufacturer's instructions (R&D Systems; Minneapolis, MN). Conditioned medium was diluted 1:1 in calibrator diluent and placed into the wells of a 96 well plate containing adsorbed antibodies to one of the four growth factors described above. After an extended incubation at room temperature, the wells were washed several times with wash buffer. Growth factor conjugate was added for one hour and washed several times thereafter. Next, substrate solution was added, which led to the development of a color that was proportional to the amount of growth factor in each conditioned medium group. The resulting colored solution was collected and the absorbance was spectrophotometrically measured at 450 nm with background subtraction at 570 nm. Absorbance values were compared with a standard curve and absolute concentrations were determined from this standard curve. The ELISA standard curve was adjusted based on the signal (noise) levels recorded in null samples.

4.2.9 Real Time RT-PCR

RNA was isolated from cell monolayers or cellularized constructs (48 hours after initial seeding) using a commercial RNeasy kit (Qiagen; Valencia, CA). RNA concentration and purity were measured using a spectrophotometer (abs: 260 nm, 280 nm and 230 nm). Afterwards, 1 μg of RNA was converted into cDNA using an Applied

Biosystems cDNA synthesis kit (Applied Biosystems, Foster City, CA). The reaction mixture was incubated for 5 minutes at 25°C, 30 minutes at 42°C and lastly, 5 minutes at 85°C. Real Time PCR was run using a total of 5 ng template cDNA for each sample. For each run, a negative control (water only, no template) was analyzed simultaneously, and each sample was run in duplicate using ABI FAST SYBR green supermix (Applied Biosystems;) for multiple genes including: ANG, IL-8, VEGF, FGF-1, ribosomal protein 13A (RPL13A), β -Actin and ribosomal protein 18S (R18S). Primer assays for each primer set were obtained from Qiagen. The fast PCR protocol consisted of an initial denaturing step at 95°C for 4 minutes. Next, samples were run at 94°C (denaturation) for 15 seconds, 60°C (annealing) for 30 seconds and 72°C (extension) for 30 seconds for 35 cycles. Relative RNA abundance was calculated using the following equation: $2^{-\Delta\Delta C_T}$, where the first delta represents threshold subtraction (“delta 1”) from the endogenous control and the second delta represents the division of “delta 1” by an internal control.

4.2.10 Hypoxia Model and Endothelial Cell Function

To evaluate paracrine functionality, hMSC were cultured in room air (~20% O₂) or under hypoxic conditions (1% O₂) for one day (Figure 4.1) as a patch or monolayer in DMEM supplemented with L-glutamine and penicillin/streptomycin (Maintenance Media; MM). Afterwards the conditioned medium was removed from the cells or patches, spun at 5000 rpm to remove debris and placed on hMVEC-C for two days in 1% O₂. Conditioned medium that was not immediately used was frozen at -80°C. Frozen medium was also used for experiments but would only be used after a single freeze/thaw cycle. After a two day culture period conditioned medium was removed from hMVEC-C and MTT (3-(4,5-Dimethylthiazol-2-yl)-2,5-diphenyltetrazolium bromide;

Sigma) reagent was added for three hours (Figure 4.1). Afterwards, the MTT reagent was removed, and a solution of 0.1 N hydrochloric acid (HCL) in anhydrous isopropyl alcohol was added to dissolve the formazan crystals. The resulting colored solution was collected, and the absorbance was spectrophotometrically measured at 570 nm with background subtraction at 690 nm. In addition, cell counts were performed to determine if cell number was affected after culture in conditioned media for 3 d in 1% O₂. hMVEC-C were removed from treated tissue culture plastic using a 0.25% trypsin/EDTA solution. Complete EGM-2V medium was added after three minutes, and the cells were collected and centrifuged. Afterwards, the cells were washed once with PBS and added to trypan blue at a 1:10 dilution. Trypan exclusion was used to determine the total number of cells and viability. Viability was recorded as (the number of live cells) / (the number of total cells).

A tube formation assay was performed to further assess the angiogenic potential of hMSC conditioned medium. hMVEC-C (15,000) were seeded onto Matrigel in a 96-well plate in the presence of conditioned medium from all groups in a 1:1 ratio with 2% fetal bovine serum in MM for 22 hours under hypoxic conditions. Images of the resultant tubes were collected with a digital camera, and the average length was manually determined (sample sizes from 50 to 70 tubes per group) using Image Pro Plus software (Media Cybernetics Inc; Bethesda, MD).

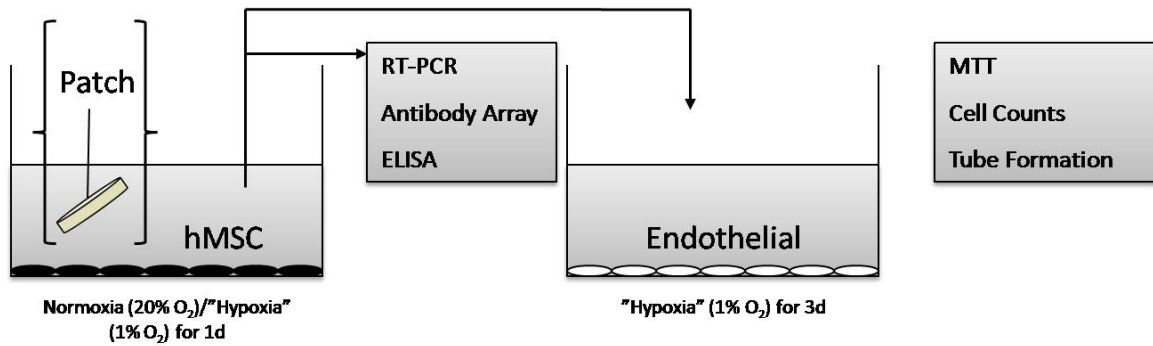


Figure 4.1) Schematic of experiments to test the paracrine effects of hMSCs. In order to investigate the paracrine effect of hMSC conditioned medium on endothelial cells, a model was set up in which conditioned medium from hMSCs cultured in room air (normoxia) or hypoxia was removed and placed on viable endothelial cells. After defined periods, the function of endothelial cells was analyzed.

4.2.11 Animal Handling

Male athymic nude rats obtained from Charles River (Wilmington, MA) were allowed to acclimate to housing conditions for at least one week before use. Rats were typically used for experiments between 8 and 12 weeks of age. All animals received care in compliance with federal and institutional guidelines with approval from the Institutional Animal Care and Use Committee.

4.2.12 Infarct Model and Patch Application

Myocardial infarction (MI) was induced by permanent ligation of the left anterior descending (LAD) coronary artery in athymic nude male rats (200-300 g). Rats were anesthetized with 5% isoflurane in pure oxygen. Afterwards, rats were weighed and intubated for mechanical ventilation. After endotracheal intubation and initiation of ventilation, isoflurane was reduced to the amount required to prevent the pedal reflex (1.5-2%). The heart was exposed via a left thoracotomy, and the proximal LAD was ligated using 6-0 silk suture. The location of the ligation was placed at the intersection of

the left atrial appendage and pulmonary conus when the LAD was not clearly visible. Noticeable effects of ligation included a change in pallor of the left ventricle (LV), transient arrhythmias and an inflated left atrial appendage. Ten minutes after ligation, either patches were applied onto the anterior wall of the infarct site and secured with fibrin glue (Baxter; Deerfield, IL; Figure 3.3) or 250,000 – 400,000 hMSC suspended in 25-40 mL saline were injected. This range of injected cells was used to account for cell loss due to leakage out of the injection site. Rats with induced infarction and without patch application or cell injection, with saline injection only, or with non-viable patches applied served as controls for the study. Additionally, a sham control, in which the pericardium was removed and suture was threaded around the LAD without ligation, was also used as a control. Buprenorphine (0.1 mg/kg) was injected subcutaneously after surgery (and as necessary), and rats were allowed to recover under close supervision. This procedure was performed on a total of 62 rats, of which 15 died within two weeks postoperatively, presumably because of infarct complications. Additionally, 22 rats were excluded because of insufficient infarct size. Therefore, a total of 25 rats were used in this *in vivo* study (Table 4.1).

4.2.13 Echocardiography

Transthoracic echocardiograms were performed on rats using a VisualSonics Vevo 770 ultrasound unit (VisualSonics, Toronto, Canada). The VisualSonics RMV 716 Scanhead with center frequency 17.5 MHz, frequency band 11.5–23.5 MHz, and focal length 17.5 mm was used for echo acquisition in rats. The animals were maintained lightly anesthetized during the procedure with 1.5% isoflurane delivered through a face mask at a rate of 3-4 L/min. The animals were kept warm on a heating pad, and the body temperature was continuously monitored using a rectal thermometer, maintaining it at between 35 and 37°C by adjusting the distance of a heating lamp. Under these

conditions, the animal's heart rate could be maintained between 300-400 beats per minute. Two-dimensional and M-mode echocardiography were used to assess wall thickness, LV dimensions and fractional shortening. Images were obtained from the parasternal long axis, parasternal short axis at the mid-papillary level and apical 4-chamber views.

Baseline echocardiograms were acquired at 3 days post-MI with additional echocardiograms acquired at 4 weeks post-MI. The baseline post-MI echocardiograms allowed determination of the extent and location of infarction. With nude rats, LAD ligation resulted in most animals developing anterolateral infarcts. Isolated anterior infarction only occurred in one animal that survived surgery.

4.2.14 Cardiac Hemodynamics

Cardiac hemodynamics were measured after the final echocardiographic examination. Rats were anesthetized with 1% isoflurane, and a 1.4 or 2 F Millar Mikro-Tip catheter (SPR-671, Millar Instruments, Houston, TX) was inserted into the right carotid artery and advanced into the left ventricle. Aortic and left ventricular (LV) pressures were recorded on a PowerLab system and analyzed using Chart v4.2.4 software (ADInstruments, Colorado Springs, CO).

Table 4.1) Animal accounting for *in vivo* model of myocardial infarction

	# Surgeries	# Dead within 24 hr	# Dead from 24 hr to 14 d	# Excluded Due to Baseline ECHO	Mass at Initial Surgery (g)	Mass at 4wk Hemo (g)	# Used in 4wk ECHO Studies	# Used in 4 wk Hemo Studies
Sham	6	0	0	1	209 ± 12	--	5	2
MI control	14	1	0	8	209 ± 8	277 ± 7	5	5
Saline Inj	15	5	0	7	233 ± 9	297 ± 18	3	3
Non-viable Patch	11	4	0	5	216 ± 8	249 ± 1	2	2
hMSC Inj	7	3	0	0	210 ± 7	267 ± 8	4	4
hMSC Patch	9	0	2	1	215 ± 7	273 ± 7	5	5

MI – Myocardial infarction; hMSC – human mesenchymal stem cells; ECHO – Echocardiography; Hemo – Hemodynamics; wk – week

4.2.15 Myocardial Histology

After the hemodynamic studies, hearts were excised under anesthesia, perfused with 4% paraformaldehyde and then cryo-protected by immersion in 30% sucrose for 48-96 hours. Isopentane cooled in liquid nitrogen was used to freeze hearts immersed in optimal cutting temperature (OCT) medium. Sections were cut to 7 µm using a commercial cryostat and used for either isolectin B4 or Masson's Trichrome staining. To calculate infarct size, at least four Masson's Trichrome stained sections at various levels along the long axis were analyzed for collagen deposition. The midline technique for infarct size determine was used as described previously [12]. Briefly, the LV midline was drawn at the center of the anterior or lateral walls along the length of the infarct. This circumference was divided by the total midline circumference of the heart to determine infarct size. Additionally, frozen heart sections were air dried, and OCT was removed by rinsing slides in PBS. Isolectin B4 (Invitrogen; Carlsbad, CA) was diluted 1:1000 in Tris buffered saline with 0.1% Tween-20. This solution was added to sections for 30 minutes at 37°C. Then, sections were washed in PBS and counterstained with DAPI for 5 minutes. Sections were rinsed in dH₂O and mounted with an antifade aqueous

mounting medium (Vector Labs; Burlingame, CA). Isolectin is used to stain endothelial cells and thus highlighted neovessel formation. Vessel density was calculated as the number of vessels (with a clear lumen and not associated with intact myocardium) per field of view (FOV). At least six FOVs were taken for each frozen section along the anterior, lateral and posterior portions of the LV.

4.2.16 Statistical Analysis and Interpretation

A Student's t-test was used to determine changes in hMSC cellularity when cultured in collagen patches. A two-way analysis of variance (ANOVA) was performed to interpret the response of hypoxic versus normoxic (20% O₂) and of patch versus monolayer in *in vitro* assays (proliferation, differentiation, viability and protein/mRNA abundance). A post-hoc Bonferroni test was used for comparison of individual results. Additionally, a one-way ANOVA with appropriate post-hoc testing (Bonferroni) was used for the interpretation of *in vivo*, endothelial cell and histological data sets. A p-value less than 0.05 indicated statistical significance.

4.3 RESULTS

4.3.1 Culture within Collagen Patches Modulates Proliferation, Differentiation and Viability of hMSC.

To determine the effects of cell culture within collagen patches on hMSC function, we assessed cell proliferation, differentiation, viability and secretion profiles. Earlier data reported in Chapter 3 noted a loss of cellularity when hMSCs were grown in patches. In order to address this, we lowered the cell number in the patch to two hundred thousand cells per patch. Two hundred thousand cells was chosen based on previous reports using cellularized collagen systems for tissue engineering purposes [13,

14] and by using the mass ratio of mice to humans to correct the number of cells given to humans in recent clinical studies of cellular cardiomyoplasty [15-17]. Upon lowering the hMSC number to 0.2 million cells per patch, we noticed slightly slower compaction but no reduced cellularity over 3 d in culture (Figure 4.2).

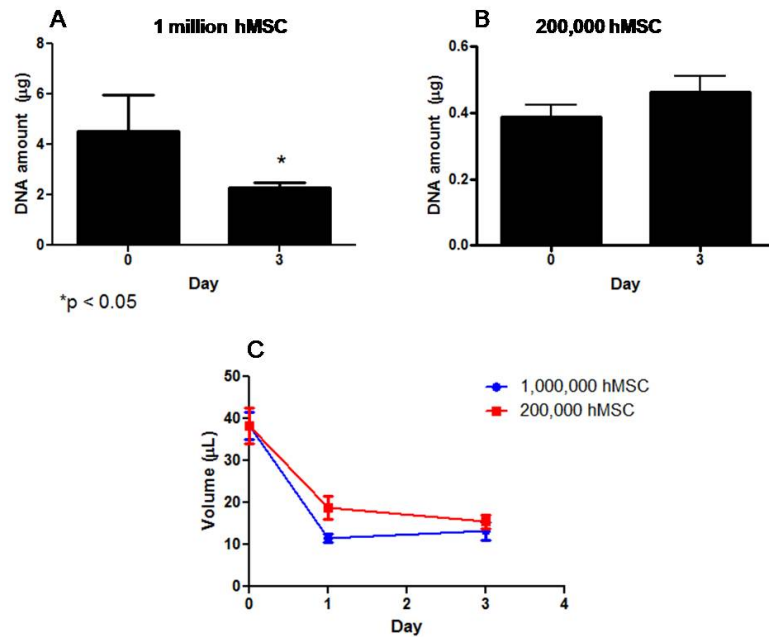


Figure 4.2) Initial cell seeding density influences cardiac patch cellularity and compaction. The seeding density of cardiac patches was lowered from 1 million to 0.2 million cells to prevent excessive cell loss while in culture. A) When 1 million cells were cultured in collagen patches, we saw a significant drop in cellularity over 3 d (Day 0: $4.5 \pm 1.4 \mu\text{g}$ vs. Day 3: $2.3 \pm 0.2 \mu\text{g}$; $p < 0.05$) B) Cardiac patches seeded with 0.2 million cells showed no decrease in cellularity over 3 d (Day 0: $0.39 \pm 0.04 \mu\text{g}$ vs. $0.46 \pm 0.05 \mu\text{g}$; $p = 0.3$). C) Cardiac patches with 1 million or 0.2 million showed little differences in compaction over 3 d.

All experiments described from this point use a seeding density of 0.2 million hMSC per patch.

Proliferation was quantified using a pulse-chase with EdU substrate (Figure 4.3). EdU incorporation into monolayer cells or cells removed from within collagen patches was measured by flow cytometry. hMSC demonstrated attenuated proliferation upon culture within collagen patches. hMSC showed a 86% reduction ($50.9 \pm 6.2\%$ EdU+ vs. $7 \pm 0.9\%$ EdU+; $p < 0.001$) compared to culture on treated plastic.

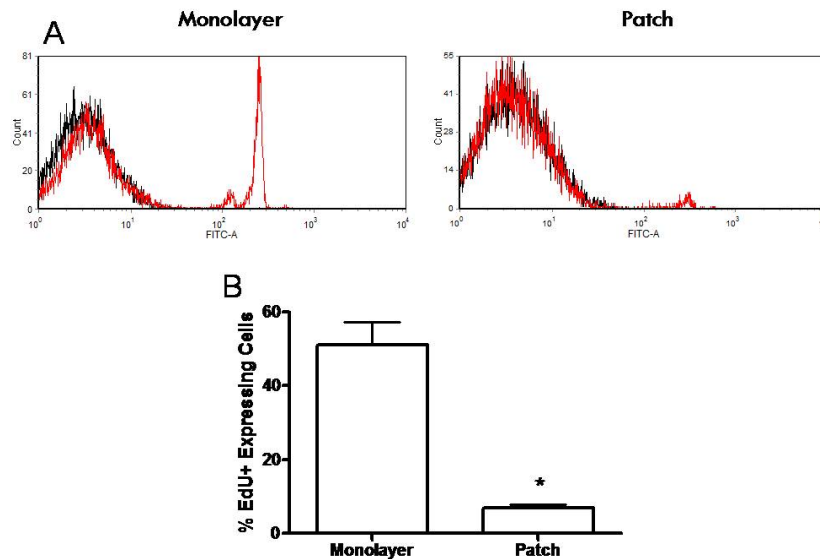


Figure 4.3) Culture of hMSC in collagen patches attenuates proliferation. A) Analysis by flow cytometry of EdU incorporation was used to determine the proliferative capacity of stem/progenitor cells cultured with patches compared to monolayers. The black histogram represents the isotype or negative control while the red histogram represents those cells stained for the EdU. Peaks beyond the isotype control, correspond to cells with positive EdU presence. B) hMSC ($50.9 \pm 6.2\%$ EdU+ vs. $7 \pm 0.9\%$ EdU+; $*p < 0.001$), demonstrated reduced EdU incorporation and thus proliferation after culture in collagen patches (hMSC: $n = 5$).

Stem cell potency for cells cultured as monolayers or within collagen patches was determined by monitoring several antigens within the progenitor/stem cell populations. CD105 and CD73 were used to determine the extent of differentiation over 7 d. There was no loss of potency in that time period for hMSCs as measured by CD105 (Monolayer: $85.6 \pm 5.5\%$ Expression vs. Patch 3 d: $76.1 \pm 8.3\%$ Expression vs. Patch 7 d: $73.1 \pm 12\%$ Expression; $p > 0.05$) and CD73 (Monolayer: $82.9 \pm 0.4\%$ Expression vs. Patch 3 d: $75.4 \pm 4.9\%$ Expression vs. Patch 7 d: $71.1 \pm 9.7\%$ Expression; $p > 0.05$).

To determine whether culture of hMSC in collagen patches promoted cardiac cell differentiation, we performed IHC on cardiac patch sections to probe for connexin43 (Cx43) and cardiac troponin T (TnT). Results reveal the presence of Cx43 localized within the cytosolic space (and near the nucleus) of cultured hMSC monolayers. This pattern of staining was maintained when hMSC were cultured in collagen patches, although the intensity of staining was less pronounced, suggesting that there was no increase in cardiac differentiation in culture. TnT was absent in hMSC monolayers and patches, confirming the maintenance of pluripotency.

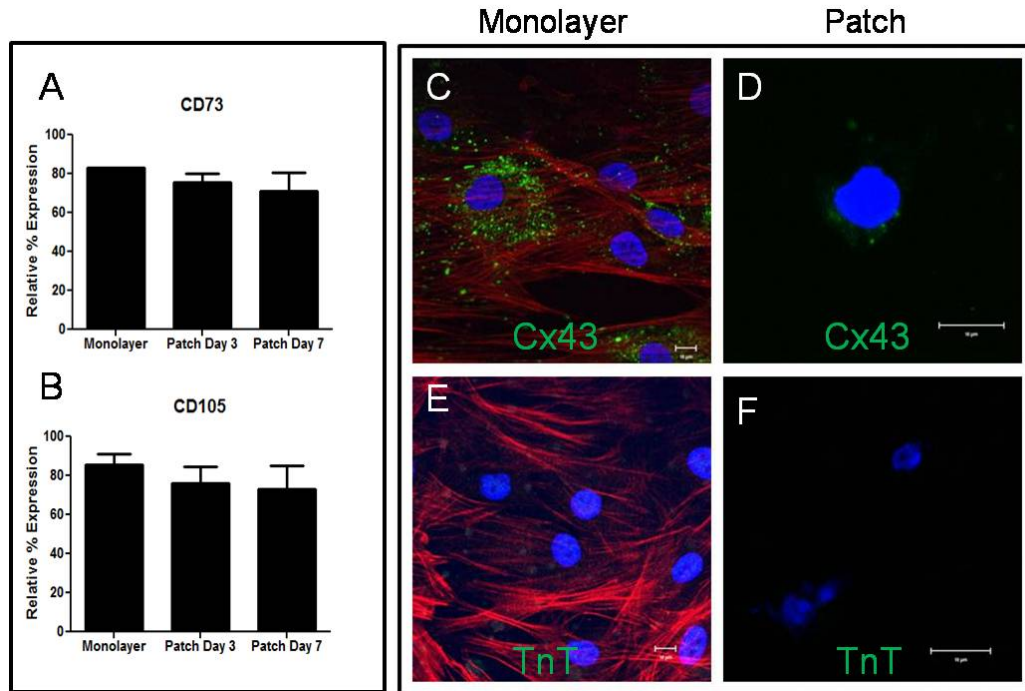


Figure 4.4) Minimal loss of cell potency after culture in collagen patches. CD73 and CD105 were used to monitor stem cell potency over 7 d in culture as monolayers or patches for hMSCs. hMSCs showed minimal to no change in A) CD73 (hMSC: monolayer: $82.9 \pm 0.4\%$ vs. patch 3 d: $75.4 \pm 4.9\%$ vs. patch 7 d: $71.1 \pm 9.7\%$; $p > 0.05$) and B) CD105 (hMSC: monolayer: $85.6 \pm 5.5\%$ vs. patch 3 d: $76.1 \pm 8.3\%$ vs. patch 7 d: $73.1 \pm 12\%$; $p > 0.05$) expression over 7 d. Additionally, culture in collagen patches did not upregulate cardiac proteins connexin43 (Cx43; C&D) or troponin T (TnT; E&F) in hMSCs (Green – Cx43 in figure C, D and TnT in figure E, F; Red – Phalloidin F-Actin; Blue – DAPI nuclear stain). Measure bars correspond to 10 μm .

Despite a maintenance of potency and little evidence of differentiation, there was a small decrease in cell viability in patches as compared to monolayers. To determine cell viability within collagen patches, hMSC were isolated using a collagenase solution after three days in culture. hMSC maintained viability above 80% after culture in collagen patches (Figure 4.6a and b). There was, however, a small but significant loss of viability of hMSC cultured in collagen patches when compared to monolayers (Monolayer: $92.8 \pm 2\%$ vs. Patch: $81 \pm 3\%$; $p < 0.05$).

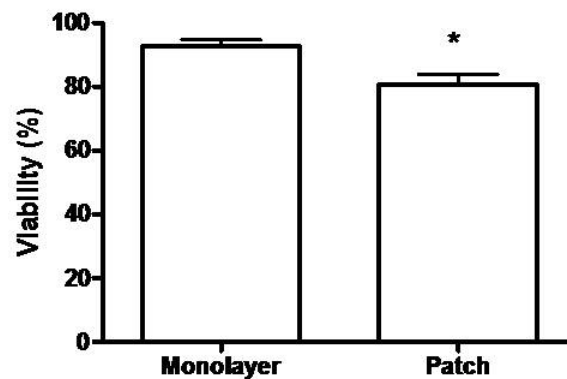


Figure 4.5) Viability of hMSC in collagen patches. Viability of hMSC was determined with a trypan exclusion assay. hMSCs culture in collagen patches resulted in a modest but statistically significant reduction in viability over 3 d (monolayer: $92.8 \pm 2\%$ vs. patch: $81 \pm 3\%$; * $p < 0.05$; $n = 5$).

4.3.2 Changes in Secretory Profiles of hMSC after Culture in Collagen Patches

Several stem cell populations are known to secrete beneficial paracrine factors which may play an important role in circumventing maladaptive pathologies. Paracrine pathways have also been suggested in potential reparative mechanisms in cellular cardiomyoplasty. The tissue engineered delivery vehicle used in this study has already

shown a propensity to alter cellular function and thus may also alter the secretion profile of hMSC. Therefore, in addition to assessing changes in cellular properties, we also assessed any changes in the secretory profiles of hMSC in collagen patches versus cultured monolayers. Conditioned medium from hMSC cultured as monolayers or within collagen patches in room air or 1% oxygen was collected and analyzed for various angiogenic factors (groups described in section 4.2.9). Additionally, RNA from hMSC was isolated from monolayers or within collagen patches and analyzed for various transcripts. Hypoxia was chosen as a model to simulate expected low oxygen conditions within ischemic tissue (such as infarcted cardiac tissue). Such a model has been used in several studies investigating cell function *in vitro*.

All hMSC conditioned media groups showed heightened protein concentrations versus a MM control (figure 4.6c). Additionally, conditioned media from all groups was placed on antibody arrays to detect the presence of pro- and anti-angiogenic factors. As shown in figure 4.6a, notable differences within groups hN, hH, hNP and hHP include the absence of IL-8 in monolayers (groups hN and hH), reduced presence of ANG, IL-6 and FGF-1 in patch samples (group hNP and hHP) and reduced presence of VEGF in normoxic monolayers (group hN).

We chose four factors depicted in figure 4.6a to quantify to verify the qualitative observations. An ELISA for VEGF, FGF-1, IL-8 and ANG was performed on conditioned media from all groups. A two-way ANOVA was also used to determine if ambient oxygen tension or culture condition (monolayer vs. patch) had a role in the regulation of secreted growth factor protein abundance. Post-hoc test were performed to compare monolayer versus patch. As shown in figure 4.6d there was significantly lower abundance of ANG found in the conditioned medium of hMSC cultured in collagen patches at both room air and hypoxia. The majority of the variance (69.9%; $p < 0.0003$) resulted from culture in collagen patches, indicating that hMSC ANG secretion was

significantly affected by culture in collagen patches. Post-hoc test revealed significant downregulation of ANG abundance by the patch in room air and in hypoxic conditions ($p < 0.05$). Ambient oxygen tension attributed little to the total variance (13.5%; $p < 0.05$). The abundance of FGF-1 found in the conditioned medium of hMSC was unchanged with culture in collagen patches versus monolayers (Figure 4.6e). Analysis of VEGF abundance (Figure 4.6f) in the conditioned medium of hMSC monolayers and collagen patches revealed a significant increase in VEGF protein abundance in hypoxic patches (29.6% of variance due to ambient oxygen tension; $p < 0.05$). Post-hoc testing confirmed this result ($p < 0.05$) and revealed a significant difference between hypoxic patches and monolayers. Lastly, there was a significant increase in IL-8 abundance attributed to culture in collagen patches (68.7% of variance was due to culture in collagen patches; $p < 0.01$). Post-hoc testing revealed a significant increase in IL-8 abundance in hypoxic patch conditioned medium compared to hypoxic monolayers. Ambient oxygen tension attributed little to total variance (3.1%; $p = 0.33$).

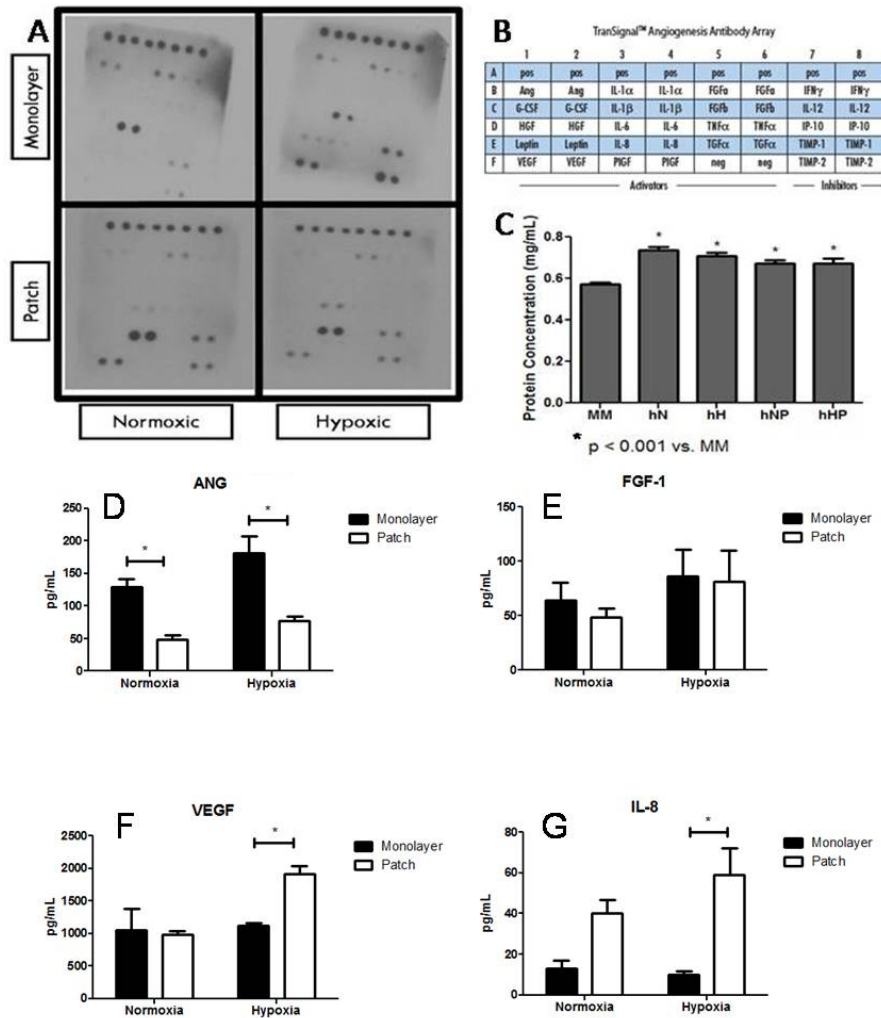


Figure 4.6) hMSC secretion profile. A and B) hMSC cultured as monolayers or within patches and exposed to normoxia (20% O₂) or hypoxia (1% O₂) display differential secretion profiles of angiogenic factors. C) There was a general increase in protein content in conditioned media from normoxic monolayers (hN; 0.74 ± 0.02 mg/mL), hypoxic monolayers (hH; 0.71 ± 0.02 mg/mL), normoxic patches (hNP; 0.67 ± 0.02 mg/mL) and hypoxic patches (hHP; 0.67 ± 0.03 mg/mL) versus a maintenance media control (MM; 0.57 ± 0.01 mg/mL; *p < 0.001). Specific analysis of pro-angiogenic factors revealed differential expressions patterns based on hMSC culture in monolayers versus collagen patches for D) ANG (Normoxia: 125.6 ± 12.2 vs. 48.4 ± 7.5 pg/mL; *p < 0.05 and Hypoxia: 180.6 ± 25.9 vs. 77 ± 7.4 pg/mL; *p < 0.05), E) FGF-1 (no statistical significance was observed; Normoxia: 63.9 ± 17.1 vs. 48.9 ± 7.7 pg/mL and Hypoxia: 86 ± 22.3 vs. 81.5 ± 28.3 pg/mL), F) VEGF (Normoxia: 1046.9 ± 333.3 vs. 981.6 ± 56.1 pg/mL and Hypoxia: 1114.1 ± 52.3 vs. 1904.8 ± 129.2 pg/mL; *p < 0.05) and G) IL-8 (Normoxia: 12.9 ± 3.4 vs. 40 ± 6.7 pg/mL and Hypoxia: 10.2 ± 1.6 vs. 58.8 ± 13.2 pg/mL; *p < 0.05); n = 3 for all groups.

To determine whether protein expression was regulated at the transcription level real time RT-PCR was performed to provide relative quantification of growth factor mRNA abundance. Two-way ANOVA of hMSC cultured as monolayers or within cardiac patches at different oxygen tensions revealed that IL-8, FGF-1, and VEGF mRNA abundance were significantly affected by culture in collagen patches. VEGF mRNA abundance was also significantly affected by ambient oxygen tension (1% O₂). Post-hoc tests revealed increased mRNA abundance of IL-8 in patches compared to monolayers in room air (58.9 ± 9.5 vs. 1 ± 0.1 ; $p < 0.01$) and increase mRNA abundance of FGF-1 and VEGF in patches compared to monolayers at 1% O₂ (FGF-1: (hHP) 9.81 ± 2.6 vs. (hH) 0.49 ± 0.02 ; VEGF: (hHP) 14.7 ± 3.54 vs. (hH) 1.14 ± 0.08 ; $p < 0.05$). There were no significant changes in ANG mRNA abundance when exposed to different conditions. Overall, the statistical analysis for both protein and mRNA abundance demonstrate that most of the changes in secretion profile were the result of culture within collagen patches and not ambient oxygen tension. These changes typically led to increased growth factor expression. Subsequent *in vitro* studies were performed using one oxygen tension (1% O₂) with condition media from hypoxic samples only.

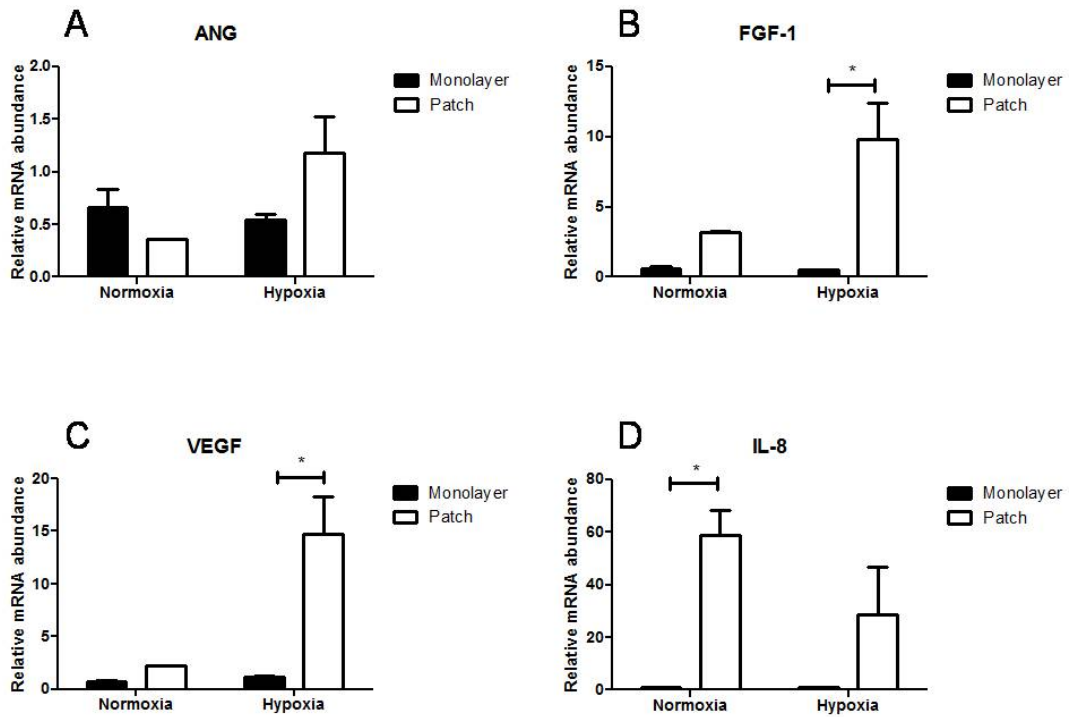


Figure 4.7) Angiogenic factor gene expression in hMSC. mRNA abundance was measure with real time RT-PCR. Results indicate differential mRNA regulatory patterns for A) ANG (no statistical significance was observed; Normoxia: 0.66 ± 0.17 vs. 0.36 ± 0.004 ; and Hypoxia: 0.55 ± 0.05 vs. 1.18 ± 0.35), B) FGF-1 (Normoxia: 0.57 ± 0.22 vs. 3.19 ± 0.1 and Hypoxia: 0.49 ± 0.02 vs. 9.82 ± 2.6 ; $p < 0.01$), C) VEGF (Normoxia: 0.7 ± 0.15 vs. 2.23 ± 0.02 and Hypoxia: 1.14 ± 0.08 vs. 14.7 ± 3.54 ; $*p < 0.01$) and D) IL-8 (Normoxia: 1.04 ± 0.05 vs. 58.9 ± 9.47 ; $*p < 0.01$ and Hypoxia: 1.06 ± 0.08 vs. 28.59 ± 18.21) for hMSC cultured as monolayers versus within 3D collagen constructs (n = 3 except ANG, FGF-1 and VEGF hNP and IL-8 hHP where n= 2).

4.3.3 hMSC Conditioned Media may Modulate Endothelial Cell Function

Since growth in collagen seemed to affect secretion of pro-angiogenic factors secreted by hMSCs favorably, we investigated potential functional consequences by comparing conditioned media from hMSC cultured as monolayers or within collagen patches on endothelial cell growth/proliferation. Conditioned media from hypoxic groups was placed on human cardiac microvascular endothelial cells (hMVEC-C) for 2 d. Afterwards MTT reagent was added for three hours and after formazan crystal formation, 0.1 N hydrochloric acid in isopropyl alcohol was added. The resulting colored solution was collected and the absorbance was spectrophotometrically measured at 570 nm (with background subtraction at 690 nm). Additionally, hMVEC-C were removed from culture after 2 d with trypsin treatment, and a trypan blue exclusion assay was performed to determine cell number. As shown in figure 4.8a, conditioned media from hypoxic hMSC groups had minimal effect on cell growth/proliferation compared to a MM control in all groups. Divergent results were obtained using direct cell counts. hMSC conditioned media from hypoxic patches increased the cell number of hMVEC-C compared to a MM control and hH conditioned media. The difference between the two methods may have resulted from the difference in culture time after addition of conditioned media (MTT: 2 d; Cell count: 3 d).

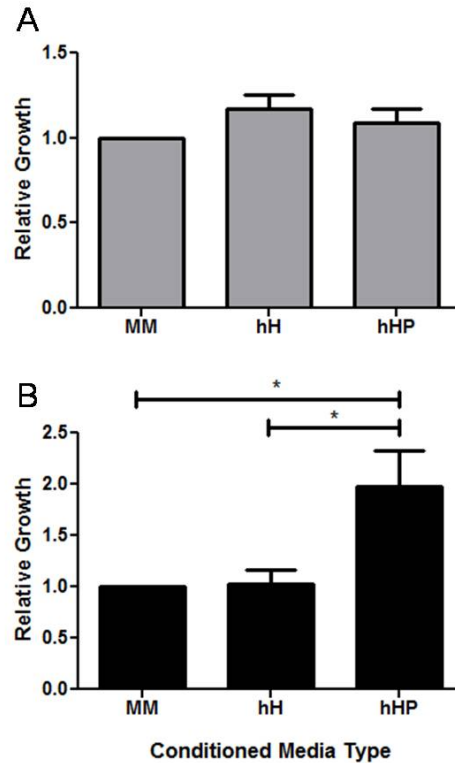


Figure 4.8) hMSC conditioned media may support endothelial cell growth/proliferation. A) A MTT assay of endothelial cells exposed to conditioned medium from hypoxic monolayers (hH) and hypoxic patches (hHP) show no change in endothelial growth/proliferation compared to maintenance media controls (MM: 1.0; hH: 1.17 ± 0.08 ; hHP: 1.09 ± 0.08). B) On the other hand, cell counts resulted in more pronounced differences growth/proliferation. Exposure of hMVEC-C to hHP conditioned media resulted in increased relative cell counts compared to both MM (1.97 ± 0.35 vs. 1.0; $*p < 0.05$) and hH exposure (1.97 ± 0.35 vs. 1.03 ± 0.14 ; $*p < 0.05$). $n = 3$ for all groups.

Angiogenic effects of conditioned media were investigated using a tube formation assay. Briefly, 15,000 hMVEC-C were seeded onto Matrigel in the presence of conditioned media and 2% fetal bovine serum for 22 hours. Images of the resultant tubes were collected and the average length was manually determined using Image Pro Plus software. In general, in the presence of hMSC conditioned media, tubes which formed were longer compared to a MM control ($N = 1$; Figure 4.9b and c). There were

no obvious differences between monolayer and patch conditioned media on tube formation (Figure 4.9a).

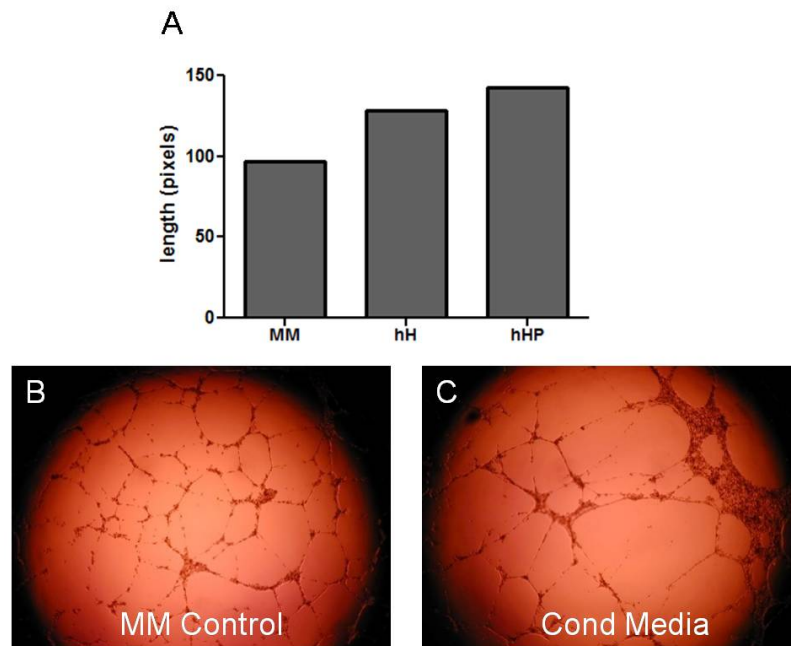


Figure 4.9) hMSC conditioned media may enhance endothelial cell tube formation properties. Conditioned media from hypoxic hMSC cultured as monolayers or within patches resulted in longer tube formation compared to a MM control when exposed to endothelial cells cultured on Matrigel (MM: 96.8; hH: 128.7; hHP: 142.8; n = 1).

4.3.4 hMSC patch application results in improved myocardial function compared to injected hMSC

In Chapter 3, we assessed the hypothesis that a tissue engineered, cardiac patch could be transplanted directly onto an infarcted site for localized and uniform delivery of human mesenchymal stem cells (hMSC) [18]. In addition to demonstrating enhanced hMSC engraftment, we also used this “proof of concept” experiment to redesign future *in vivo* studies. This allowed us to optimize cell survival in order to adequately compare the effects of direct injection and cardiac patch delivery of hMSC to infarcted myocardium. Strategies for optimization included lowering the seeding density of hMSC within cardiac patches and using a nude rat myocardial infarct model. Initial

analysis revealed no change in infarct size at four weeks amongst the different experimental groups (Figure 4.10). Additionally, there was successful induction of infarction in all groups compared to sham. All groups suffered attenuated fractional shortening and adverse LV remodeling.

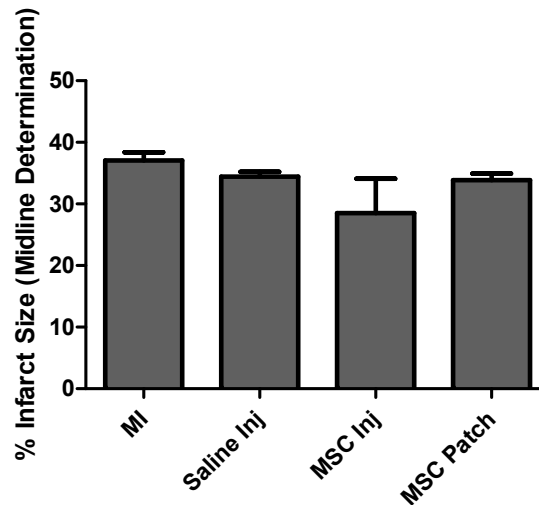


Figure 4.10) No change in infarct size with cardiac patch transplantation. Infarct size was determined by measuring the infarct midline circumference of Masson's Trichrome stained tissue sections. Analysis revealed no change in infarct size 4 weeks after initial LAD ligation when comparing MI ($37.1 \pm 1.4\%$) and saline injected controls, ($34.4 \pm 0.8\%$) hearts treated with MSC injection ($28.5 \pm 5.6\%$) or hearts treated with MSC patches ($33.9 \pm 1.1\%$) MI – Myocardial infarction controls; Saline Inj – Saline injection; MSC Inj – Mesenchymal stem cell injection; MSC Patch – Mesenchymal stem cell patch. (n = 3 for all groups except saline inj where n = 2).

Baseline echocardiograms taken 3 d post infarction were compared with echocardiograms taken at four weeks post infarction. The extent of functional loss/gain and remodeling were calculated as a percent change over the duration of the experiment. When cardiac patches were applied to infarcted heart, fractional shortening and infarct wall thickness were augmented in animals treated with patch versus MI

controls and NV patches (Table 4.2). There were no statistical differences between groups in regards to left ventricular systolic and diastolic diameter (Table 4.2).

Table 4.2 - Corrected echocardiographic measures after myocardial infarction

Corrected	MI (n=5)	Saline Inj (n=4)	MI+NV Patch (n=2)	MSC Inj (n=3)	MI+ MSC Patch (n=4)
FS ($\Delta\%$)	-38 \pm 19	-11 \pm 15	-4 \pm 15	-6 \pm 3	11 \pm 10 ^a
AWTh ($\Delta\%$)	-97 \pm 25	-87 \pm 27	-80 \pm 13	-62 \pm 12	19 \pm 12 ^{a,b}
LVIDs ($\Delta\%$)	19 \pm 4	18 \pm 4	14 \pm 9	8 \pm 6	6 \pm 1
LVIDd ($\Delta\%$)	14 \pm 4	23 \pm 3	15 \pm 6	10 \pm 5	11 \pm 2

^ap < 0.05 vs. MI, ^bp < 0.05 vs. MI + NV Patch

MI: Myocardial Infarction

NV: Non-viable

MSC: Mesenchymal Stem Cell

Inj: Injection

LVIDd: Left ventricular internal diameter at diastole

LVIDs: Left ventricular internal diameter at systole

FS%: Percent fractional shortening

AWTh: Anterior wall thickness

Invasive hemodynamics were performed to determine the functionality of the LV chamber after infarction and in the presence of cell treatment (Table 4.3). There were no statistically significant events when contractility, end diastolic pressure (EDP) or τ (time constant for pressure fall during cardiac relaxation) were measured and calculated.

Table 4.3 - Hemodynamic measures after myocardial infarction

	MI (n=5)	Saline Inj (n=4)	MI+NV Patch (n=3)	MSC Inj (n=3)	MI+ MSC Patch (n=4)
+dP/dt (mmHg/s)	8133 ± 306	8213 ± 241	6862 ± 279	7381 ± 540	8145 ± 158
-dP/dt (mmHg/s)	-6510 ± 372	-6785 ± 224	-5882 ± 63	-6976 ± 703	-8252 ± 640
EDP (mmHg)	11 ± 3	10 ± 1	17 ± 5	7 ± 0.5	8 ± 3
τ (msec)	16 ± 3	14 ± 1	17 ± 3	16 ± 3	12 ± 0.3

MI: Myocardial Infarction

NV: Non-viable

MSC: Mesenchymal Stem Cell

Inj: Injection

+ dp/dt: Maximum rate of rise in left ventricular pressure during systole

- dp/dt: Maximum rate of decrease in left ventricular pressure during diastole

EDP: Left ventricular end-diastolic pressure

τ: Time constant for pressure fall during cardiac relaxation

One possible mechanism by which hMSC can prevent or delay the onset of adverse remodeling after myocardial infarction is by mediating the formation of functional blood vessels within the infarcted area. To determine if there was any difference in the number of blood vessels that occupied the LV wall across the infarct we performed histology for isolectin B4. Staining revealed no change in blood vessel presence in the infarct area when cardiac patches were applied to infarcted hearts compared to MI controls and hMSC injection (Figure 4.11; p = 0.1, MSC patch vs. MI control). Observed blood vessels were most prominent in the peri-infarct region near the epicardial surface of the anterior wall (Figure 4.11b – 4.11d).

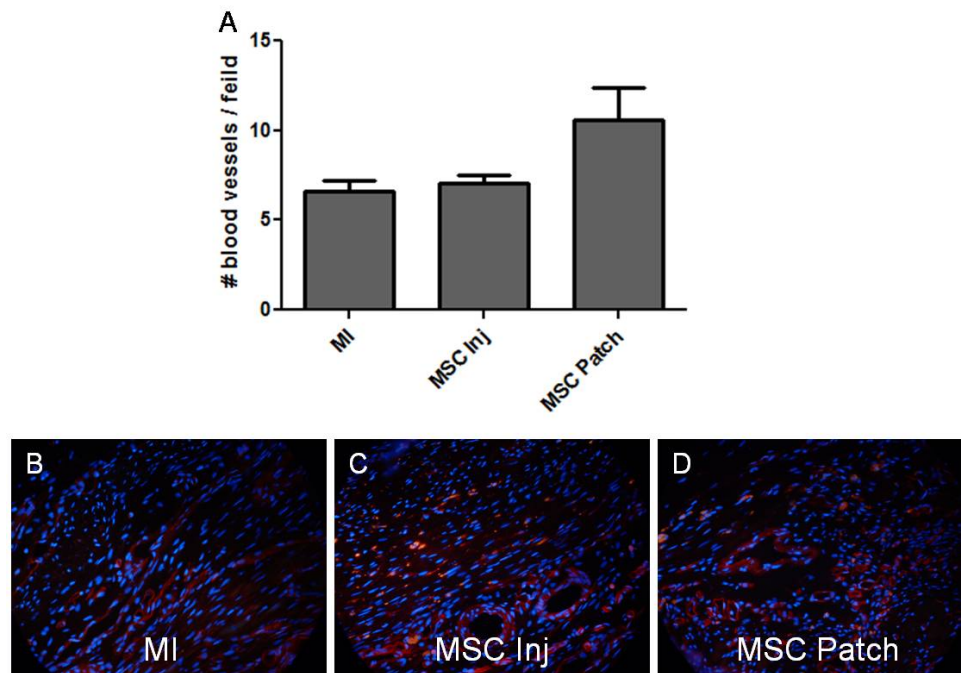


Figure 4.11) Application of hMSC patch does not change blood vessel presence. four weeks after LAD ligation hearts were probed for neo-vessel formation. A) hMSC patch application does not affect neo-vessel formation compared to MI controls and hMSC injection (MI: $7 \pm 1\%$, MSC Inj: $7 \pm 0.4\%$ and MSC Patch: $11 \pm 2\%$; ANOVA $p = 0.1$). Histological analysis of B) MI control hearts; $n=3$, C) hMSC injected hearts; $n=2$ and D) hMSC patch treated hearts; $n=3$ was performed to assess neo-vessel formation.

4.4 DISCUSSION

Cellular cardiomyoplasty offers a novel therapeutic approach to myocardial repair and preservation. Unfortunately, conventional cell delivery strategies are less than optimal. This thesis explores a tissue engineered vehicle, called a cardiac patch that can be applied directly to the infarct site for homogenous and localized cell delivery, overcoming this limitation. In this chapter, we investigated the behavior of cells once embedded within cardiac patches. In a series of experiments, we identified alterations of cell function caused by cell culture within 3D collagen constructs. These studies reveal specific changes between cells cultured as monolayers and within patches with little

dependence on ambient oxygen tension. For instance, cells cultured in collagen patches display reduced proliferation and viability. Additionally, cell culture within collagen patches tended to augment the secretion of several angiogenic growth factors. These differences may induce deviations in downstream effects for myocardial repair after infarction when using a cardiac patch for cell delivery versus direct injection.

One observation from *in vitro* characterizations of cardiac patches was that culture of hMSC in 3D collagen constructs attenuated their proliferative response as assessed via their ability to incorporate EdU. Similar *in vitro* models have shown the tendency of cells embedded within 3D scaffolds to have suppressed cell proliferation [19]. This could indicate reconfigured bioenergetics to support cell differentiation or enhance protein production. It is well documented that MSC cultured in collagen gels can undergo both chondrogenic and osteogenic differentiation [20, 21]. Nevertheless, there was no loss of potency over 7 d with hMSC in collagen patches, and cell viability remained consistently above 80% in hMSC patches. Thus, cellular differentiation is an unlikely event mediating reduced proliferation.

Reduced cell proliferation may also indicate increased protein production. It has already been reported that hMSC secrete a variety of different growth factors under normal and hypoxic culture conditions. Such factors include: VEGF [22, 23], IGF-1 [24], SDF-1 [25] and MCP-1 [26]. To date, little research has been performed to assess the effect of 3D culture on protein production of stem/progenitor cells. In our studies, ANG, FGF-1, VEGF and IL-8 were observed to secrete from hMSC monolayers. Upon culture in collagen patches, this response increased for VEGF and IL-8 compared to monolayers. Additionally, the mRNA abundance of VEGF, IL-8 and FGF-1 increased upon culture in collagen patches. Ambient oxygen tension did not appear to affect these results. Similar results were shown when hMSC were grown as spheroids via a traditional hanging drop method. These cells demonstrated increased angiogenic

growth factor production that was thought to be mediated by an autocrine feedback loop where enriched growth factors continually promoted additional production of angiogenic factors [23], although this hypothesis was not tested. The proliferative state of hMSC in spheroids was also not tested. Wong et. al., however, have noted that reduced proliferation is associated with increased protein production [27] given the reduced need to expend energy for cell division. The data demonstrate reduced proliferation with culture in cardiac patches. This event may explain the increased protein and mRNA expression observed.

There were instances where protein and mRNA expression did not correlate. For instance, culture of hMSC in collagen patches caused substantial upregulation of FGF-1 transcripts. This effect, however, was not apparent when conditioned media was analyzed for the presence of FGF-1. It is possible that the lack of a secretory signal peptide on FGF-1 transcripts [28] results in FGF-1 accumulating near the cell surface or within the surrounding extracellular matrix and would be released only upon matrix degradation.

Additionally, ANG is a very potent angiogenic factor which is thought to be necessary for VEGF and FGF to elicit their pro-angiogenic effects [29]. ANG is an RNase capable of binding to endothelial cells to promote proliferation and protease activity which aids in the breakdown of basement membrane [30]. The secretion of ANG was downregulated upon culture in collagen patches although no differences in mRNA abundance were observed. Rajashekhar and colleagues have reported that ANG shows differential regulation depending on cell type, extracellular matrix and oxygen tension [31].

We were unable demonstrate conclusive positive effects of hMSC patch conditioned medium on endothelial cell proliferation/growth and tube formation. Conditioned media from hMSC had no effect on endothelial cell growth as assessed via

MTT analysis but did demonstrate enhanced endothelial cell growth after performing cell counts. Specifically hMVEC-C exposed to hHP conditioned media demonstrated improved cell number versus a MM control and hMVEC-C exposed to hH conditioned medium. The culture of hMVEC-C in hN conditioned media also increased cell number versus a MM control. The differences between these two assays may be the result of the time hMVEC-C were exposed to conditioned media before cell collection and assaying (MTT: 2 d; Cell counts: 3 d). hMSC conditioned medium appeared to have promoted the production of longer tubes when cultured with endothelial cells on Matrigel. This effect did not depend on whether hMSC were cultured in 3D collagen patches or monolayers, although more experiments are needed to calculate statistical significance. The results presented support the hypothesis that culture of stem cells in collagen constructs modulates cell function but seems to suggest that angiogenic factors and vessel formation may not explain the improvements in function after cardiac patch application noted *in vivo*.

The data suggest that hMSCs delivered in collagen have a more beneficial effect than those directly injected. This might have been explained by changes in the secretory profile of angiogenic factors. Nevertheless, *in vitro* and *in vivo* data does not support that to be the main cause. Specifically, when we analyzed infarcted hearts for neovessel formation we observed no change in neovessel formation throughout the LV infarct wall. These results are similar to the observations reported in Chapter 3 where there was no statistically significant change in neovessel formation after cardiac patch transplantation. There are several studies which indicate increased neovessel formation after hMSC delivery, however [32, 33]. For instance, Li and colleagues concluded that anoxic pretreatment of hMSC significantly improved their positive effects in cardiomyopathies by enhancing capillary density in addition to other trophic effects [34]. These studies typically delivered more cells, via direct injection, to infarcted myocardium

than our experiments, however. Other causes for improved function after cardiac patch transplantation may include the accumulation of myofibroblasts [18], a modulated fibrotic response, endogenous stem cell recruitment and activation or improved net engraftment. These responses have been demonstrated in Chapter 3.

In other studies that inject hMSC, more cells were initially injected than what was used in this study. This difference may account for why we were unable to observe significant improvements in myocardial function after hMSC injection. The positive results observed after cardiac patch application (which also contained a small cell number) may indicate that localized (and concentrated) delivery of cells provides for better local responses involved in infarct repair. In Chapter 3 a cardiac patch initially seeded with one million cells and transplanted onto an immunocompetent model demonstrated enhanced remodeling parameters (FS%, AWTh, LVIDd and LVIDs) compared to MI and NV patch controls. The initial seeding density and animal model used may account for the differences observed between the two studies. Dose response studies in nude and immunocompetent animal models are needed to help comprehend these differences.

In conclusion, the culture of hMSC in collagen patches alters their behavior and cells delivered in collagen patches show increased cardiomyoplasty efficacy compared to cells directly injected. This may be explained by increased paracrine secretion of hMSC grown in patches. Nevertheless, the mechanism by which this happens is not clear, since vessel formation is similar between hearts with patches and those subject to direct injection. Other paracrine responses may be involved in cardiac repair, however. Additionally, an increase in net engraftment may explain the favorable effects of cardiac patch application compared to direct injection. hMSC culture and delivery within collagen patches may represent an option to promote local reparative response involved

myocardial repair after cellular cardiomyoplasty and thus improve global cardiac function.

4.5 LIMITATIONS and RECOMMENDATIONS

Chapter 4 discusses the modulation of hMSC function when cultured in collagen patches. There are clear differences in several functions including proliferation and growth factor expression when cells are embedded in a collagen matrix. The mechanism for such changes was not clearly identified, however. Reduced proliferation was one factor thought to mediate changes the hMSC secretory profiles. The mechanism promoting reduced proliferation was not addressed. Protein measurements and analysis after preventing proliferation with cell cycle inhibitors may aid in uncovering specific mechanisms involved in protein modulation. Comparing these mechanisms with those involved in cardiac patch mediated suppression of cell proliferation will help determine how culture in collagen patches reduces proliferation and its consequences on the production of specific proteins.

Additionally, several studies within Chapter 4 were performed to demonstrate variations in growth factor expression after culture in collagen patches. These experiments were completed under the assumption that modulation in paracrine function will produce differential reparative responses after cellular cardiomyoplasty. Unfortunately, there is no direct evidence which would suggest that the changes in hMSC growth factor expression upon culture in collagen patches affected local or global reparative responses *in vivo*. This is a very difficult hypothesis to investigate given the number of potential paracrine factors and likely redundancy of function. Although the use of *in vitro* experiments will help answer some questions related to paracrine functions, the mechanisms of action for several *in vivo* responses will likely prevent reliable correlations. Thus, investigating general responses such as angiogenesis, fibrosis or cell mobilization may aid in discovering classes of paracrine factors which play

important roles in myocardial repair. From these classes, “cocktails” can be developed and used *in vitro* and *in vivo* to help determine specific paracrine factors which mediate efficient myocardial repair. Of course, the dose will have to be accounted for in the experimental design.

Our *in vivo* studies also contained limitations. We chose to decrease the seeding density within cardiac patches to sustain cellularity and stem cell potency.

Unfortunately, the positive effects of cardiac patch application as described in Chapter 3, was attenuated. Thus we only observed minor changes in myocardial repair. This effect was also likely caused by the change in animal model (immunocompetent vs. nude).

Unfortunately, the role seeding density and immune status in mediating myocardial repair after infarction are ill-defined. For this reason, it is difficult to precisely determine why neither hMSC injection nor hMSC cardiac patch application resulted in more pronounced augmentation of myocardial function. Dose response studies (using both injection and TE constructs for cell delivery) in immunocompetent and immunocompromised physiologic models would aid in developing a more complete hypothesis for the role of seeding density and immune status in myocardial repair.

4.6 REFERENCES

1. S. Miyagawa, Y. Sawa, S. Sakakida, et al. Tissue cardiomyoplasty using bioengineered contractile cardiomyocyte sheets to repair damaged myocardium: their integration with recipient myocardium. *Transplantation*. 2005 Dec 15;80:1586-95.
2. W. H. Zimmermann, I. Melnychenko, G. Wasmeier, et al. Engineered heart tissue grafts improve systolic and diastolic function in infarcted rat hearts. *Nat Med*. 2006 Apr;12:452-8.
3. M. K. El Tamer and R. L. Reis. Progenitor and stem cells for bone and cartilage regeneration. *J Tissue Eng Regen Med*. 2009 May 5.
4. A. Samadikuchaksaraei. An overview of tissue engineering approaches for management of spinal cord injuries. *J Neuroeng Rehabil*. 2007;4:15.

5. A. Mol, A. I. Smits, C. V. Bouten and F. P. Baaijens. Tissue engineering of heart valves: advances and current challenges. *Expert Rev Med Devices*. 2009 May;6:259-75.
6. W. J. Zhang, W. Liu, L. Cui and Y. Cao. Tissue engineering of blood vessel. *J Cell Mol Med*. 2007 Sep-Oct;11:945-57.
7. T. Freyman, G. Polin, H. Osman, et al. A quantitative, randomized study evaluating three methods of mesenchymal stem cell delivery following myocardial infarction. *Eur Heart J*. 2006 May;27:1114-22.
8. D. Hou, E. A. Youssef, T. J. Brinton, et al. Radiolabeled cell distribution after intramyocardial, intracoronary, and interstitial retrograde coronary venous delivery: implications for current clinical trials. *Circulation*. 2005 Aug 30;112:1150-6.
9. W. Dai, S. L. Hale, B. J. Martin, et al. Allogeneic mesenchymal stem cell transplantation in postinfarcted rat myocardium: short- and long-term effects. *Circulation*. 2005 Jul 12;112:214-23.
10. W. Jiang, A. Ma, T. Wang, et al. Homing and differentiation of mesenchymal stem cells delivered intravenously to ischemic myocardium in vivo: a time-series study. *Pflugers Arch*. 2006 Aug 17.
11. M. Kudo, Y. Wang, M. A. Wani, M. Xu, A. Ayub and M. Ashraf. Implantation of bone marrow stem cells reduces the infarction and fibrosis in ischemic mouse heart. *J Mol Cell Cardiol*. 2003 Sep;35:1113-9.
12. J. Takagawa, Y. Zhang, M. L. Wong, et al. Myocardial infarct size measurement in the mouse chronic infarction model: comparison of area- and length-based approaches. *J Appl Physiol*. 2007 Jun;102:2104-11.
13. J. T. Butcher, B. C. Barrett and R. M. Nerem. Equibiaxial strain stimulates fibroblastic phenotype shift in smooth muscle cells in an engineered tissue model of the aortic wall. *Biomaterials*. 2006 Oct;27:5252-8.
14. C. L. Cummings, D. Gawlitta, R. M. Nerem and J. P. Stegemann. Properties of engineered vascular constructs made from collagen, fibrin, and collagen-fibrin mixtures. *Biomaterials*. 2004 Aug;25:3699-706.
15. B. Assmus, J. Honold, V. Schachinger, et al. Transcoronary transplantation of progenitor cells after myocardial infarction. *N Engl J Med*. 2006 Sep 21;355:1222-32.
16. K. Lunde, S. Solheim, S. Aakhus, et al. Intracoronary injection of mononuclear bone marrow cells in acute myocardial infarction. *N Engl J Med*. 2006 Sep 21;355:1199-209.
17. V. Schachinger, B. Assmus, M. B. Britten, et al. Transplantation of progenitor cells and regeneration enhancement in acute myocardial infarction: final one-year results of the TOPCARE-AMI Trial. *J Am Coll Cardiol*. 2004 Oct 19;44:1690-9.

18. D. Simpson, H. Liu, T. H. Fan, R. Nerem and S. C. Dudley, Jr. A tissue engineering approach to progenitor cell delivery results in significant cell engraftment and improved myocardial remodeling. *Stem Cells*. 2007 Sep;25:2350-7.
19. M. J. Schuliga, I. See, S. C. Ong, et al. Fibrillar Collagen Clamps Lung Mesenchymal Cells in a Non-Proliferative and Non-Contractile Phenotype. *Am J Respir Cell Mol Biol*. 2009 Mar 27.
20. E. Donzelli, A. Salvade, P. Mimo, et al. Mesenchymal stem cells cultured on a collagen scaffold: In vitro osteogenic differentiation. *Arch Oral Biol*. 2007 Jan;52:64-73.
21. D. Bosnakovski, M. Mizuno, G. Kim, S. Takagi, M. Okumura and T. Fujinaga. Chondrogenic differentiation of bovine bone marrow mesenchymal stem cells (MSCs) in different hydrogels: influence of collagen type II extracellular matrix on MSC chondrogenesis. *Biotechnol Bioeng*. 2006 Apr 20;93:1152-63.
22. Y. L. Tang, Q. Zhao, Y. C. Zhang, et al. Autologous mesenchymal stem cell transplantation induce VEGF and neovascularization in ischemic myocardium. *Regul Pept*. 2004 Jan 15;117:3-10.
23. I. A. Potapova, G. R. Gaudette, P. R. Brink, et al. Mesenchymal stem cells support migration, extracellular matrix invasion, proliferation, and survival of endothelial cells in vitro. *Stem Cells*. 2007 Jul;25:1761-8.
24. L. Chen, E. E. Tredget, P. Y. Wu and Y. Wu. Paracrine factors of mesenchymal stem cells recruit macrophages and endothelial lineage cells and enhance wound healing. *PLoS ONE*. 2008;3:e1886.
25. M. Zhang, N. Mal, M. Kiedrowski, et al. SDF-1 expression by mesenchymal stem cells results in trophic support of cardiac myocytes after myocardial infarction. *FASEB J*. 2007 Oct;21:3197-207.
26. S. C. Hung, R. R. Pochampally, S. C. Chen, S. C. Hsu and D. J. Prockop. Angiogenic effects of human multipotent stromal cell conditioned medium activate the PI3K-Akt pathway in hypoxic endothelial cells to inhibit apoptosis, increase survival, and stimulate angiogenesis. *Stem Cells*. 2007 Sep;25:2363-70.
27. H. L. Wong, M. X. Wang, P. T. Cheung, K. M. Yao and B. P. Chan. A 3D collagen microsphere culture system for GDNF-secreting HEK293 cells with enhanced protein productivity. *Biomaterials*. 2007 Dec;28:5369-80.
28. D. Gospodarowicz, N. Ferrara, L. Schweigerer and G. Neufeld. Structural characterization and biological functions of fibroblast growth factor. *Endocr Rev*. 1987 May;8:95-114.
29. G. F. Hu, S. I. Chang, J. F. Riordan and B. L. Vallee. An angiogenin-binding protein from endothelial cells. *Proc Natl Acad Sci U S A*. 1991 Mar 15;88:2227-31.
30. G. F. Hu and J. F. Riordan. Angiogenin enhances actin acceleration of plasminogen activation. *Biochem Biophys Res Commun*. 1993 Dec 15;197:682-7.

31. G. Rajashekhar, A. Loganath, A. C. Roy, S. S. Chong and Y. C. Wong. Extracellular matrix-dependent regulation of angiogenin expression in human placenta. *J Cell Biochem.* 2005 Sep 1;96:36-46.
32. K. H. Schuleri, L. C. Amado, A. J. Boyle, et al. Early improvement in cardiac tissue perfusion due to mesenchymal stem cells. *Am J Physiol Heart Circ Physiol.* 2008 May;294:H2002-11.
33. N. Derval, L. Barandon, P. Dufourcq, et al. Epicardial deposition of endothelial progenitor and mesenchymal stem cells in a coated muscle patch after myocardial infarction in a murine model. *Eur J Cardiothorac Surg.* 2008 Aug;34:248-54.
34. J. H. Li, N. Zhang and J. A. Wang. Improved anti-apoptotic and anti-remodeling potency of bone marrow mesenchymal stem cells by anoxic pre-conditioning in diabetic cardiomyopathy. *J Endocrinol Invest.* 2008 Feb;31:103-10.

Chapter 5

Human Embryonic Stem Cell Derived-Mesenchymal Cells: Exploring the Efficacy of a Possible Substitute for Mesenchymal Stem Cells in Cellular Cardiomyoplasty

5.1 INTRODUCTION

One issue limiting advancements in clinical cellular cardiomyoplasty is determining an optimal cell source. Traditionally, cells intended for human use have been limited to those that can be isolated in large quantities (thus limiting the need for *ex vivo* expansion) and/or that are autologous. As a result, bone marrow mononuclear cells have become very popular in clinical studies. The use of this heterogeneous population of cells imparts difficulties in trying to assess which cell type(s) contributes to improved function and which do not. One population within unfractionated bone marrow which may be useful is mesenchymal stem cells (MSC). This defined cell population has proven successful in both preclinical and clinical studies. Unfortunately, MSCs represent a very small portion of the bone marrow and may require *ex vivo* expansion to maximize their efficacy. Derivation of MSC-like cells that can be made available “off-the-shelf” might help address these problems.

Unlike other organs of the body, the myocardium does not regenerate appreciably because of the limited pool of cardiac specific progenitor cells present and the inability of adult cardiomyocytes to proliferate [1]. Recently, cellular cardiomyoplasty has been proposed as a strategy to repair myocardial damage after injury. Cell sources include: cardiomyocytes [2-4], skeletal myoblasts [5-7], smooth muscle cells [8], cardiac progenitors [9-11], bone marrow stem cells [12-17], embryonic stem cells [18-21], endothelial cells [22], activated macrophages [23], amniotic fluid stem cells [24, 25], cord blood stem cells [26], and adipose derived stem cells [27]. When delivered to infarcted

myocardium, cell therapy results in improved measures of cardiac function. Clinical studies have also shown success with cell treatment [28-36]. Larger controlled trials using bone marrow mononuclear cells indicate statistically significant improvements in several cardiac indices; although the absolute change may not be physiologically relevant.

Although the kinds of cells used for cellular cardiomyoplasty is vast, MSC continue to prove resourceful for mediating cardiac repair after injury. Bone marrow stem cells (BMSC) include both mesenchymal and hematopoietic cell types. Mesenchymal stem cell (MSCs) are adult progenitor cells that have the potential to differentiate into tissues from the mesoderm [37]. These include fibroblast, muscle, bone, tendon, ligament, and adipose tissue. These cells also successfully differentiate into cardiomyocytes *in vitro* [38]. When human MSCs are injected into normal mouse myocardium they attain a “cardiac-like” phenotype [39] determined by the expression of several cardiac related markers. Unfortunately, few studies have shown well-defined cardiomyogenic differentiation of MSCs delivered to infarcted hearts [12-14, 40]. Clinical use of MSCs has recently begun. Preliminary results indicate that MSCs are safe and feasible as a therapeutic platform. Nevertheless, the need for *ex vivo* expansion was required.

Boyd et al. recently described the derivation of hESC derived mesenchymal cells [41]. H9 hESC (as well as BG01 hESC) were cultured in endothelial basal medium for 20-30 days until epithelial outgrowths form a confluent sheet within the culture dish. Upregulated genes during hESC differentiation included several mesodermal markers such as BMP4, GATA4 and RUNX1. After several passages of these cells MSC markers began to appear including CD73, CD90, CD105 and CD166. Although there is no clear definition as to what constitutes a mesenchymal stem cell, the expression of these markers is typically observed. These derived cells were also tested for their ability

to differentiate down osteogenic, adipogenic and chondrogenic lineages. The ability of MSCs to differentiate into these components of the mesoderm has also been used to define MSCs. Osteogenic and chondrogenic differentiation was observed, however, adipogenic differentiation was not. Similar to MSCs, hES-MC could also contract a collagen lattice. Despite the lack of adipogenic differentiation, hES-MC do possess several genetic and phenotypic similarities to MSCs. These cells are relatively easy to derive and culture and may represent a suitable alternative to MSC-based therapies. Therefore, we hypothesized that hES-MC (referred to as B4 progenitor cells throughout this and subsequent chapters) would display similar responses when cultured in 3D culture compared to hMSC. In addition, similar indices of myocardial improvement will be presented upon delivery of B4 progenitor cells to infarcted heart when compared to hMSC.

5.2 MATERIALS AND METHODS

5.2.1 Animal Handling

Male athymic nude rats (200-300 g) obtained from Charles River (Wilmington, MA) were allowed to acclimate to housing conditions for at least one week before use. All animals received care in compliance with federal and institutional guidelines with approval from the Institutional Animal Care and Use Committee.

5.2.2 Cell Culture

CD34 negative female hMSC obtained from Lonza were cultured in complete media consisting of Dulbecco's Modified Eagle's Medium (DMEM) containing 10% MSC qualified serum, L-glutamine and penicillin/streptomycin at 37°C in 5% CO₂. B4 progenitor cells obtained from Dr. Stephen Stice (University of Georgia) were cultured in complete EGM-2V medium containing 5% FBS at 37°C in 5% CO₂. At 80-90%

confluency hMSC or B4 progenitor cells were passaged by treating cells with 0.25% Trypsin/EDTA for three minutes. Cells were collected and replated at a lower cell density (usually one-third of the original cell density) onto new tissue culture treated flasks.

5.2.3 Formation of Cell Seeded Collagen Patches

hMSC (female) expanded to P3 – P6 or B4 progenitors (female, also known as hESC derived mesenchymal cells) expanded to P4 - P12 were embedded into a rat tail type I collagen matrix to form cardiac patches. To produce cardiac patches for progenitor cell delivery, 0.2 million hMSC or 0.2 million B4 progenitor cells were mixed in a solution of rat tail type I collagen, 5x DMEM and 10% fetal bovine serum such that the final collagen concentration was 2 mg/mL. Upon addition of sodium hydroxide (to neutralize acidic collagen solution) and placement of patches at 37°C for 15 minutes, the collagen solution gelled. The solution was placed in individual wells of a non-tissue culture-treated 48-well plate in order to create a patch that is between 0.3 – 0.7 cm in diameter. Patches were cultured at 37°C in 5% CO₂ for 1 d before usage. For the control experiments, non-viable cardiac patches were prepared by freezing 1 d old patches overnight in phosphate buffered saline at -80°C. The patches were thawed at room temperature and used for subsequent experiments. Non-viable patches were only exposed to a single freeze-thaw cycle.

5.2.4 Viability Assays

To assess cell viability within the construct, patches containing hMSC or B4 progenitor cells were digested 3 d after production in type I collagenase (500 U/mL) diluted in DMEM for 30 min at 37°C with intermittent mixing. Each patch was submerged in 2 mL of the collagenase solution and placed into at 37°C water bath. The solution

was triturated every 5 minutes to assist in the digestion of the construct. At the end of the incubation period, collagenase activity was inhibited by the addition of 500 μ L of 100% FBS and 8 mL of complete hMSC or B4 progenitor cell medium (see section 5.2.2). Viability was measured using a 1:10 dilution of the cell suspension by trypan blue exclusion. Counts were made using a hemocytometer. Viability was recorded as (the number of live cells) / (the number of total cells). For comparison, the viability of hMSC and B4 progenitor cells cultured on treated plastic dishes was determined using the same trypan blue exclusion and counting methodology. Cells were removed from culture dishes on day three using 0.25% Trypsin/EDTA.

5.2.5 Proliferation

Proliferation was determined by measuring the incorporation of 5-ethynyl-2'-deoxyuridine (EdU); a nucleoside analog to thymidine which is incorporated into DNA during synthesis. Cellularized constructs or cells cultured as a monolayer were pulsed with 10 mM EdU (Invitrogen; Carlsbad, CA) for 72 hours after their initial formation. Afterwards, constructs were washed in PBS and digested using collagenase to isolate cells as described above (5.2.4). Next, cells were washed using a 1% bovine serum albumin (BSA)/PBS solution and then fixed using the Click-iT fixative (Invitrogen; Carlsbad, CA) for 15 minutes at room temperature. Cells were permeabilized with Triton X-100 and then stained using the Click-iT cocktail mixture for 30 minutes at room temperature. Afterwards, cells were washed with 1% BSA/PBS and used for flow cytometry. To simplify analysis, hMSC or B4 progenitor cells were gated using an unstained sample (no antibody) on a forward scatter versus side scatter dot plot. This procedure helped to remove excess debris. Next, a positive control (using hMSC or B4 progenitor cells cultured on treated plastic) was run to determine the proper levels for positive signal. Samples were run and analyzed for positive fluorescein isothiocyanate

(FITC) signal using the histogram option of the BD FACS Diva software package (BD Biosciences; San Jose, CA). Positive signal was compared with the appropriate isotype controls, which allowed for accurate background subtraction. Analysis of data was performed using FCS Express 3.0 software and the histogram subtraction function (De Novo Software; Los Angeles, CA).

5.2.6 Assessment of Cell Differentiation

Differentiation of hMSC and B4 progenitor cells within the patch was measured by monitoring the expression of markers for stem cell potency over several days. hMSC and B4 progenitors isolated from the patch were stained and analyzed for the expression of CD105 and CD73 by flow cytometry. After cells were isolated from the patch, they were fixed using a 4% paraformaldehyde (PFA) for 15 minutes on ice. Next, cells were stained with the appropriate primary antibodies for 30 minutes on ice. If necessary, fluorescent conjugated secondary antibodies were added afterwards for 25 minutes at 0°C (Santa Cruz Biotechnology; Santa Cruz, CA). Cells were washed in a 0.3% BSA/PBS solution and analyzed via flow cytometry as described above (5.2.5). A two-way analysis of variance or Student t-test was used to determine differences in expression between culture methods (i.e. treated plastic vs. collagen gel).

5.2.7 Real Time RT-PCR

RNA was isolated from cell monolayers or cellularized constructs (48 hours after initial seeding) using a commercial RNeasy kit (Qiagen; Valencia, CA). RNA concentration and purity were measured using a spectrophotometer (abs: 260 nm, 280 nm and 230 nm). Afterwards, 1 µg of RNA was converted into cDNA using an Applied Biosystems cDNA synthesis kit (Applied Biosystems, Foster City, CA). The reaction

mixture was run for 5 minutes at 25°C, 30 minutes at 42°C and lastly, 5 minutes at 85°C. Real Time PCR was run using a total of 5 ng template cDNA for each sample. For each run, a negative control (water only, no template) was analyzed. Each sample was run in duplicate using ABI FAST SYBR green supermix (Applied Biosystems;) for multiple genes including: ANG, FGF-1, VEGF, FGF-2, Stromal Derived Factor (SDF-1), CXCR4, ribosomal protein 13A (RPL13A), β -Actin and ribosomal protein 18s (R18s). Primer assays for each primer set was obtained from Qiagen. The fast PCR protocol consists of an initial denaturing step at 95°C for 4 minutes. Next, samples are run at 94°C (denaturation) for 15 seconds, 60°C (annealing) for 30 seconds and 72°C (extension) for 30 seconds for 35 cycles. Relative RNA abundance was calculated using the following equation: $2^{-\Delta\Delta CT}$ (where the first delta represents threshold subtraction (“delta 1”) from the endogenous control and the second delta represents the division of “delta 1” by an internal control).

5.2.8 Infarct Model and Patch Application

Myocardial infarction (MI) was induced by permanent ligation of the left anterior descending (LAD) coronary artery in athymic nude male rats. Rats were anesthetized with 5% isoflurane in pure oxygen. Afterwards, rats were weighed and intubated for mechanical ventilation. After endotracheal intubation and initiation of ventilation, isoflurane was reduced to effect (1.5-2% vol/vol). The heart was exposed via a left thoracotomy, and the proximal LAD coronary artery was ligated using 6-0 silk suture. The location of ligation was placed at the intersection of the left atrial appendage and pulmonary conus whenever the LAD was not clearly visible. Diagonal branches of the main LAD were also ligated if the developed infarct was small. Noticeable effects of LAD coronary artery ligation included a change in pallor of the left ventricle (LV),

transient arrhythmias and an inflated left atrial appendage. Ten minutes after ligation, either viable or non-viable cardiac patches were applied onto the anterior wall of infarct site and secured with fibrin glue (Baxter; Deerfield, IL; Figure 3.3). Cardiac patches were secured to heart directly beneath the ligation site and covered approximately 30-40% of the LV wall. Rats with induced infarction and without construct application, with a non-viable construct, or with sham ligations (left thorocotomy with pericardium removal and suture place around LAD coronary without ligation) served as controls. Buprenorphine (0.1 mg/kg) was injected subcutaneously after surgery (and as necessary), and rats were allowed to recover under close supervision.

5.2.9 Echocardiography

Transthoracic echocardiograms were performed on rats using a VisualSonics Vevo 770 ultrasound unit (VisualSonics, Toronto, Canada). The VisualSonics RMV 716 Scanhead with center frequency 17.5 MHz, frequency band 11.5–23.5 MHz, and focal length 17.5 mm was used for echo acquisition in rats. The animals were maintained lightly anesthetized during the procedure with 1.5% isoflurane delivered through a face mask at a rate of 3-4 L/min. The animals were kept warm on a heating pad and the body temperature was continuously monitored using a rectal thermometer probe and maintained between 35 and 37°C by adjusting the distance of a heating lamp. Under these conditions, the animal's heart rate could be maintained between 300-400 beats per minute. Two-dimensional and M-mode echocardiography were used to assess wall thickness, LV dimensions and fractional shortening. Images were obtained from the parasternal long axis, parasternal short axis at the mid-papillary level and apical 4-chamber views.

Baseline echocardiograms were acquired at 3 d post-MI with additional echocardiograms acquired at 28 d post-MI. The baseline post-MI echocardiograms allowed us to determine whether incidence of infarction was successful (via a substantial reduction in myocardial shortening/thickening) and the extent and location of infarction. With nude rats, we noticed that LAD ligation resulted in most animals developing anterio-lateral infarcts. Isolated anterior infarctions only occurred in one case which survived surgery and other procedural stages of the overall experiment.

5.2.10 Cardiac Hemodynamics

Cardiac hemodynamics were measured after the final echocardiographic examination. Rats were anesthetized with 1% isoflurane, and a 1.4 or 2F Millar Mikro-Tip catheter (SPR-671, Millar Instruments, Houston, TX) was inserted into the right carotid artery and advanced into left ventricle. Aortic and left ventricular (LV) pressures were recorded on a PowerLab system and analyzed using Chart v4.2.4 software (ADInstruments, Colorado Springs, CO). After the procedure, rats were intravenously injected with 30% potassium chloride to paralyze/relax the heart before excision for histology.

5.2.11 Myocardial Histology

After the hemodynamic studies, hearts were excised, perfused with 4% paraformaldehyde and then cryo-protected by immersion in 30% sucrose for 48-96 hours. Isopentane cooled in liquid nitrogen was used to freeze hearts immersed in optimal cutting temperature (OCT) medium. Sections were cut to 7 μm using a commercial cryostat and used for either isolectin B4 or Masson's Trichrome. To calculate infarct size, at least four Masson's Trichrome stained sections at various levels along the long axis were analyzed for collagen deposition. The midline technique for

infarct size determination was used as described previously [42]. Briefly, the LV midline was drawn at the center of the anterior (lateral) wall along the length of the infarct. This circumference was divided by the total midline circumference of the heart to determine infarct size. Frozen sections were air dried, and OCT was removed by rinsing slides in PBS. Isolectin B4 was diluted 1:250 in Tris buffered saline with 0.1% Tween-20. This solution was added to sections for 1 hour at 37°C. Afterwards, sections were washed in PBS and counterstained with DAPI for 5 minutes. Sections were rinsed in dH₂O and mounted with an anti-fade aqueous mounting media (Vector Labs, Burlingame, CA).

5.2.12 Statistical Analysis and Interpretation

Two-way analysis of variance (ANOVA) was performed to interpret the response of hMSC and B4 progenitor cells in collagen patches in several *in vitro* assays (proliferation, differentiation and viability). A post-hoc Bonferroni testing was used to determine statistical significance between culture conditions for the two cell types. Additionally, a one-way ANOVA with appropriate post-hoc testing (Bonferroni) was used for the interpretation of *in vivo* and histological data sets. A p-value less than 0.05 indicated statistical significance. A Student's t-test was used to determine changes in mRNA abundance fold change between hMSC and B4 progenitor cells.

5.3 RESULTS

5.3.1 Culture within Collagen Patches Modulates Proliferation, Differentiation and Viability of hMSC and B4 Progenitor Cells

To determine how culture of cells within collagen patches affected stem cell function, we measured proliferation, differentiation and viability of hMSC and B4 progenitor cells as monolayers or isolated from collagen patches. Proliferation was

quantified using a pulse-chase with EdU substrate (Figure 4.3). EdU incorporation within cell types as monolayers or removed from within collagen patches was measured with flow cytometry. hMSC and B4 progenitor cells demonstrated attenuated proliferation upon culture within collagen patches. hMSC showed a 86% reduction in EdU incorporation (50.9% EdU+ vs. 7% EdU+; $p < 0.001$). B4 progenitors showed a 57% reduction (60% EdU+ vs. 25.5% EdU+; $p < 0.01$). A two-way ANOVA revealed that 55.3% of the variance was due to the culture of cells in collagen patches ($p < 0.0001$). The cell types used only accounted for 6.9% of the variance ($p = 0.022$), suggesting that patches reduced proliferation and the effect was similar but not identical between cell types.

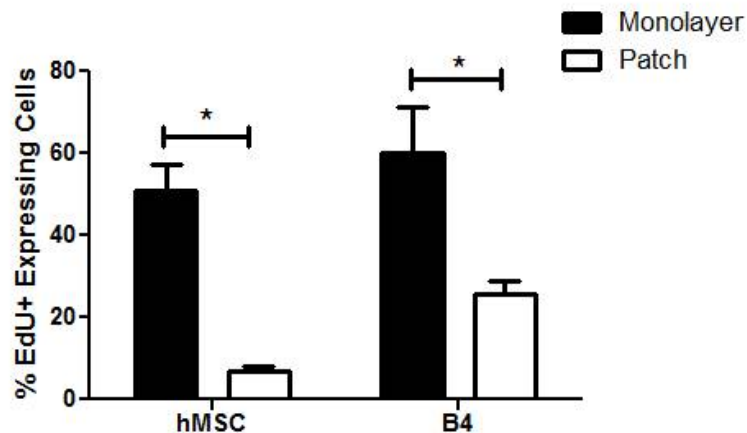


Figure 5.1) Proliferation of hMSC and B4 progenitor cells in collagen patches. Flow cytometry for EdU incorporation into hMSC and B4 progenitor cells was used to determine the proliferative capacity of stem/progenitor cells in 3D culture. Both hMSC ($50.9 \pm 6.2\%$ vs. $7 \pm 0.9\%$; $*p < 0.001$) and B4 ($60.1 \pm 11.1\%$ vs. $25.5 \pm 3.2\%$; $*p < 0.01$) progenitor cells demonstrated attenuated proliferation in collagen patches as compared to culture as monolayers.

Additionally, stem cell potency for cells cultured as monolayers or within collagen patches was determine by monitoring several antigens within the progenitor/stem cell

populations. For both hMSC and B4 progenitors, CD105 and CD73 were used to determine the extent of differentiation over 3 d. There was no loss of potency over 3 d in hMSC for both CD105 (Monolayer: 85.6% Expression vs. Patch 3 d: 76.1% Expression; $p > 0.05$) and CD73 (Monolayer: 82.9% Expression vs. Patch 3 d: 75.4% Expression; $p > 0.05$). In addition, there was no loss of potency in B4 progenitors over 3 d for CD105 (Monolayer: 78.2% Expression vs. Patch 3 d: 81% Expression; $p > 0.05$) or CD73 (Monolayer: 96.8% Expression vs. Patch 3 d: 95.3% Expression; $p > 0.05$). Despite the lack of change of markers in collagen patches, CD73 was higher in B4 progenitors than hMSC ($p = 0.0002$), suggesting a higher percentage of B4 cells expressed this multipotent marker at baseline.

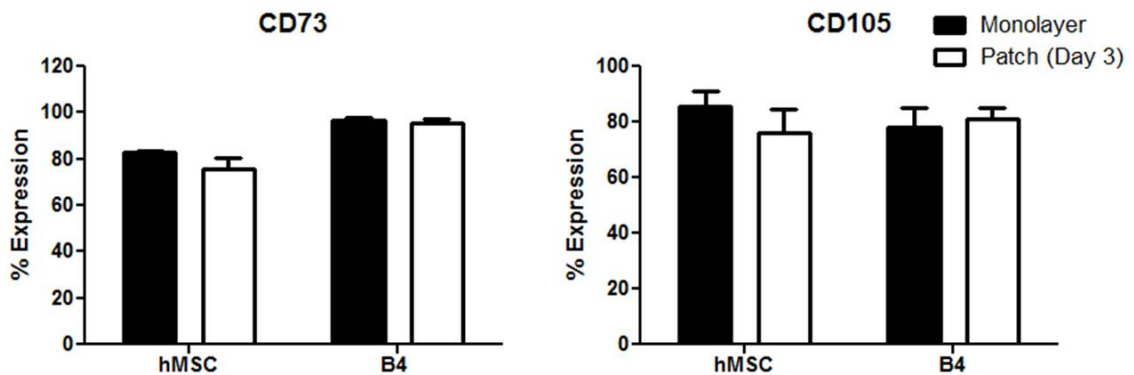


Figure 5.2) No loss of hMSC or B4 progenitor cell potency after culture in collagen patches. CD73 and CD105 were used to monitor stem cell potency over 3 d in culture as monolayers or patches for hMSC and B4 progenitor cells. hMSC showed no change in CD73 (hMSC: monolayer: $82.9 \pm 0.4\%$ vs. patch 3 d: $75.4 \pm 4.9\%$) and CD105 (hMSC: monolayer: $85.6 \pm 5.5\%$ vs. patch 3 d: $76.1 \pm 8.3\%$) expression over 3 d. B4 progenitor cells also displayed no change in CD73 (B4: monolayer: $96.8 \pm 1.1\%$ vs. patch 3 d: $95.3 \pm 1.7\%$) and CD105 (hMSC: monolayer: $78.2 \pm 6.8\%$ vs. patch 3 d: $81 \pm 4\%$). A two-way ANOVA revealed significant variation between cell types in regard to CD73 expression ($p = 0.0002$).

To determine cell viability within collagen patches, hMSC and B4 progenitors were isolated using a collagenase solution after 3 d in culture. Both hMSC and B4 progenitor maintained viability above 80% after culture in collagen patches (Figure 5.3). There was a slight but significant loss of viability of hMSC cultured in collagen patches (Monolayer: $92.8 \pm 2\%$ Expression vs. Patch: $81 \pm 3\%$ Expression) that was not seen in B4 cells (Monolayer: $96.6 \pm 6.5\%$ vs. Patch: $91.3 \pm 2.9\%$).

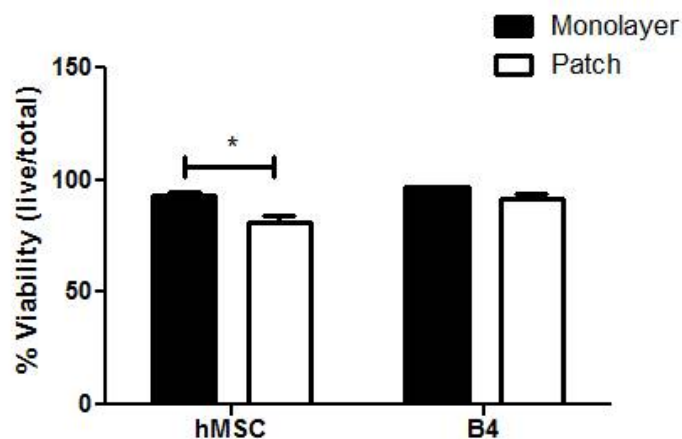


Figure 5.3) Viability of hMSC and B4 progenitor cells in collagen patches. Viability was measured using a trypan blue exclusion assay. hMSC displayed a small and significant reduction in viability after culture in collagen patches ($92.8 \pm 2\%$ vs. $80.8 \pm 3\%$; * $p < 0.05$). B4 progenitor cells demonstrated no change in viability when cultured collagen patches compared to culture as monolayers ($96.6 \pm 6.5\%$ vs. $91.3 \pm 2.9\%$).

5.3.2 Culture within 3D Collagen Patches Modulates Growth Factor mRNA

Abundance of hMSC and B4 Progenitor Cells

Paracrine pathways may play an important role hMSC mediated repair of damaged myocardium. Therefore, we performed real time RT-PCR to determine the effect of progenitor/stem cell culture in collagen patches on growth factor mRNA abundance. We investigated six growth factors: IL-8, ANG, VEGF, FGF-1, FGF-2, and

SDF-1 α . All data were taken from cells/patches exposed to hypoxia (1% O₂) to mimic likely conditions in the infarct region. Comparison of hMSC and B4 progenitor cells was represented as fold difference between monolayer and cardiac patches. Analysis revealed that hMSC and B4 cells responded similarly for IL-8 (upregulation; p = 0.4), ANG (upregulation; p = 0.3), FGF-2 (downregulation; p = 0.3) and SDF-1 α (downregulation; p = 0.1). Although both hMSC and B4 progenitor cells modulation expression of VEGF and FGF-1 upon culture in collagen patches, the extent of change was significantly greater in hMSC (VEGF: 13.3 \pm 3.3 vs. 1.5 \pm 0.2; *p < 0.05; FGF-1: 20 \pm 5.3 vs. 0.7 \pm 0.3; *p < 0.01)

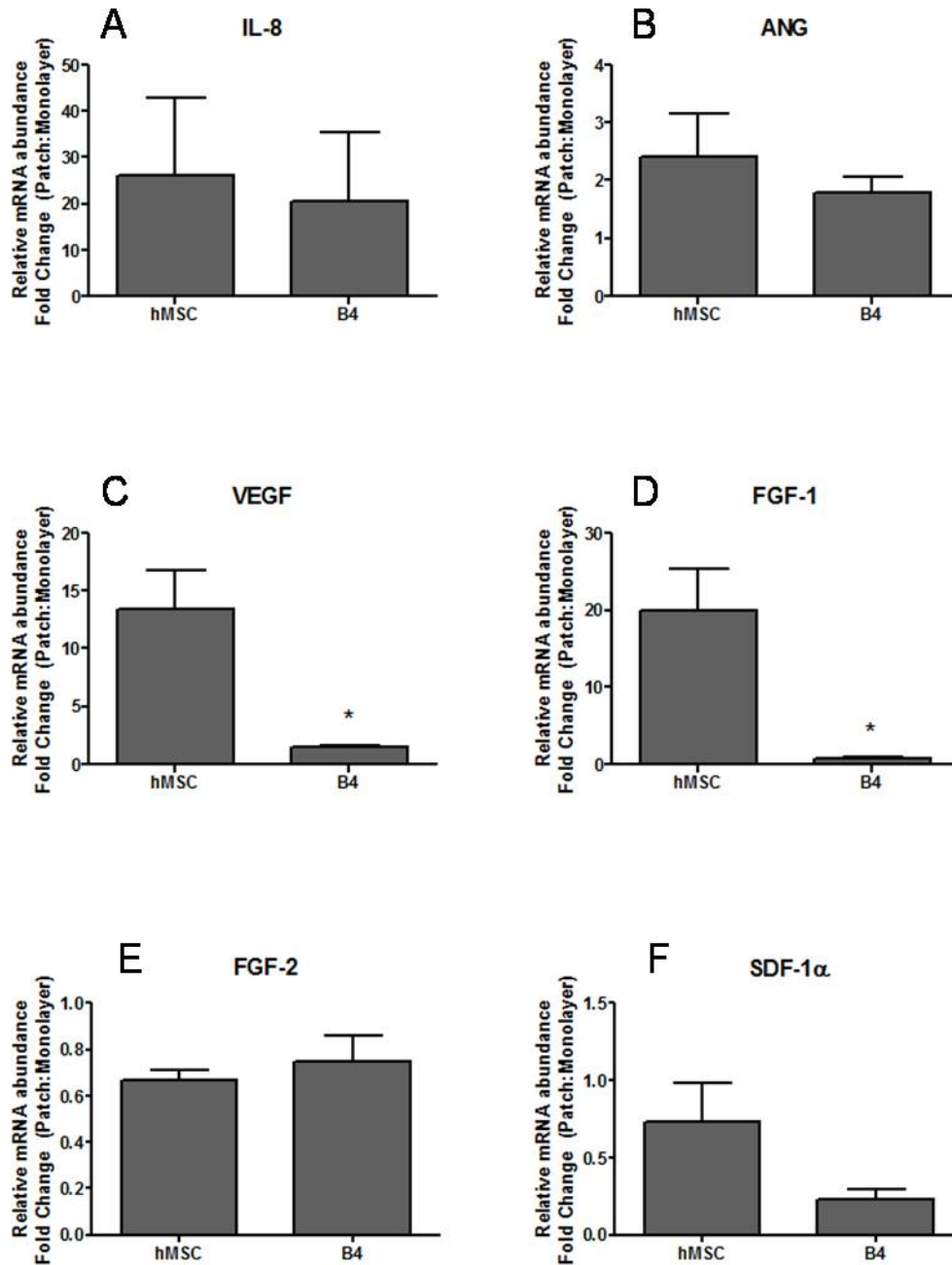


Figure 5.4) Angiogenic growth factor mRNA abundance fold change in hMSC and B4 progenitor cells. mRNA abundance was measure with real time RT-PCR. Results indicate similar mRNA regulatory patterns between hMSC and B4 progenitor cells for A) IL-8 (26 ± 16.7 vs. 20.3 ± 15 ; $p = 0.4$), B) ANG (2.4 ± 0.7 vs. 1.8 ± 0.3 ; $p = 0.3$), E) FGF-2 (0.7 ± 0.04 vs. 0.8 ± 0.1 ; $p = 0.3$) F) SDF-1 (0.7 ± 0.3 vs. 0.2 ± 0.1 ; $p = 0.1$). mRNA regulatory patterns were significantly different for the growth factors C) VEGF (13.3 ± 3.3 vs. 1.5 ± 0.2 ; $*p < 0.05$) and D) FGF-1 (20 ± 5.3 vs. 0.7 ± 0.3 ; $*p < 0.05$).

5.3.3 Cardiac Patch Application to Injured Myocardium does not Alter the Developed Infarct Size

In vivo models of myocardial infarction are well documented and involve the ligation the left anterior descending coronary artery. This artery supplies the anterior portions of the heart. The high death and exclusion rates seen in Table 4.1 and Table 5.1 suggest variability in infarct surgery or coronary anatomy. To determine if there were any differences in final (28 d) infarct size between different groups represented in the study, we measured infarct size by midline evaluation. As shown in figure 5.4 there were no differences in infarct size between MI control hearts, hMSC patch treated hearts and B4 progenitor cell patch treated hearts (MI: $37 \pm 1\%$, MSC Patch: $34 \pm 1\%$, and B4 Patch: $34 \pm 6\%$; $p = 0.71$).

Table 5.1 – Animal accounting for *in vivo* model of myocardial infarction

	# Surgeries	# Dead within 24 hr	# Dead from 24 hr to 14 d	# Excluded Due to Baseline ECHO	Mass at Initial Surgery (g)	Mass at 4wk Hemo (g)	# Used in 4wk ECHO Studies	# Used in 4 wk Hemo Studies
Sham	6	0	0	1	209 ± 12	--	5	2
MI control	14	1	0	8	209 ± 8	277 ± 7	5	5
Non-viable Patch	11	4	0	5	216 ± 8	249 ± 1	2	2
hMSC Patch	9	0	2	1	215 ± 7	273 ± 7	5	5
B4 Patch	12	5	0	1	216 ± 8	254 ± 14	6	6

MI – Myocardial infarction; hMSC – human mesenchymal stem cells; LAD – Left anterior descending coronary artery; ECHO – Echocardiography; Hemo – Hemodynamics; wk – week

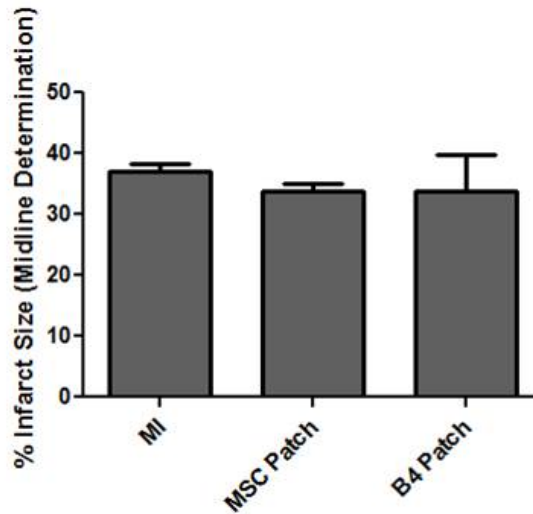


Figure 5.5) No change in infarct size with cardiac patch transplantation. Infarct size was determined by measuring the infarct midline circumference of Masson's Trichrome stained tissue sections. Analysis revealed no change in infarct size 4 weeks after initial LAD ligation when comparing MI controls, hearts treated with MSC patches or hearts treated B4 progenitor cell treatment (MI: $37 \pm 1\%$, MSC Patch: $34 \pm 1\%$, and B4 Patch: $34 \pm 6\%$; $p = 0.71$). MI – Myocardial infarction controls; MSC – Mesenchymal stem cells; B4 – B4 progenitor cells.

Although there was no change in infarct size, there were distinct differences in the composition of the infarct area. (Figure 5.5). Echocardiography, invasive hemodynamics and histology for neovessel formation were performed to help elucidate this effect.

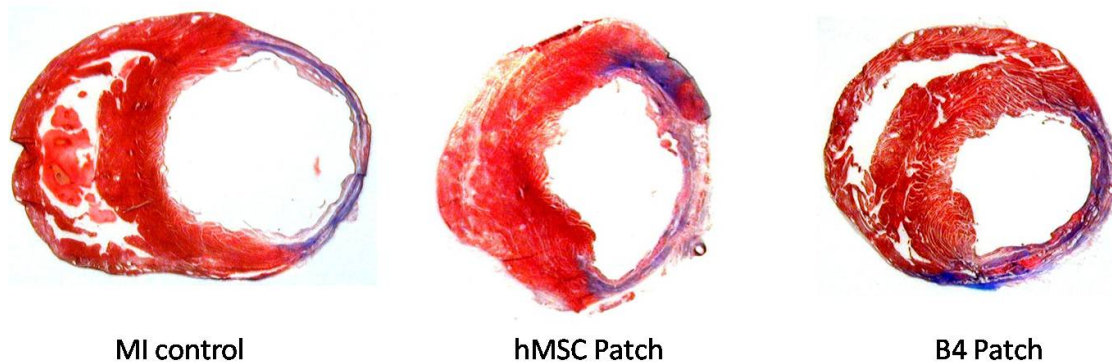


Figure 5.6) Myocardial infarct development at treatment with a cardiac patch. hMSC and B4 progenitor cell patches were applied to infarcted hearts. 4 weeks later, histological analysis revealed qualitative differences in infarct composition between all groups. This included in the presence of blood vessels and LV wall thickness.

5.3.4 hMSC and B4 Progenitor Cell Cardiac Patch Application Improves

Parameters of Cardiac Remodeling and Function after Myocardial Infarction

To adjust for variable infarct size within each group, echocardiographic data was normalized within each rat for the 3 d baseline. After this correction, both hMSC and B4 progenitor cardiac patches had a beneficial role in preventing adverse remodeling. Specifically, hMSC and B4 progenitor cells helped to maintain fractional shortening and infarct wall thickness (Table 5.2). There was no difference between hMSC patch or B4 progenitor cell treatment. Additionally, there were no significant differences observed with LV chamber dimensions between all groups.

Table 5.2 - Corrected echocardiographic measures after myocardial infarction

Corrected	MI (n=5)	MI+Nv Patch (n=2)	MI+ MSC Patch (n=4)	MI+ B4 Patch (n=5)
FS ($\Delta\%$)	-38 \pm 19	-4 \pm 15	11 \pm 10 ^a	14 \pm 10 ^a
AWTh ($\Delta\%$)	-97 \pm 25	-80 \pm 13	19 \pm 12 ^{a,b}	-22 \pm 14 ^a
LVIDs ($\Delta\%$)	19 \pm 4	14 \pm 9	6 \pm 1	12 \pm 7
LVIDd ($\Delta\%$)	14 \pm 4	15 \pm 6	11 \pm 2	15 \pm 5

^ap < 0.05 vs. MI, ^bp < 0.05 vs. MI + NV Patch

MI: Myocardial Infarction

NV: Non-viable

MSC: Mesenchymal Stem Cell

LVIDd: Left ventricular internal diameter at diastole

LVIDs: Left ventricular internal diameter at systole

FS%: Percent fractional shortening

AWTh: Anterior wall thickness

Additionally, invasive hemodynamics were performed to assess myocardial function after cardiac patch application. Similar to previous experiments using this model (see Chapter 3 and Chapter 4), there were few hemodynamic changes between the different groups 28 d after the initial infarct surgery (Table 5.3). hMSC patch application, however, did improve the dP/dt min compared to MI and non-viable patch controls. Other measures including dP/dt max, end diastolic pressure and τ did not show any statistical significance when comparing viable patch treatment to controls.

Table 5.3 - Hemodynamic measures after myocardial infarction

	MI (n=5)	MI+ NV Patch (n=3)	MI+ MSC Patch (n=4)	MI+ B4 Patch (n=5)
+dP/dt (mmHg/s)	8133 ± 306	6862 ± 279	8145 ± 158	7664 ± 355
-dP/dt (mmHg/s)	-6510 ± 372	-5882 ± 63	-8252 ± 640 ^{a,b}	-7009 ± 59
EDP (mmHg)	11 ± 3	17 ± 5	8 ± 3	6 ± 1
τ (msec)	16 ± 3	17 ± 3	12 ± 0.3	15 ± 2

^ap < 0.05 vs. MI, ^bp < 0.05 vs. MI + NV Patch

MI: Myocardial Infarction

NV: Non-viable

MSC: Mesenchymal Stem Cell

+ dp/dt: Maximum rate of rise in left ventricular pressure during systole

- dp/dt: Maximum rate of decrease in left ventricular pressure during diastole

EDP: Left ventricular end-diastolic pressure

τ: Time constant for pressure fall during cardiac relaxation

5.3.5 B4 Progenitor Cell Patch Application does not Alter Neovessel Formation after Myocardial Infarction.

One possible explanation as to why hMSC application (either injected or delivered with a tissue engineered patches) improves cardiac function is through the release of beneficial paracrine factors once engrafted. Such factors can act by decreasing cardiomyocyte apoptosis, preventing adverse fibrosis or increasing angiogenesis. To determine whether B4 progenitor cell patch application had an effect on neovessel formation after myocardial infarction, histological evaluation for isolectin B4 was performed. The data indicated that hMSC and B4 progenitor cell patches did not alter blood vessel formation compared to MI controls (MI: 6.6 ± 0.6 vs. hMSC: 10.6 ± 1.8 vs. B4: 11.9 ± 2.6 ; ANOVA p = 0.18; Figure 5.6).

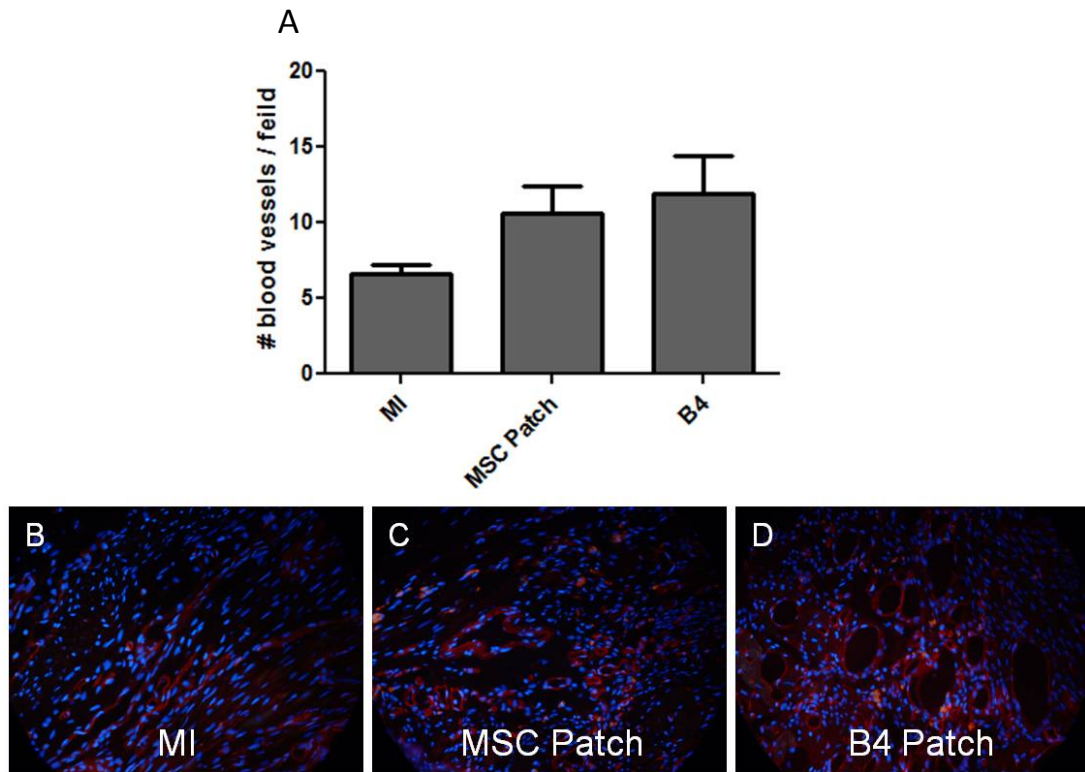


Figure 5.7) Application of B4 patch showed no improvement in neovessel formation. 4 weeks after LAD ligation, hearts were analyzed for neo-vessel formation. A) hMSC and B4 progenitor cell patch application showed no statistical evidence of increased neo-vessel formation compared to MI controls (MI: 6.6 ± 0.6 vs. hMSC: 10.6 ± 1.8 vs. B4: 11.9 ± 2.6 ; ANOVA $p = 0.18$). Histological analysis of B) MI control hearts; $n=3$, C) hMSC patch treated hearts; $n=3$ and D) B4 patch treated hearts; $n=3$ was performed to assess neo-vessel formation.

5.4 DISCUSSION

The choice of cell source used in human clinical trials is limited by the need to expand specific cell populations after isolation. This is the case with mesenchymal stem cells, which have to be purified and expanded before transplantation into patients. This delay represents a potential problem when treating patients with cellular cardiomyoplasty. Given the difficulties of harvesting mesenchymal stem cells for preventive therapy, it is essential to develop novel techniques for deriving “off-the-shelf” hMSC substitutes. B4 progenitor cells represent one possible solution to the development of hMSC substitutes. It has been reported that these cells display a similar phenotype to hMSC, however, the reparative potential of B4 progenitor cells in cellular cardiomyoplasty was not yet evaluated. In this study, we compared hMSC to B4 progenitor cells delivered to infarcted myocardium. A tissue engineered approach to cell delivery was chosen given evidence that cardiac patches provide relatively large cell engraftment efficiencies and provide enhanced prevention of adverse cardiac remodeling (Chapter 3 and Chapter 4, respectively)

In general, hMSC and B4 progenitor cells responded similarly when embedded in collagen patches. Both cell types demonstrated attenuated proliferation with maintenance of stem cell potency and viability. It has already been reported by Boyd et al. that B4 progenitor cells are phenotypically similar to hMSC [41]. This manuscript also described the use of a contraction assay to demonstrate the ability of B4 progenitor cells to respond to external stresses. Similar responses have been reported for MSCs by other investigators and in Chapters 3 and 4. We expanded on this approach of comparing hMSC and B4 progenitor cell function in collagen hydrogels by assessing proliferation, potency and viability. The comparable responses of hMSC and B4 progenitor cells in collagen patches suggests these cells may respond similarly in other applications such as cellular cardiomyoplasty.

As reported in Chapter 4, the culture of stem cells in collagen patches alters mRNA expression of several growth factors. Several growth factors (including IL-8, ANG, FGF-2 and SDF-1) were similarly regulated when cultured in collagen patches for hMSC and B4 progenitor cells. These cells also displayed differential regulatory patterns for other growth factors (VEGF and FGF-1), however. This implies that hMSC and B4 progenitor cell paracrine actions may promote different downstream local responses. Differences in mRNA regulation may be due to variations in derivation or isolation procedures.

The mechanisms involved in the differential modulation of mRNA abundance for hMSC and B4 progenitor cells may include cell responsiveness to physical stresses. This may induce cytoskeletal reorganization because of cellular interaction (or lack of interaction) with the collagen microstructure or modulation of cell bioenergetics. The data shows similar cellular behavior for proliferation, differentiation and viability between hMSC and B4 progenitor cells. Therefore differences in mRNA regulation may be due to differences in available stress-induced transcriptional elements within the individual cells before culturing in patches. Understanding these mechanisms will aid in optimizing or modifying paracrine actions of different stem/progenitor cell populations for cellular cardiomyoplasty.

In order to determine the effectiveness of B4 progenitor cell patch transplantation in mediating cardiac repair after infarction, we assessed function using echocardiography and invasive hemodynamics. Although B4 progenitor cells did not perform as well as hMSC in this model (i.e. hemodynamic measures), they did provide for a similar level of cardiac repair and preservation (FS% and AWTh). Interestingly, hMSC patch application resulted in improved $-dP/dt$ when compared to MI and nonviable patch controls. This level of improvement was absent when B4 progenitor cell patches were transplanted onto infarcted hearts. This may be the result of differential

paracrine actions that affect myofibroblast presence, neovessel formation or endogenous stem cell recruitment. These perceived paracrine responses were shown to be important in Chapter 3. These actions represent a few possible explanations for the differences in hMSC and B4 progenitor cell mediated repair, but given the number of paracrine factors secreted by stem/progenitor cells other mechanisms are also likely to be playing an important role. Other responses include differential engraftment/migration efficiencies or cell differentiation.

The accumulation of blood vessels within the wall can aid in the prevention of adverse remodeling by allowing for improved infarct volume and compliance and reduced apoptosis of viable muscle. The local angiogenic effects of B4 progenitor cells were similar to hMSC, but were not statistically significant compared to MI controls.. The lack of enhanced neovessel formation in both hMSC and B4 progenitor cells suggests other reparative mechanisms are involved in myocardial repair. Given differences in growth factor regulation upon culture in cardiac patches, the initiation or lack of several paracrine actions may account for differences hMSC and B4 progenitor cell mediated myocardial repair. Another mechanism involves differences in engraftment (migratory) potential. For instance, hMSC may be more prone to engraft into injured myocardium after culture in cardiac patches than B4 progenitor cells. Therefore the local effects of hMSC would be more pronounced than B4 progenitor cells. This hypothesis has yet to be tested.

In conclusion, cellular cardiomyoplasty with the use of B4 progenitor cells may represent a suitable alternative to hMSC therapy. B4 progenitors displayed similar responses to hMSC in 3D culture in terms of retention of pluripotency and longevity. Additionally, there were similar trends in the indices of myocardial repair after delivery with hMSC and B4 progenitor cell patches. There were several differences that suggest differential paracrine actions after engraftment, however. Such differences highlight a

need to investigate potential mechanisms by which hMSC and B4 progenitor cells enhance cardiac function and remodeling. Nevertheless, B4 progenitor cells do offer another effective cell source for cellular therapies.

5.5 LIMITATIONS and RECOMMENDATIONS

B4 progenitor cells may represent a potential cell source substitute for hMSC-based therapies. We tested this hypothesis by comparing the response of hMSC and B4 progenitor cells in 3D culture and by comparing the reparative potential of hMSC and B4 progenitor cells (delivered within collagen patches) in an *in vivo* model of myocardial infarction. There are several limitations to these studies. One hypothesis investigated in Chapter 5 concerns the response of B4 progenitor cells in collagen patches compared to hMSC. Although there were several responses that were similar (i.e. reduced proliferation, maintenance of potency and growth factor expression), this response may not be cell specific. The use of a control stem cell (such as an embryonic stem cell) would benefit this study so that generic and specific responses can be identified.

Additionally, hMSC improved myocardial function and prevented adverse remodeling more effectively than B4 progenitor cells. The reason for such differences is not specifically addressed, however. Possible mechanisms include differential myofibroblast presence, stem cell recruitment or engraftment (migration) efficiencies. Many of these mechanisms were addressed in Chapter 3. To investigate the hypothesis more conclusively, these experiments will have to be undertaken. Additional experiments to determine changes in cell migration potential are also necessary.

hMSC patch application led to improved prevention of wall thinning. This effect was also observed with the use of immunocompetent animal models in Chapter 3. Other measures such as LV dimensions were not improved, however. This is contrary to the results of Chapter 3. Additionally, improved lusitropy was not observed with the use of

immunocompetent animal models. This collection of data (Chapter 3 and Chapter 5) suggests the immune status of the host may play a role in hMSC patch mediated repair. Understanding this effect is essential to determining the role of the immune response in cellular cardiomyoplasty and may demonstrate a benefit to allogenic therapies. A nude rat may allow for longer engraftment and thus allow hMSC to favorably affect lusitropy. Additionally, a strong immune response may promote enhanced remodeling and repair. Experiments necessary to investigate this hypothesis involve monitoring engraftment and the immune response over several time points in immunocompromised and immunocompetent animal models.

5.6 REFERENCES

1. M. G. Klug, M. H. Soonpaa, G. Y. Koh and L. J. Field. Genetically selected cardiomyocytes from differentiating embryonic stem cells form stable intracardiac grafts. *J Clin Invest.* 1996 Jul 1;98:216-24.
2. R. K. Li, Z. Q. Jia, R. D. Weisel, et al. Cardiomyocyte transplantation improves heart function. *Ann Thorac Surg.* 1996 Sep;62:654-60; discussion 60-1.
3. T. Sakai, R. K. Li, R. D. Weisel, et al. Fetal cell transplantation: a comparison of three cell types. *J Thorac Cardiovasc Surg.* 1999 Oct;118:715-24.
4. G. Y. Koh, M. H. Soonpaa, M. G. Klug and L. J. Field. Long-term survival of AT-1 cardiomyocyte grafts in syngeneic myocardium. *Am J Physiol.* 1993 May;264:H1727-33.
5. M. Horackova, R. Arora, R. Chen, et al. Cell transplantation for treatment of acute myocardial infarction: unique capacity for repair by skeletal muscle satellite cells. *Am J Physiol Heart Circ Physiol.* 2004 Oct;287:H1599-608.
6. G. Invernici, S. Cristini, P. Madeddu, et al. Human adult skeletal muscle stem cells differentiate into cardiomyocyte phenotype in vitro. *Exp Cell Res.* 2007 Aug 16.
7. C. E. Murry, R. W. Wiseman, S. M. Schwartz and S. D. Hauschka. Skeletal myoblast transplantation for repair of myocardial necrosis. *J Clin Invest.* 1996 Dec 1;98:2512-23.
8. R. K. Li, Z. Q. Jia, R. D. Weisel, F. Merante and D. A. Mickle. Smooth muscle cell transplantation into myocardial scar tissue improves heart function. *J Mol Cell Cardiol.* 1999 Mar;31:513-22.

9. A. P. Beltrami, L. Barlucchi, D. Torella, et al. Adult cardiac stem cells are multipotent and support myocardial regeneration. *Cell*. 2003 Sep 19;114:763-76.
10. B. Dawn, A. B. Stein, K. Urbanek, et al. Cardiac stem cells delivered intravascularly traverse the vessel barrier, regenerate infarcted myocardium, and improve cardiac function. *Proc Natl Acad Sci U S A*. 2005 Mar 8;102:3766-71.
11. E. Messina, L. De Angelis, G. Frati, et al. Isolation and expansion of adult cardiac stem cells from human and murine heart. *Circ Res*. 2004 Oct 29;95:911-21.
12. W. Dai, S. L. Hale, B. J. Martin, et al. Allogeneic mesenchymal stem cell transplantation in postinfarcted rat myocardium: short- and long-term effects. *Circulation*. 2005 Jul 12;112:214-23.
13. W. Jiang, A. Ma, T. Wang, et al. Homing and differentiation of mesenchymal stem cells delivered intravenously to ischemic myocardium in vivo: a time-series study. *Pflugers Arch*. 2006 Aug 17.
14. M. Kudo, Y. Wang, M. A. Wani, M. Xu, A. Ayub and M. Ashraf. Implantation of bone marrow stem cells reduces the infarction and fibrosis in ischemic mouse heart. *J Mol Cell Cardiol*. 2003 Sep;35:1113-9.
15. D. Orlic, J. Kajstura, S. Chimenti, et al. Bone marrow cells regenerate infarcted myocardium. *Nature*. 2001 Apr 5;410:701-5.
16. Y. L. Tang, Q. Zhao, X. Qin, et al. Paracrine action enhances the effects of autologous mesenchymal stem cell transplantation on vascular regeneration in rat model of myocardial infarction. *Ann Thorac Surg*. 2005 Jul;80:229-36; discussion 36-7.
17. Y. L. Tang, Q. Zhao, Y. C. Zhang, et al. Autologous mesenchymal stem cell transplantation induce VEGF and neovascularization in ischemic myocardium. *Regul Pept*. 2004 Jan 15;117:3-10.
18. I. Kehat, D. Kenyagin-Karsenti, M. Snir, et al. Human embryonic stem cells can differentiate into myocytes with structural and functional properties of cardiomyocytes. *J Clin Invest*. 2001 Aug;108:407-14.
19. D. Kumar, T. J. Kamp and M. M. LeWinter. Embryonic stem cells: differentiation into cardiomyocytes and potential for heart repair and regeneration. *Coron Artery Dis*. 2005 Mar;16:111-6.
20. C. Mummery, D. Ward-van Oostwaard, P. Doevendans, et al. Differentiation of human embryonic stem cells to cardiomyocytes: role of coculture with visceral endoderm-like cells. *Circulation*. 2003 Jun 3;107:2733-40.
21. J. Nussbaum, E. Minami, M. A. Laflamme, et al. Transplantation of undifferentiated murine embryonic stem cells in the heart: teratoma formation and immune response. *FASEB J*. 2007 May;21:1345-57.

22. G. Condorelli, U. Borello, L. De Angelis, et al. Cardiomyocytes induce endothelial cells to trans-differentiate into cardiac muscle: implications for myocardium regeneration. *Proc Natl Acad Sci U S A*. 2001 Sep 11;98:10733-8.
23. J. Leor, L. Rozen, A. Zuloff-Shani, et al. Ex vivo activated human macrophages improve healing, remodeling, and function of the infarcted heart. *Circulation*. 2006 Jul 4;114:194-100.
24. A. Chiavegato, S. Bollini, M. Pozzobon, et al. Human amniotic fluid-derived stem cells are rejected after transplantation in the myocardium of normal, ischemic, immunosuppressed or immuno-deficient rat. *J Mol Cell Cardiol*. 2007 Apr;42:746-59.
25. S. Sartore, M. Lenzi, A. Angelini, et al. Amniotic mesenchymal cells autotransplanted in a porcine model of cardiac ischemia do not differentiate to cardiogenic phenotypes. *Eur J Cardiothorac Surg*. 2005 Nov;28:677-84.
26. J. Leor, E. Guetta, M. S. Feinberg, et al. Human umbilical cord blood-derived CD133+ cells enhance function and repair of the infarcted myocardium. *Stem Cells*. 2006 Mar;24:772-80.
27. K. Schenke-Layland, B. M. Strem, M. C. Jordan, et al. Adipose Tissue-Derived Cells Improve Cardiac Function Following Myocardial Infarction. *J Surg Res*. 2008 Apr 10.
28. B. Assmus, J. Honold, V. Schachinger, et al. Transcoronary transplantation of progenitor cells after myocardial infarction. *N Engl J Med*. 2006 Sep 21;355:1222-32.
29. A. C. Diederichsen, J. E. Moller, P. Thayssen, et al. Effect of repeated intracoronary injection of bone marrow cells in patients with ischaemic heart failure the Danish stem cell study--congestive heart failure trial (DanCell-CHF). *Eur J Heart Fail*. 2008 Jul;10:661-7.
30. K. Hamano, M. Nishida, K. Hirata, et al. Local implantation of autologous bone marrow cells for therapeutic angiogenesis in patients with ischemic heart disease: clinical trial and preliminary results. *Jpn Circ J*. 2001 Sep;65:845-7.
31. K. Lunde, S. Solheim, S. Aakhus, et al. Intracoronary injection of mononuclear bone marrow cells in acute myocardial infarction. *N Engl J Med*. 2006 Sep 21;355:1199-209.
32. A. N. Patel, L. Geffner, R. F. Vina, et al. Surgical treatment for congestive heart failure with autologous adult stem cell transplantation: a prospective randomized study. *J Thorac Cardiovasc Surg*. 2005 Dec;130:1631-8.
33. E. C. Perin, H. F. Dohmann, R. Borojevic, et al. Transendocardial, autologous bone marrow cell transplantation for severe, chronic ischemic heart failure. *Circulation*. 2003 May 13;107:2294-302.
34. V. Schachinger, B. Assmus, M. B. Britten, et al. Transplantation of progenitor cells and regeneration enhancement in acute myocardial infarction: final one-year results of the TOPCARE-AMI Trial. *J Am Coll Cardiol*. 2004 Oct 19;44:1690-9.

35. H. F. Tse, Y. L. Kwong, J. K. Chan, G. Lo, C. L. Ho and C. P. Lau. Angiogenesis in ischaemic myocardium by intramyocardial autologous bone marrow mononuclear cell implantation. *Lancet*. 2003 Jan 4;361:47-9.
36. K. C. Wollert, G. P. Meyer, J. Lotz, et al. Intracoronary autologous bone-marrow cell transfer after myocardial infarction: the BOOST randomised controlled clinical trial. *Lancet*. 2004 Jul 10-16;364:141-8.
37. M. F. Pittenger, A. M. Mackay, S. C. Beck, et al. Multilineage potential of adult human mesenchymal stem cells. *Science*. 1999 Apr 2;284:143-7.
38. W. S. Shim, S. Jiang, P. Wong, et al. Ex vivo differentiation of human adult bone marrow stem cells into cardiomyocyte-like cells. *Biochem Biophys Res Commun*. 2004 Nov 12;324:481-8.
39. C. Toma, M. F. Pittenger, K. S. Cahill, B. J. Byrne and P. D. Kessler. Human mesenchymal stem cells differentiate to a cardiomyocyte phenotype in the adult murine heart. *Circulation*. 2002 Jan 1;105:93-8.
40. A. A. Mangi, N. Noiseux, D. Kong, et al. Mesenchymal stem cells modified with Akt prevent remodeling and restore performance of infarcted hearts. *Nat Med*. 2003 Sep;9:1195-201.
41. N. L. Boyd, K. R. Robbins, S. K. Dhara, F. D. West and S. L. Stice. Human Embryonic Stem Cell-Derived Mesoderm-like Epithelium Transitions to Mesenchymal Progenitor Cells. *Tissue Eng Part A*. 2009 Jan 15.
42. J. Takagawa, Y. Zhang, M. L. Wong, et al. Myocardial infarct size measurement in the mouse chronic infarction model: comparison of area- and length-based approaches. *J Appl Physiol*. 2007 Jun;102:2104-11.
43. N. G. Frangogiannis, C. W. Smith and M. L. Entman. The inflammatory response in myocardial infarction. *Cardiovasc Res*. 2002 Jan;53:31-47.
44. E. E. Creemers, J. N. Davis, A. M. Parkhurst, et al. Deficiency of TIMP-1 exacerbates LV remodeling after myocardial infarction in mice. *Am J Physiol Heart Circ Physiol*. 2003 Jan;284:H364-71.
45. R. Mukherjee, T. A. Brinsa, K. B. Dowdy, et al. Myocardial infarct expansion and matrix metalloproteinase inhibition. *Circulation*. 2003 Feb 4;107:618-25.
46. N. Sivasubramanian, M. L. Coker, K. M. Kurrelmeyer, et al. Left ventricular remodeling in transgenic mice with cardiac restricted overexpression of tumor necrosis factor. *Circulation*. 2001 Aug 14;104:826-31.
47. M. L. Lindsey, D. L. Mann, M. L. Entman and F. G. Spinale. Extracellular matrix remodeling following myocardial injury. *Ann Med*. 2003;35:316-26.

Chapter 6

Conclusions and Future Directions

6.1 ADDRESSING CELLULAR CARDIOMYOPLASTY IN FIVE STAGES

Heart failure represents a major cause of death in the United States. The progressive decline in cardiac function after myocardial infarction (MI) represents one etiology that leads to heart failure. Typical approaches to preventing heart failure after MI is through the use of pharmaceuticals which act to restore inotropic function or to minimize the energy demands of the heart. Unfortunately, these approaches do not allow for improvements in left ventricular (LV) remodeling or regeneration of lost myocardium. One experimental therapy which is gaining much ground is cellular cardiomyoplasty. This involves the delivery of cell alternatives to aid in infarct repair. Although this method has resulted in improved cardiac function in both preclinical and clinical studies, there are still limitations in cell delivery and cell sourcing. To address these issues, we developed a tissue engineered vehicle for progenitor cell delivery. This involved embedding progenitor cell populations within collagen matrices and transplanting the resultant cellularized patch onto infarcted myocardium. The hypothesis was that the application of a tissue engineered patch onto the infarct site would localize more cells and distribute them more evenly across the injured region. This would allow for higher engraftment rates than other delivery strategies and ultimately increased improvement in cardiac function. There are several stages to this project that warrant further discussion in order for this hypothesis to be thoroughly investigated (Figure 6.1). Each stage presents known and unknown problems associated with mechanism and application.

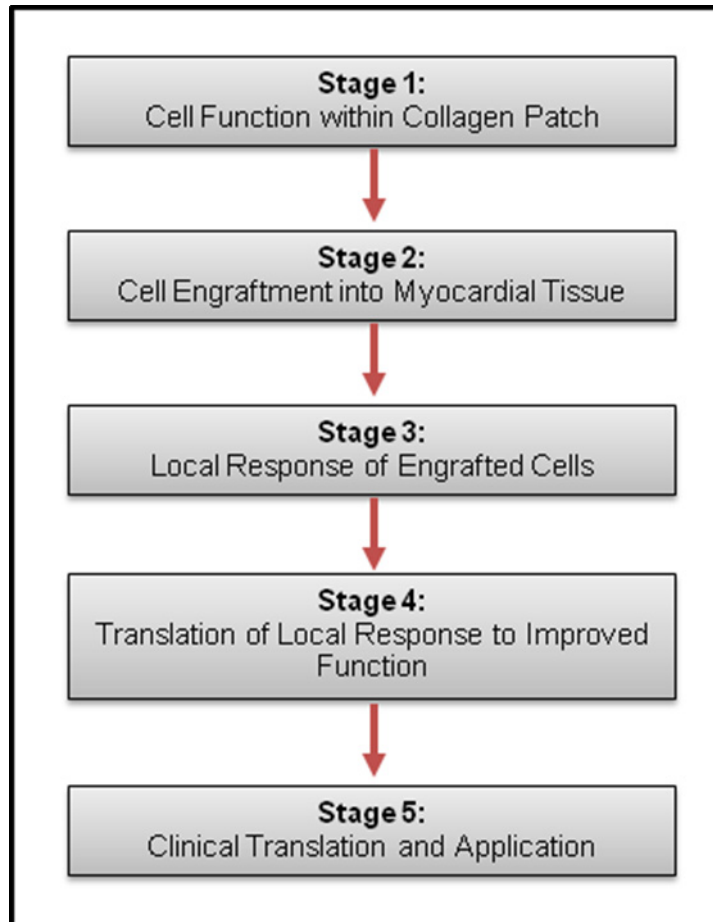


Figure 6.1) Five stages of cardiac patch mediate responses that require additional research.

Stage 1

The first stage revolves around the formation and characterization of cardiac patches. Throughout this study, type I collagen was used as a bioscaffold material and provided most of the mechanical support for the patch. Collagen was chosen based on previous studies which describe the formation of viable constructs for tissue engineering (TE) purposes [1-3] and because collagen is biodegradable, relatively non-immunogenic and can interact with adhesion dependent cell types such as MSCs. Chapters 4 and 5 provide evidence that different progenitor cell populations undergo changes in behavior after culture within collagen patches. This modulation in function may be mediated by cellular responsiveness to physical stresses such as oxygen tension or cellular interaction with the collagen microstructure.

When cells are deprived of oxygen, some cells respond by upregulating survival genes and modulating bioenergetics by inducing glycolysis, erythropoiesis and angiogenesis. For instance, hMSC typically respond to hypoxia by increasing HIF-1 α expression, a heterodimeric transcription factor [4]. One outcome of this response is increasing the production of vascular endothelial growth factor (VEGF) and other trophic factors such as IL-8. There was a measurable increase in VEGF and IL-8 production and mRNA abundance when hMSC were cultured in cardiac patch exposed to hypoxia compared to monolayers. Therefore, patches may help modulate desirable paracrine factors. Future experiments may show that this modulation is important for cellular myoplasty.

In Chapters 4 and Chapter 5, reduced proliferation was apparent for both hMSC and B4 progenitor cells cultured within collagen patches. HIF-1 α and p53 may play a role in this response. HIF-1 α is known to promote growth arrest. Carmeliet and colleagues demonstrated the anti-proliferative function of HIF-1 α by exposing ESC void of HIF-1 α

and normal ESC to hypoxia [5]. Results indicate that in the absence of HIF-1 α , cells retained a high proliferative capacity compared to wild type ESC. These HIF-1 α knock out ESCs also downregulated p53 expression, a known mediator of stress induced growth arrest and apoptosis [6]. Given that HIF-1 α can stabilize p53 [7], it was concluded that HIF-1 α mediated growth arrest was mediated through the p53 pathway.

Matrix interactions with cells are also known to influence cellular properties through integrin binding and outside-inside signaling pathways. Collagen matrices are rich in RGD and other integrin binding sequences. Therefore, progenitor cell integrin binding to collagen within cardiac patches may affect cellular properties.

The extent to which a gradient of oxygen tension and cell-collagen interaction play in modulating cell function in a patch is unknown. Investigators have shown that the presence of ECM such as collagen can regulate differentiation of MSCs. For example, culture of MSCs on or within collagen matrix induces both adipogenic and osteogenic differentiation [8]. Understanding how culture of stem cells in collagen patches affects differentiation may aid in directed cardiomyogenesis or reducing differentiation to unwanted cell types.

Future Directions: Stage 1

Studies involved in specifically deciphering the role of oxygen tension and integrin binding on progenitor cell function in collagen matrices will provide further insight as to how researchers can optimize and tailor TE patches for different applications. Studies that utilize different bioscaffolds, cell sources and seeding densities need to be explored to understand the usefulness of other forms of “cardiac patches”. Other studies will involve the use of oxygen generating biomaterials which may help sustain oxygen tension and prevent hypoxia-mediated modulations[9]. Additionally, the use of PEG-

ylated fibrin [10] or Matrigel [11] as a bioscaffold induces proliferation and resistance to apoptosis of different progenitor cell types. Thus, the use of different matrices for cardiac patch formation may induce more desirable modulations in cell function.

Stage 2

The second stage addresses issues related to cell engraftment after transplantation of the cardiac patch. We showed that hMSC have the ability to migrate out of the patch in response to injury. One potential injury signal mediating this migration is stromal derived factor-1 α (SDF-1 α). It is well documented that there is a multifold increase in endogenous SDF-1 α levels after myocardial infarction. Ma and colleagues [12] recently described the time course of SDF-1 α expression after the induction of MI in mice. They concluded there was a bimodal response with SDF-1 α expression peaking after 1 d and returning to basal levels by 8 d. Also known is that MSCs express CXCR4 (the receptor for SDF-1 α) and can migrate toward a chemotactic gradient of SDF-1 α upon activation of cytokines, growth factors or hypoxia [12-15]. The role of the SDF-1 α :CXCR4 axis in the migration of progenitor cells has been implicated in cellular cardiomyoplasty as well as other injury models [16]. Based on preliminary data obtained, the intracellular SDF-1 α :CXCR4 axis of hMSC embedded within collagen patches is significantly altered. Results indicate decreased SDF-1 α expression with increased CXCR4 expression. These changes may result from decreased oxygen tension or cellular interaction with the collagen microstructure. This suggests that hMSC have increased migratory potential when embedded in collagen patches.

Another possible determinant of progenitor cell migration into infarcted myocardium is integrin binding. CD29 is constitutively expressed on MSCs at high levels. Additionally, the binding partners for CD29 (such as Tenascin –C and VCAM-1)

are upregulated after MI. When CD29 was blocked using antibodies on MSCs, the engraftment rate of these cells was severely reduced [17]. Thus, MSCs may also migrate toward injury by binding to adhesion molecules down a chemotactic gradient.

Another unknown is the role of protease secretion (i.e. MMPs) in facilitating migration. This hypothesis has not yet been tested but determining the mechanism for transmigration and engraftment by cells embedded within cardiac patches will aid in the engineering of cells/matrix with an enhanced ability to promote migration into the infarct. This would effectively increase cell engraftment beyond current levels and also possibly enhance cardiac repair.

The idea that increased cell engraftment (or increased cell number initially delivered) is necessary in augmenting cardiac repair may not always hold true. Logically, if more cells engraft into injured myocardium, greater benefit would be expected. Delivery of a relatively small number of cells however, demonstrates comparable benefit. As shown in Table 6.1, 50,000 – 10 million cells have been delivered to infarcted myocardium in rats and mice. In all cases augmentation of myocardial function and remodeling was observed.

Table 6.1) Correlation of cell number to improved myocardial function

Study	In vivo Model	Cell Type	# Cells Delivered	Engraftment (if reported)	Result
Grinnemo et al. [18]	Nude Rat	Human MSC	1-2 million	% not reported but few cells present at 3 d	30% increase FAC at 1wk compared to controls; difference gone by 6 wk
Dai et al. [19]	Rat	Rat MSC	2 million	Not reported	12% increase FS at 4 wk compared to controls; difference gone by 6 months
Uemura et al. [20]	Mouse	Mouse MSC	1 million	0.01%	Increased EF% compared to controls
Nagaya et al. [21]	Rat	Rat MSC	1-5 million	Not reported though it was reported that at 5 wk 8% of isolated MSC expressed cardiac markers	1 million cell showed no substantial difference; 5 million increased FS% compared to controls
Kudo et al. [22]	Mouse	Mouse MSC	0.05-0.5 million	Not reported	68% decrease in infarct size compared to controls
Tang et al. [23]	Rat	Rat MSC	10 million	Not reported	60% increase in FS at 8 wk compared to controls
Hou et al. [24]	IS Rat	Human MSC	2 million	Not reported though few cells present at 4 wk	Increased FS% compared to control at 4 wk

EF – ejection fraction; FS – fractional shortening; FAC – fractional area change; MSC – mesenchymal stem cells

Whether graft size/cell number correlates with cardiac function is still an unanswered question. For instance, our studies utilized two types of animal models (immunocompetent vs. immunocompromised) with two different seeding densities to determine if patch application had an effect on myocardial function (Chapter 3 and 4). We observed similar patterns in infarct repair when using 1 million (immunocompetent) or 0.2 million (immunocompromised) cells within cardiac patches. The use of 1 million cells appeared to provide more benefit (although this could be an effect of the model and not cell number). Dose response studies intended to determine optimal cell number and graft sizes would greatly benefit ongoing investigations that use cardiac patches.

Future Directions Stage 2

The application of cardiac patches onto infarcted myocardium allows for localized delivery of progenitor cells at relatively high engraftment rates. The mechanism by

which cells are able to migrate from the patch and engraft into the injured tissue, however, is unknown. Studies to determine the migratory potential of cells within cardiac patches to known chemotactic (or growth factor) gradients present after MI will help to uncover new and useful information about this process. For instance, progenitor can be engineered to overexpress receptors for the most effective chemotactic signals present after an infarct. It may well be that localized delivery is only one advantage of cardiac patches. Another advantage is enhanced migratory potential due to cell culture in a 3D construct. More in depth studies into the SDF-1:CXCR4 axis and integrin/adhesion molecule profile of progenitor cells will help determine the role of bioscaffolding in modulating cellular migratory potential. Additional studies to determine the location and activity levels of secreted proteases will help to investigate how progenitor cells traverse the ventricular wall for efficient engraftment. Enhancing this process with gene therapy may help increase engraftment rates. Lastly, dose response studies will need to be performed to determine whether there are optimal graft sizes. In these studies one will have to consider cell number, the size of injury, the type of cell used and the immune status of the model. It is expected that the data from these studies will help to answer the question, “How many cells are necessary to have a positive effect on myocardial function?”

Stage 3

The third stage addresses the response of progenitor cells after engraftment. Reports have speculated that a variety of events may take place and include: cell differentiation, secretion of paracrine factors and/or cell death. MSCs are typically defined by their ability to differentiate into osteocytes, chondrocytes and adipocytes [25]. These multipotent cells have also been reported to differentiate into cardiomyocytes [26] or neural cells [27, 28] with the proper stimuli. Several cases of MSC differentiation to

cardiomyocytes have been reported after the delivery of MSCs to infarcted myocardium [19, 29]. Unfortunately, the functions of these “cardiac-like” cells and the mechanisms mediating differentiation *in vivo* have not been investigated. Interestingly, researchers have also reported a lack of differentiation potential from these cells after engraftment [30]. In Chapter 3 we noted improved cardiac function without cardiomyocyte differentiation or hMSC presence long term. These conflicting results make necessary studies in understanding differentiation of MSCs after engraftment.

Another possible local response of engrafted progenitor cells is to secrete paracrine factors. Potential paracrine factors include angiogenic, anti-apoptotic, mitogenic and progenitor cell mobilizing factors. Such factors may aid in the induction of neo-vessel formation, survival of energy starved myocardium and the proliferation and mobilization of endogenous cardiac progenitor cells. Interestingly, the mechanisms that are mediating the secretion of paracrine factors may be related to the mechanisms involved in the modulation of the hMSC secretion profile as described in Chapter 4. After delivery, progenitor cells engraft into a 3D hypoxic/ischemic tissue placing similar stresses on the cells as that imposed by the cardiac patch. The presence of endogenous chemokines and growth factors after a MI may also play a role in the induction of progenitor cells to secrete paracrine factors. For instance, angiotensin II, a potent vasoconstrictor regulated via the renin-angiotensin system (see Chapter 2), can induce VEGF synthesis in MSCs. The mechanism for this effect was via binding of Ang II to AT₁ receptors and activation of the extracellular signal-regulated kinase 1/2 and Akt pathways [31].

Oxygen tension, cellular interaction with the myocardial microstructure or stimulation via endogenous chemokines/growth factors may also play a role in the apparent differentiation of engrafted progenitor cells. Recent data suggest that Wnt-related signaling events are upregulated in the peri-infarct region of a MI [32].

Additionally, it has been suggested that both canonical and non-canonical Wnt signaling pathways play a role in cardiomyogenesis [33, 34] and that MSCs have the molecular machinery in place to participate in these signaling cascades [35]. Studies aimed at deciphering the role of Wnt signaling in cell differentiation after engraftment, may aid in uncovering “tunable” mechanisms involved in enhancing cardiomyogenesis.

Given the volatile and highly ischemic properties of the heart after infarction, many engrafted cells will simply die. This effectively reduces engraftment over time and may reduce the effect progenitor cells have on possible repair and preservation of the myocardium.

Future Direction Stage 3

Progenitor cells which have migrated and engrafted into infarcted myocardium generate local responses which may (or may not) contribute to repair. Such responses include cell differentiation and the secretion of paracrine factors. Cell differentiation may occur via Wnt signaling. Tracking and isolating progenitor cells for mRNA (i.e. laser capture) may aid researchers in understanding the role of the Wnt pathway in progenitor cell cardiomyogenesis after engraftment. If this pathway is shown to play a significant role, than the use of stem cells which overexpress Frizzled receptors may enhance differentiation.

Another local response is the secretion of paracrine factors. Studies aimed at understanding the role of hypoxia/ischemia, the myocardial microstructure (mechanics and content) and chemokines/growth factors at inducing progenitor cell paracrine responses will aid in understanding how researchers can prime or modify MSCs for optimal performance. For instance, the use of a cardiac patch may aid in the acclimation and modulation of progenitor cells to survive and enhance secretion specific factors necessary for effective repair. The choice of scaffold, cell number and bioactive factors

will have to be addressed when designing such studies. These local responses are key to understanding the reported benefits of cellular cardiomyoplasty. Answering the question: “How do local responses translate into global benefit?” is a lofty task but has to be done in order to progress this field forward.

Stage 4

How local cellular responses might translate into improved myocardial function is the focus of Stage 4. During the discussion of Stage 3, two major local responses were described, cell differentiation and secretion of paracrine factors. Under an appropriate sets of stresses and bioactive signals, progenitor cells may differentiate into cardiomyocytes. If these cells are able to integrate into the synticium of the myocardium and produce a contractile force, they may contribute to improved systolic function.

One question is how many cells are necessary to have a beneficial effect? Under normal conditions, there are millions of cells working together to actively contract and relax the heart. After cellular cardiomyoplasty, the number of cells which actually engraft reduces the likelihood that a necessary number of cells differentiate into cardiomyocytes and integrate with the endogenous system. Therefore, cell differentiation alone may not account for improved myocardial function after infarction.

Several groups contend that preserved ejection fraction or fractional shortening suggests improved contractility and thus the emergence of new, working myocytes. This, however, may be due to compensatory hypertrophic responses, reduced deposition of collagen or reduced infarct size. These responses can be explained via the interaction of endogenous cells with beneficial paracrine factors secreted from engrafted progenitor cells. For instance, several pathways are involved in pathological hypertrophy of cardiomyocytes and include: G-protein coupled receptor (GPCR), mitogen activated protein kinase and cytokine activated pathways (via NF- κ b). Factors

secreted from progenitor cells such as insulin-like growth factor-1 (IGF-1) can bind receptor tyrosine kinases (or other receptors such as GPCR or specific cytokine receptors) to induce hypertrophy of the viable myocytes (most likely in the peri-infarct region). This hypertrophic response can preserve ejection fraction though may also act as a catalyst for diastolic dysfunction.

Paracrine factors from progenitor cells may also reduce fibrosis by inhibiting MMP activity via TIMP secretion or by attenuating myofibroblasts production of collagen via IGF-1 or adrenomedullin [36]. MMPs are involved in the initial breakdown of the cardiac microstructure which provides the necessary space for myofibroblast to lay down scar tissue. Additionally, relaxin [37], a member of the IGF family of growth factors, has been cited as an antifibrotic growth factor which can act on myofibroblasts. Both of these efforts will help reduce fibrosis.

A reduction in infarct size can also aid in preserving cardiac function. This is most efficiently done by reperfusion of an infarction. The complete block of a coronary artery may not always allow for reperfusion and thus neovessel formation mediated by paracrine factors secreted from engrafted progenitor cells may help. Several angiogenic factors have been reported to secrete from progenitor cells in response to hypoxia and *in vivo* after infarction. These factors actively assist in the recruitment, proliferation and stabilization of endothelial cells. In Chapter 4 and 5 we describe the pro-angiogenic responses of progenitor cells delivered via a cardiac patch. There was no change in neoessel formation *in vivo*, however. Therefore, neovessel formation may not play as big a role in infarct repair as thought. Other paracrine-mediated events may be attributing to repair, however. For instance, in Chapter 3 we noted enhanced myofibroblast presence after patch delivery. Myofibroblasts are responsive to several paracrine stimuli.

Lastly, paracrine factors from engrafted progenitor cells can aid in the recruitment and proliferation of endogenous progenitor cells. In Chapter 3 we presented preliminary

data which suggest that the application of a cardiac patch increases the number of c-kit+ cells in the infarct region after MI. Endogenous progenitor cells have the capacity to differentiate into cardiomyocytes or vascular cell types (i.e. endothelial cells and/or smooth muscle cells). Given sufficient differentiation, this response may aid in the replenishment of necrotic/apoptotic myocytes and the formation of functional blood vessels.

Future Directions Stage 4

Understanding how local responses after cellular cardiomyoplasty translate into improved global myocardial function will allow researchers to determine optimal cell types for delivery, how cells can be engineered for optimal performance (possibly via modulation in cardiac patches) and which responses provided the most benefit. Cell differentiation is one response that may aid in improved cardiac function after infarction. Studies aimed at determining the contractile and integration potential of these cells will have to be completed. For instance, labeled progenitor cells (GFP label driven by an MCL-2v promoter to isolate progenitor cells which have differentiated to cardiomyocytes) can be isolated and contractile properties analyzed using published cell shortening analysis techniques. Additionally, patch clamp studies will help to understand the electrophysiological state of isolated cells. Optical mapping techniques can also be used to determine whether differentiated progenitor cells have integrated electrically with the endogenous myocardium. Optical mapping will also aid in determining the location of differentiated progenitor cells to help correlate location with function. If differentiated cells are shown to significantly contribute the cardiac function, methods intended to promote cardiac cell differentiation should be explored.

Although some differentiation is possible after progenitor cell engraftment, it may not be enough to explain the augmented function reported after cellular cardiomyoplasty.

Thus, cellular responses to paracrine factors should be studied. These include hypertrophy, apoptosis, angiogenesis, fibrosis and progenitor cell recruitment. All of these responses provide potential benefits to cardiac repair. Studies aimed at understanding the extent by which these responses aid in cardiac repair should be explored. Additionally, studies to determine what factors (and how much) are most beneficial are imperative.

Stage 5

Translating the use of cardiac patches into clinical arenas must be considered. Considerations include: cell source, immune response and transplantation of the cardiac patch. In Chapter 5 the effect of B4 progenitor cell patch application on myocardial function after infarction was described. B4 progenitor cells were chosen based on several limitations to hMSC. A major limitation with hMSC is the need for *ex vivo* expansion. This inherently delays the turnover before treatment. Given the similarities between B4 progenitor cells and hMSC [38] it was expected that these two cell types would perform similarly. In fact, we did observe similar indices of functional improvement compared to MI controls. Therefore B4 progenitor cells may represent a suitable alternative to hMSC therapy. The need for *ex vivo* expansion is just one limitation to progenitor cells use. Other cell types may be less prone to secrete paracrine factors or more prone to differentiate into unwanted cell types. Because of the multitude of cell responses, the choice of one “optimal” cell type may not be possible. Thus several cell types may be necessary. For instance, one cell type can be used to limit infarct expansion by inducing neovessel formation, another cell may differentiate into working myocytes and integrate with the host tissue and another cell may assist in limiting fibrosis through enhanced IGF-1 secretion. If a cardiac patch is chosen as the delivery vehicle than its role in the modulation of cell function will have to be addressed.

The question of cell source has no easy answer and will likely require many more years of research before significant progress is achieved.

One major issue with the use of B4 progenitor cells is they will likely have to be provided as an allogenic transplant. Thus, the likelihood of an immunological response is foreseeable. It will be interesting to determine the extent of immune response elicited due to B4 progenitor cell delivery (or any allogenic cell source). Such experiments would proceed similarly to what was performed with hMSC and would involve the delivery of B4 progenitor cells to immune-competent models of MI. This experiment will help to answer whether B4 progenitor cells have any immunoprivileges and whether they can continue to elicit a beneficial effect in the presence of an immunological response. This effect was indirectly addressed in the Chapters 3 and 4. The use of immunocompetent and immunocompromised animal models for a xenotransplant provided for similar indices of repair. The mechanisms governing each repair process are untested, however.

The transplantation of cardiac patches may present problems for cardiac surgeons. In most surgical settings, the use of non-invasive or minimally invasive procedures is preferred. This produces less tissue trauma for the patient. Thus, if the cardiac patch is to be used in a clinical setting, effective and minimally invasive ways to transplant the patch are preferred. Given the increase in temperature during an inflammatory responses and occurrence of acidosis after MI, physically responsive bioscaffolds may allow for localized delivery of cardiac patches. Thus, thermoresponsive (or pH-responsive) bioscaffolds [39] or the injection of a pre-gelled patch directly into the myocardium [40] using an image modality to guide the surgeon to an injection site may provide suitable alternatives to a complete thoracotomy.

The use of a cardiac patch provides plenty of benefits. Unexpected occurrences can blunt any positive effect, however. For instance, unwanted differentiation, the

secretion of non-beneficial paracrine factors or induction of adverse mechanical strain on the heart are just a few potential problems. Although we did not address this specifically, any unwanted events should be addressed throughout an experimental design.

Future Directions Stage 5

Effectively translating cellular cardiomyoplasty and cardiac patch application into the clinic is a work in progress. Several factors related to cell sourcing (which cell(s) will provide the greatest benefit and how can cardiac patches be used to aid in this benefit?), the immune response (if allogenic cells are to be used, how does the immune response effect local cellular responses?) and surgical transplantation of the cardiac patch (how to do so in a minimally invasive fashion?) have to be addressed. Studies aimed at determining optimal cell types and whether a cell “cocktail” could be more beneficial will have to be explored. These studies will proceed as described in Chapter 3, 4, and 5 except the cell type will vary. Additionally, studies aimed at understanding the role of the immune responses in cell mediated repair will allow researchers to either expand the cell source pool (if the immune response is shown to induce minimal changes in local cellular responses) or shrink the cell source pool. Lastly, innovative methods for minimally invasive delivery of the cardiac patch will need to be explored if this technique is to translate into the clinic. This may involve the use of thermo- or pH-responsive bioscaffolds for localized delivery of cardiac patches.

6.2 CONCLUSIONS

It is clear that a tissue engineered approach to cell delivery can enhance engraftment and modulate cell function. Whether these processes can be further advanced is a work in progress. Issues related to how cells migrate from the patch, how

they affect myocardial improvement, and how to deliver a patch in a minimally invasive manner need to be addressed, however.

6.3 REFERENCES

1. K. L. Christman and R. J. Lee. Biomaterials for the treatment of myocardial infarction. *J Am Coll Cardiol*. 2006 Sep 5;48:907-13.
2. J. T. Butcher, B. C. Barrett and R. M. Nerem. Equibiaxial strain stimulates fibroblastic phenotype shift in smooth muscle cells in an engineered tissue model of the aortic wall. *Biomaterials*. 2006 Oct;27:5252-8.
3. W. H. Zimmermann, I. Melnychenko and T. Eschenhagen. Engineered heart tissue for regeneration of diseased hearts. *Biomaterials*. 2004 Apr;25:1639-47.
4. H. Okuyama, B. Krishnamachary, Y. F. Zhou, H. Nagasawa, M. Bosch-Marce and G. L. Semenza. Expression of vascular endothelial growth factor receptor 1 in bone marrow-derived mesenchymal cells is dependent on hypoxia-inducible factor 1. *J Biol Chem*. 2006 Jun 2;281:15554-63.
5. P. Carmeliet, Y. Dor, J. M. Herbert, et al. Role of HIF-1 α in hypoxia-mediated apoptosis, cell proliferation and tumour angiogenesis. *Nature*. 1998 Jul 30;394:485-90.
6. D. A. Liebermann, B. Hoffman and R. A. Steinman. Molecular controls of growth arrest and apoptosis: p53-dependent and independent pathways. *Oncogene*. 1995 Jul 6;11:199-210.
7. W. G. An, M. Kanekal, M. C. Simon, E. Maltepe, M. V. Blagosklonny and L. M. Neckers. Stabilization of wild-type p53 by hypoxia-inducible factor 1 α . *Nature*. 1998 Mar 26;392:405-8.
8. L. Meinel, V. Karageorgiou, R. Fajardo, et al. Bone tissue engineering using human mesenchymal stem cells: effects of scaffold material and medium flow. *Ann Biomed Eng*. 2004 Jan;32:112-22.
9. S. H. Oh, C. L. Ward, A. Atala, J. J. Yoo and B. S. Harrison. Oxygen generating scaffolds for enhancing engineered tissue survival. *Biomaterials*. 2009 Feb;30:757-62.
10. G. Zhang, X. Wang, Z. Wang, J. Zhang and L. Suggs. A PEGylated fibrin patch for mesenchymal stem cell delivery. *Tissue Eng*. 2006 Jan;12:9-19.
11. T. Kofidis, J. L. de Bruin, G. Hoyt, et al. Myocardial restoration with embryonic stem cell bioartificial tissue transplantation. *J Heart Lung Transplant*. 2005 Jun;24:737-44.
12. J. Ma, J. Ge, S. Zhang, et al. Time course of myocardial stromal cell-derived factor 1 expression and beneficial effects of intravenously administered bone marrow

stem cells in rats with experimental myocardial infarction. *Basic Res Cardiol.* 2005 May;100:217-23.

13. R. F. Wynn, C. A. Hart, C. Corradi-Perini, et al. A small proportion of mesenchymal stem cells strongly expresses functionally active CXCR4 receptor capable of promoting migration to bone marrow. *Blood.* 2004 Nov 1;104:2643-5.

14. S. Bhakta, P. Hong and O. Koc. The surface adhesion molecule CXCR4 stimulates mesenchymal stem cell migration to stromal cell-derived factor-1 in vitro but does not decrease apoptosis under serum deprivation. *Cardiovasc Revasc Med.* 2006 Jan-Mar;7:19-24.

15. J. Ringe, S. Strassburg, K. Neumann, et al. Towards in situ tissue repair: human mesenchymal stem cells express chemokine receptors CXCR1, CXCR2 and CCR2, and migrate upon stimulation with CXCL8 but not CCL2. *J Cell Biochem.* 2007 May 1;101:135-46.

16. M. S. Penn. Importance of the SDF-1: CXCR4 axis in myocardial repair. *Circ Res.* 2009 May 22;104:1133-5.

17. J. E. Ip, Y. Wu, J. Huang, L. Zhang, R. E. Pratt and V. J. Dzau. Mesenchymal stem cells use integrin beta1 not CXC chemokine receptor 4 for myocardial migration and engraftment. *Mol Biol Cell.* 2007 Aug;18:2873-82.

18. K. H. Grinnemo, A. Mansson-Broberg, K. Leblanc, et al. Human mesenchymal stem cells do not differentiate into cardiomyocytes in a cardiac ischemic xenomodel. *Ann Med.* 2006;38:144-53.

19. W. Dai, S. L. Hale, B. J. Martin, et al. Allogeneic mesenchymal stem cell transplantation in postinfarcted rat myocardium: short- and long-term effects. *Circulation.* 2005 Jul 12;112:214-23.

20. R. Uemura, M. Xu, N. Ahmad and M. Ashraf. Bone marrow stem cells prevent left ventricular remodeling of ischemic heart through paracrine signaling. *Circ Res.* 2006 Jun 9;98:1414-21.

21. N. Nagaya, K. Kangawa, T. Itoh, et al. Transplantation of mesenchymal stem cells improves cardiac function in a rat model of dilated cardiomyopathy. *Circulation.* 2005 Aug 23;112:1128-35.

22. M. Kudo, Y. Wang, M. A. Wani, M. Xu, A. Ayub and M. Ashraf. Implantation of bone marrow stem cells reduces the infarction and fibrosis in ischemic mouse heart. *J Mol Cell Cardiol.* 2003 Sep;35:1113-9.

23. Y. L. Tang, Q. Zhao, X. Qin, et al. Paracrine action enhances the effects of autologous mesenchymal stem cell transplantation on vascular regeneration in rat model of myocardial infarction. *Ann Thorac Surg.* 2005 Jul;80:229-36; discussion 36-7.

24. M. Hou, K. M. Yang, H. Zhang, et al. Transplantation of mesenchymal stem cells from human bone marrow improves damaged heart function in rats. *Int J Cardiol.* 2007 Feb 7;115:220-8.

25. M. F. Pittenger, A. M. Mackay, S. C. Beck, et al. Multilineage potential of adult human mesenchymal stem cells. *Science*. 1999 Apr 2;284:143-7.
26. X. J. Xie, J. A. Wang, J. Cao and X. Zhang. Differentiation of bone marrow mesenchymal stem cells induced by myocardial medium under hypoxic conditions. *Acta Pharmacol Sin*. 2006 Sep;27:1153-8.
27. Z. Lei, L. Yongda, M. Jun, et al. Culture and neural differentiation of rat bone marrow mesenchymal stem cells in vitro. *Cell Biol Int*. 2007 Sep;31:916-23.
28. S. Wislet-Gendebien, G. Hans, P. Leprince, J. M. Rigo, G. Moonen and B. Rogister. Plasticity of cultured mesenchymal stem cells: switch from nestin-positive to excitable neuron-like phenotype. *Stem Cells*. 2005 Mar;23:392-402.
29. J. Y. Min, M. F. Sullivan, Y. Yang, et al. Significant improvement of heart function by cotransplantation of human mesenchymal stem cells and fetal cardiomyocytes in postinfarcted pigs. *Ann Thorac Surg*. 2002 Nov;74:1568-75.
30. L. C. Amado, A. P. Saliaris, K. H. Schuleri, et al. Cardiac repair with intramyocardial injection of allogeneic mesenchymal stem cells after myocardial infarction. *Proc Natl Acad Sci U S A*. 2005 Aug 9;102:11474-9.
31. R. Z. Shi, J. C. Wang, S. H. Huang, X. J. Wang and Q. P. Li. Angiotensin II induces vascular endothelial growth factor synthesis in mesenchymal stem cells. *Exp Cell Res*. 2009 Jan 1;315:10-5.
32. W. A. LaFramboise, K. L. Bombach, R. J. Dhir, et al. Molecular dynamics of the compensatory response to myocardial infarct. *J Mol Cell Cardiol*. 2005 Jan;38:103-17.
33. M. P. Flaherty, A. Abdel-Latif, Q. Li, et al. Noncanonical Wnt11 signaling is sufficient to induce cardiomyogenic differentiation in unfractionated bone marrow mononuclear cells. *Circulation*. 2008 Apr 29;117:2241-52.
34. L. Ling, V. Nurcombe and S. M. Cool. Wnt signaling controls the fate of mesenchymal stem cells. *Gene*. 2009 Mar 15;433:1-7.
35. S. L. Etheridge, G. J. Spencer, D. J. Heath and P. G. Genever. Expression profiling and functional analysis of wnt signaling mechanisms in mesenchymal stem cells. *Stem Cells*. 2004;22:849-60.
36. L. Li, S. Zhang, Y. Zhang, B. Yu, Y. Xu and Z. Guan. Paracrine action mediate the antifibrotic effect of transplanted mesenchymal stem cells in a rat model of global heart failure. *Mol Biol Rep*. 2009 Apr;36:725-31.
37. X. J. Du, Q. Xu, E. Lekgabe, et al. Reversal of cardiac fibrosis and related dysfunction by relaxin. *Ann N Y Acad Sci*. 2009 Apr;1160:278-84.
38. N. L. Boyd, K. R. Robbins, S. K. Dhara, F. D. West and S. L. Stice. Human Embryonic Stem Cell-Derived Mesoderm-like Epithelium Transitions to Mesenchymal Progenitor Cells. *Tissue Eng Part A*. 2009 Jan 15.

39. H. Naito, Y. Takewa, T. Mizuno, et al. Three-dimensional cardiac tissue engineering using a thermoresponsive artificial extracellular matrix. *ASAIO J.* 2004 Jul-Aug;50:344-8.
40. T. Kofidis, D. R. Lebl, E. C. Martinez, G. Hoyt, M. Tanaka and R. C. Robbins. Novel injectable bioartificial tissue facilitates targeted, less invasive, large-scale tissue restoration on the beating heart after myocardial injury. *Circulation.* 2005 Aug 30;112:1173-7.

APPENDIX A

Performing a Successful Left Anterior Descending Coronary Artery Ligation

A.1 INTRODUCTION

The following appendix provides a step-by-step protocol for performing a successful left anterior descending coronary ligation in rats. *In vivo* models of myocardial infarction have become essential to investigating the efficacy of cellular cardiomyoplasty. Unfortunately there is no published in depth protocol for this procedure. Surgical technique and equipment (and instruments) will be presented.

A.2 MATERIALS

Surgical Pack

- Chest tube
- 20mL syringe
- Scalpel handle (#3)
- Rib retractor
- Needle Holder (auto-locking)
- 12 cm hemostats (curved; x2)
- Small scissors
- 12 cm forceps (straight)
- 10 cm forceps (curved; x2)
- 14 cm Surgical scissors (straight; used for cutting non-tissue)
- gauze (1 – 2, 4x4 inch pieces)
- Cotton swabs (x8)

Surgical Equipment

- Rodent Anesthesia Workstation
- Isoflurane vaporizer
- Heating Pad
- EKG monitor
- Rectal Probe
- Hair Clippers
- Scale
- Surgical lamp (fiber optics)
- Trachea tube
- Nose cone (small and medium sizes)

Anesthesia and Analgesics

- Bupenorphine (Dose: 0.1mg/kg)
- Bupivacaine (Dose: 0.3mL 0.25% solution)
- Isoflurane

Miscellaneous

- 1mL Insulin syringes
- Isolation gown
- Face mask
- Gloves (both sterile and non-sterile)
- Sterile Drapes
- Shoe covers
- Sterile Saline
- Sterile beaker (small)
- Hemostats and forceps for intubation
- Surgical bed (i.e. Styrofoam lids)
- Clean rodent cage (with food and water)
- Suture (4-0 nylon, 5-0 nylon, 6-0 silk)

A.3 PRE-OP

Before performing this surgery, make sure that all materials described in section A.2 are available.

1) Retrieve rat from housing and bring to surgical suite. Allow animal at least 20 minutes to acclimate to new environment. If your animal facilities require laminar flow hoods to be used when opening cages, place animal under an operating hood during this time.

2) During the acclimation period prepare aliquots of 0.9% saline in 1mL insulin syringes (for each rat 0.5mL of warm saline will be injected SC post-op into two sites). Also prepare 0.1mg/mL Bupenorphine and 0.25% Bupivacaine in 1mL insulin syringes. Bupenorphine will be delivered SC post-op at 0.1mg/kg and Bupivacaine will be delivered IM (directly beneath the initial incision site) at 0.3mL per rat.

Turn on the heating pad, check isoflurane levels and add as needed, clean surgical space with 70% ethanol or Clidex, turn on rectal thermometer and ECG monitor.

3) Retrieve acclimated rat using a medium size nose cone. Once rodent is inside nose cone, place onto a flat surface near vaporizer. Attach vaporizer to nose cone. Turn on oxygen, rodent workstation (make sure ventilation function is off) and set isoflurane level to five (or max) and oxygen flow rate to 0.5 L/min. During this time watch for three responses:

Excitability: Initially the rodent will appear calm in the nosecone but after a few minutes he/she will appear more excited and restless. This response is normal.

Flickering of Eyelids: After the excitability response the rodent will begin to settle down and the eyelids will begin to quickly flicker. The cessation of this response is a good indicator that one can move to the next step

Respiration: Throughout this process the breathing rate of the rodent will steadily decrease. Monitoring respiration is a good method to determine the depth of anesthesia.

4) Once respiration is down to 1 breath per second or the eyelids have stopped flickering, turn off anesthesia, remove the rodent from nosecone and weigh. Record this weight for later use. Next place the rodent in a supine position with a small nosecone attached. Return isoflurane levels back to max. Again monitor respiration. Once the breath rate is down to one per second the surgeon should proceed to the next step. While waiting, secure the rodent to a surgical bed on top of heating pad using surgical tape. Place a rolled piece of gauze (no more than 0.75 inch thick) under the chest of the rodent to lift the heart slightly. The gauze should be placed directly inferior to the armpit of the rodent. The surgeon should modify the supine position slightly so that the left leg

crosses over to the right leg. Use surgical tape to secure this position. This modification displaces the heart slightly so that the anterior portion is more visible after rib retraction.

5) Once the breath rate has returned to one per second, turn off the anesthesia and remove nose cone. Position the surgical bed (to which the rodent is secured to) such that the nose of the rodent is toward the surgeon. Place rubber bands (or some other restraint) around the incisors of the rodent so that its head remains flat. Direct the light source to the throat of the rodent. Gently displace the tongue and use a 14 cm curved hemostats to lift the jaw. At this point the surgeon should see the vocal cords. Insert trachea tube into the trachea when the cords are **OPEN**. Do not force the tube down the trachea as this will cause severe trauma. Once the tube is in the trachea, attach it to the rodent workstation, set isoflurane level to 1.5 – 2, turn on mechanical ventilation and increase oxygen such that pO_2 is above 10mmHg. The ventilation rate should be set to 80 per minute for rats. Check the rodent to make sure the chest expands and collapses with the ventilator. If not, remove tube and try again. Do not try more than 3 times to avoid serious throat trauma. For most surgeons, this will be the hardest skill to master for this surgery.

6) Secure trachea tube and connections using surgical tape. Place ointment onto the eyes of rodents to prevent infection and severe drying during surgery. Shave the rodent (if hair is present) and vacuum excess hair. Be sure there is no loose hairs present around the surgical sight. Clean sight with surgical scrub (70% ethanol) to clean and pick up any loose hair. Attach ECG monitor and insert rectal probe (body temperature should be maintained at 37°C). Next, inject 0.3mL of bupivacaine IM directly under the proposed incision sight (just lateral to the sternum). Use surgical scrub to

clean the area again and then place iodine onto the area for one minute. Remove iodine with sterile ethanol wipes.

7) Aseptically place sterile drape over the rodent. Be sure there is a hole in the drape which should be big enough to see the entire surgical site. Next, aseptically open the surgical pack and sterile beaker. Place sterile saline into the beaker and set close to surgery area. Adjust light source to desired intensity and location. Aseptically put on sterile gloves and proceed to the surgery area.

A.4 SURGICAL PROCEDURE

1) Using a scalpel with sharp blade (do not reuse the blades), make a 3-4 cm parasternal incision just left of the sternum. Be sure not to press with too much force. Use blunt dissection to lift skin from muscle layer. At this point you will see a thick muscle layer. (note: There are actually two muscle layers here with the other being directly under the visible muscle layer). Use scalpel to make a 3 cm parasternal incision in the top layer only. If there is bleeding, be sure it is under control before proceeding. Displace the second layer (which covers the ribcage) to the left side of the rodent by slowly cutting the connective tissue beneath this layer. The use of a scalpel or scissors works well for this step. Use hemostats secure this layer to the side of the rodent such that the ribcage is clearly visible.

2) Find the largest intercostal space and insert 12 cm curved hemostats into this area at the peak of the rib (Each rib extends from the sternum going down. The rib will peak at a particular location and extend upwards toward the left arm). Rotate the hemostats so that the tip goes beneath the rib more proximal to the heart and out the

adjacent intercostal space. Slightly lift and open the hemostats and cut rib. This procedure aids in preventing unwanted damage to the lung which is in the area. Place a small piece of damp gauze through the hole to move the lung slightly to the left. Use scissors to cut up toward the next proximal rib but do not cut this rib. Use scissors to cut down toward the next distal rib. Cut through this rib and continue cutting until the next rib. Do not cut through this rib. In total two ribs and three intercostal spaces should be cut (note: during this step always be aware of where the lung is located. Damage to the lung is very traumatic).

3) Retract the ribs. Use additional damp gauze to displace the lung so that the anterior portion of the heart is visible. Gently remove the pericardium using forceps and displace the left atrial appendage slightly upward to gain a better view of the LAD (traditionally, the LAD branches from the left main at the intersection of the left atrial appendage and pulmonary conus. These are the best landmarks if the surgeon is unable to visualize the LAD). Reduce intensity of the light source and inspect the heart for the LAD. The LAD is not bright red (these are veins) or superficial. It will be directly beneath the epicardium and will look pinkish (and very pale). It will continue straight down toward the apex of the heart and will most likely branch 1-3 mm from the base of the heart into the lateral myocardium.

4) Obtain sterile 6-0 silk suture and ligate the LAD 1-2 mm from the intersection of the left atrial appendage and pulmonary conus (note: 1-2 mm is just a typical number that seems to work for most surgeries. For nude rats, however, this may be too proximal and it is suggested that the ligation be made 2-4 mm from the intersection. If the ligation is made too proximal, the infarct will be too big and the rodent will die. If the ligation is made too distal however, the infarct will be very small and thus useless in your analysis.

The surgeon should practice several surgeries to determine optimal ligation parameters). If a successful ligation has been made there will be immediate ST-elevation on the EKG monitor and pallor of the myocardium. The myocardium will look grey in the anterio-lateral portions of the heart. If these changes do not occur than up to two more ligations can be made. Ligation of LAD branches may also help in making a good infarct.

5) Monitor the rodent for 10 minutes after ligation for adverse arrhythmias, respiration (remove gauze from lung so that lungs can fully inflate) and fusion of ST-segment with the QRS complex on the EKG. Also make sure the ligation does not come loose by observing maintained pallor. Make sure that any bleeding (especially from the heart) is under control before continuing.

6) Clean pleural cavity with gauze to remove excess blood and fluid. Remove excess gauze, retractor and hemostats from surgical area. Suture the rodent closed in three layers:

Ribcage: 4-0 interrupted; inserted chest tube before tightening of last suture; bite size should be < 1 mm

Muscle: 5-0 continuous; bite size should be < 1 mm

Skin: 4-0 continuous; bite size should be 1-2 mm

7) Right before the skin suture is secured, restore negative pressure using a 20mL syringe attached to the chest tube. Blood and other fluids will also be drawn into the syringe.

8) Clean skin with saline.

A.5 POST-OP

1) Turn off anesthesia, removed rolled gauze from under chest, remove drape and rectal thermometer. Inject 0.5 mL of warm saline SC (any location other than the surgical site is fine). Also inject bupenorphine SC at a dose of 0.1mg/kg. This mass of the rodent taken pre-op should be used to determine the dose. Maintain ventilation and O₂ levels until it is clear that the rodent is breathing on its own. Turn off ventilation and set the O₂ flow rate to 0.5. Allow the rodent to take in pure O₂ for at least 5 minutes and then remove the trachea tube. Watch to make sure the rodent continues breathing for 5 minutes and then return to cage. The rodent should be placed on its side and the cage should be clean and contain moist food on top of the bedding. One half of the cage should be place on a heating pad. This will help generate a temperature gradient that so the rodent can choose a comfortable area for eating or sleeping.

2) Return live rodent to housing room. Watch the rodent for consecutive three days. If there are signs of pain (porphyrin red staining around the eyes, lack of appetite, loss of body mass, lack of activity) give more bupenorphine at the same dose.

APPENDIX B

Modulation of Human Embryonic Stem Cell Function in Collagen Patches

B.1 INTRODUCTION

In chapters 3 and 4 we describe the use of a TE approach (combination of cells and matrix) to locally and homogeneously deliver cells to an infarct. Typical cell source choices are limited in their ability to differentiate into working cardiomyocytes. To address this issue, human embryonic stem cells (hESCs) have been considered as an alternative for cardiomyocyte replacement. Such cells have been shown to readily differentiate into cardiomyocytes under specific conditions [1-3] and may offer a superior platform for cardiac regeneration. The culture of hESCs within TE constructs, however, may alter their function. We hypothesize that culture of hESCs within collagen gels will modulate cellular viability, proliferation and differentiation compared to cells cultured as monolayers.

B.2 MATERIALS and METHODS

B.2.1 Cell Culture

hESC obtained from a NSF-sponsored core lab at Emory University, were cultured in a 90% DMEM/Ham's F12 Mixture (1:1), 20% Knock-Out Serum Replacement, 1% glutamine, 1% non-essential amino acids and 10 ng/mL human recombinant basic fibroblast growth factor at 37°C in 3% O₂ and 5% CO₂ on mitomycin C treated mouse embryonic feeder cells.

B.2.2 Formation of Cell Seeded Collagen Patches

H9 (female) hESC expanded to P30-P50 were embedded into a rat tail type I collagen matrix to form cardiac patches. To produce cardiac patches for stem cell

delivery, 0.2 million hESCs (resuspended as small clumps) were mixed in a solution of rat tail type I collagen, 5x DMEM and serum replacement such that the final collagen concentration was 2 mg/mL. The solution was placed in individual wells of a non-tissue culture-treated 48-well plate in order to create a patch that is between 0.3 – 0.7 cm in diameter. Patches were cultured at 37°C in 5% CO₂ for 1-7 d before usage

B.2.3 Viability Assays

To assess cell number within the construct, patches containing hESC were digested in type I collagenase (250 U/mL) diluted in DMEM for 30 min at 37°C with intermittent mixing. Each patch was submerged in 2mL of the collagenase solution and placed into at 37°C water bath. The solution was triturated every 5 minutes to assist in the digestion of the construct. At the end of the incubation period, collagenase activity was inhibited by the addition of 500µl of 100% FBS and 8 ml of complete hESC medium (see section B.2.1). Counts were made using a hemocytometer on day three. In addition, a more qualitative measure of viability was completed via fluorescence microscopy using a commercial live/dead kit. Constructs were washed in (PBS) to remove serum. Fluorescent EthD-1 (4µM, red) and SYTO 10 (4µM, green) (Molecular Probes; Eugene, Oregon) were then added for 30 minutes. Afterwards, constructs are washed three times in PBS and viewed under a confocal microscope. Although this technique only offers finite penetration into the construct it did provide a general sense as to the viability of cells within the collagen matrix.

B.2.4 Proliferation

Proliferation was determined by measuring the incorporation of 5-ethynyl-2'-deoxyuridine (EdU); a nucleoside analog to thymidine which is incorporated into DNA

during synthesis. Cellularized constructs or cells cultured as a monolayer were pulsed with 10mM EdU at (Invitrogen; Carlsbad, CA) for 24 hours after their initial formation. Afterwards constructs were washed in PBS and digested using collagenase to isolate cells as described above (B.2.3). Next, cells were washed using a 1% bovine serum albumin (BSA)/PBS solution and then fixed using the Click-iT fixative (Invitrogen; Carlsbad, CA) for 15 minutes at room temperature. Cells were permeabilized with Triton X-100 and then stained using the Click-iT cocktail mixture for 30 minutes at room temperature. Afterwards, cells were washed with 1% BSA/PBS and used for flow cytometry. To simplify analysis, hESCs were gated using an unstained sample (no antibody) on a forward scatter vs. side scatter dot plot. This procedure helped to remove excess debris. Next, a positive control (using hESCs cultured on treated plastic) was run to determine the proper levels for positive signal. Samples were run and analyzed for positive fluorescein isothiocyanate (FITC) signal using the histogram option of the BD FACS Diva software package (BD Biosciences; San Jose, CA). Positive signal was compared with the appropriate isotype controls which allowed for accurate background subtraction. Analysis of data was performed using FCS Express 3.0 software (De Novo Software; Los Angeles, CA) and the histogram subtraction function.

B.2.5 Assessment of Cell Differentiation

Differentiation of hESCs within collagen patches was measured by monitoring the expression of markers for stem cell potency over several days. hESC isolated from the patch by treatment in collagenase (B.2.3) were stained and analyzed for the expression of Oct 3/4, SSEA 4 and anti-TRA 1-81 by flow cytometry. After cells are isolated from the patch, they were fixed using a 4% paraformaldehyde (PFA) for 15 minutes on ice. Next, cells were stained with the appropriate primary antibodies for 30 minutes on ice. If necessary, fluorescent conjugated secondary antibodies were added

afterwards for 25 minutes on ice (Santa Cruz Biotechnology; Santa Cruz, CA). Cells were washed in a 0.3% BSA/PBS solution and analyzed via flow cytometry as described above (B.2.4). A Student's t-test was used to determine statistical significance.

B.3 RESULTS

B.3.1 Culture of hESCs within Collagen Patches Modulates Proliferation, Differentiation and Viability.

To determine the effect of cell culture within collagen patches on hESC function, we performed a series of test to assess cell proliferation, differentiation and viability. Proliferation was quantified using a pulse-chase with EdU substrate (Figure 4.3). EdU incorporation within cell types as monolayers or removed from within collagen patches was measured with flow cytometry. hESC demonstrated attenuated proliferative capacity upon culture within collagen patches (hESC showed a 92% reduction).

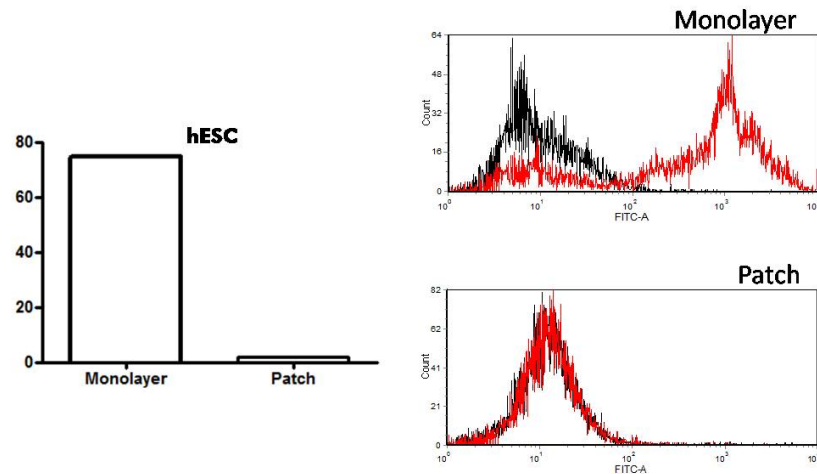


Figure B.1) Culture of hESCs in collagen patches attenuates proliferation. Analysis by flow cytometry of EdU incorporation was used to determine the proliferative capacity of hESCs cultured within patches compared to monolayers. hESC demonstrated a 92% reduction in EdU incorporation and thus proliferation after culture in collagen patches (n = 1).

hESC demonstrated slight modulations in potency after culture in collagen patches. SSEA4, Oct 3/4 and Tra 1-81 were used to monitor potency of hESC over 3 d. There was no change in SSEA4 expression on hESC when cultured in collagen patches (Monolayer: 77% Expression vs. Patch: 78% Expression; Figure 4.5a). We did notice attenuated expression levels of Oct 3/4, however. Oct 3/4 showed a significant reduction in expression of 64.7% (Figure 4.5b; Monolayer: 43.6% Expression vs. Patch: 15.4% Expression; $p < 0.05$). There was also a non-statistical reduction in Tra 1-81 expression (Figure 4.5c; Monolayer: 69.4% Expression vs. Patch: 56.1% Expression; $p = 0.1$) in hESC cultured in collagen patches.

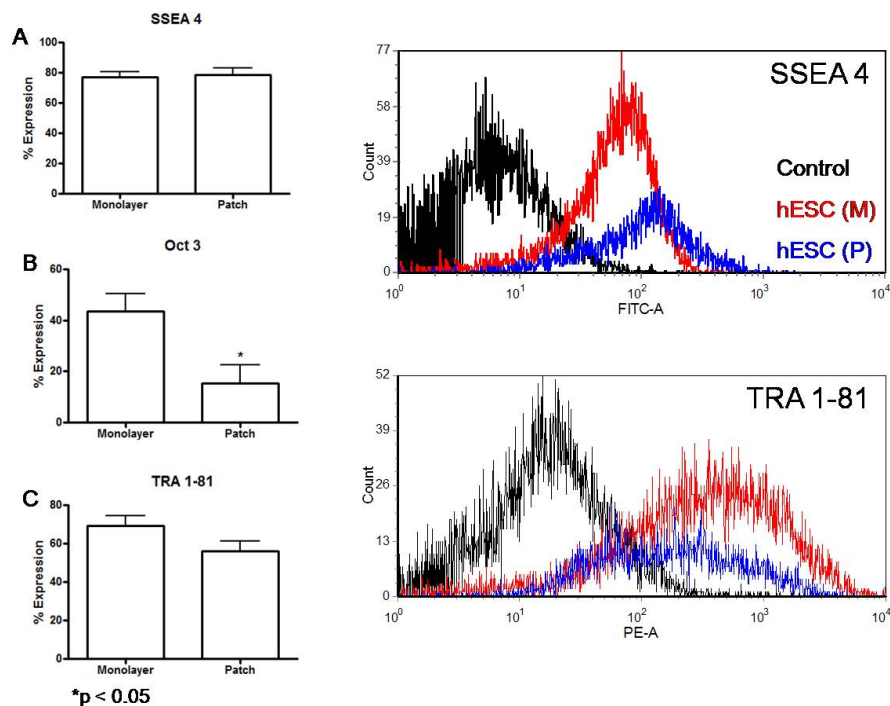


Figure B.2) Culture of hESC in collagen patches modulates potency. hESC evaluated for the expression of A) SSEA (Monolayer: $77 \pm 3.7\%$ vs. Patch: $78 \pm 4.4\%$; $p = 0.8$) B) Oct 3/4 (Monolayer: $43.6 \pm 6.7\%$ vs. Patch: $15.4 \pm 7.1\%$; * $p = 0.04$) and C) TRA 1-81 (Monolayer: $69.4 \pm 4.9\%$ vs. Patch: $56.1 \pm 5.2\%$; $p = 0.1$) demonstrate attenuated expression of Oct 3/4 upon culture in collagen patches. SSEA 4 and TRA 1-81 expression remains statistically unchanged over 3 d in culture. ($n > 3$ for all groups)

hESC demonstrated variable cell morphology and viability after 3 d in collagen patches (Figure 4.6e-f). As shown in Figure 4.6d-f, there were instances of small embryoid body-like structures developing in some samples and in most others there was complete loss of cell viability with no body formation. In addition, there were instances where cell yield was as low as 1800 cell per patch and at other times as many as 116,000 cells could be isolated with collagenase treatment after 3 d in culture (Figure 4.6c). Most instances resulted in low cell yield. This variability in cell survival and morphology prompted us to exclude hESC from potential *in vivo* experiments as it was concluded that under the current conditions, undifferentiated hESC would not represent a viable option for tissue engineered-based cell delivery strategies. Additionally, teratoma formation (a significant disadvantage to the use of undifferentiated ESC *in vivo*) was still an unresolved risk.

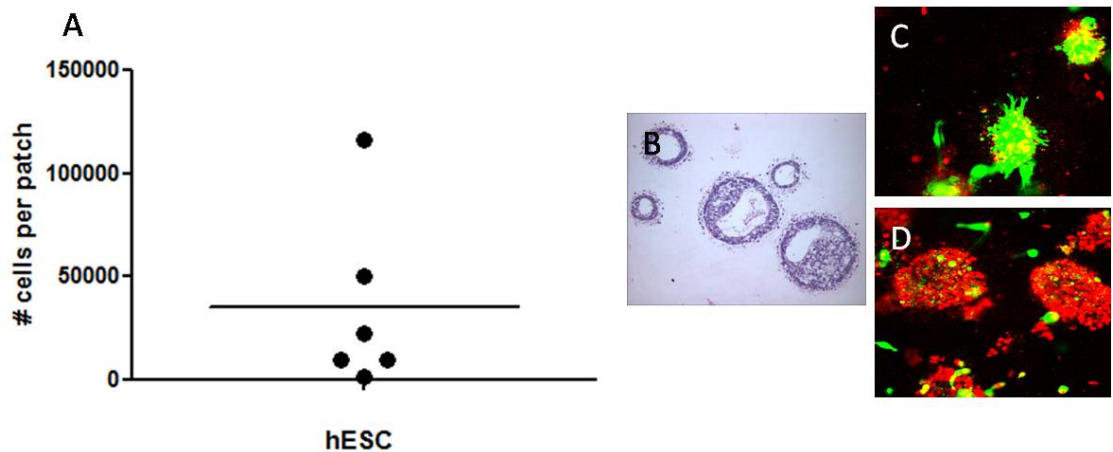


Figure B.3) Viability of hESCs cells in collagen patches. A live/dead assay was used to determine the viability of hESC in collagen patches given the low and variable cell yield after patch treatment with collagenase (A; n = 6). hESC demonstrated a tendency to form small embryoid bodies with collagen patches (B), though this occurred on rare instances. C and D) There was also variability in hESC viability in collagen patches (green – live cells, red – dead cells).

B.4 DISCUSSION

There are several cell sources marked for use in cellular cardiomyoplasty. hESC are attractive because they readily differentiate into working cardiomyocytes. Unfortunately, our experiments show that hESC display variable growth and viability patterns and thus do not represent a good option for cell delivery in collagen constructs. It has already been suggested that hESC are fairly intolerant to hypoxia [4] but hESC must also be grown as colonies. Thus single celled hESC are more likely to undergo apoptosis [5] than those grown as colonies. Even when grown as colonies, however, hESC continue to display incidences of cell death. On the other hand there were also cases of embryo body formation within collagen matrices. This is likely due to initial colony size. It is assumed that if colonies were large enough they would continue to grow. If colonies did not meet a particular threshold, however, they would assume the same fate as single cells. Variations in initial colony size were due to mild enzymatic treatment and gentle trituration of hESC. This treatment may also have induced cell death before culture in collagen patches. The use of small colonies in TE delivery vehicles however, foreshadow teratoma formation once transplanted in vivo. Thus this strategy does not represent a suitable option for hESC delivery. It may be possible to use ROCK inhibitors to allow for single cell survival in collagen patches [6]. Whether or not hESCs will migrate out of the patch and into the adjacent myocardium will have to be investigated if this strategy is to be explored.

In conclusion, using the conditions and experimental procedures described, the use of undifferentiated hESC would not represent a viable option of TE-based delivery strategies. Methods for improving cell survival in TE constructs and preventing adverse teratoma formation would aid in advancing the use of hESC in translational research.

B.5 REFERENCES

1. C. Mummery, D. Ward-van Oostwaard, P. Doevendans, et al. Differentiation of human embryonic stem cells to cardiomyocytes: role of coculture with visceral endoderm-like cells. *Circulation*. 2003 Jun 3;107:2733-40.
2. C. Mummery, D. Ward, C. E. van den Brink, et al. Cardiomyocyte differentiation of mouse and human embryonic stem cells. *J Anat*. 2002 Mar;200:233-42.
3. I. Kehat and L. Gepstein. Human embryonic stem cells for myocardial regeneration. *Heart Fail Rev*. 2003 Jul;8:229-36.
4. S. M. Prasad, M. Czepiel, C. Cetinkaya, et al. Continuous hypoxic culturing maintains activation of Notch and allows long-term propagation of human embryonic stem cells without spontaneous differentiation. *Cell Prolif*. 2009 Feb;42:63-74.
5. R. Peerani, B. M. Rao, C. Bauwens, et al. Niche-mediated control of human embryonic stem cell self-renewal and differentiation. *EMBO J*. 2007 Nov 14;26:4744-55.
6. K. Watanabe, M. Ueno, D. Kamiya, et al. A ROCK inhibitor permits survival of dissociated human embryonic stem cells. *Nat Biotechnol*. 2007 Jun;25:681-6.

APPENDIX C

Secretion Profile for B4 Progenitor Cells

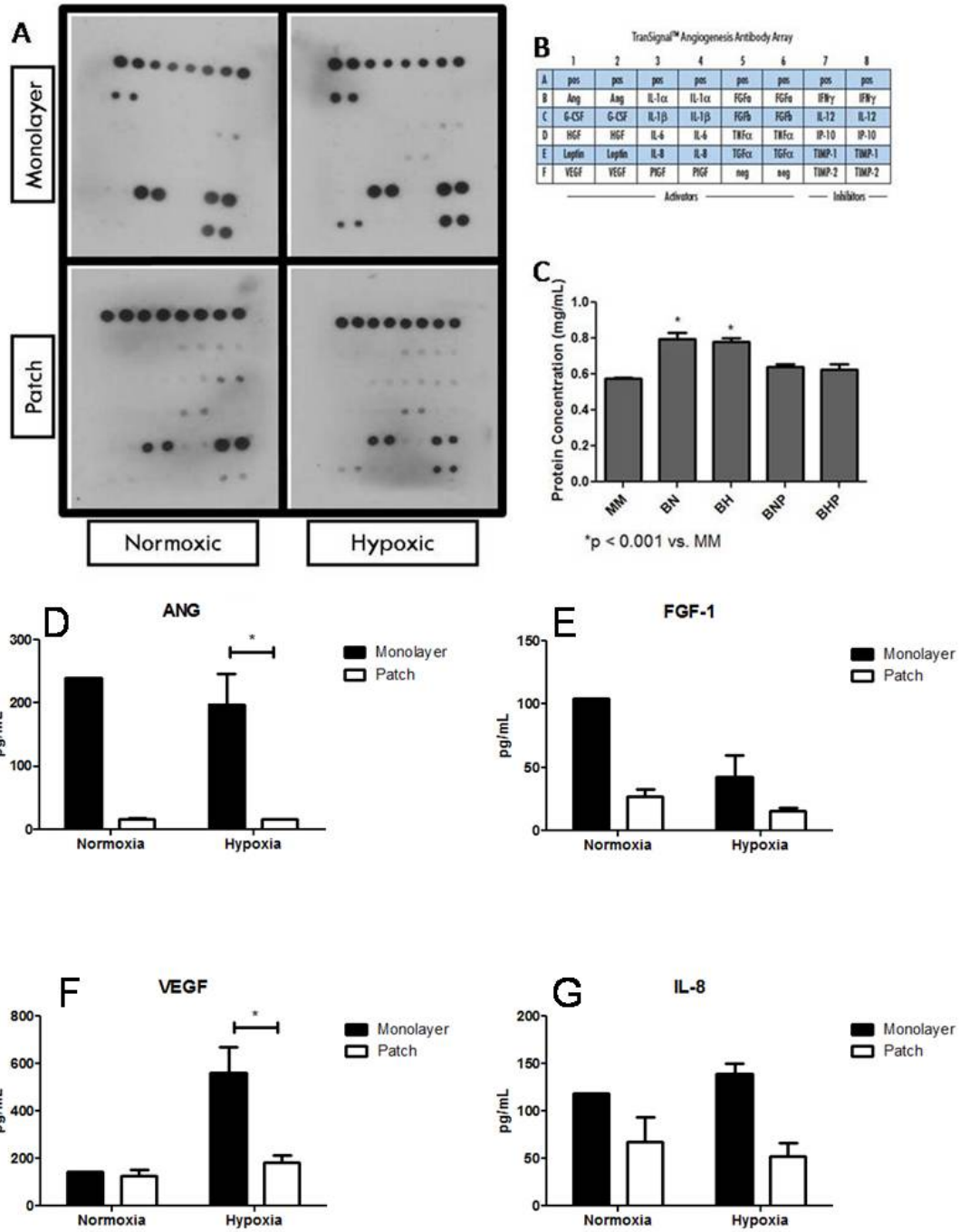


Figure C.1) B4 Progenitor Cell Secretion Profile. A & B) B4 progenitor cells cultured as monolayers or within patches and exposed to normoxia (20% O₂) or hypoxia (1% O₂) display differential secretion profiles of angiogenic factors. C) There was a general increase in protein content in conditioned media from normoxic monolayers (BN; 0.8 ± 0.03 mg/mL) and hypoxic monolayers (BH; 0.78 ± 0.02 mg/mL), versus a maintenance media control (MM; 0.57 ± 0.01 mg/mL; *p < 0.001). There was no statistical difference between normoxic patches (BNP; 0.64 ± 0.02 mg/mL) and hypoxic patches (BHP; 0.62 ± 0.03 mg/mL) versus a MM control. Specific analysis of pro-angiogenic factors revealed differential expressions patterns based on hMSC culture in monolayers versus collagen patches for D) ANG (Normoxia: 239.3 vs. 16.5 ± 1.6 pg/mL; and Hypoxia: 198 ± 49.2 vs. 15.6 ± 1 pg/mL; *p < 0.01), E) FGF-1 (no statistical significance was observed; Normoxia: 104.9 vs. 26.8 ± 6.4 pg/mL and Hypoxia: 42.7 ± 17.1 vs. 15.6 ± 2.3 pg/mL), F) VEGF (Normoxia: 144.8 vs. 128.6 ± 23.8 pg/mL and Hypoxia: 562.3 ± 107.1 vs. 184.7 ± 30.5 pg/mL; *p < 0.01) and G) IL-8 (no statistical significance was observed; Normoxia: 118.5 vs. 68 ± 26.1 pg/mL and Hypoxia: 139 ± 10.7 vs. 52.5 ± 13.8 pg/mL) n > 3 for all groups for panel C; n = 3 for BNP and BHP; n = 2 for BH and n = 1 BN for ELISAs.

VITA

David L. Simpson

David Lemar Simpson was born to David and Mable Evans on March 15, 1981 in Norfolk, Virginia. He graduated from East Kentwood High School in 1999 and obtained his B.S. in Engineering Science from the University of Virginia in 2003. Following graduation, David entered into the joint biomedical engineering Ph.D program at Georgia Tech and Emory University. He will graduate with his Ph.D in December 2009.